TESI DOCTORAL

UVIC
UNIVERSITAT DE VIC
UNIVERSITAT CENTRAL
DE CATALUNYA

Doctorate program in Environmental Sciences and Technology

Assessment of the ecological impact of metal and salts mining effluents on freshwater bodies.

Lidia Vendrell Puigmitjà

June 2021

Dra. Laia Llenas Argelaguet

Dra. Meritxell Abril Cuevas

Agraïments

Aquesta secció està dedicada a totes aquelles persones que d'alguna manera o altre m'han acompanyat durant aquesta etapa.

M'agradaria agrair a les meves directores, la Laia i la Txell, per la seva confiança i suport durant aquests anys, sense elles no hauria estat possible. A la Laia, moltes gràcies per donar-me l'oportunitat, la confiança i el suport durant tot el camí. Txell, potser ets la que m'has hagut de "patir" més, i se que a vegades no és una tasca fàcil... gràcies per la paciència, per guiar-me durant aquests anys, per els consells, la motivació i tot el que m'has ensenyat.

Als meus companys de doctorat, m'heu acompanyat en els bons i els mals moments. Iman i Nagore, m'heu aixecat els ànims sempre que ho he necessitat, sempre heu estat disposades a ajudar-me i heu confiat en mi quan jo no ho feia, quina sort trobar-vos i tenir-vos! Carmen, gràcies per la disposició a ajudar-me sempre en tot el que he necessitat, pels riures i, per les xerrades del cafè a primera hora del matí! Als nois; Jordi, Lluís, Pablo, Ipan, Daniel, Carlos y Mostafa, sens dubte heu sigut la font dels millors riures i heu sabut veure la part divertida, i tant necessària, de cada situació. Heu fet que el camí fos més fàcil. En definitiva, aquesta experiència no hagués estat la mateixa sense vosaltres.

A tot l'equip del BETA, sou un gran equip ple de persones que valeu moltíssim, m'heu ajudat sempre i he après molt de cada un de vosaltres. Quina sort haver-vos conegut, moltes gràcies! Especialment a en Lorenzo, sens dubte has estat una de les persones de les que més he après. Moltes gràcies per la implicació, disponibilitat, la paciència i el suport al llarg d'aquest viatge.

Als meus amics, Daniel, Jorge, Soukaina, Júlia, Marina i Cintia, ens hem vist menys del que hauria volgut en aquests últims tres anys, però sempre heu estat al meu costat i, sobretot, m'heu ajudat a desconnectar, agafar aire i continuar, gràcies. A la Sheila, la Kate i en Marc, us vau posar les mans al cap quan us vaig dir on em ficava, però tot i així m'heu fet costat, ajudat, escoltat i aconsellat, tinc molta sort de tenir-vos.

A la Marta, la Judit i la Joni, sou les persones amb les que vaig començar la meva experiència laboral i m'heu ensenyat tant! Moltes gràcies per tot, per com em vau acollir, pels consells, els ànims i el suport i per encoratjar-me a seguir el meu camí.

A la meva cosina Judit, sempre has estat al meu costat, en els bons i en els mals moments. M'has recolzat en totes les decisions que he pres i m'has ajudat incondicionalment. Gràcies, sobretot gràcies per fer-me riure fins que m'ha faltat l'aire.

Al Kostas, la persona que ha viscut en primera persona i ha patit aquest procés. Moltes gràcies per ser-hi sempre, estar disposat a donar-me un cop de mà en qualsevol moment, a confiar en mi més que jo mateixa, a fer-me veure les coses des d'un altre punt de vista i sobretot per la paciència.

Als meus pares, heu lluitat per ajudar-nos a arribar tant lluny com volguéssim. M'heu ensenyat a no rendir-me mai i a lluitar per els meus somnis. M'heu aconsellat i donat suport sempre en totes les decisions que he pres i m'heu ajudat a seguir el camí que jo vaig escollir. Als meus germans Oscar i Jordi, els millors del món! M'heu fet riure per sobre de tot, m'heu recolzat, sempre heu estat al meu costat i m'heu fer veure i viure la vida d'una manera única.

Moltes gràcies a tots!

LAIA LLENAS ARGELAGUET, deputy director and project manager of the BETA Technological Center, and MERITXELL ABRIL CUEVAS, senior researcher of the BETA Technological Center,

CERTIFY:

that the PhD student LIDIA VENDRELL PUIGMITJA has carried out under our direction the work with title "Assessment of the ecological impact of metal and salts mining effluents on freshwater bodies" that is presented in this report and that constitutes her Thesis to apply for a Doctor's Degree from the University of Vic - Central University of Catalonia.

Dra. Laia Llenas Argelaguet

Dra. Meritxell Abril Cuevas

Abstract

Mining activities have been crucial for the economic and social development of Europe over the centuries. However, nowadays there are significantly more abandoned than operational mines in Europe, which cause serious impacts on freshwater ecosystems mostly through the uncontrolled and still non-regulated discharge of polluted effluents to the receiving water bodies. Among the different type of abandoned mining effluents, those with high loads of metals and salts are of special environmental concern to nearby citizens and the surrounding environment, as they can affect water supplies, water resources and damage freshwater ecosystems. The presence of those mobilised heavy metals and dissolved ions in mining effluents can be either in dissolved form or adsorbed to particles and can be transported downstream of the river, deposited, and accumulated in sediments by fluvial river processes. However, not many studies exist addressing this problem from the aquatic ecosystems point of view, especially in the case of saltinisation. Additionally, even though new treatment technologies and management strategies are being developed, it is still an unresolved issue.

Effluents from abandoned mines represent a source of chronic uncontrolled pollution because of the lack of any regulation about this wastewater treatment. The specific hazards posed by chemical stressors harboured in mine effluents to the aquatic environment depend mainly on its fate which influence its bioavailability and consequently its ecotoxicity. In this regard, biofilm communities have been considered as a good ecological indicator of freshwater pollution due to its capacity to integrate early effects and long-term responses produced by chemical and environmental stressors.

In this thesis, biofilm communities have been used to assess the efficiency of different remediation methods, including treatment technologies for the metal mining effluent and applying dilutions for the saline effluent. Specifically, the new treatment technologies developed by the LIFE DEMINE (LIFE16 ENV/ES/000218) project were used. LIFE DEMINE is a demonstration project funded by the European Commission that puts in practice, tests, and evaluates an innovative treatment technology at pre-industrial scale to treat abandoned mining effluents by combining membrane technologies and electrocoagulation processes. The two mining effluents used during the work developed, where from two different abandoned mining sites, a metal effluent from Frongoch abandoned metal mine (Wales, UK) and a hypersaline effluent from Menteroda potash abandoned mine (Germany).

To assess the effects of these mining effluents on freshwater ecosystems and its reduction through different methodologies, biofilm communities has been used as bioindicators, at field study and microcosms experiments.

The results obtained in the experiments developed during this thesis demonstrated that the mining effluents from the two abandoned mines sites (Frongoch and Menteroda) had severe effects in functional and structural variables of biofilm communities under both, metal and hypersaline mining effluents. Short-term exposures of the biofilm to the mining effluents caused rapid responses in biofilm function (i.e., photosynthetic efficiency and nutrient uptake), while the structural shifts were appreciated after mid-term exposures. Additionally, both metal and hypersaline mining effluents promoted changes in the diatom growth rate, size, biodiversity, and taxa dominance favouring pioneer and tolerant species to growth. This shift in the community composition entailed an increase community tolerance to metal and salt pollution. However, biofilm communities exposed to metal and hypersaline mining effluents gradually recovered its functionality when the polluted effluent was removed, despite the community structure remained affected.

On the other hand, the results obtained from the biofilm performance regarding the efficiency of the treatment technologies in reducing the ecological impact caused by metal mining effluents, demonstrated that, despite high metal removal rates were achieved, its efficiency depended also on the dilution factor of the receiving stream where the most significant effects on the biofilm response were found at Zn concentrations up to 1.41 mg L^{-1}. Furthermore, as a treatment method, it was also explored the salinity thresholds from which irreversible impact can be observed on the biofilm structure and functioning, and thus the optimal concentration to be achieved when discharging hypersaline mining effluents to the receiving water bodies. In this regard, although structural effects were observed in biofilm exposed to all salinities tested, significant effects on biofilm functioning were observed only under salinities above 15 g L^{-1}.

Overall, the results of this thesis demonstrated the feasibility of using biofilm communities as a bioindicator of freshwater pollution and, especially, for the functional variables of biofilm, that were the ones responding faster to the stress and the recovery. Additionally, new evidence of the effects of hypersaline effluents on biofilm communities were provided throughout this study. The biofilm response proved the efficiency of the new treatment technologies in reducing abandoned metal mining effluents impacts on freshwater ecosystems, even though the dilution capacity of the receiving stream should be considered when discharging. Additionally, this thesis

provided new evidence of the potential salinity thresholds from which impacts on freshwaters can achieve a point of no return.

Resum

Les activitats mineres han estat crucials per al desenvolupament econòmic i social d'Europa al llarg dels segles. No obstant, avui en dia a Europa hi ha significativament més mines abandonades que operatives que causen greus impactes sobre els ecosistemes aquàtics, principalment mitjançant l'abocament incontrolat, i encara no regulat, d'efluents contaminants als rius receptors. Entre els diferents tipus d'efluents miners procedent de mines abandonades, són d'especial preocupació els efluents amb una elevada càrrega de metalls i sals ja que poden afectar als recursos hídrics i danyar els ecosistemes aquàtics. Els metalls pesants i ions en els efluents miners es poden trobar tant dissolts com adsorbits en partícules, això fa que puguin ser transportats, depositats i acumulats en sediments riu avall. Tot i així, no existeixen gaires estudis que abordin aquest problema des del punt de vista dels ecosistemes aquàtics, especialment en el cas de la salinització. A més a més, tot i que s'estan desenvolupant noves tecnologies de tractament i estratègies de gestió, aquest continua sent un problema ambiental sense resoldre.

Per tot això, els efluents procedents de mines abandonades representen una font crònica i incontrolada de contaminació, ja que no hi ha cap regulació que abordi el tractament d'aquest tipus d'aigua residual. Els impactes específics causats per els contaminants presents en els efluents miners en els ecosistemes aquàtics depenen principalment del seu destí, que influeix en la seva biodisponibilitat i, en conseqüència, en la seva ecotoxicitat. En aquest sentit, els biofilms són considerats com un bon indicador ecològic per a detectar la contaminació en els ecosistemes d'aigua dolça degut a la seva capacitat d'integrar efectes primerencs i respostes a llarg termini produïdes per contaminants químics i ambientals.

En la present tesis, els biofilms s'han fet servir per avaluar l'eficiència de diferents metodologies de remediació, incloent tecnologies de tractament en el cas dels efluents metàl·lics i diferents dilucions per als efluents salins, per reduir els impactes d'aquests efluents ens els ecosistemes aquàtics. Específicament, s'han utilitzat les noves tecnologies desenvolupades en el marc del projecte europeu LIFE DEMINE (LIFE16 ENV/ES/000218), el qual avalua una tecnologia innovadora, que combina tecnologies de membrana i electrocoagulació, a escala preindustrial per a tractar efluents miners abandonats. Al llarg d'aquesta tesis, s'han utilitzat com a referència dos efluents miners procedents de dues mines abandonades: un efluent metàl·lic de la mina abandonada de Frongoch (Gal·les, Regne Unit) i un efluent hipersalí de la mina abandonada de potassa de Menteroda (Alemanya).

Per avaluar els impactes d'aquest dos efluents miners en els ecosistemes aquàtics, així com la reducció d'aquests gràcies a les diferents metodologies de remediació, es van usar els biofilms com a bioindicadors en un estudi de camp i diferent experiments en microcosmos.

Els resultats obtinguts en els experiments desenvolupats durant aquesta tesi van demostrar que els efluents miners de les dues mines abandonades (Frongoch i Menteroda) tenien efectes severs en les variables funcionals i estructurals de les comunitats de biofilms. Durant el període d'exposició, a curt termini es va apreciar un canvi en les respostes funcionals (eficiència fotosintètica i captació de nutrients), mentre que els canvis estructurals es van veure al cap de mig termini. A més a més, tant els efluents miners metàl·lics com els hipersalins van promoure canvis en la taxa de creixement, la mida, la biodiversitat i la dominància de la comunitat de diatomees, afavorint el creixement de les espècies pioneres i tolerants. Aquest canvi en la composició de la comunitat va causar un augment en la tolerància de la comunitat a la contaminació per metalls i sals. No obstant, un cop eliminat l'efluent contaminant, les comunitats de biofilms exposats als dos tipus d'efluents miners van recuperar gradualment la seva funcionalitat, però no la seva estructura.

Per altra banda, les tecnologies de tractament van aconseguir elevats índex d'eliminació de metalls. No obstant això, les respostes del biofilm davant dels diferents tractaments van demostrar que la seva eficiència també depenia del factor de dilució del riu receptor. En aquest sentit, segons la resposta del biofilm, els efectes més significatius es van trobar a concentracions de Zn de fins a 1.41 mg L^{-1}. A més a més, com a mètode de tractament, també es van explorar els llindars de salinitat a partir dels quals es pot observar un impacte irreversible sobre l'estructura i el funcionament del biofilm, i, per tant, la concentració òptima que s'ha d'assolir en descarregar efluents hipersalins en els ecosistemes aquàtics. En aquest sentit, tot i que es van observar efectes estructurals en els biofilms exposats a totes les salinitats testades, només es van observar efectes significatius sobre el funcionament del biofilm en salinitats superiors a 15 g L^{-1}.

En general, els resultats d'aquesta tesi demostren la viabilitat d'utilitzar els biofilms com a bioindicador de la contaminació dels ecosistemes aquàtics i, especialment, l'ús de les variables funcionals del biofilm, essent les que van respondre més ràpidament a l'estrès i la recuperació. A més a més, durant aquest estudi, es van obtenir noves evidències dels efectes dels efluents hipersalins sobre els biofilms, no descrites fins al moment. La resposta dels biofilms va demostrar l'eficiència de les noves tecnologies de tractament per reduir els impactes dels efluents metàl·lics abandonats sobre els ecosistemes aquàtics, tot i que és necessari tenir en

compte la capacitat de dilució del riu receptor a l'hora de descarregar. Per altra banda, aquesta tesi proporciona noves evidencies que poden ajudar a determinar dels llindars de salinitat a partir dels quals els impactes sobre les els ecosistemes aquàtics poden assolir un punt de no retorn.

Index

LIST OF FIGURES

LIST OF TABLES

CHAPTER 1.

GENERAL INTRODUCTION

Photo: Frongoch mine (Wales, UK), by Life DEMINE project

1. INTRODUCTION

1.1. MINING IN EUROPE

Mining activities have been crucial for the economic and social development of Europe over the centuries (Wirth et al., 2012). Mining is the process used to extract valuable resources from the Earth, such as minerals or other geological materials that cannot be obtained through agricultural activities or created artificially. Europe is rich in natural resources, and the extraction and supply of minerals continues to play a crucial role in the European economy (Euromines, n.d). In that sense, the European Union (EU) is a major international producer of many industrial minerals like magnesite, kaolin or potash, and also produces metals like iron, chromium, copper, lead, and zinc (Cassard et al., 2015) (Figure 1.1). The EU's production of metals is about the 20% of world production, by extracting 1.7% nickel, 2% iron ore, 5% copper, 8.5% zinc and 2% bauxite of the world's production (Reichl et al., 2016). Extracted metals are used in alloys such as brass, nickel, silver, and aluminium solder, and in the manufacture of many products such as paints, rubber, pharmaceuticals, soaps, batteries, and electrical equipment (Emsley, 2011). On the other hand, the EU produced the 13% of potash of the world's production (European Commission, 2016), which is used as a fertiliser and in the manufacturing of chemicals, such as detergents, ceramics, and pharmaceuticals (Garrett, 2012).
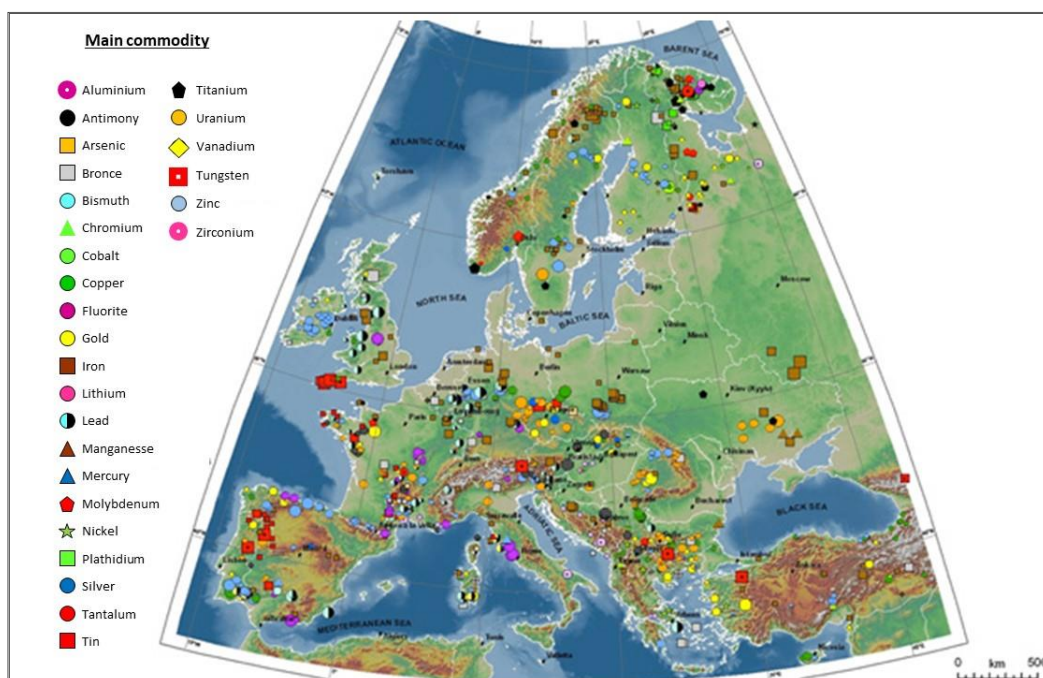
Figure 1.1: Main mineral deposits in Europe (Cassard et al., 2015).

Regarding mining activities, four main types of mining methods are currently used in Europe: underground, open surface, placer, and in-situ mining (Jain et al., 2016; Figure 1.2). a)

Underground mining consists of digging into the earth tunnels or shafts to reach buried ore deposits (Balt and Goosen, 2020); b) *Open surface mining* involves the removal of surfaces topsoil, vegetation, dirt, and, if necessary, layers of bedrock to reach buried deposits (Espinoza et al., 2013); c) *Placer mining* is a combination of different mining methods that use water to separate valuable ore from the surrounding sediments (Heikkinen et al., 2008); d) *In-situ mining extraction* involves pumping a lixiviant into the ore body via a borehole, which circulates through the porous rock dissolving the ore and is extracted via a second borehole (Society for Mining, Metallurgy, and Exploration, 2008).

Each mining step within these mining methods involves removing surfaces, topsoil, vegetation, dirt, and bedrock layers, generating different kinds of mining waste material with different physical and chemical properties (Figure 1.2). For example, in the EU the total waste generated in 2018 was 2.3 billion tons of which the 26% was generated in mining activities (Eurostat, 2018). The most abundant waste types generated during mining activities are: a) *waste rock*, which is the rock that is excavated to reach the ore and it is generally stored indefinitely in piles and heaps (Mossa and James, 2013); b) *tailings*, that are deposits of non-valuable fine-grained mineral sand obtained after separating the value minerals from the ore (Charbonnier 2001) and; c) *mining effluents*, which are generated at mining regions through 3 main processes: i) the water table elevates above the mine subsurface, ii) the water reaches the depth of an open cast mine and, iii) during the discharge of washing water throughout rock fractures, shafts, tunnels and open pits (Jain and Das 2017). Within the mining effluents, acid mine drainage (AMD) is one of the most studied pollution problems caused by mining activities (Gray, 1998; Akcil and Koldas, 2006; Motsi et al., 2009). It consists in the outflow of acidic water from metal or coal mines and is formed when pyrite (an iron sulphide) is exposed and reacts with air and water to form sulfuric acid and dissolved iron (Johnson and Hallberg 2005; Jain and Das 2017). However, other forms of mining effluents can be generated by the weathering of previously stable minerals causing the release of heavy metals and other potentially toxic solutes that contribute to the pollution of the water body in which they are released (Ermite Consortium, 2004). This type of mining effluents is less studied and is the main targeted waste of this PhD thesis.

Mining waste such as waste rocks and tailings generated during mining operation can cause severe environmental impacts on the natural water environment (Ermite Consortium, 2004) through run-off, leaching and the direct discharge (Figure 1.2). The run-off occurs during periods of heavy rainfall when more water reaches the tailings than their ability to hold the discharge and ends in the surrounding rivers and streams (Younger and Wolkersdorfer, 2004). On the

other hand, leaching occurs when water carrying soluble substances or small particles within the waste rock leak into surrounding rivers and streams (Clothier and Green, 2005). All these effluents generated from mining wastes can potentially damage the freshwater ecosystems. Therefore, this waste can become a major environmental concern in mining areas, and it must be properly managed to avoid pollution of surrounding environments, as required at European level by the Mining Waste Directive (Directive 2006/21/EC).
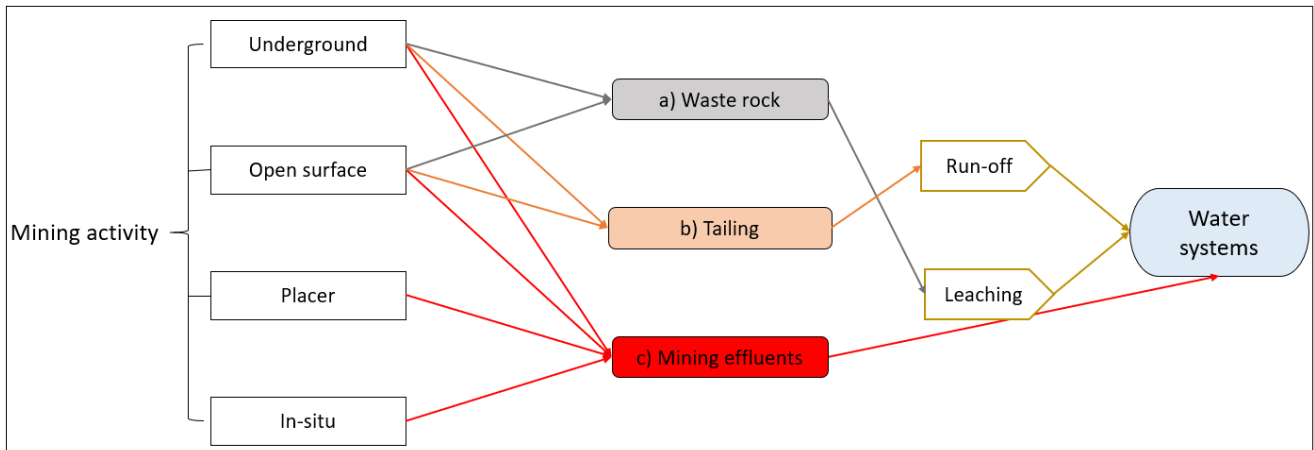
Figure 1.2: Examples of mining waste and leachate generation during the mining operation that can reach water systems. Adapted from Jain and Das (2017).

1.2.   ABANDONED MINES IN EUROPE

Nowadays, in Europe there are significantly more abandoned than operational mines (Jarvis et al., 2012). Abandoned mines are areas whereby mining activities were ceased as a result of incomplete closure or improper reclamation occurrence. Before the existence of environmental regulations, the land used for mining was commonly left without any remediation when mine extraction activities were completed. At that time, few countries had government mine regulations and reclamation programs, making it difficult to calculate the exact number of abandoned mines that we have nowadays. However, it is estimated that there could be more than one million of abandoned mines worldwide (Coelho et al., 2011).

Although these zones are abandoned, they continue to discharge toxic substances from its build-up residue causing a dangerous hazard (Issaka and Ashraf, 2021). Consequently, considerable attention is focused on addressing the environmental problems associated with these orphan sites, such as the release of the abandoned mining effluents. Abandoned mining effluents are certain to be of appreciable concern to nearby citizens, as they can affect regional water supplies, contaminate water resources and damage sensitive aquatic habitats (Jain et al., 2016). Among the abandoned mining effluents, those with high loads of metals and potash are of

special environmental concern. They consist of wastewater with a high concentration of heavy metals or salts, respectively generated due to the contact between water and various types of minerals in the piles of waste rocks and tailings or from the mine itself (Weiss et al., 2016). Additionally, the impacts caused by the presence of heavy metals and the high amounts of salts can have lasting socio-economic consequences (such as community development, service access, livelihood, land and assets impact, health and security) and can be extremely difficult and costly to address through remedial measures (Strake. 2002).

In 2019, around 100 million tons of metal ores were extracted worldwide (Eurostat, 2021). Most of the mined minerals are relatively chemically stable, although some of them (e.g. sulphide minerals such as sphalerite (ZnS), galena (PbS), chalcopyrite ($CuFeS_2$), millerite (NiS) and arsenopyrite (FeAsS), releasing both sulphate and their constituent metal ions) are especially vulnerable to weathering (i.e. breaking down of rocks and minerals) when they are exposed to the influence of atmospheric oxygen and water (Younger et al., 2004) which increases their solubility and mobilization in the environment (Kaasalainen et al., 2019).

On the other hand, the world potash production in 2018 was estimated in 37 million tons (Ober, 2016). The processing of potash ores comprises four stages: (1) potash ore is crushed and ground to release the potash minerals from the ore; (2) potash minerals are separated from unwanted salt minerals (e.g., halite) by froth-floatation; (3) the potash minerals are dried and size-graded; and finally (4) further purification takes places by dissolving the potash minerals in hot brine to remove impurities (European Commission, 2016). The unwanted salt mineral and wastes produced from potash mining operations, such as tailings dominated by sodium chloride (NaCl), are one of the world's largest chronic waste concerns (Cañedo-Argüelles et al., 2017). These mining effluents can include both cations and anions such as Na^+, K^+, Ca^{2+}, Mg^{2+}, Cl, HCO_3^-, and SO_4^{2-} that might modify the ionic matrix of the stream water (Kunz et al., 2013).

Considering all the aspects mentioned in the previous section, it can be stated that mining effluents generated during mining activities are important sources of water pollution that can arise while the mine is active but, without remediation action, they can persist long after the mining operation ceases (Younger and Wolkersdorfer, 2004). Nowadays, water pollution in Europe is mainly associated with abandoned mine sites. Indeed, so many are the catchments in which pollution from abandoned mines is the single greatest cause of freshwater pollution (Amezaga et al., 2011).
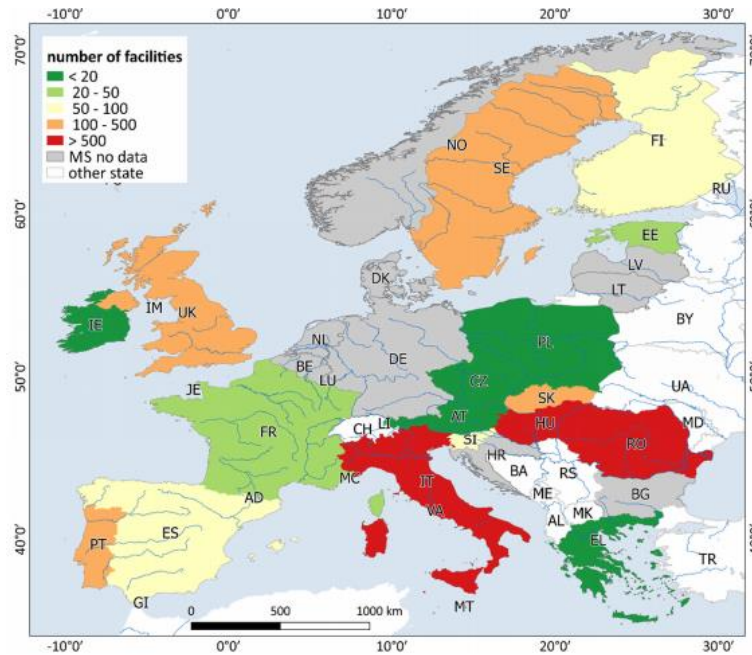
Figure 1.3: Closed or abandoned mining waste facilities in Europe (June 2017). Source: European Commission, (2017).

At European level (18 states), there are a total of 3.462 mining waste facilities, either closed or abandoned (Figure 1.3) (European Commission, 2017). A mine facility is considered closed when the mining activity is ceased and there is an identified former owner or license that have closed the mining facility following the national regulations. Abandoned mines and waste facilities, by contrast, are facilities without any identified former owner or licences and/or they have not been closed in a regular manner (European Commission, 2012). From those closed and abandoned mining facilities, 1.027 (30%) correspond to mines of metallic minerals, 3% non-metallic minerals, 2% fuels, 2% coal, 1% precious metals, 5% of mines with a combination of minerals, while the remaining 47% is still unspecified (Figure 1.4; European Commission, 2017), evidencing the scarce information currently available regarding closed and abandoned mining and waste facilities around Europe.
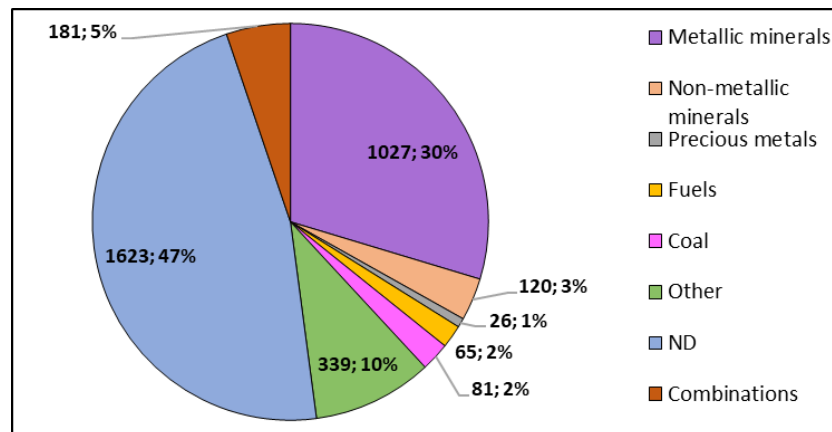
Figure 1.4: Minerals mined in closed and abandoned mining facilities in the European Union (European Commission, 2017)

In abandoned mining sites, mining effluents are discharged uncontrollably into the surrounding aquatic ecosystems without being treated (Figure 1.5). Freshwater pollution from abandoned mining effluents is particularly difficult to deal with, since it lasts for a very long time if no mine remediation is done (Kivinen, 2017). Abandoned mining effluents discharges are considered as a source of pollution which alters the quality of the receiving stream water (Johnston et al., 2008). Moreover, no-one is legally responsible for the great majority of them. According to the Water Framework Directive (WFD), each national public water administration in Europe is responsible for the good quality status of its water bodies. Although the quality of water bodies is monitored, in abandoned mining areas there is no accountability for its management, and therefore the environmental pollution remains. For that reason, there is an urgent need for management and technological solutions to deal with abandoned mines wastewaters, preventing damage to freshwater ecosystems and securing the goods and services that they provide to our societies.
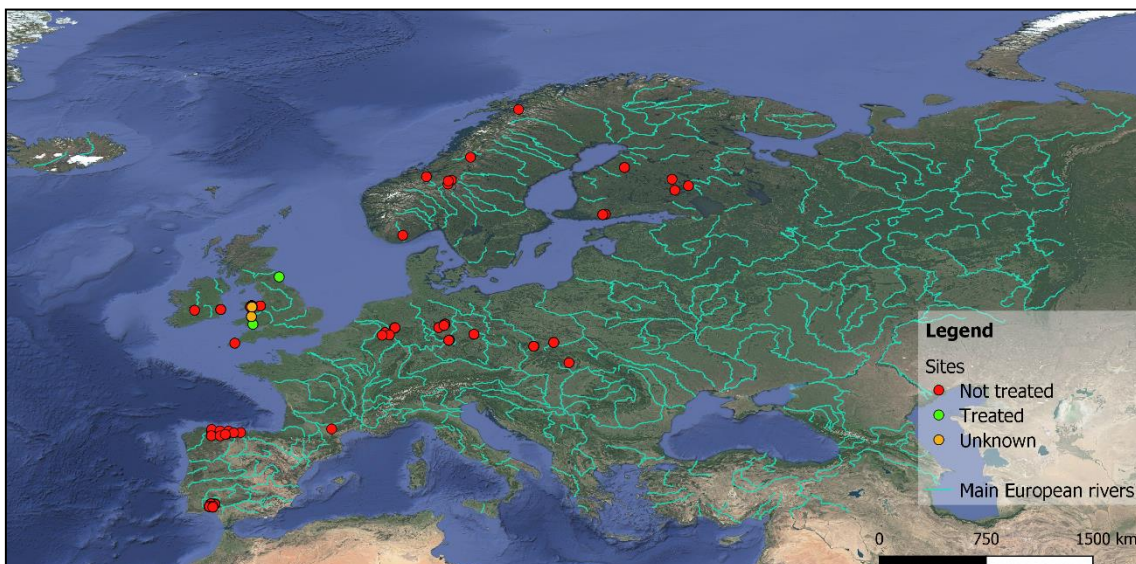
Figure 1.5: An overview of treated and untreated mining effluents from 90 different European mining sites based on the LIFE DEMINE database.

1.3. IMPACTS OF MINING EFFLUENTS ON FRESHWATER ECOSYSTEMS

The presence of those mobilised heavy metals and dissolved ions in mining effluents can be either in dissolved form or adsorbed to particles and can be transported downstream of the river, deposited, and accumulated in sediments by fluvial river processes (Jarvis and Potter, 2006).

One of the main environmental problems caused by mining effluents from abandoned mine on freshwater ecosystems is salinisation. Mining activities and the mining waste generated are

among the main sources of river salinisation in Europe (Bäthe and Coring, 2011). The stockpiles of non-profitable residues from potash extraction may contain water-soluble parts that can be washed as hypersaline effluents into adjacent water bodies during heavy precipitation events (Cañedo et al., 2014) affecting both, groundwaters and surface waters. The discharge of these hypersaline effluents into freshwater ecosystems can increase the salinity levels from 5 to 220 times in a matter of few hours or days (Johnson et al., 2010, Cañedo-Argüelles et al., 2012). The impacts caused by this increase on aquatic organisms affect the ecosystem structure and functioning (Sauer et al., 2016) and can change the ecosystem services provided by freshwater ecosystems (Cañedo-Argüelles, 2020). In these ecosystems, species richness decreases along a salinity gradient since many species do not survive when a certain salinity threshold is exceeded (Cañedo-Argüelles, Kefford, and Schäfer 2019). In fact, freshwater organisms have different sensitivities towards salinity stress, and hence it is expected that its increase alters the composition of the freshwater communities (Berger, Frör, and Schäfer 2019).

For instance, in Catalonia (Spain), potash mining represents a relevant economic activity causing high salinity levels in surrounding rivers (Figure 1.6). This is the case of Llobregat River, one of the most important rivers of the region with a length of 170 km, that suffers from salinity problems derived from potash mining activities causing changes in the macroinvertebrate community (Cañedo-Argüelles et al., 2012). The salinisation problem is also affecting Germany where the main source of this pollution is caused by dumps of abandoned potash mines causing high chloride concentration in the river system Wipper - Unstrut (North Thuringia), where the annual average concentration of chloride is around 1100 to 1300 mg L^{-1}, being the maximum observed concentration 1600 mg L^{-1} of chloride (Südharz and Sommer, 2014, Figure 1.6). Although it has been known for a long time that human activities alter the salinity and composition of ions in freshwater ecosystems (Cañedo-Argüelles, Kefford and Schäfer, 2019), this environmental issue has been hardly studied (Cañedo-Argüelles, 2020).

Figure 1.6: Sallent (Spain) salt mine waste stockpiles in Sallent (Spain) and Werra River (Germany).

On the other hand, heavy metals are among the most pollutant and dangerous wastes produced in mining activities (Fashola et al., 2016). The specific hazards posed by heavy metals harboured in mining effluents to the aquatic environment are highly dependent on metal speciation, which, in turn, determines bioavailability, toxicity (Tessier and Turner, 1995) and metal accumulation (Meylan et al., 2004). Additionally, its impact on freshwater ecosystems will be influenced by the dilution capacity of the receiving stream. The dilution effect depends on the mining effluent load, stream flow and heavy metals bioavailability (Tchounwou et al., 2012). Flow fluctuations determine the dilution capacity of the stream that can influence biogeochemical processes and surface water quality through complex interactions between hydrology and biogeochemical processes, including the production, release, and transport of natural materials and anthropogenic pollutants such as mining effluents (Park et al., 2011). The metal bioavailability could lead to its bioaccumulation and, consequently, the biomagnification of the metal throughout the trophic food web (Younger et al., 2004). Those heavy metals dissolved in water are easily absorbed by fish (through the lungs and gastrointestinal tract, and even to a certain extent by intact skin; Tchounwou et al., 2012) and other aquatic organisms such as aquatic biofilms (through metal binding sites located in either organic matrix at the surface of cells or in the organic particles trapped by the biofilm; Bere et al., 2012) that are the aquatic ecosystems' primary producers at the base of the food web (Solomon, 2008). For instance, this environmental problem caused by metal abandoned mines is common in England and Wales, where pollution from abandoned mines is a significant cause of surface watercourses' degradation (Tipping et al., 2008). Specifically, the Frongoch Mine was one of Wales' most productive lead mines during the mining renaissance of the 18th and 19th centuries (Edwards et al., 2016) (Figure 1.7) which nowadays, it is ranked as Wales' second most polluting mine, discharging annually 23 and 1.5 tons of zinc and lead (Mullinger 2004) into the Frongoch stream, which causes the failure of the water quality standards defined in the Water Framework Directive and the Water Environment (England and Wales) Regulations (DEFERA, 2014).

Figure 1.7: Frongoch (UK) abandoned metal mine impoundment and the channelling of the effluent release to the river.

In addition, very few studies have experimentally addressed the recovery of freshwater communities after the pollution reduction in streams (Lambert et al., 2012; Arini et al., 2012b; Pandey and Bergey, 2018). The recovery after exposure may be variable depending on the biological compartment assessed and the magnitude of the induced toxic response (Pandey and Bergey, 2018). For instance, diatom-dominated biofilm transferred from metal polluted to unpolluted site needed 40 to 60 days to recover according to the trophic diatom index (TDI) (Rimet et al., 2005). On the other hand, Arini et al. (2012a) observed incomplete recovery after 56 days of exposure to water free of metals. Additionally, it was reported that a decrease in the salinity changes the primary producers' community which lead to a higher primary production, supporting greater secondary production (Gutiérrez-Cánovas et al., 2009).

1.3.1. POTENTIAL SOLUTIONS TO REDUCE THE IMPACT OF ABANDONED MINING EFFLUENTS

To minimise the high environmental and ecological impacts that abandoned mining effluents are causing to water bodies, different treatment technologies exist. The conventional active methods for pollution removal from wastewaters include chemical precipitation, chemical oxidation, ion exchange, nanofiltration, reverse osmosis, electrocoagulation and electrodialysis (Tripathi and Rawat Ranjan, 2015).

Despite the existence of these technologies, the treatment of mining effluents coming from abandoned mines continues to be a major environmental problem, due to the high treatment costs and the lack of establishment actors, responsible to deal with the treatment. Currently there are different research and innovation activities aiming to study and develop new solutions to this problem. One of these activities is the LIFE DEMINE (LIFE16 ENV/ES/000218) project. LIFE DEMINE is a demonstration project funded by the European Commission that puts in practice, tests, and evaluates an innovative treatment technology at pre-industrial scale to treat abandoned mining effluents by combining membrane technologies (nanofiltration and microfiltration) and electrocoagulation. The first one, is nanofiltration which is a membrane technology and has been in use since the early 1980s. The technology uses the combination of small pore size (nanometre range, MWCO < 2000 Da) and a charged surface to selectively remove divalent cations from solution while allowing monovalent ions to permeate (Mohammad et al., 2015). As a result, this technology has found industrial application in food and beverages, wastewater treatment and drinking water production (Oatley-Radcliffe et al., 2017). The second one is microfiltration, that is a pressure-driven membrane separation process capable of removing suspended particles with sizes down to $0.1 – 0.2$ µm (organic compounds) as well as inorganic contaminants such as heavy metals (Keerthi and Balasubramanian, 2013;

Basile et al., 2015). Finally, electrocoagulation, which is essentially chemical precipitation of the metal species by formation of the metal hydroxide, in this case the hydroxyl ions are formed by splitting water at an electrode (Moussa et al., 2017). Any metal that is insoluble in hydroxyl form will then precipitate, thus removing heavy metals but allowing common salts to remain.

Apart from the possible treatment technologies, other solutions exist to minimize the impact of abandoned mining effluents on freshwater ecosystems. One of the most effective solutions used to reduce the quantity of water that requires treatment is the stream diversions. This technique is used to prevent that waste units or areas of contaminations directly reach surface waters and becoming contaminated. For instance, surface waters may be diverted to avoid contact with stockpiled waste rock; this would prevent the water from becoming acidified. Examples of run-on controls would include retaining walls, gabion dams, check dams (both permanent and temporary), and diversion ditches (Ceto and Mahmud, 2000). Another common method is the point source discharge of pollutants, which is any single identifiable source of pollution from which pollutants are discharged, such as a pipe, where emissions can easily be metered. This concept lies in assessment of the maximum pollutant load a waterbody can accept before becoming impaired and in the measurement of changes (Meals et al., 2013). For both metals and salts, these thresholds (not described for salts) will be explored throughout this thesis.

1.4. EUROPEAN FRESHWATER POLICIES AND LEGISLATION

The main legislation concerning the protection and sustainable use of freshwater resources in the European Union is the Water Framework Directive (WFD, Directive 2000/60/EC). The WFD is the most important European legislation which concerns the protection of inland surface water, groundwater, estuarine water, and coastal water. The WFD establishes an integrated approach for the monitoring and assessment of the environmental (including ecological and chemical) quality status of water bodies. The Directive's main objectives are: 1) the prevention of the deterioration of the status of all surface and groundwater bodies, and 2) the protection, improvement, and restoration of all surface and groundwater bodies to achieve an excellent ecological quality. It is mainly focused on the overall environmental quality, replacing previous water policies focused only physical and chemical status, by adopting a realistic approach that include also biological aspects to define ecological status (Howarth, 2007).

There are two status categories, ecological and chemical. The ecological status classification considers, i) the condition of biological quality elements (i.e., fish and benthic invertebrates); ii) concentrations of supporting physicochemical elements such as oxygen or ammonia; iii) concentrations of specific pollutants (e.g., copper) and iv) hydromorphology (Figure 1.8). The

biological quality elements are identified as the composition, abundance and biomass of phytoplankton, other aquatic flora, benthic invertebrates, and fish. The hydrological elements supporting the biology are given as depth variation, bed's quantity, structure and substrate, intertidal zone structure and freshwater flow.

The WFD, by the Directive 2008/105/EC defines the chemical status by two types of chemical substances that need to be monitored, and thresholds above which damage to the aquatic ecosystem may be incurred (Environmental Quality Standards or EQS): 1) *Priority Hazardous Substances*, that are those chemicals with high toxicity potential on aquatic ecosystems and include hydrocarbons, pesticides and some metals (i.e. lead) , and 2) *Specific pollutants,* which are substances that can be harmful to ecological communities and may be identified by member states as being discharged to water bodies in "significant quantities", including cyanides, arsenic and other metals. The EQS determine threshold below which it is not expected adverse effects to occur.

Considering this chemical, ecological and morphological aspects of the surface water body its status is classified in 5 levels (high, good, moderate, poor, and bad) (Figure 1.8).
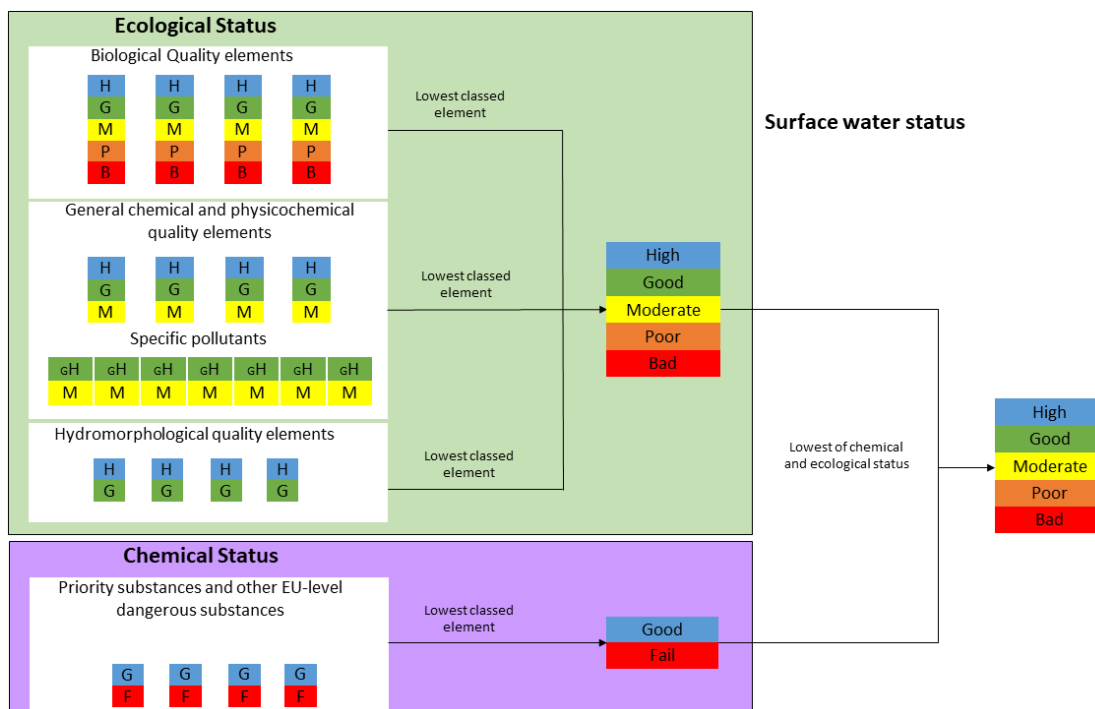
Figure 1.8: Classification scheme of surface water status; H: high status, G: good status, M: moderate status, P: poor status, B: bad status. Adapted from Ternjej and Mihaljevic (2017).

Even though in the WFD it is well described how to assess the chemical and hydromorphological characteristics, it does not specify which indices or metrics should be used to assess the biological quality status (Hering et al., 2010). In fact, this decision was left to the EU Member

States and, consequently, there are many different biological methods used around Europe that connote different patterns among methods assessing the same quality elements or water categories (Brik et al., 2012). Some of the most used biological methods to monitor the ecological status of water bodies are based on benthic invertebrates or diatoms (Hering et al., 2006; Torrisi et al., 2010). The ecological information given by these organisms are used to detect changes in natural surroundings as well as to indicate negative or positive impacts (Parmar et al., 2016).

1.5. AQUATIC BIOFILM AS A MONITORING TOOL

Aquatic biofilm are microbial communities made up of autotrophic (green algae, diatoms, and cyanobacteria) and heterotrophic (bacteria, fungi, and protozoa) organisms located in close physical contact, embedded in an exopolysaccharide matrix (EPS), and adhered on different solid substrates (e.g., sand, cobbles, wood) in contact with water (Sabater et al., 2007) (Figure 1.9). They are primary producers located at the base of the freshwater trophic food chain (Vannote et al., 1980). Moreover, aquatic biofilm communities fulfil other essential tasks relevant at ecosystem level such as the interception of dissolved and particulate matter from the water column that contributes to the nutrient cycle and the self-depuration capacity of river systems (Bunn et al., 2010, Kupilas et al., 2016, Lepori et al., 2005).
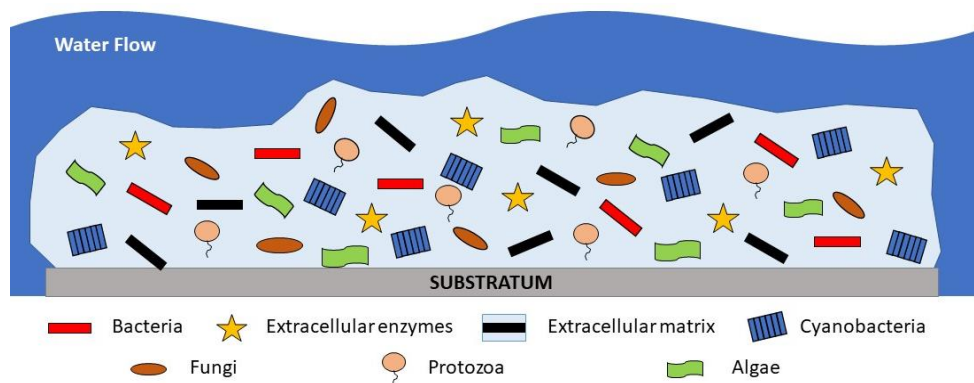
Figure 1.9: Scheme of the freshwater biofilm community structure. Adapted from Romaní et al (2010).

Aquatic biofilms are commonly used in ecotoxicology since the quantification of the effects of pollution on different biofilm components, allows evaluating direct effects of pollutants on the most sensitive community (e.g., algae and bacteria) and their indirect effects on the rest of biofilm components and on higher trophic levels because all of them are closely related through biological interactions (Guasch et al., 2016). These properties give these communities the capacity to integrate the effects of environmental conditions and the opportunity to evaluate the effects of toxic exposure over extended periods (Guasch et al., 2003; Sabater et al., 2007;

Bonet et al., 2013). Consequently, biofilms have been defined as powerful ecosystem health indicators (Larson and Passy, 2005). Ecotoxicological experiments with biofilm have been used to investigate the direct and indirect effect of contaminants under microcosms or mesocosms conditions (Gold et al., 2003; Morin et al., 2007; Bonnineau et al., 2011; Bonet et al., 2012; Corcoll et al., 2012; Cañedo et al., 2012 and 2016) as well as in field experiments (Guasch et al., 2003; Tlili et al., 2011; Corcoll et al., 2012; Bonet et al., 2014).

Among the most toxic substances for aquatic ecosystems are heavy metals. Heavy metals may be stored in aquatic ecosystems or seep into the water table, which leads to contamination of underground water courses (Johnson and Hallberg, 2005; Ermite Consortium et al., 2004). Metal pollution could lead to a variety of biofilm responses including structural and functional changes with different ecological implications. For example, kinetics of algal growth, photosynthetic activity, chlorophyll- a concentration, nutrient uptake capacity and community composition may be altered in response to chemical stressors (Corcoll et al., 2011; Proia et al., 2017), as the ones harboured in mining effluents. Specifically, metal exposure can produce metabolic and functional alterations on the biofilm and, after long-term exposures, when the accumulation of increases, it causes structural changes (Morin et al., 2012; Guasch et al., 2012; Wu, 2016). These effects might persist when effluents are no longer polluted, causing accumulated effects that delay the ecosystem's recovery capacity (Arini et al., 2012). Although the effects are widely recognized, very few studies have experimentally addressed the recovery (Morin et al., 2010; Corcoll et al., 2012; Morin et al., 2012b; Lambert et al., 2012; Arini et al., 2012b; Pandey and Bergey, 2018). The velocity of recovery following metal exposures varies (Steinman and Mcintire, 1990). For instance, diatom-dominated biofilm transferred from polluted to unpolluted site needed 40 to 60 days of recovery (Rimet et al., 2005). On the other hand, Arini et al. (2012a) reported incomplete recovery after 56 days of exposure to water free of metals.

On the other hand, little is known about the consequences of extreme salinities on the biofilm functioning and whether and to what extent changes in the species community structure can affect the biofilm functionality. Freshwater salinisation has an impact on freshwater communities, including biofilm communities (Cañedo-Argüelles et al., 2017). Freshwater organisms only tolerate specific salinity ranges, and at high salt concentrations, it becomes toxic to many of them (Hintz and Relyea, 2017; Olson and Hawkins, 2017; Velasco et al., 2019). Nevertheless, salinity's toxic effects depend on the ionic composition of the salinisation sources (Sala et al., 2016). The most studied form of salt pollution is NaCl, but other salt compounds, including different combinations of Ca, Mg, Na, K, sulphate (SO_4^{2-}), chloride (Cl^-), and bicarbonate (HCO_3^-), as well as other ions (Kunz et al., 2013), can also contribute to freshwater

salinisation (Kaushal et al., 2018). Nevertheless, there is still much uncertainty about the effects of salinisation on ecosystem functioning, and specifically on important ecosystem functions performed by freshwater biofilm, such as nutrient uptake or microbial respiration, and photosynthetic efficiency (Cañedo-Arguelles et al., 2013; 2017). Previous studies reported effects of salinity on algal biomass and chlorophyll-a concentration (Silva et al., 2000; Ros et al., 2009; Rotter et al., 2013), as well as drastic reductions in macroinvertebrate and biofilm abundance and surviving taxa (Cañedo-Argüelles et al., 2012; Dunlop et al., 2008 and Kefford et al., 2011) under salinities between 4 and 10 g L^{-1}. However, few studies have examined salinity tolerance thresholds on biofilm communities (Cañedo-Arguelles et al., 2017; Bonada et al., 2004) or the biofilm community's recovery capacity after the stressor disappearance, which can cause shifts in biofilm communities in both structure and function due to developed tolerances (Gutiérrez-Cánovas et al., 2009)

The ecotoxicological response of biofilm can be affected by some physicochemical and biological factors (Bonet 2013). Different sensitivities to toxicants have been found depending on the biofilm community's age and succession status (Ivorra et al., 2000). Moreover, environmental factors, such as temperature, discharge light intensity, or nutrients, can influence biofilm sensitivity to toxicants (Guasch and Sabater 1998; Navarro et al., 2008; Villeneuve et al., 2010; Tlili et al., 2010). Therefore, environmental parameters play a double role concerning biofilm: as stressors and as modifiers of toxic effects (Bonnineau et al., 2011).

Biofilm composition tests are potentially more trustworthy tools to indicate aquatic ecological status than some tests proposed by the WFD. They are pertinent indicators of ecosystem health since their omnipresence, important role in primary production, nutrient fluxes and trophic cascades and their sensitivity to organic and inorganic pollutants (Guasch et al., 2003; Sabater and Admiraal 2005; and Sabater et al., 2007). Due to its complexity and structure, freshwater biofilms can be considered as micro-ecosystems with different levels of biological organization. As a result, multiple biomarkers have been developed to assess both function (such as photosynthetic efficiency, extracellular enzymes peptidase and glucosidase) and structure (diatom community composition) of the different biofilm components integrating the whole biofilm response (Bonnineau et al., 2011; Ylla et al., 2011). Additionally, most of these biomarkers focused on functions directly linked with essential processes for the whole aquatic ecosystem (i.e., primary production) (Bonnineau et al., 2012). Biofilm tests range from simple chemical measurements (i.e., pigment content) to detailed analysis (i.e., phospholipids fatty acids, respiration, photosynthesis, determination of species composition, or microbial community DNA profiling) (Vinten et al., 2011). By contrast, the trophic diatom index (TDI),

which is one of the established methods by the WFD, is time-consuming and only considers one component of the biofilm community. For that reason, it is necessary to explore the utility of a range of potential microbial community tests to better characterize the use of benthic biofilm as an indicator of stream ecological status.

Overall, given the biofilm potential to become a powerful tool to monitor and assess the aquatic ecological status, it could be used to test the efficiency of different treatment technologies to reduce the ecological impacts caused by water pollutants such as mining effluents. In this regard, this thesis will test biofilm communities as a tool to detect the impacts caused by mining effluents but also the efficiency of these biofilm to assess whether different treatment methods can reduce these impacts.

CHAPTER 2.

OBJECTIVES AND HYPOTHESIS

Photo: Nant Cell River (Wales, UK), by the author

2. OBJECTIVES AND HYPOTHESIS

2.1. MAIN OBJECTIVES

The main objective of this PhD thesis is to evaluate the ecological impact caused by abandoned mining effluents and determine the reduction of their effects (by using different treatment technologies and dilutions) on freshwater ecosystems using biofilm communities as a bioindicator.

To reach this main objective, the following specific objectives have been defined:

1. To assess the ecological status of a heavy metal polluted stream by comparing the Water Framework Directive methodologies with biofilm community responses.

   CHAPTER 4: Assessment of the ecological status of a river affected by a metal mining effluent from an abandoned mine using the biofilm as bioindicator.

2. To investigate the ecological impact caused by untreated abandoned metal mining effluent in freshwater bodies and the efficiency of treatment technologies based on electrocoagulation and membrane processes in reducing this impact.

   CHAPTER 5: Assessing the effects of metal mining effluents on freshwater ecosystems using biofilm as an ecological indicator: Comparison between nanofiltration and nanofiltration with electrocoagulation treatment technologies.

   CHAPTER 6: Responses and recovery of freshwater biofilms receiving treated and untreated metal mining effluents under different river dilution scenarios.

3. To assess the ecological impact of a salinity gradient to freshwater biofilm communities to establish a salinity threshold from which aquatic organisms might be permanently affected.

   CHAPTER 7: Effects of a hypersaline effluent from an abandoned potash mine on freshwater biofilm and diatom communities.

   CHAPTER 8: Effects of a hypersalinity gradient on biofilm communities structure and functioning: a microcosm approach.

4. To assess the biofilm community ability to recover after a mid-term exposure to metal (Chapter 6) and hypersaline mining effluents (Chapter 8).

5. To evaluate the use of aquatic biofilm as freshwater bioindicator of metal (CHAPTER 4, 5 and 6) and hypersaline pollution (CHAPTER 7 and 8).

2.2. GENERAL HYPOTHESIS

Based on the current knowledge about the abandoned mining effluents effects on freshwater ecosystems and biofilm community response, the following hypotheses had been formulated:

1. Metal mining effluents would cause functional alterations on the biofilm after short-term exposure and, after mid-term exposures, cause structural changes.

2. Hypersaline mining effluents would severely affect the functionality and structure of aquatic biofilm, but these effects would change depending on the salinity concentration.

3. Biofilm exposed to both metal and hypersaline mining effluents will be able to recover their functions and structure whit the transition from the impacted to the non-impacted scenario.

4. Treated metal mining effluent would reduce the ecological impacts to freshwater ecosystems, but the level of the reduction will depend on the dilution capacity of the river.

5. Diluted hypersaline mining effluents would reduce the ecological impacts caused by this mining effluents to freshwater ecosystems.

6. Biofilm communities could be a useful bioindicator tool to assess the efficiency of different treatment technologies in reducing the ecological impacts of mining effluents into freshwaters.

CHAPTER 3.

MATERIALS AND METHODS

Photo: Experimental set-up, by the author
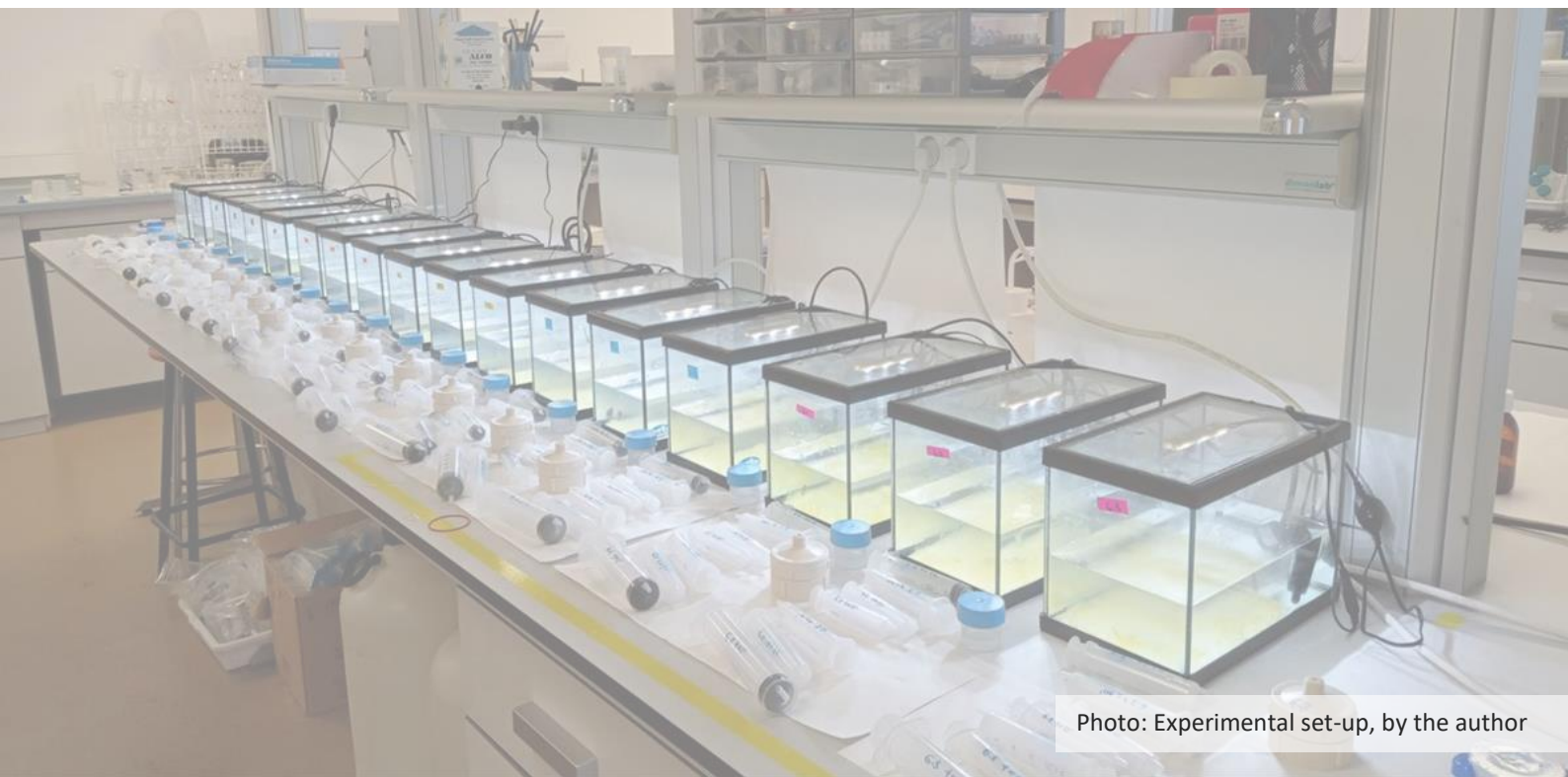
3. MATERIALS AND METHODS

In this chapter the methodologies applied in this thesis are described. In the first section (3.1) it is explained the different experimental approaches and mining effluents used throughout the thesis. In the second section (3.2), it is provided a detailed description of the procedures used for the water samples analysis, and in the third section (3.3), the methodology related to the biofilm analysis is detailed.

3.1. EXPERIMENTAL APPROACH

To achieve the objectives of this thesis, different experimental approaches have been applied. A field study (with high ecological realism; Chapter 4) and microcosms experiments (high control conditions) in aquariums (Chapter 5 and 7) or artificial streams (Chapter 6 and 8) have been performed to assess the impact of abandoned mining effluents on freshwater ecosystems (Figure 3.1). Small scale laboratory experiments in microcosms, where biofilm communities are exposed to different environmental conditions, have lower ecological relevance but are easily replicated and provide tight control over experimental variables. Artificial streams are smaller and less complex than real-world systems but offer the opportunity to develop ecosystem-level research in replicated test systems under controlled conditions having greater ecological relevance (Roussel et al., 2007). The use of microcosms or artificial streams in which biofilm communities can develop may fulfil the necessary settlement between simplification and standardization of the natural system and required replicability and repeatability (Sabater et al., 2007). This system is specially appropriated in ecotoxicological studies, given the impossibility of experimentally releasing toxicants to the natural environment. Finally, field experiments allow to evaluate *in situ* the effects of the abandoned metal mining effluent to the stream and freshwater communities with higher realism and greater ecological relevance (Serra, 2009).
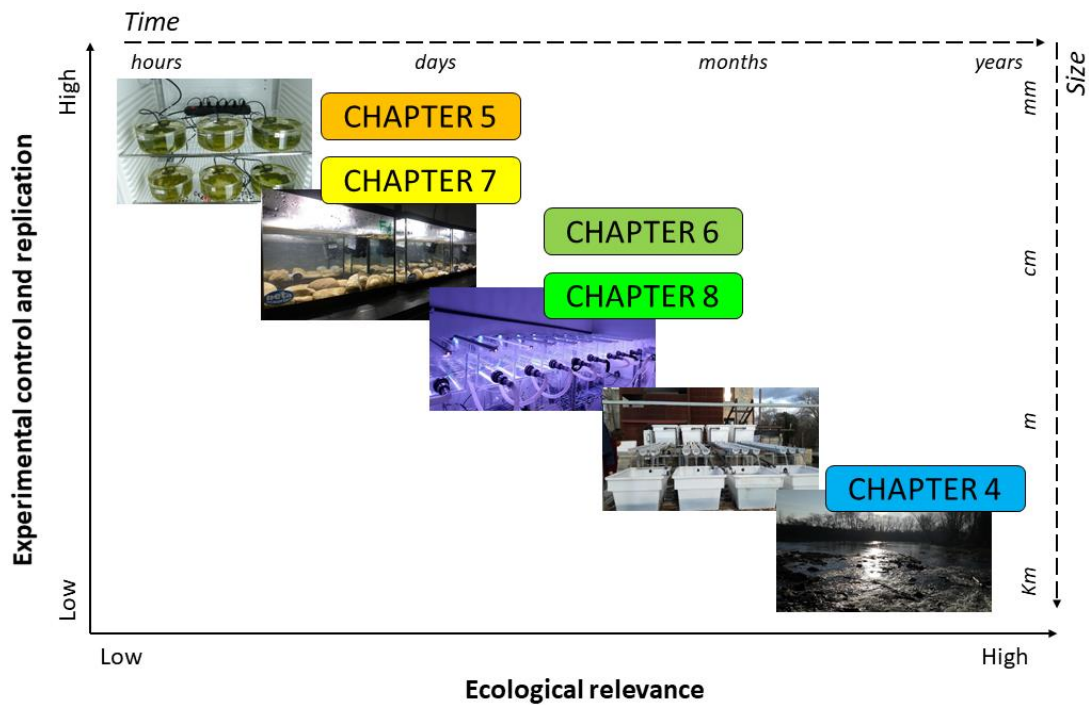
Figure 3.1: Experimental approach of this Thesis, adapted from Clements and Newman (2002).

3.1.1. MICROCOSMS

In this thesis two different microcosms set-ups have been used to assess the short (24h) and mid-term (14 and 21 days) ecological impacts of abandoned metal mining effluents: aquariums and artificial streams.

In this thesis the microcosms system used in Chapter 5 and 7 consisted of a set of 6L glass aquariums of size 26 × 15 × 17 cm (length × width × height) placed in a chamber under controlled temperature and light conditions. Each aquarium had a submersible pump (EDEN 105, Eden Water Paradise, Italy) to promote water recirculation and a LED light (LENB 135-lm, LENB/14.97/11.98) to control the photoperiod based on the experimental requirements (Figure 3.2).

Figure 3.2: Set of aquariums used as microcosms in this thesis (Chapter 5 and 7).

Each microcosm contained 15 previously scraped and autoclaved stream cobbles that were used as substrata for natural in situ biofilm colonization. To promote biofilm colonisation, 15 mL of natural biofilm suspension obtained by scraping cobbles collected from Viladrau pristine and forested stream (Natural Park of Montseny, Spain) were inoculated in each microcosm. Each microcosm was filled with 3 L of artificial water providing a deep column height of 10 cm. Artificial water was prepared to mimic a pristine stream as described in Ylla et al. (2009). The artificial water was obtained by dissolving pure salts in distilled water creating a chemical composition of 0.75 mg N L^{-1}, 0.10 mg P L^{-1}, 15.83 mg Na^+ L^{-1}, 8.17 mg Ca^{2+} L^{-1}, 0.52 mg K^+ L^{-1}, 0.19 mg Mg^{+2} L^{-1}, 8.89 mg SO_4^{2-} L^{-1}, 10.71 mg SiO_3^{2-} L^{-1}, 14.94 mg Cl^{2-} L^{-1} and 14.52 mg HCO_3^- L^{-1}.

The artificial streams systems used in Chapter 6 and 8 was confirmed by a set of methacrylate canals of size 50 x 12 x 10 cm (length × width × height) (Figure 3.3, a) placed in a chamber under controlled light and temperature conditions. Each stream unit was designed to maintain the water column height at 2 cm. Water input at the head of the first channel unit was provided by a 5 L carboy using a pump (EDEN 105, Eden Water Paradise, Italy) connected with silicone tubes. The system was supplied by artificial water made up following Ylla et al. (2009). Light emitting diodes (LEDs 135-lm, LENB/14.97/11.98) were used to provide the desired photoperiod (Figure 3.3 b). The bottom of each channel was covered with a sandblasted glass substratum of three different sizes (1, 3 and 200 cm^2) used as artificial substrata. Biofilm colonisation and growth

were promoted at each artificial stream by adding, 50 mL of natural biofilm suspension obtained by scraping cobbles collected from Viladrau stream (Natural Park of Montseny, Spain).
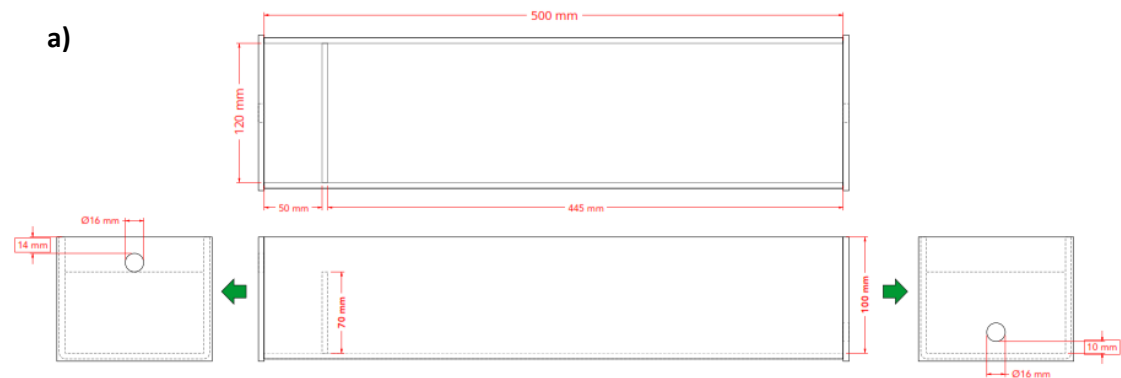
Figure 3.3: Artifical streams: a) scheme of the artificial streams. b) artificial streams placed in the chamber under controlled conditions.

3.1.2. MINING EFFLUENTS

In this thesis, two different effluents from two different abandoned mining sites were used directly as a reference of polluted effluent. The first mining effluent was from Frongoch abandoned mine (Wales, UK; Figure 3.4) and was directly studied in the field (Chapter 4) and used in microcosms experiments (Chapter 5 and 6). The second one, was a real hypersaline mining effluent from Menteroda (Germany; Figure 3.3) was directly used in aquarium (Chapter 7) and re-created (Chapter 8) in artificial streams experiments.

The Frongoch abandoned metal mine is located near the village of Pont-rhyd-y-groes, Ceredigion (UK) and covers approximately 11ha. The mine was exploited for lead (Pb) and zinc (Zn) for almost 200 years until the early 1900s (Figure 3.4). Frongoch mining effluent discharges into the Afon Ysywyth catchment and it is characterized by a high metal content with a specific

composition of 6.91 mg Pb L^{-1}, 0.55 mg Cd L^{-1} and 76.07 mg Zn L^{-1}, 0.79 mg L^{-1} of dissolved inorganic nitrogen (DIN), 0.03 mg L^{-1} of phosphate (PO_4^{3-}), 13.56 mg L^{-1} of sulphate (SO_4^{2-}), pH of 6.91 and alkalinity of 12.13 mg L^{-1} on historical average (from 1975 to 2015).

Figure 3.4: Frongoch (UK) abandoned mine site and its effluent (Source: Life DEMINE project).

Menteroda (Germany) is an abandoned potash mine, which stored the wastes of the potash extraction in a large dump next to the mine (Figure 3.5). The leaching waters from the dump are currently stored in a reservoir from which they can reach the surface waters by flowing through embankments or through the base of the tailing pile. This mining effluent is characterized by an extreme salinity, as evidenced by the high concentrations of dissolved inorganic ions: 78 200 mg Na^+ L^{-1}, 6 700 mg K^+ L^{-1}, 117 000 mg Cl^- L^{-1} and 1 210 mg Mg^{2+} L^{-1}.

Figure 3.5: Menteroda abandoned mining site, with the hypersaline water collection and the abandoned potash wastes. (Source: Life DEMINE project)

3.2. WATER PHYSICOCHEMICAL ANALYSIS

3.2.1. PH, ELECTRICAL CONDUCTIVITY, TEMPERATURE AND DISSOLVED OXYGEN

Dissolved oxygen concentration and saturation, temperature, pH and conductivity (YSI professional plus, YSI Incorporated, USA), were measured directly at each microcosm at each water renewal or *in situ* in the river with sensor probes. The probes were calibrated every day using commercial tampons of 4, 7 and 10 for the pH, and a buffer of 1413 μS cm^{-1} for the conductivity. The oxygen was calibrated in the probe cover after being cleaned with distilled water. When the probes were calibrated, they were introduced into the water and all measures were taken when all the parameters stabilized. Probes were rinsed with distilled water after each use between different microcosm and river sites.

3.2.2. NUTRIENT CONTENT

3.2.2.1. SOLUBLE REACTIVE PHOSPHOROUS (SRP)

A colorimetric technique described by Murphy and Riley (1962) was used to determine the soluble reactive phosphorous (SRP) concentration. 10 mL of each water sample were collected and filtered through a 0.22 μm pore diameter glass microfiber filter (Prat Dumas Filter Paper, Couze-St-Front, France). Then 1 mL of mixed reagent was added to each water sample and mixed, placed in the dark for 4 hours and subsequently measured using a spectrophotometer (A3-50S17R-U R01101900571) at 890 nm.

To create the mixed reagent a mix of four different reagents were combined:

-   Ammonium molybdate: 11.2 g of tetrahydrate ammonium molybdate [$(NH_4)_6Mo_7O_{24} \cdot 4H_2O$] was weighted and dissolved in 500 mL of milliQ water.
-   Sulfuric acid: 900mL of milliQ water were placed in a 1L flask and 140 mL of H_2SO_4 were added.
-   Ascorbic acid: 27 g of ascorbic acid were dissolved in 500 mL of milliQ water.
-   Antimony potassium tartrate: 0.34 g of antimony potassium tartrate ($C_4H_4O_7SbK$) were dissolved in 250 mL of milliQ water.

All the reagents were stored in the dark in the refrigerator. Because the mixed reagent is not stable, it was prepared every analysis day.

For the calibration curve, a phosphate stock solution of 1000 mg L^{-1} of $PO_4 - P$ (S1) was prepared by weighting and dissolving in 1L milliQ water 1.3609 g of potassium phosphate diacid KH_2PO_4. Then, intermediate solutions of 10 and 1 mg L^{-1} (S2 and S3, respectively) were prepared from the stock solution. The calibration curve was prepared using the intermediate solutions as described in Table 3.1.

Table 3.1: Volume in mL of each intermediate solution and milliQ water to obtain the different concentrations of the calibration curve.

Standard (mg L^{-1})	0	0.1	0.2	0.5	1	2	5	10
S2 (mL)						0.2	0.5	1
S3 (mL)	0	0.1	0.2	0.5	1			
milliQ (mL)	10	9.9	9.8	9.5	9	9.8	9.5	9

3.2.2.2. AMMONIUM

Two different methods were used to analyse ammonium (NH_4^+) in water samples, the first method was used for freshwater samples, and the second one to analyse the samples with high salinities.

For the ammonium determination of freshwater samples, a colorimetric test described by Reardon et al., (1966) was performed. 10 mL of each water sample were collected and filtered through a 0.22 µm pore diameter glass microfiber filter (Prat Dumas Filter Paper, Couze-St-Front, France). On each sample, 1 mL of both reagents 1 and 2 (see below) were added and mixed, placed in the dark for 4 hours and subsequently measured using a spectrophotometer (A3-50S17R-U R01101900571) at 690 nm.

The preparation of the reagents used for ammonium determination was done by weighting the following reagents:

- Reagent 1: 8.5 g of sodium salicylate, 10 g of sodium citrate and 0.1 g of sodium nitroprusside, dissolved in 250 mL of milliQ water.
- Reagent 2: 5 g of sodium hydroxide and 0.4 g of sodium dichloroisociaturate, dissolved in 500 mL of milliQ water.

Besides, for the calibration curve, intermediate solutions of 10 and 1 mg L^{-1} (S2 and S3 respectively) were obtained from a commercial ammonium stock solution of 1 mg L^{-1} (PanReac - AppliChem). Using these intermediate solutions, the calibration curve was prepared as indicated in Table 3.2.

Table 3.2: Volumes of the intermediate solutions to obtain the different concentrations of ammonium within the calibration curve.

Standard (mg L^{-1})	0	0.02	0.04	0.05	0.1	0.2	0.4	0.5	0.8	1	2
S2 (mL)										1	2
S3 (mL)	0	0.2	0.4	0.5	1	2	4	5	8		
milliQ (mL)	10	9.8	9.6	9.5	9	8	6	5	2	9	8

To determine the ammonium concentration on saline samples, a colorimetric test described by Kanda (1995) for saline waters was used. For this determination, 5 mL of each water sample were filtered through a 0.22 µm pore diameter glass microfiber filter (Prat Dumas Filter Paper, Couze-St-Front, France). Different reagents were used and prepared as follows:

- Reagent 1: trisodium citrate dihydrate (400 g) was dissolved in milliQ water and the final volume was made up to 1000 mL.

- Reagent 2: sodium hydroxide (2 g) and 4 g of o-phenylphenol was dissolved in milliQ water successively, and the final volume was made up to 100 mL.

- Reagent 3: the commercial solution of sodium hypochlorite (4 mL) was diluted with deionized water and the final volume was made up to 100 mL.

- Reagent 4: sodium nitroprusside (0.05 g) was added to 100 mL of sodium hydroxide solution (120 g L^{-1}).

To each 5 mL of filtered water sample, 1 mL of Reagent (1), 0.1 mL of (2), and 0.05 mL of (3) were added successively. The test tube was swirled between each addition of reagent. Between 2 and 5 min after the addition of Reagent (3), 0.1 mL of Reagent (4) was added and swirled. The tubes were placed in a water bath of 40°C for 15 min, and absorbance was measured at 670 nm using a spectrophotometer (A3-50S17R-U R01101900571).

Additionally, a calibration curve was prepared as described in Table 3.2 using the solutions S2 and S3. An example of the calibration curve is shown in.

3.2.2.3. NITRATE

The nitrate concentration was determined as described in APHA (1992b). 45 mL of water sample of each treatment was collected and filtered through a 0.22 µm pore diameter glass microfiber filter (Prat Dumas Filter Paper, Couze-St-Front, France). To each sample, 1 mL of HCl (37.5 g L^{-1}), was added and mixed, then the sample was measured using a spectrophotometer (A3-50S17R-U R01101900571) at 220 and 275 nm.

For the calibration curve, a commercial stock solution of 1 mg L^{-1} of nitrate (PanReac − AppliChem) were used to create the intermediate solutions of 100 and 10 mg L^{-1} (S2 and S3 respectively). Using these intermediate solutions, the calibration curve was prepared as described in Table 3.3.

Table 3.3: Volumes of the intermediate solution to obtain the different nitrate concentrations within the calibration curve.

Standard (mg L^{-1})	0	1	2	4	6	10	15	18
S2 (mL)				1.8	2.7	4.5	6.7	8.1
S3 (mL)		4.5	9					
milliQ (mL)	45.0	40.5	36.0	43.2	42.3	40.5	38.3	36.9

After measuring the absorbance, the final absorbance was obtained as indicated in the following equation:

$$\text{Final absorbance} = \text{Abs.}\,220\text{nm} - 2 \cdot \text{Abs.}\,275\text{nm} \quad [\text{Eq 1}]$$

3.2.2.4. NITRITE

Nitrite concentration was determined as described in APHA (1992a). 45 mL of water sample of each treatment was collected and filtered through a 0.22 µm pore diameter glass microfiber filter (Prat Dumas Filter Paper, Couze-St-Front, France). To each sample, 2 mL of color reagent was added and mixed. After 10 minutes the sample was measured using a spectrophotometer (A3-50S17R-U R01101900571) at 543 nm.

The color reagent was prepared by mixing 100 mL of 85% phosphoric acid and 10 g of sulfanilamide in 800 mL of milliQ water. When dissolved, 1 g of N-(1-naphthyl) ethylenediamine dihydrochloride was added and completed up to 1 L.

For the calibration curve, the intermediate solutions were prepared by using a nitrite commercial stock solution of 1 g L^{-1} (PanReact − AppliChem). From the stock solution, the intermediate solutions of 100 and 10 m g L^{-1} (S2 and S3 respectively) were prepared. The calibration curve was made as indicated in Table 3.4, and show an example of this curve.

Table 3.4: Volumes of the intermediate solutions to obtain the nitrite calibration curve.

Standard (m g L^{-1})	0	0.1	0.2	0.4	0.6	0.8	1
S3 (mL)		0.5	0.9	1.8	2.7	3.6	4.5
milliQ (mL)	45.0	44.5	44.1	43.2	42.3	41.4	40.5

3.2.3. METALS ANALYSIS: MICROWAVE PLASMA ATOMIC EMISSION SPECTROSCOPY

Water samples were filtered through a 0.22 µm pore diameter glass microfiber filter (Prat Dumas Filter Paper, Couze-St-Front, France) to analyse metal concentrations in water (Chapter 4) using a Microwave Plasma Atomic Emission Spectroscopy (MP-AES model 240/280, Agilent technologies, UK). Specifically, concentrations of Zinc (Zn), Lead (Pb) and Cadmium (Cd) were analysed using the corresponding lamps.

Three different standard concentrations were used for the different elements depending on their absorbance graph. The standards were of 100 mg Zn L^{-1} (PanReac - Applichem), 1000 mg Pb L^{-1} (PanReac - Applichem) and 1000 mg Cd L^{-1}(PanReac - Applichem). Samples with concentrations that exceeded those of the standards were diluted to fit within the calibration rank. The quantification limits were 0.04, 0.1 and 0.02 mg L^{-1} for the Zn, Pb and Cd, respectively. Moreover, the detection limits for Zn, Pb and Cd were 0.012, 0.03 and 0.006 mg L^{-1}, respectively. The instrument was controlled using the SpectrAA software, version 5.3 PRO.

3.2.4. CHLORIDE ANALYSIS

The chloride content of the water samples from the experiments done with hypersaline effluents (Chapter 8), was determined by ionic chromatography (Dionex Integrion HPI System - Thermo Fisher Scientific) following the protocol established by Gómez-Ordóñez et al. (2010).

A commercial standard anion solution of 1000 mg L^{-1} of Cl^- for ionic chromatography (Fisher Chemical) with a purity of 99.8%, was used to obtain the calibration curve. This standard was diluted in milliQ water to obtain the desired concentrations that ranged from 0.01 to 100 mg L^{-1}. 10 mL of water samples were filtered through 0.22 $µL^{-1}$ pore diameter glass microfiber filter (Prat Dumas Filter Paper, Couze-St-Front, France), diluted, and measured by triplicate. In between the samples, a known standard of 2.5 and 25 mg L^{-1} of Cl^- were measured as quality check.

The instrument was controlled using the Chromeleon CDS software, version 7.2 and was attached to an Advanced Sample Processor with an injection Valve Unit with a 500 µL sample loop. The equipment was also equipped with a Pump, an Eluent Degasser and a Liquid Handling Unit that required a minimal volume of 10 µL for the samples. Detection was performed with a Conductivity Detector. Separation was performed in a 5.1 x 5.5 x 8.4 cm 4 µm particle size column (CR-ATC 500). All measurements were carried out at 35°C (column temperature) under the following eluent conditions: 976.5 µg L^{-1} potassium hydroxide at 1 mL min^{-1} as mobile phase.

Under the working conditions the anion was separated completely, and total analysis was 16 min 26 seconds. Cl- in samples were identified by the coincidence of their retention times with those of commercial standard anion. Peak areas were used for quantitative analysis.

3.3. BIOFILM SAMPLING AND ANALYSIS

Biofilm parameters were measured directly on the cobbles (Chapter 4, 5 and 7) and the artificial substrata (Chapter 6 and 8) to measure the photosynthetic efficiency and the community composition, then were scrapped, and suspended in a known water volume to analyse the chlorophyll-*a*, ash free dry mass, metal accumulation in biofilm, diatom metrics and microbial respiration. The area of the cobbles was measured by placing aluminum foil over the scratched surface and drawing the area of the stone and recalculating depending on the foil weight (Graham et al., 1988).

3.3.1. PHOTOTROPHIC COMMUNITY COMPOSITION

The phototrophic community composition was measured *in situ* using the BenthoTorch portable fluorimeter probe (bbe Moldaenke, Schwentinenta, DK). The fluorescence excitation is undertaken by seven diodes (LEDs) that emitted light at three wavelengths to detect cyanobacteria, green algae, and diatoms (470, 525 and 610 nm, respectively). An additional LED of 700nm is used to compensate the effects of background reflection. The BenthoTorch measures the resulting fluorescence of Chlorophyll-*a* emitted at 680nm. The calculation of the respective biomass of the photosynthetic groups is via algorithm based on the fluorescence response to all different excitation wavelengths. The calculation algorithms are based on characteristic spectral fingerprints (fluorescence spectral signature) for each photosynthetic group. It was used for a real-time measuring of the main photosynthetic groups' densities (diatom, cyanobacteria, and green algae) of biofilm communities.

Measurements were done directly covering the colonized cobble with the probe outside the microcosm, to determine the concentration of the main photosynthetic groups in µg chl-*a*/cm^2 (Echenique-Subiabre et al., 2016).

3.3.2. BIOFILM PHOTOSYNTHETIC EFFICIENCY

The portable pulse amplitude modulated (PAM) fluorometer (Mini-PAM-II, HeinzWalz, Effeltrich, Germany), were used for the in vivo fluorescence analysis. The measures were performed *in situ* by placing the light-emitting diode sensor to a constant distance of the samples. The Mini-PAM gave information about the minimum fluorescence yield that can be

used as an estimation of the algal biomass (F_0) and the yield (Yeff). The settings were verified to be correct and were maintained during all samplings. The established settings were Damp = 3, Gain = 7 and Meas-int = 8. The zero to calibrate the Mini-PAM was done in a clean cobble or glass substrata surface.

The measurements were done before the biofilm dried in each cobble or artificial substrata by triplicate in three different random places. To ensure the reliability of the measurement, the F value must be above 130, if not the case, it indicated that there was not enough biomass to perform a valid yield and it was not considered.

3.3.3. CHLOROPHYLL-A

The Chlorophyll-a concentration (Chl-*a*) was used to estimate the algal biomass in biofilm, as described by Jeffrey and Humphrey (1975). All Chl-*a* samples were always taken by triplicate and stored in the dark to avoid its degradation caused by the light.

A known volume (5 mL) of the scraped biofilm suspension taken during the biofilm sampling were filtered through a 1.2 μm pore filter (A0258855 Prat Dumas) (GF/C) to remove the contained water. Then the samples were prepared by doing an extraction using 10 mL of 90% acetone and stored for 24 hours in the dark at 4 ˚C. After 24h, the suspension was filtered through pore filter of 47 mm diameter and 1.2 μm pore filter (A0258855 Prat Dumas). Chlorophyll-a concentration was then determined in the filtrate by spectrophotometric measurements (NanoPhotometer™ P-360) at 430 (carotenoid peak), 665 (Chl-*a* peak) and 750 (turbidity peak) nm. The autozero was done using the 90% acetone.

When the 430 nm peak was higher than 2, the sample was diluted by adding acetone to the filtrate. If the 750 nm peak was higher than 0.02 the sample were filtrated again until adjusting to the value.

The Chl-*a* concentration was calculated as follows:

$$\mathrm{Chl-a\;(\mu g\;cm^{-2})} = \frac{(\mathrm{Abs.665-Abs.750nm})\cdot 11.4\cdot \mathrm{AV}}{\mathrm{SS}} \qquad \text{[Eq 2]}$$

Where *Abs. 665nm* is the absorbance value read at 665nm wavelength, *Abs. 750nm* is the absorbance read at 750nm wavelength, *AV* is the acetone volume (in mL), *11.4* is the error of the absorbance coefficient, and *SS* is the scraped surface (in cm^2).

Additionally, the Margalef index (MI) was calculated as described by Margalef (1983) applying the following equation:

$$MI = Abs. 430nm / Abs. 665nm \quad \text{[Eq 3]}$$

Were *Abs. 430nm* is the value read at 430nm and *Abs. 665nm* is the absorbance read at 665nm.

The basis of this index remains in the fact that Chlorophyll-*a* is the pigment that is synthesized and degraded more quickly, while other pigments accumulate and are more resistant to degradation than Chlorophyll-*a*. Thus, all populations that have low productivity, are characterized by lower concentrations of pigments and, therefore, the relationship of Chlorophyll-*a* with the rest of the pigments is lower or higher depending on the age of the populations. Therefore, with this index, low values are obtained in population that grow rapidly and increase when the population is more mature and with a low renewal rate (Margalef, 1960).

3.3.4. ASH FREE DRY MASS

Total biofilm biomass was measured as ash free dry mass (AFDM). 47 mm GF/F Whatman glass-fibber filters (0.7 µm pore size) were pre-combusted for 4h at 500°C (Carbolite muffle ELF 11/14B) and weighted (W1, Eq 4). Then, a known volume from the biofilm suspension was filtered using the pre-weighted filers, dried for 72h at 60°C (Forced air oven, MEMMEERT IFE500) and weighted again (W2, Eq 4 and 5) to calculate the dry mass (DM). Finally, the samples were combusted at 500°C for 4h (Carbolite muffle ELF 11/14B) and weighted again (W3, Eq 5). The differences in filter mass before and after drying for DM (72h at 60°C) and after combustion (4h at 500°C) subtracted from DM were calculated to obtain AFDM.

$$DM = W2(g) - W1(g) \quad \text{[Eq 4]}$$

Where, *W1* is the weight of the filter before filtering de sample, and *W2* is the weight of the filter after 72h in the oven.

$$AFDM \; (g) = W3(g) - W2(g) \quad \text{[Eq 5]}$$

Where, *W2* is the weight of the filter after 72h in the oven, and *W3* is the weight of the filter after 4h in the muffle.

The results were standardized by the surface of the cobbles or artificial substrata, as shown in the following equation:

$$AFDM(g \; m^{-2}) = \frac{W3(g) - W2(g)}{scraped \; surface \; (m^2)} \quad \text{[Eq 6]}$$

The percentage of organic matter (OM) were then calculated as follows:

$$OM\ (\%) = \frac{W3\ (g\ m^{-2})}{AFDM\ (g\ m^{-2})} \qquad \text{[Eq 7]}$$

Additionally, the Autotrophic Index (AI) was measured. In this index, values above 200 indicate a predominance of heterotroph in front of autotroph organisms in biofilm (Weber, 1973) and it was calculated as follow:

$$AI = \frac{AFDM\ (g\ m^{-2})}{Chl-a\ (g\ m^{-2})} \qquad \text{[Eq 8]}$$

3.3.5. METAL ACCUMULATION IN BIOFILM

In order to measure the total metal accumulation in biofilm, dried biofilm samples from one cobble (Chapter 4 and 5) or glass substratum (Chapter 6) were lyophilized and weighed (g) to determine the dry weight (DW). Then, 200 mg of DW were digested with 4 mL of concentrated HNO_3 (65%, suprapure) and 1 mL of H_2O_2 (31%, suprapure). After dilution with milliQ water, water samples were acidified (1% nitric acid suprapure) and stored at 4 ˚C, as described by Meylan et al. (2004). Total dissolved metals of the digested samples of Chapter 5, were analysed by ICP-MS (7500c Agilent Technologies, Inc. Wilmington, DE). The quantification limits were 1.65, 0.012 and 0.376 µg L^{-1} for the Zn, Pb and Cd, respectively. Moreover, the detection limits for Zn, Pb and Cd were 0.495, 0.003 and 0.113 µg L^{-1}, respectively. Dissolved metals of the digested samples of Chapter 1 and 3, were analysed by Microwave Plasma Atomic Emission Spectroscopy (MP-AES model 240/280, Agilent technologies, UK) and the detection and quantification limits are the same as the explained in section 3.2.3. Metal accumulation was expressed as dissolved metal contents per biofilm dry weight (µg g^{-1} DW).

3.3.6. DIATOM METRICS

To evaluate the diatom metrics, a volume of 5 mL of the biofilm suspension, taken during the biofilm sampling, was placed in a 15 mL Falcon and preserved using 5 mL Ethanol 70%. Then, before the analysis, they were ultrasonicated to isolate the aggregated cells without damaging the frustules, and 125 µL of each sample was pipetted onto a Nageotte counting chamber to count the total number of diatom cells following Morin et al., (2010). Data were recorded as cells per sample substrate area (number of cells cm^{-2}). Two different types of counting were performed; empty cells considered as 'dead', and cells occupied by chloroplasts considered as 'alive'. According to Guillard (1973), the diatom community growth rates were determined (in cell divisions day^{-1}) by using live diatom counts (expressed in cells mL^{-1}).

To identify the species level, hydrogen peroxide (30%) was used to clean diatom samples to remove the organic material and dissolve calcium carbonates according to Leira and Sabater

(2005). Cleaned frustules were mounted on permanent glass slides using Naphrax (Brunel Microscopes Ltd, UK; RI=1.74). Using standard references and recent nomenclature updates listed in Coste et al. (2009) and Prygiel and Coste (2000), about 400 random frustules per slide were counted at 1,000x magnification, and diatom were measured and identified to the lowest taxonomic level feasible. Relative abundances of species (percentage of the total abundance) were estimated, and diversity was calculated using the Shannon-Weaver index (H') (Shannon and Weaver, 1963). From species relative abundances and their individual biovolumes, a mean cell length (µm) of the community was calculated the lenght of 25 randomly selected valves per species as described in Barral-Fraga et al., (2016).

3.3.7. MICRORESPIRATION

The microbial respiration of biofilm analysed using the MicroResp^{TM}, a microplate-based respiration system. This technique offers the possibility for measuring CO_2 production in short-term incubations. MicroResp is a colorimetric method described by Campbell et al., (2003) based on the colour change of a pH indicator dye caused by CO_2 release. The system consists of two 96-well microplates placed face-to-face. One is a deep-well microplate (1.2 mL capacity, NUNC) in which each well contains 750 µL of biofilm suspension. The second microplate contained the indicator solution (detection plates).

The indicator stock solution was prepared dissolving 18.75 mg of cresol red, 16.77 g of potassium chloride (KCl) and 0.315 g of sodium bicarbonate (NaHCO$_3$), for the indicator solution in 900 mL of millliQ water over a low heat (<65°C) before diluting to 1000mL. The indicator solution was stored at 4°C.

The detection plates were prepared with previously autoclaved material as follows:

- 3% purified agar were prepared by weighting 3g and dissolving it in 100mL of milliQ water in a low setting microwave and cooled the agar until 60°C in a water bath.
- Two times of the indicator solution were measured and placed into a bottle and warm it in a water bath to 60°C.
- Once the temperature of each solution has equilibrated, the indicator solution and agar were transferred into a beaker and mixed thoroughly, maintaining the heat at 60°C with constant stirring.
- 150µg aliquots were dispensed into the microplate.

The plates were stored in the dark at room temperature in a desiccator with self-indicating soda lime in the base and a beaker of water.

Before the incubation, the microplate was read with a spectrophotometer microplate reader (Thermo Scientific Multiskan EX) at 560nm. From the biofilm suspension, 750 µL were spilled into the deepwell plate. For the incubation, microplates were connected to the deep wells with the seal and then the Perspex sheet were placed on the top of the filling device and using the fingerholds, tapped the assembly on the bench. The incubation lasted 16h in the darkness. After the 16h the colour variations were measured with a spectrophotometer microplate reader (Thermo Scientific Multiskan EX) at 560nm.

Then, the absorbance data were normalized for both times:

$$0\text{h data}: \text{Ai} = (\text{At0}/\text{At0}) \cdot \text{Mean}(\text{At0}) \qquad \text{[Eq 9]}$$

$$16\text{h data}: \text{Ai} = (\text{At16}/\text{At0}) \cdot \text{Mean}(\text{At0}) \qquad \text{[Eq 10]}$$

Where, *Ai* is the normalised data, *At0* is the value of the lecture before the incubation and *At16* is the value of the lecture after 16h of incubation.

Then the 16h normalised data were converted to %CO_2 produced:

$$\%CO_2 = A + B / (1 + D \cdot Ai) \qquad \text{[Eq 11]}$$

Where, A = -0.2265, B = -1.606, D = -6.771 which are given parameters calculated from a calibration using Emax Microplate reader (Molecular Devices, USA) using a wavelength of 570 nm, and Ai is the normalised data for the 16h.

Finally, the CO_2 rate were also calculated, in µg CO_2 – C g h^{-1}, as:

$$\frac{((\%CO_2) \cdot \text{vol} \cdot (44/22.4) \cdot (12/44) \cdot (273 / (273 + T))}{\text{incubation time}} \qquad \text{[Eq 12]}$$

Where, *T* is the temperature in °C, *vol* is the headspace volume in the well (µm), and *44, 22.4, 12, 44 and 273* values are gas constants and constants for incubation.

3.3.8. NUTRIENT UPTAKE CAPACITY

The soluble reactive phosphorus (SRP) (Chapter 7) and ammonium (Chapter 6 and 8) uptake capacity of biofilm was measured at each sampling day directly on each microcosm with the remaining cobbles in the microcosm's experiments (Chapter 7) and moving the 11 x 18 glass substrata to different aquariums for the artificial channels (Chapter 6 and 8). These two nutrients were chosen since they are essential resources and their availability could determine changes in the structure and the function of microbial benthic communities (Proia et al., 2012).

The phosphorus and ammonium uptake rate were calculated measuring the temporal decay after a controlled spike (Proia et al., 2017). If the nutrient decay in time fitted the negative exponential model, it allowed the calculation and comparison of the nutrient decay (k). The

basal nutrient concentration was previously determined, and each aquarium was later spiked with the appropriate volume of Na_2PO_4 stock solution (1.42 g L^{-1}) and NH_4^+ solution (1 g L^{-1}) in order to quadruple the background concentration of both nutrients. Aliquots of water (10 mL) for SRP and NH_4^+ concentration measurements were then taken at 1, 5, 30, 60, 120, 180 and 240 min after spiking, immediately filtered through 0.22 μm nylon membrane filters (GNWP04700) and stored at −20 °C until analyses. The SRP and NH_4^+ uptake rate (U, μgPcm^{-2} h^{-1} and μg NH_4^+cm^{-2} h^{-1}) were calculated as:

$$U = \frac{P_\circ - Pf}{A \cdot Tf} \qquad \text{[Eq 13]}$$

Where P_0 is the initial mass of each nutrient after the spike (μg); Pf is the final mass of the nutrient at the end of incubation (μg); A is the area colonized by biofilm (cm^2) and Tf is the time of incubation end (h).

Each nutrient uptake rate coefficient (k, min^{-1}) was calculated as the coefficient of the negative exponential model represented by the decay of SRP and NH_4^+ concentration over time. The k coefficient was considered valid as a measure of the k-SRP only when data significantly fitted the negative exponential model describing the kinetics decay.
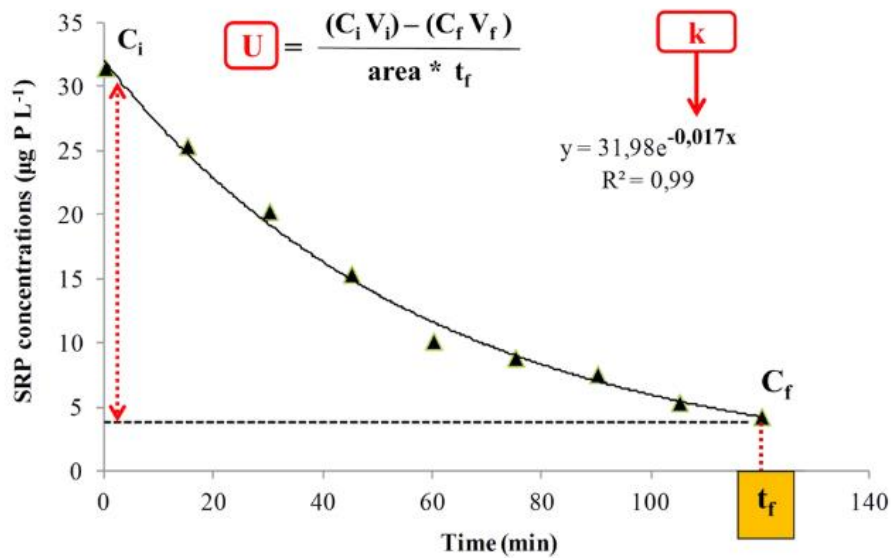
Figure 3.6: Example of dissolved inorganic P decay in time after controlled spike in response to biotic uptake by biofilm. Uptake rate coefficient (k, min^{-1}) is calculated by fitting negative exponential curve to the data. Source: Proia et al. (2017)

3.3.9. POLLUTED INDUCED COMMUNITY TOLERANCE (PICT)

The polluted induced community tolerance (PICT) is a concepted based in that toxicant-tolerant organisms can survive exposure, whereas most toxicant-sensitive organisms will be eliminated,

resulting in an increased PICT indicative of a globally more tolerant community (Tlili et al., 2011b). This concept applied to biofilm communities allow to establish a cause-effect relationship between a pollutant and its impact on biological communities, which considers the contamination history of the ecosystem at community level (Tlili and Montuelle, 2011). The PICT is assessed by a toxicity test in which a specific endpoint is measured for evaluating exposure-effects relations of pollutants at community level. The measure used is the EC_{50} (half maximal effective concentration), that represents the concentration of a toxicant where the 50% of its maximal effect is observed thus the 50% of the population respond after a specific exposure (Blanck et al., 1998). In this thesis the endpoint selected to assess the PICT was the photosynthetic efficiency (Chapter 8). For that, eight colonised glass substrata of 1x1 cm were taken from each mesocosm and were exposed during 24h to eight increasing, salt concentrations based on the Menteroda mining effluent under controlled temperature and in constant agitation.

The increasing salt concentrations were created from a mother solution of 290 g L^{-1} (265 g NaCl L^{-1}, 17.1 g KCl L^{-1} and 17.1 g $Cl_2Mg·6H_2O$ L^{-1}) which included two concentrations above the most concentrated treatment that allowed to assess potential tolerances of the most concentrated treatment (Blanck, 2002). From that mother solution the following concentrations were made as described in Table 3.5.

Table 3.5: Volume of the saline mother solution and microcosmos water to create the increasing salinity concentrations for the PICT assessment.

	Salinity	A	B	Total volume
C0	0	0	10	10
C1	4.50	0.16	9.84	10
C2	9.00	0.31	9.69	10
C3	18.00	0.62	9.38	10
C4	36.30	1.25	8.75	10
C5	72.50	2.50	7.50	10
C6	145.00	5.00	5.00	10
C7	290.00	10.00	0.00	10

Where *A* is the volume of saline mother solution, *B* is the volume of each microcosms water, and *C* is the concentration code.

After the 24h of exposure period, the photosynthetic efficiency was measured using the Mini-PAM as described above.

3.4. BIOLOGICAL QUALITY INDEXES

3.4.1. TROPHIC DIATOM INDEX (TDI)

The Trophic Diatom Index (TDI) is an index for monitoring the trophic status of rivers based on the diatom composition. The index is based on a suite of 86 taxa selected both for their indicator value and ease of identification. To calculate the TDI, it was generated a list of the diatom taxa at each sampling site and then taxon weightings described in Kelly and Whitton (1995) were applied to calculate the index following the next equation:

$$\text{Index} = \Sigma\ (A_i\ v_i\ j_i)\ /\ (A_i\ v_i) \qquad \text{[Eq 14]}$$

Where *A* is the relative abundance of species *i, v* is the indicator value of the species and *j* its sensitivity. The value of TDI can range from 0 to > 100 according to the water quality (Table 3.6).

3.4.2. BIOLOGICAL MONITORING WORKING PARTY (BMWP)

The BMWP was developed in 1976 (Biological Monitoring Working Party, 1978), and revised to a final version, 1980 (National Water Council, 1981), as a simplified system to assess water quality, using benthic macroinvertebrates (Hawkes, 1997). The index is based on species assemblages and associated environmental sensitivities within their respective regions. The BMWP Score system is based on identification of macroinvertebrates to family level (National Water Council, 1981; MINAE, 2007). Each of the identified families is allocated a score, ranging from 1 to 10 (National Water Council, 1981) and 1 to 9 (MINAE, 2007). The most sensitive organisms (e.g., mayfly and stonefly nymphs), either score 10 (National Water Council, 1981) or 9 (MINAE, 2007), molluscs 3 and the least sensitive (Oligochaeta) 1 (National Water Council, 1981; MINAE, 2007). The values for each family are summed up independently from their abundance and generic diversity, thus sensitivity scores higher than 120 points indicate an undisturbed (excellent) aquatic system, while those lower than 15 points indicate highly polluted (poor) aquatic system (MINAE, 2007; Stein et al., 2008). Based on the BMWP total scores, six levels of water quality may be established (Alba-Tercedor, 1996; Table 3.6).

3.4.3. AVERAGE SCORE PER TAXON (ASPT)

The total BMWP score can also be divided by the number of taxa to produce the Average Score Per Taxon, ASPT (Chapman, 1996), which is less influenced by season and sample size (Armitage et al., 1983; Muralidharan et al., 2010). A high ASPT score (e.g., greater than 7) indicates clean water, containing a large number of high scoring taxa (Table 3.6) (Armitage et al., 1983; O'Callaghan and Kelly-Quinn, 2013).

Throughout this thesis, theBiological Monitoring Working Party (BMWP) and the Average Score Per Taxon (ASPT) reported in Chapter 4 were calculated by Welsh Government environmental agency Natural Resources Wales (NRW).

Table 3.6: Categories of water quality as defined by the numerical values and colours of the Throphic Diatom Index (TDI), Biological Monitoring Working Party (BMWP) and Average Score per Taxon (ASTP) index.

Water quality category	Colour	TDI	BMWP	ASTP
Waters with excellent quality			>120	
Waters with good quality, no contaminations or obvious distortions		> 100	101 – 120	> 7
Waters with regular quality, Eutrophic, moderate contamination		60 – 100	61 – 100	6 – 6.9
Waters with bad quality, Contaminated		45 – 60	36 – 60	5 – 5.9
Waters with bad quality, very contaminated		30 – 45	16 – 35	4 – 4.9
Waters with very bad quality, extremely contaminated		< 30	<15	< 3.9

CHAPTER 4.

Assessment of the ecological status of a river affected by a metal mining effluent from an abandoned mine using the biofilm as bioindicator.

Photo: Frongoch stream (Wales, UK), by Life DEMINE project

4. ECOLOGICAL IMPACT ASSESSMENT OF FRONGOCH ABANDONED MINE ON FRONGOCH STREAM (WALES, UNITED KINGDOM)

4.1. INTRODUCTION

England and Wales have a long history of metal mining dating back to the Bronze Age (Pattrick and Polya, 1993; Ixer and Budd, 1998). Hundreds of thousands of tons of lead, zinc, and copper ore have been extracted from several major mining areas since this time. The last major mine closed in the late twentieth century, and currently, there are no operating metal mines neither in England nor in Wales (Hudson-Edwards et al., 2008). However, this history of metal mining has generated a legacy of abandoned mines across these regions with important environmental implications, especially for water bodies. Nowadays, Wales has more than 1.300 abandoned metal mines, impacting more than 67 water bodies (Edwards et al., 2016). One of the most common mining methods applied in Wales was placer mining which involved water and led to the transfer of significant quantities of metal-rich, fine-grained sediment and water to river systems (Hudson-Edwards et al., 2008).

Focusing on the environmental impacts that abandoned mines have caused in Wales, one of the most affected catchments by mining-related metal contamination is the Ystwyth River catchment (mid-Wales), where there is an abandoned lead-zinc mine (Frongoch Mine). This mine is one of the 50 Welsh sites prioritised by the Environmental Agency of Wales (Palumbo-Roe et al., 2012) for remediation in 2002. Frongoch Mine is a primary source of zinc pollution to the river Ystwyth, causing important chemical and ecological impacts on downstream watercourses (i.e. Frongoch stream, and Rivers Nant Cell, Nant Cwmnewydion and Magwe) that are currently failing to achieve the Environmental Quality Standards (EQS) for zinc, lead and cadmium required by the European Water Framework Directive (WFD) (Edwards and Williams 2016).

According to the Life DEMINE data base, the annual average (from 1975 to 2015) concentrations of zinc (Zn), lead (Pb) and cadmium (Cd) of Frongoch mining effluent were of 102 mg Zn L^{-1}, 4.73 mg Pb L^{-1} and 0.24 mg Cd L^{-1}, with an annual average flow of 2.16 L s^{-1} to the receiving stream (Table 4.1). After the discharge of this mining effluent to the Frongoch stream (average from July 2004 to March 2016 of 17 L s^{-1}, Williams, and Stanley 2016), from July 2004 to March 2016 the average Zn, Pb and Cd concentration in the Frongoch stream were 13.3 mg L^{-1}, 1.2 mg L^{-1} and 0.02 mg L^{-1} (Edwards, Williams, and Stanley 2016), exceeding the metal (Zn, Pb and Cd) standards

established for freshwaters by both the WFD in Europe and the US Environmental Protection Agency (WFD; US EPA, 2006). According to the WFD, the maximum heavy metal concentrations thresholds recommended for freshwater ecosystems is 14 µg L^{-1} of Pb, 10.9 µg L^{-1} of Zn, and 0.45 to 1.5 µg L^{-1} of Cd (depending on the hardness of the water as specified in five class categories; Class 1: < 40 mg $CaCO_3$ L^{-1}, Class 2: 40 to < 50 mg $CaCO_3$ L^{-1}, Class 3: 50 to < 100 mg $CaCO_3$ L^{-1}, Class 4: 100 to < 200 mg $CaCO_3$ L^{-1} and Class 5: ≥ 200 mg $CaCO_3$ L^{-1}).

Since 2013, Natural Resources Wales (NRW) is the regulatory body responsible for managing water resources in Wales. In the last decade, following the Mine Strategy for Wales (Johnston, 2004), NRW has carried out extensive investigations and feasibility studies to prioritise and deal with the most polluting mines, including an assessment of their impacts according to the WFD in over 90 waterbodies across Wales, such us the Ystwyth catchment affected by Frongoch abandoned mine.

NRW uses a range of methodologies and approaches to assess the water quality of the streams surrounding mining areas based on biological indexes such as the Biological Monitoring Working Party (BMWP) scoring system, Number of Taxa (NoT) and Average Score per Taxon (ASPT) scores for the macroinvertebrate community, and the Trophic Diatom Index (TDI) for the diatom community. To do so, monthly samplings are carried out up and downstream of the pollution source (i.e., mining effluent). Water physicochemical, metal composition and macroinvertebrate metrics are determined at each sampling site, and then the BMWP, NoT and ASTP indexes are calculated.

In the last report performed by NRW in Frongoch abandoned mine (2008), the waterbodies surrounding this mine showed Pb, Zn, and Cd concentrations above the EQS recommended range. It was observed a decrease in macroinvertebrate species diversity, abundance and richness and increase on evenness compared to the control sites, that caused a decrease in BMWP and NoT after the input of the abandoned mine effluent into the main stream course, even though they could not find any pattern within the diatom community. Additionally, the high levels of dissolved metal concentrations, were eventually limiting the presence of trout populations in these waterbodies (Environment Agency Wales 2008). For all these reasons, the Frongoch mine was included in the priority 50 list of abandoned mine causing significant impacts on waterbodies in Wales.

It is important to state that biofilm community responses have not been included in the studies that NRW have carried out, although diatoms have been used to assess the water quality of the stream. Biofilm community responses can be helpful to assess the ecological status since they

contribute significantly to the mechanisms of absorption and processing of nutrient and pollutants, leading to the self-depuration of running water ecosystems (Sabater et al., 2007). Biofilms are at the base of the food chain and are particularly important for assessing the level of metal accumulation and potential trophic transfer to higher trophic levels (Leguay et al., 2016). The effects of pollutants on biofilm can be expressed as variations of community composition, growth (i.e., biomass), and physiological properties (e.g., photosynthesis or respiration). These variations on its properties are expressed in a variety of temporal and spatial scales enabling more or less reversibility (Sabater et al., 2007). Additionally, they have commonly been used for biomonitoring in rivers since their rapid response to environmental changes which makes them appropriate as early warning systems for toxicity evaluation (Sabater et al., 2007). Phototrophic organisms of biofilm (such as diatoms) are recognized for the WFD to be one of the components of the "biological quality elements" (BQEs) for the assessment of the ecological status of water systems. Therefore, for all these reasons, biofilm could be a useful tool to assess the ecological impact of Frongoch abandoned mine on Frongoch stream since it could be a feasible supporting tool to assess the water status of the stream.

In order to deal with metal pollution in water bodies caused by mining effluents from abandoned mines, both active and passive remediation options have been developed and applied at different mining sites (Tripathi and Rawat Ranjan, 2015; US EPA, 2014), including Frongoch abandoned mine (Edwards and Williams, 2016) In this context, a new treatment technology based on electrocoagulation and ultrafiltration processes has been developed in the context of the LIFE DEMINE project to decrease the ecological impacts caused by mining effluents from abandoned mines on aquatic ecosystems. This treatment technology was implemented in Frongoch mining site during 2019-2020 to treat the abandoned metal mining effluent of the abandoned metal mine before being discharged to the stream.

In this context, an assessment of the ecological status of Frongoch stream was carried out before implementing the LIFE DEMINE technology in Frongoch abandoned mine. A sampling campaign along the Frongoch stream was carried out in collaboration with NRW before the pilot plant operation started (October 2019), and adding the biofilm as an ecological indicator to complement the NRW's common monitoring tasks. Besides, the response of freshwater biofilm was assessed to be further used in microcosms, under controlled conditions, to assess the impacts of different abandoned mining effluents under different conditions. Additionally, the comparison between the biofilm responses to the data commonly collected and used by NRW was made.

Table 4.1: Environmental Quality Standards (EQS) and mining water composition from 1975 to 2015 of the Wales closed and abandoned mining effluents. The "Frongoch Mine (Tailings Culvert)" effluent is the mining effluent evaluated in this study. Values calculated as the average registered during all the years at each mining site (Mean ± SD).Q, Flow; EC, electrical conductivity; n.a, not available data; nd, not detected. Data source: Life DEMINE data base.

Location	Produced mineral	Q (m³ day⁻¹)	pH	EC (µS cm⁻¹)	Al	Ba	Ca	Cd	Cr	Cu	Fe	K	Mg	Mn	Na	Ni	Pb	SO₄	Zn
										(mg L⁻¹)									
River Teifi	lead, zinc	326 (± 133)	6.84 (± 0.26)	171 (± 43.4)	0.32 (±0.58)	0.01 (±0.00)	8.98 (±1.38)	0.04 (±0.02)	0.00 (±0.00)	0.01 (±0.02)	0.63 (±1.14)	1.35 (±0.31)	2.75 (±0.55)	0.05 (±0.04)	6.16 (±0.94)	0.00 (±0.00)	1.47 (±2.06)	43.3 (±13.8)	16.7 (±6.40)
Afon Clarach	silver, lead	864 (± 61.0)	7.12 (± 0.22)	125 (± 21.1)	0.01 (±0.01)	n.a	10.2 (±1.51)	0.00 (±0.00)	n.a	0.00 (±0.00)	0.03 (±0.02)	0.47 (±0.03)	3.46 (±0.49)	0.02 (±0.03)	7.76 (±0.42)	0.00 (±0.00)	0.11 (±0.02)	15.3 (±1.37)	0.38 (±0.02)
Pontrhydfendig aid, Afon Teifi	lead, zinc	241 (± 127)	7.30 (± 0.11)	109 (± 20.0)	0.04 (±0.03)	n.a	9.88 (±1.62)	0.00 (±0.00)	n.a	0.00 (±0.00)	0.15 (±0.08)	1.82 (±0.39)	2.63 (±0.43)	0.07 (±0.05)	5.52 (±0.63)	0.00 (±0.00)	0.01 (±0.01)	11.2 (±1.03)	0.76 (±0.25)
Aberystwyth, Rheidol mines	lead, zinc	253 (± 145)	2.89 (± 0.32)	1584 (± 317)	27.2 (±17.8)	0.01 (±0.00)	59.9 (±16.3)	0.30 (±0.26)	0.01 (±0.01)	0.19 (±0.16)	127 (±86.6)	0.89 (±1.82)	38.6 (±10.7)	3.52 (±1.54)	10.6 (±1.81)	1.44 (±0.05)	0.13 (±0.29)	822 (± 253)	110 (±74.5)
Nant y Mwyn Mine	lead	0.03 (±0.02)	7.12 (±0.62)	273 (±24.8)	0.02 (±0.02)	n.a	24.3 (±3.62)	0.03 (±0.01)	n.a	0.02 (±0.00)	0.07 (±0.06)	0.75 (±0.13)	8.47 (±1.18)	0.03 (±0.01)	8.07 (±1.24)	0.04 (±0.00)	0.09 (±0.02)	50.8 (±4.92)	10.1 (±2.98)
Frongoch Mine (Tailings Culvert)	lead, zinc	187 (±61.0)	5.30 (±0.22)	425 (±138)	0.83 (±0.36)	n.a	7.56 (±2.55)	0.24 (±0.13)	n.a	0.15 (±0.06)	0.05 (±0.02)	1.44 (±0.42)	2.19 (±0.37)	0.31 (±0.05)	4.25 (±0.33)	0.05 (±0.03)	4.73 (±3.13)	143 (±16.3)	102 (±38.5)
Frongoch Mine (Frongoch Adit)	lead, zinc	1404 (±1085)	6.94 (±0.30)	107 (±23.9)	0.09 (±0.41)	0.01 (±0.00)	6.78 (±2.59)	0.01 (±0.01)	0.02 (±0.01)	0.01 (±0.01)	0.18 (±0.43)	0.75 (±0.39)	1.81 (±0.58)	0.03 (±0.03)	5.81 (±0.96)	0.02 (±0.01)	0.39 (±0.49)	16.3 (±8.38)	3.78 (±4.56)
Esgair Mwyn Mine, Esgair Mwyn Adit	lead	339 (±119)	6.96 (±0.31)	60.1 (±7.35)	0.10 (±0.03)	n.d	4.84 (±0.93)	0.00 (±0.00)	n.d	0.01 (±0.00)	0.56 (±0.25)	0.34 (±0.09)	2.09 (±0.25)	0.08 (±0.04)	3.66 (±0.19)	0.00 (±0.00)	0.58 (±0.09)	n.a	0.60 (±0.11)
Esgair Mwyn Mine, Llwyn Llwyd Adit	lead	150 (±116)	7.06 (±0.27)	48.6 (±5.42)	0.15 (±0.05)	n.d	2.27 (±0.51)	0.00 (±0.00)	n.d	0.01 (±0.00)	1.14 (±0.72)	0.87 (±0.14)	1.16 (±0.16)	0.10 (±0.05)	3.02 (±0.40)	0.00 (±0.00)	0.39 (±0.12)	n.a	1.68 (±0.12)
EQS (mg L⁻¹)			6-9	-	-	-	-	0.001	0.005	0.001	1.00	-	-	0.0175		0.05	0.004	-	0.12

4.2. MATERIALS AND METHODS

The study area was in the mining region of Frongoch abandoned mine, near Pontrhyd-y-groes (Ceredigion, Wales, UK) and covers approximately 11 hectares. The mine exploited for lead (Pb) and zinc (Zn) ore extraction from the late 1700s until the early 1900s. This abandoned mine is a major source of metal pollution, causing downstream chemical and ecological impacts on watercourses. Indeed, this mine is the primary cause of failing the environmental quality standards for Zn, Pb and Cd required by the European Water Framework Directive (WFD) at Frongoch stream, and Rivers Nant Cell, Nant Cwmnewydion and Magwe, all of them located downstream of the abandoned mine (Edwards and Williams, 2018).

4.2.1. STUDY AREA AND SAMPLING DESIGN

Different sampling sites along the Frongoch stream and Nant Cell were selected to cover the metal pollution gradient from the source, at Frongoch stream, to its confluence with the Nant Cell. The sampling was performed at the end of October 2019 in collaboration with NRW.
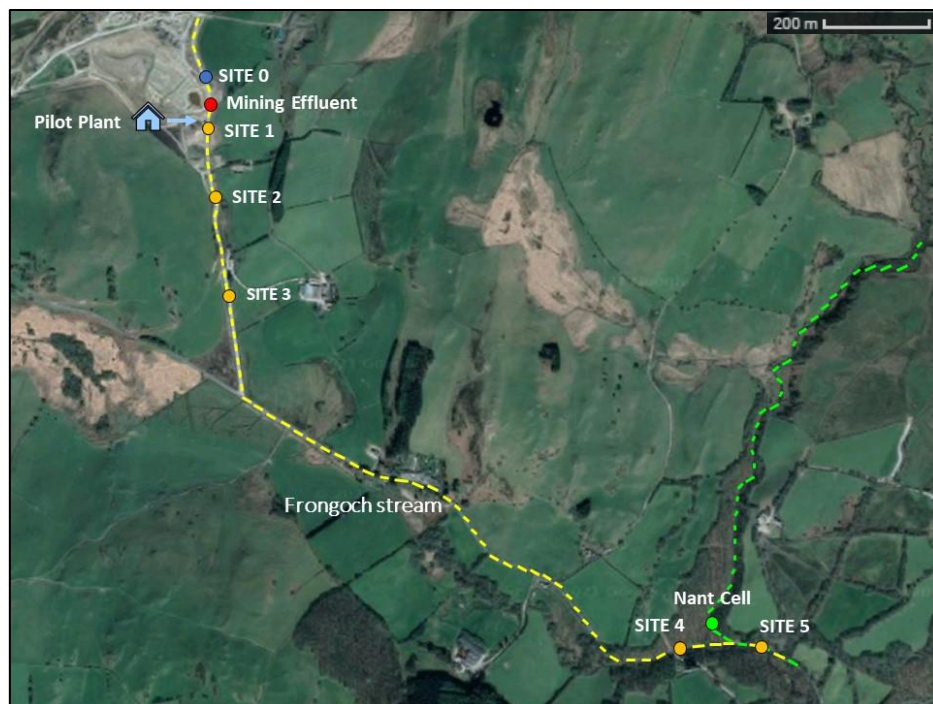
Figure 4.1: Study area around the Frongoch abandoned mine with the selected sampling sites. yellow dash line indicates the Frongoch stream, green one indicates Nant Cell stream. Coloured dots indicate the metal pollution grandient: blue dot is the up-stream point before the entrance of the mining effluent (ME), the red one is the entrance of the ME to the stream being the most metal polluted site, orange dots are the sampled sites downstream the ME and, and green dot is the Nant Cell sampling site taken as an unpolluted reference stream.

Specifically, the sampling sites were chosen according to the points usually sampled by NRW along Frongoch stream to monitor its ecological status (Figure 4.1, Figure 4.2). Specifically, seven sampling points were selected along 2-km river reach: a) SITE 0, upstream the metal mining

effluent entrance; b) Mining Effluent (ME), c) SITE 1 to SITE 4: located at 20 m, 170 m, 420 m and 1700 m, respectively, downstream the ME entrance and, d) SITE 5, (1900 m from the ME) after the confluence of Frongoch with Nant Cell streams. An additional sampling point located at the Nant Cell stream (NANT CELL) was selected as a reference site since it is consider by NRW as a pristine stream belonging to the same catchment (Figure 4.1, Figure 4.2).
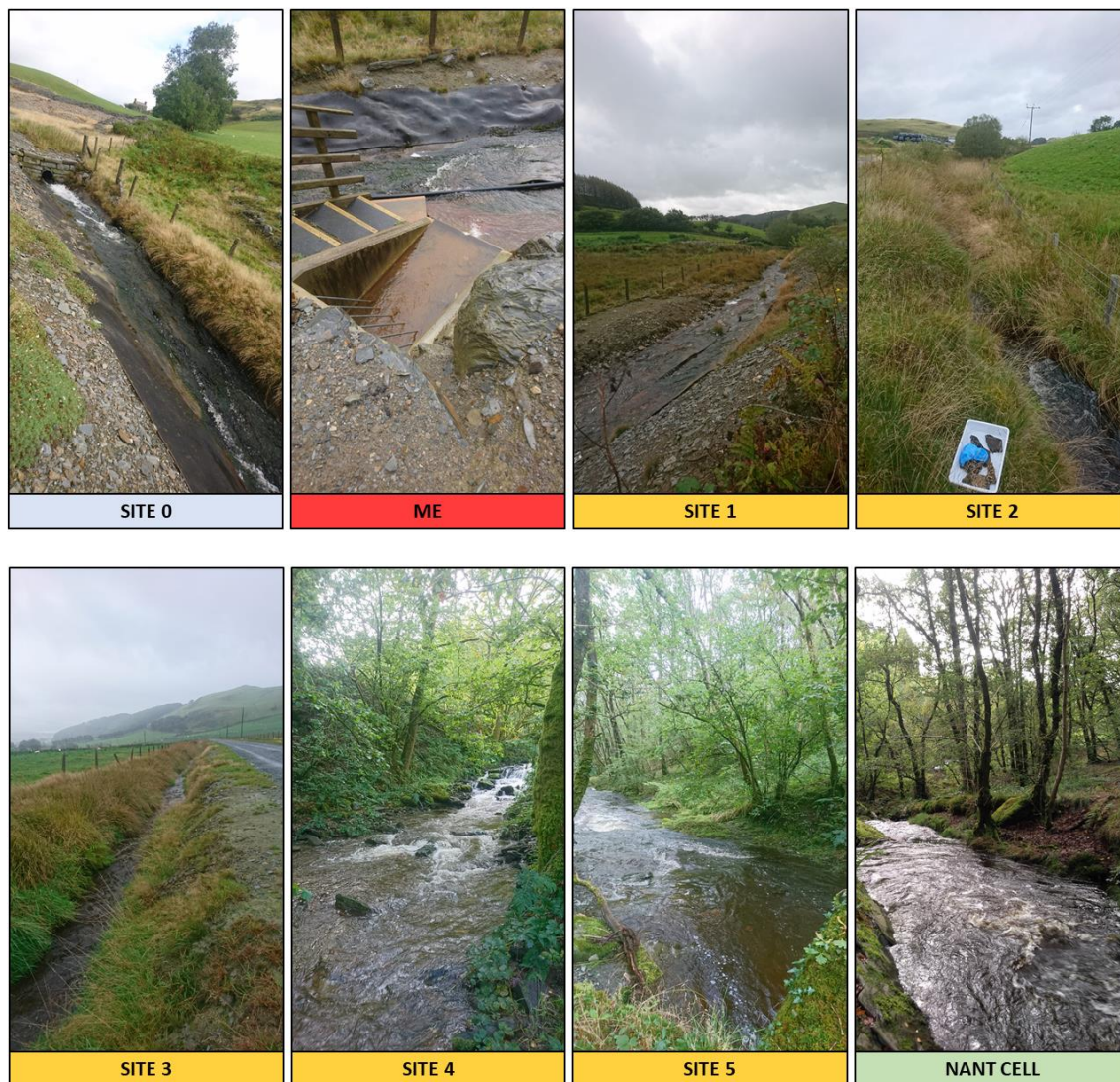
Figure 4.2: Sampling sites along Frongoch and Nant Cell streams. ME: mining effluent.

One value of the water physicochemical characteristics (i.e., water temperature, pH, dissolved oxygen, and conductivity) and metal concentration, at each sampling point, were provided by NRW. Triplicate water samples at each sampling sites (excepting SITE 1, due to methodological setbacks) were collected at each point and filtered through 0.22 µm pore diameter glass microfiber filter (Prat Dumas Filter Paper, Couze-St-Front, France) before the nutrient analysis (i.e., SRP, NH_4^+ and NO_3^-). Because of the adverse meteorological conditions in autumn season, water samples were not collected at SITE 5, and therefore, data regarding water

physicochemical parameters from SITE 5 is not provided in this study. Biofilms were sampled at each sampling point (Figure 4.1,Figure 4.2) by collecting three random cobbles. Biofilm photosynthetic activity and the phototrophic community composition were measured immediately after collection, directly with an amplitude modulated fluorometer (Mini-PAM fluorometer, Walz, Effeltrich, Germany) and a BenthoTorch portable fluorometer probe (bbe Moldaenke, Schwentinenta, DK), respectively. The biofilm from each of the three cobbles taken at each sampling site was scrapped, suspended, and homogenized separately in 45 mL of the corresponding sampling site water. Aliquots were distributed for analyses of diatom metrics, organic matter (OM), Margalef index (MI), chlorophyll-a (chl-a) concentration and metal accumulation. Diatom samples were stored with 90% ethanol, whereas metal accumulation, chl-a and OM samples were stored at −20 °C until analysis. All these measurements were analysed as described in CHAPTER 3.

Macroinvertebrates were sampled by NRW, by collecting macroinvertebrate samples with a net for three minutes (<1 mm mesh net) with an additional one-minute hand search, following standard procedures (Murray-Bligh and Ferguson,1999), only at sampling sites 3, 4, 5 and NANT CELL due to adverse meteorological conditions and high flow conditions during the sampling campaign-. The Shannon-Wiener Index, the total and relative macroinvertebrate abundance (total of all absolute abundance scores for all individual taxa recorded at each site) and taxa richness (the total number of reliably recognizable different taxa) were obtained.

Finally, the different biological indicators based on the macroinvertebrate (BWMP and ASTP) and diatom community (TDI) were calculated as described in Chapter 3.

4.2.2. DATA ANALYSIS

Differences in SRP, NH_4^+ and NO_3^-, biofilm variables (photosynthetic efficiency, MI, chl-a, OM and metal accumulation), and diatom metrics (species richness) between sampling sites along the studied reach were evaluated using one-way ANOVA. One-way ANOSIM tests (using Bray-Curtis similarity coefficients) were carried out with Bonferroni correction on the biofilm community composition, diatom, and macroinvertebrate taxa in Past3 version 3.23. Statistical significance for all tests was set at $p < 0.05$. Pearson's correlation analysis was performed to analyse the correlation between water physicochemical characteristics and biofilm variables along the studied reach. Normality was assessed with the Kolmogorov-Smirnov test and homogeneity of variances with the Bartlett. Statistical analysis was carried out using SPSS Statistics software (version 21).

Threshold Indicator Taxa Analysis (TITAN) was applied to identify diatom indicator taxa and diatom community sensitivity thresholds to the pollution gradient. Change points or thresholds are detected when there is a synchronous change in the abundance of a number of taxa lying within a narrow range of the predictor variable (Sultana et al., 2020). Taxa with occurrences < 3 were not considered, following Baker and King's (2010) recommended minimum TITAN variable in terms of z scores. This method is based on IndVal (indicator values from species indicator analysis) (Dufrêne and Legendre, 1997) and incorporates a bootstrap procedure to find taxon responses that are pure and reliable. Correlations between environmental variables were performed to select the most significant ones using matrix of scatter plots in R studio.

The relation between biofilm variables and physico-chemical composition was also evaluated using Redundancy Analysis (RDA) in R Studio software (version 3.6.0) using the 'ordiR2step' function of the Vegan Package (Oksanen et al., 2013). Biological data were square-root transformed and included chlorophyll-a, photosynthetic efficiency and diatom, green algae and cyanobacteria abundance. All environmental data were transformed by $\log10 (x + 1)$ to reduce skewed distributions. To avoid co-linearity, the variables were selected based on the inspection of variance inflation factors (VIF < 20) (ter Braak and Smilauer, 1998). Forward selection was used to reduce the environmental variables that criterion. TITAN distinguishes taxa responding positively or negatively to the specific predictor. Forward selection was used to reduce the environmental variables that significantly explained the responses of biofilms at a cut-off point of $p < 0.05$.

4.3.   RESULTS

4.3.1. PHYSICOCHEMICAL CHARACTERISTICS OF THE STREAM WATER

Nutrient concentration varied among sampling sites and significant differences were found in SRP (one-way ANOVA F = 115, $p < 0.001$) and NH_4^+ (one-way ANOVA F = 11.2, $p < 0.001$) among them (Table 4.2). By contrast, non-significant differences were found in NO_3^- concentration among sampling sites that ranged between 0.43 ($\pm$ 0.26) and 1.19 ($\pm$ 0.77) mg L^{-1} (Table 4.2). The pH was lower and electrical conductivity (EC) were higher at SITE 0, ME and 1 compared to the other sampling sites, whereas the dissolved oxygen concentration (DO) decreased at ME and SITE 1. Additionally, the metal concentrations (Zn, Pb and Cd) were significantly higher in the ME and in the Frongoch stream sites after its entrance (one-way ANOVA F = 6.12, $p < 0.001$) compared to the other sites. NANT CELL had the lowest metal concentrations, but the Zn concentrations were, still, considerably high. However, metal concentrations in water decreased downstream the ME and the DO, pH and EC values increased all along the stream (Table 4.2).

Table 4.2: Physico-chemical conditions on each sampling site (3 replicates per site) (mean ±SD). Tukey-b test indicate significant differences between sites. DO, dissolved oxygen; EC, electrical conductivity; T, temperature; n.a, not available data; n.d, not detected.

	DO (mg L^{-1})	pH	EC (µS cm^{-1})	T (°C)	Flow (L s^{-1})	NO$_3^-$ (mg L^{-1})	SRP (µg L^{-1})	NH$_4^+$	Zn (mg L^{-1})	Pb	Cd
SITE 0	10.87	6.35	227	10.4	2.05	1.07 (±0.41)	54.3 [a] (±2.72)	9.95 [c] (±3.55)	33.3	10.30	0.06
ME	4.16	5.03	528	11.3	n.a	0.61 (±0.19)	n.d [d]	0.03 [b,c] (±0.01)	136	14.90	0.36
SITE 1	7.36	6.39	227	10.8	n.a	n.a	n.a	n.a	133	22.10	0.03
SITE 2	11.3	7.36	93.0	9.90	129.3	1.19 (±0.77)	9.21 [b,c,d] (±1.08)	32.7 [b,c] (±11.5)	35.4	0.09	0.01
SITE 3	10.37	7.29	94.4	10.6	80.0	0.74 (±0.11)	29.8 [b] (±1.43)	45.5 [b,c] (±5.77)	33.9	0.19	n.d
SITE 4	11.27	7.26	87.5	9.70	n.a	0.61 (±0.45)	14.6 [b,c,d] (±1.63)	14.2 [c] (±4.45)	27.4	0.06	n.d
SITE 5	n.a	n.a	n.a	n.a	n.a	0.43 (±0.26)	8.67 [c,d] (±1.96)	60.7 [a,b] (±18.4)	n.a	n.a	n.a
NANT CELL	9.90	8.19	72.0	11.1	n.a	1.09 (±0.53)	9.76 [b,c] (±1.08)	87.0 [a] (±0.82)	0.15	n.d	n.d

4.3.2. BIOFILM COMMUNITIES

Regarding biofilm communities, significant differences were found in the chlorophyll-*a* concentration (chl-*a*; one-way ANOVA F = 18.2, p < 0.001) and organic matter content (OM) (one-way ANOVA F = 18.5, p < 0.001) among sampling sites. Both parameters decreased after the entrance of the ME to the Frongoch stream (SITE 1), but while the OM tended to increase downstream, the chl-*a* presented variations all along the stream (Table 4.3). Furthermore, SITE 0 and NANT CELL differed significantly in chl-*a* (one-way ANOVA F = 19.9, p < 0.05) and OM (one-way ANOVA F = 15.6, p = 0.017). In addition, significant differences were observed in the Margalef index (MI) among sites (one-way ANOVA F = 5.36, p < 0.001). According to the MI values, high variability was found among sampling points being higher at SITE 2 and 3 (Table 4.3).

Significant differences were found in the Zn (one-way ANOVA, F = 22.4, p < 0.001), Pb (one-way ANOVA, F = 5.07, p < 0.001) concentration in biofilm among the three-sampling site (SITE 0, 1 and 2) of which data is available (Table 4.3). Biofilm at SITE 1 presented higher Zn and Pb concentration. SITE 0 were the sampling site with less metal accumulation in biofilm.

Table 4.3: Structural (Chl-*a*, OM, community composition, diatom metrics) and functional (photosynthetic efficiency: Y_{eff}) biofilm variables measured during the sampling campaign (Mean ± SD). Tukey-b test indicate significant differences between sites. Accumulation of Cd were below the detection limit. Chl-a, chlorophyll-a; OM, organic matter; MI: Margalef index, Y_{eff}, photosynthetic efficiency, n.a: not available, n.d: not detected.

	Accumulation in biofilm		Community composition							Diatom metrics	
	Zn	Pb	Y_{eff}	Green algae	Diatom	Cyanobacteria	OM	Chl-*a*	MI		
	(mg g^{-1})			(µg chl-*a* cm^{-2})			(%)	(µg chl-*a* cm^{-2})		H'	S
SITE 0	0.55 [a] (±0.32)	0.44 [a] (±0.30)	0.44 [a,b,c] (±0.05)	2.36 [a] (±1.96)	0.97 [b] (±0.43)	0.52 [b] (±0.22)	58.3 [a,b] (±4.81)	3.39 [a] (±0.74)	2.12 [a] (±0.05)	2.78	33
ME	n.a	n.a	0.34 [a] (±0.02)	2.79 [a,b] (±0.52)	0.00 [c] (±0.00)	0.34 [a,b] (±0.02)	26.2 [b] (±3.57)	0.23 [b,c] (±0.02)	2.04 [a] (±0.02)	2.33	17
SITE 1	7.33 [b] (±2.51)	7.00 [b] (±1.96)	0.50 [a,b,c,d] (±0.03)	0.17 [b] (±0.07)	0.40 [b] (±0.14)	0.43 [a,b] (±0.22)	23.3 [b] (±1.80)	0.15 [b,c] (±0.05)	2.00 [a] (±0.03)	2.27	31
SITE 2	2.06 [a] (±1.05)	1.93 [c] (±0.10)	0.43 [a,b] (±0.03)	n.d [b]	1.20 [a] (±0.63)	1.39 [c] (±0.62)	76.6 [b,c] (±15.9)	0.68 [c] (±0.11)	3.73 [b] (±0.32)	2.75	43
SITE 3	n.a	n.a	0.46 [a,b,c] (±0.02)	n.d [b]	0.48 [b,c] (±0.28)	0.61 [a,b] (±0.23)	88.7 [c] (±11.3)	0.08 [b] (±0.01)	6.07 [c] (±0.35)	2.93	42
SITE 4	n.a	n.a	0.57 [b,c,d] (±0.05)	1.73 [a] (±0.73)	1.09 [a] (±0.16)	1.34 [d] (±0.14)	90.1 [c] (±1.55)	0.10 [b] (±0.04)	2.09 [a] (±0.30)	2.91	37
SITE 5	n.a	n.a	0.64 [d] (±0.01)	2.13 [a] (±0.69)	0.68 [b] (±0.24)	0.49 [a,b] (±0.53)	43.2 [a,b] (±2.46)	0.20 [b,c] (±0.02)	1.81 [a] (±0.01)	2.83	40
NANT CELL	n.a	n.a	0.62 [c,d] (±0.06)	2.62 [a] (±0.69)	0.38 [b,c] (±0.24)	0.20 [a] (±0.04)	33.4 [a] (±3.79)	0.08 [b] (±0.01)	1.74 [a] (±0.05)	3.08	36

Furthermore, the biofilm photosynthetic efficiency (Y_{eff}) presented significant differences among sampling sites (one-way ANOVA F = 4.36, p < 0.05), being the lowest value in the ME and increasing gradually from the first sampling site (SITE 0) to the last one (SITE 5) correlating positively with the decrease of the metal concentration in water (Table 4.3, Pearson correlation, r = -0.651, p < 0.001), and the distance among sampling sites (Pearsons correlation r = 0.89, p < 0.05). On the other hand, the biofilm community composition, presented significant differences along the Frongoch stream (one-way ANOSIM R = 0.39, p < 0.001). In the ME the community were dominated by green algae (2.79 µg chl-a cm^{-2}), but just after the ME entrance to the Frongoch stream (SITE 1), green algae decreased and were not detected at sampling points 2 and 3 (Table 4.3). In these sites, the community were co-dominated by diatoms and cyanobacteria, but an increase on the green algae community was observed at the downstream sampling sites (SITE 4 and 5) (Table 4.3).

Over 45 diatom taxa were identified from the different biofilm samples. Although diatom diversity index (H') was similar among sampling points along the stream (from 2.27 to 3.08) significant differences were found between sites with higher metal concentrations in surface water (i.e., SITE 1 and 2) and NANT CELL (one-way ANOVA F = 0.15, p < 0.001) (Table 4.3). Additionally, the number of diatom species identified throughout the sampling sites differed significantly between them (one-way ANOVA F = 7.19, p < 0.001). In the ME, significantly lower number of species were identified (17) whereas they increased downstream being SITE 2 the site with higher number of species identified (42,Table 4.3).

Furthermore, significant differences were found in the diatom community composition among sampling sites (one-way ANOSIM R = 0.85, p < 0.001). The most significant difference was found between the diatom community found at the mining effluent (ME) compared to the other sampling sites. The diatom community at ME was dominated by PMIC, PRUP and PGIB, while at the rest of the sites, ACMI was the most abundant diatom species. ADPY and FCON, presented similar abundances in all sampling sites, except for the ME, where this last two species were not detected (Figure 4.3).
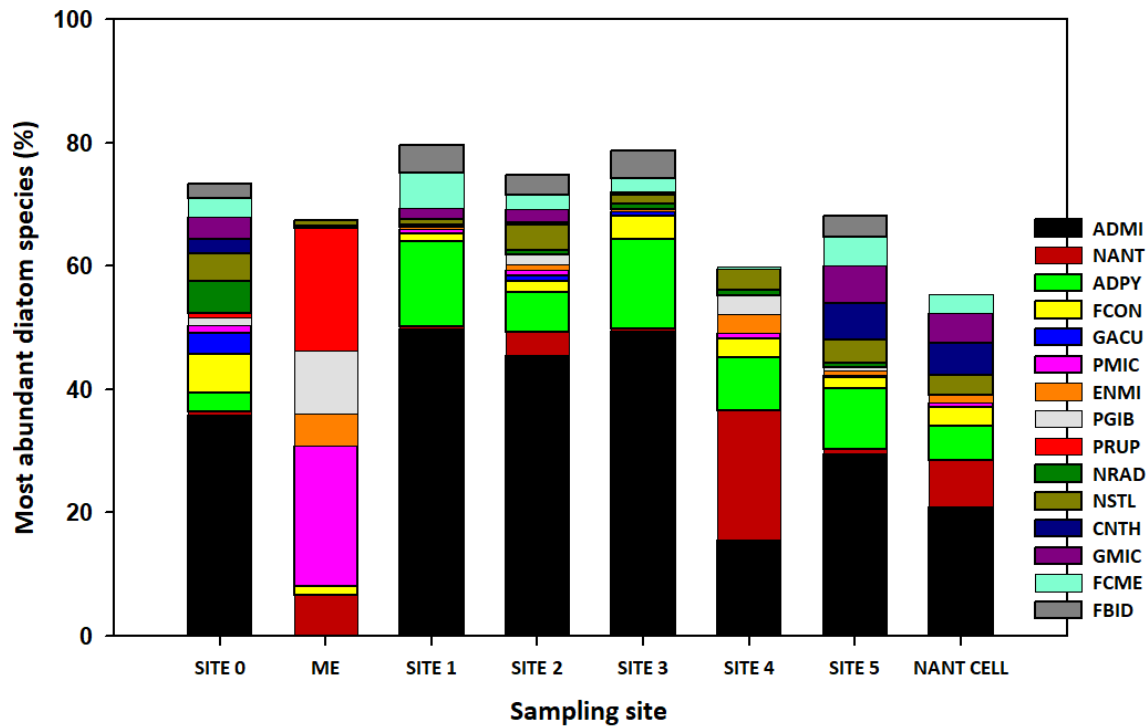
Figure 4.3: Relative abundance (mean value, n=3) of the 16 major diatom species (>3%) within diatom communities collected at each sampling site. ACMI: Achnanthidium minutissimum (Kützing), NANT: Navicula antonii (Lange-Bertalot), ADPY: Achnanthidium pyrenaicum (Hustedt), FCON: Fragilaria construens (Ehrenberg) Grunow, GACU: Gomphonema acuminatum (Ehrenberg), NRAD: Navicula radiosa (Kützing), NSTL: Navicula striolata (Grunow), CNTH: Cocconeis neothumensis (Krammer), GMIC: Gomphonema micropus (Kützing), FCME: Fragilaria capucina var. mesolepta (Rabenhorst), FBID: Fragilaria bidens (Heiberg), PMIC: Pinnularia microstauron (Ehrenberg), ENMI: Encyonema minutum (Hilse) D.G.Mann, PGIB: Pinnularia gibba (Ehrenberg), PRUP: Pinnularia subrupestris (Krammer).

The diatom species richness (Pearson correlation, r = -0.886, p = 0.001) and the photosynthetic efficiency of the biofilm (Pearson correlation, r = -0.651, p = 0.001) were negatively correlated with the total metal concentration in water (sum of the concentrations in water of the three metals), showing that the sites with higher metal concentrations tended to have the lowest diversity (i.e., the predominance of tolerant diatom taxa) and lower photosynthetic efficiencies. The diatom species richness was positively correlated with pH (Pearson correlation, r = -0.805, p = 0.016) suggesting that sites with the lowest pH had the lowest diatom biodiversity.

4.3.3. MACROINVERTEBRATES

Regarding macroinvertebrates, a total of 66 taxa were identified across the four sampling sites (SITE 3, 4, 5 and NANT CELL). Significant differences were found among sites (one-way ANOSIM R = 0.95, p = 0.01). The macroinvertebrate community composition at SITE 3 and 4 were significantly different from SITE 5 and NANT CELL (Figure 4.4). The first two sites (3 and 4) were dominated by *Protonemura meyeri* (19% and 35%, respectively), *Baetis rhodani* (27 and 19%), *Rhithrogena semicolorata* (21% and 24%), while the most abundant species at SITE 5 and NANT CELL were *Rhithrogena semicolorata* (29% and 21%). At these two sites, the species *Ecdyonurus*

had greater abundances (Figure 4.4). The number of species was significantly lower in SITE 3 (i.e., 28 taxa), than in other Frongoch sites, being higher in SITE 5 (i.e., 43 taxa).
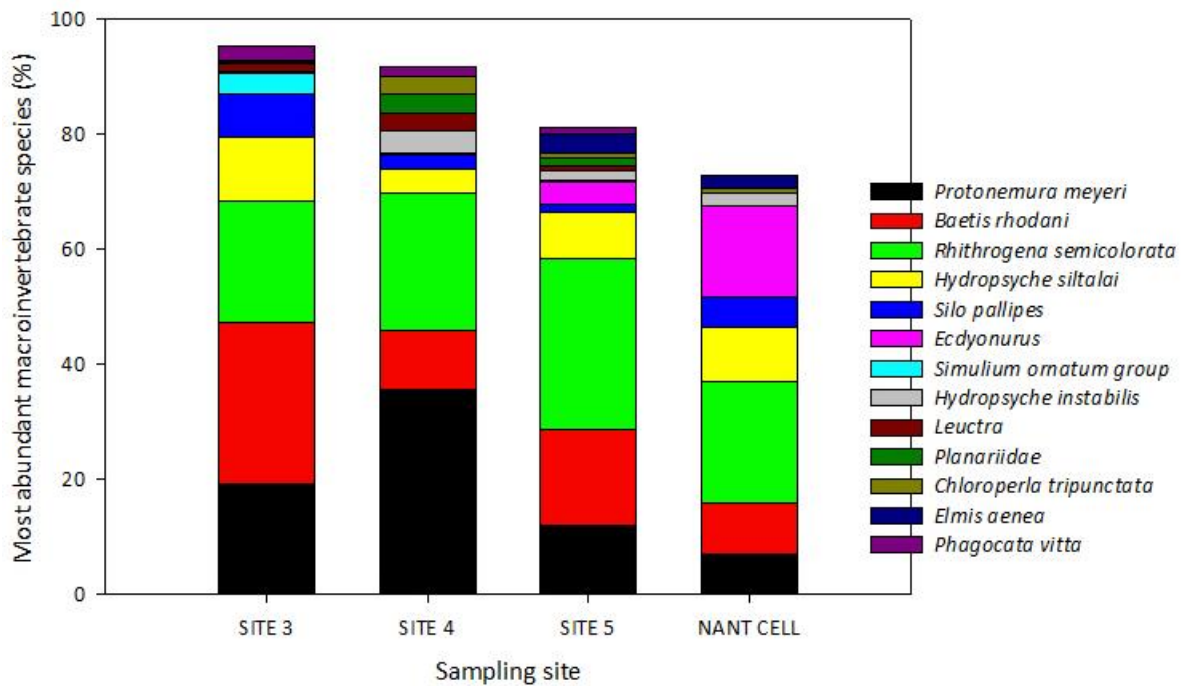
Figure 4.4: Relative abundance (mean value, n=3) of the 13 major macroinvertebrate species (>3%) within macroinvertebrates collected at each sampling site. (p < 0.005).

4.3.4. INTERACTION BETWEEN BIOFILM AND CHEMICAL VARIABLES

An RDA was performed to evaluate the relationship between the water physiochemical parameters and the biofilm function and structure. The percentahe of explained variation was 40.85%. The environmental dataset included 3 variables: pH, Zn and Pb concentration in water. This RDA accounted for 43.2% of the variance. According to the first axis, SITE 2 and 3 differed from the other sampling sites presenting higher chl-a, photosynthetic efficiency and diatom and cyanobacteria abundances but lower green algae abundance (Figure 4.5). The second axis explained the 5.72% of the variance and mainly separated SITE 0, 2 and ME from the rest due to higher metal concentration and lower pH values (Figure 4.5).
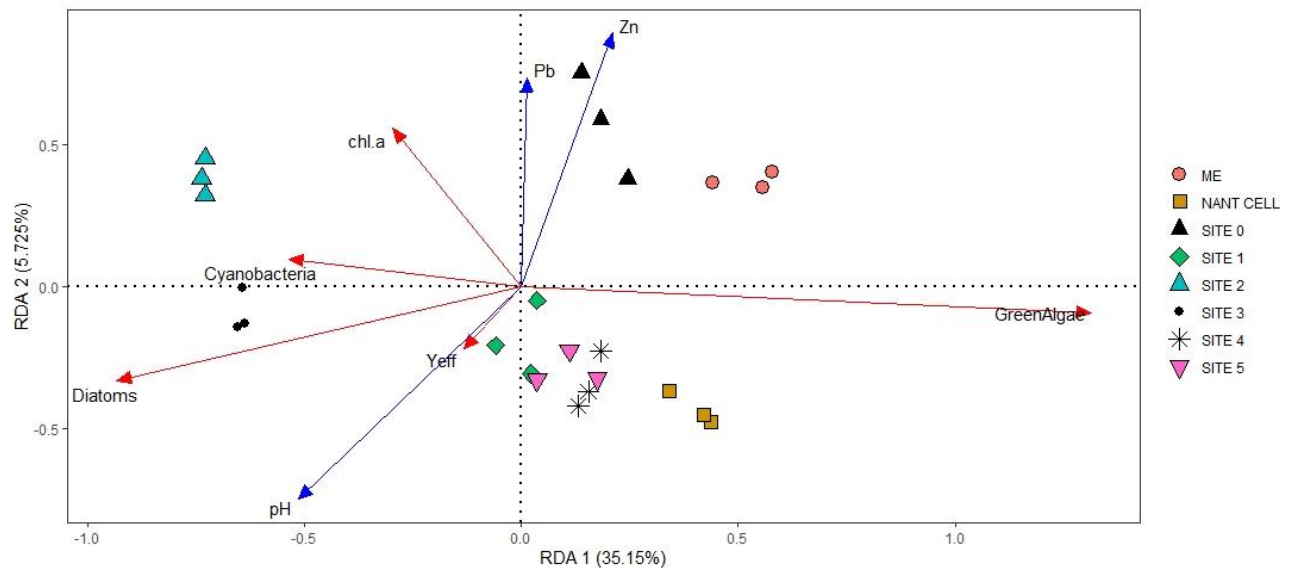
Figure 4.5: Redundancy Discriminant Analysis (RDA) at the different sampling sites along Frongoch stream, including biofilm functional and structural metrics and physicochemical variables (Zn and Pb total dissolved in water and pH). chl.a: chlorophyll-a, Yeff: photosynthetic efficiency.

4.3.5. THRESHOLD INDICATOR TAXA ANALYSIS (TITAN ANALYSIS)

TITAN analysis was applied to identify diatom indicator taxa and diatom community sensitivity thresholds to the pollution gradient. This analysis could not be applied to the macroinvertebrate community because the amount of data available was not enough. In this study, Zn and pH were the environmental variables to which the diatom community demonstrated significant responses. This analysis revealed that most negative responder taxa decreased sharply at community-level change points of 2 mg Zn L^{-1} (Figure 4.6). The community-level change points for the positive responder taxa were calculated at a pH of 6.2 (Table 4.4 A). Most of the positive responder taxa were associated with higher pH, and negative responder taxa were related to high Zn concentrations. Using TITAN, we found that only a subset of the diatom taxa (range: 2%–20% of the 46 taxa depending on the environmental variable considered) responded reliably to the two environmental variables (Table 4.4 B). More taxa were identified as negative responders (4 – 20%) than as positive responders (2 – 17%) (Table 4.4B). The sampling site where the diatom community structure showed major changes were the most polluted sampling site (ME).
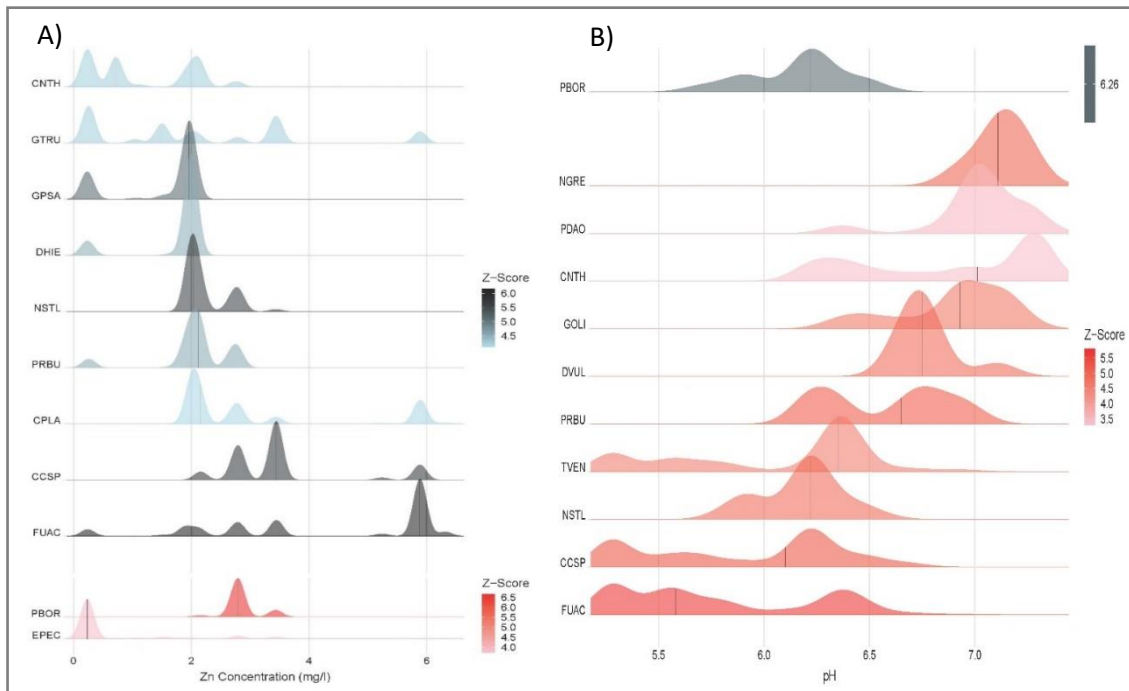
Figure 4.6: Plot of sum z-scores for responding taxa along the A) Zn and B) pH environmental gradient. Steep slopes indicate major change points in abundance. Red corresponds genera that increased with the increasing Zn and pH values (z+), and in blue the genera that negatively responded to the increase in pH and Zn (z-).

Table 4.4: A. Diatom community change point along the four environmental variables that indicates a threshold at which a synchronous change in the abundance and occurrence of many taxa happens. The community change points (or thresholds) correspond to the maximum sum(z) of the taxa identified as reliable positive or negative responders in TITAN and the 5th and 95th percentiles (in parentheses following the observed value) correspond to the frequency distribution of change points from 1000 bootstrap replicates that provides an estimation of uncertainty associated to the community change points. B. Number of OTUs (taxa) identified as positive, negative or no responders using TITAN.

	Community-level change points [sum(z)]	
(A)	Zn (mg L^{-1})	pH
positive responders	5.89	6.22
(5th and 95th percentiles)	(0.20 - 6.33)	(5.70 – 6.92)
negative responders	5.89	6.22
(5th and 95th percentiles)	(1.88 - 6.33)	(5.70 – 6.50)
(B)		
Number of taxa with:	Zn	pH
Positive response (TITAN)	2	10
Negative response (TITAN)	9	1
No response (TITAN)	35	35

4.3.6. ECOLOGICAL STATUS OF FRONGOCH STREAM

The overall ecological status of the Frongoch stream was calculated according to the ecological indexes established by the WFD and used by NRW based on the diatom (TDI), and the macroinvertebrate community composition (BMWP and ASTP). The results obtained based on the TDI evidenced the "poor" ecological status of Frongoch stream, while the NANT CELL quality was "moderate" (Figure 4.7). However, the macroinvertebrate BMWP index showed "good" quality at SITE 3, 4 and NANT CELL, whereas SITE 5 presented "high" ecological quality. By

contrast, the ASTP index demonstrated "poor" quality at SITE 3 and 4 but "high" quality at SITE 5 and NANT CELL (Figure 4.7). Based on the WFD rules in which the worst status prevails when combining the quality indexes, all sampling sites along Frongoch stream had a "poor" quality status, whereas the quality at the NANT CELL was "moderate" (Figure 4.7).

Figure 4.7: Ecological status of Frongoch stream based on diatom and macroinvertebrates indexes along the stream. TDI: Trophic Diatom Index, IBD: Biological Diatom Index, BMWP: Biological Monitoring Working Party, ASPT: Average Score Per Taxon. The numbers indicate the value of each index and the colors the category of water quality.

4.4. DISCUSSION AND CONCLUSION

The main aim of this study was to investigate *in situ* the effects of the mining effluent to the ecological status of the Frongoch stream before the operation of the LIFE DEMINE pilot plant in the Frongoch Mine (Frongoch Adit), using the current methodologies used by NRW together with the response of biofilm communities. The metal mining effluent from Frongoch abandoned mine was characterised by high Zn, Pb and Cd concentrations, causing the Frongoch stream, to exceed the Zn and Pb limits (0.12 and 0.004 mg L^{-1} respectively) determined by the European Water Framework Directive (WFD) (Directive 2000/60/EC, 2000) in all the sampling points, and Cd at sampling sites 0, 1, 2, 3 and, ME.

In this study, differences in stream water physiochemical characteristics and biofilm structure and functioning were found between sampling sites along the stream. In the field, physical parameters like current velocity or light irradiance (Hill et al., 2000) and water chemistry, e.g., nutrient bioavailability (Lozano and Pratt, 1994; Lawrence et al., 2005) may have a significant impact on metal accumulation and toxicity. In this study high metal concentrations (136, 14.9 and 0.36 mg L^{-1} of Zn, Pb and Cd, respectively) were discharged to the Frongoch stream by the metal effluent (ME), and metal concentrations gradually decreased downstream probably because of both the dilution effect and the accumulation occurring along the stream (Bonet et al., 2013). The changes in the stream physicochemical characteristics might be caused by the occurrence of metal-complexing substances from the mining effluent entrance to the stream resulting in a variation of the metals load and hence in its conductivity (Barrado et al., 1998) and cause a decrease in the pH water (pH <5.6). The decrease of the pH can be caused by acid mine drainage or by the breakdown (oxidation) of organic matter and formation of organic acids, which can cause the dissolution of metal-bearing silicate, carbonate, sulphide and oxide minerals and release of their metals to the solute phase (Jain and Das 2017). Metal concentration in water and other factors affecting its bioavailability (i.e., pH, temperature, or hardness) may also influence the accumulation (Meylan et al., 2003).

The exposure to metals along the stream caused biofilm community alterations, including changes in the photosynthetic efficiency, community composition and metal accumulation. In this study higher metal accumulation in biofilm were found where higher the metal concentration in water was. As previously reported, metal toxicity in biofilm is mainly related to bioaccumulation than to concentration in water (Bradac et al., 2010; Bonet et al., 2014; Corcoll et al., 2012). Biofilms accumulate metals at intra and extra-cellular level trough adsorption on extracellular polymeric substances, cell surface or intracellular absorption (Holding et al., 2003). In this study, the metal accumulation in biofilm lead to a decrease on the photosynthetic efficiency, as observed by Leal-Alvarado et al. (2016) and Miller et al. (2017). This decrease is caused by two main reasons: a) the mode of action of metals potentially targeting several photosynthetic processes of diatoms, green algae and cyanobacteria (Corcoll et al., 2012). For example, the in vivo substitution of magnesium, which is the central atom of chlorophyll-*a*, by heavy metals (such as Zn), leading to a breakdown in photosynthesis (Corcoll et al., 2011). And b) the physical effect of metal accumulation in biofilm acting as a light barrier (Ivorra et al., 2000).

In addition to the differences observed in the photosynthetic efficiency, differences in the biofilm community composition, chlorophyll-*a* (chl-*a*) and organic matter (OM) were also observed along the stream. The observed decrease of chl-*a* suggests that metal exposure inhibited the electron transport flow (Juneau et al., 2007), which also affected the overall biofilm biomass by jeopardizing the community growth (Wong 1988). Under controlled conditions in microcosm, where causal relationships can be identified, Corcoll et al. (2011) reported similar results at Zn concentrations of 400 µg Zn L^{-1} after a few hours of exposure. Ivorra et al. (2000), observed similar trends 2 days after the addition of Zn spike at 2216 µg Zn L^{-1} in microcosms conditions. By contrast, Tlili et al. 2011 and Bonet et al. 2014 reported an increase of Chl-*a* in metal polluted sites, possible due to the greening effect.

In this study green algae were found to be dominant in those biofilm communities under the ME where higher metal concentrations were observed. In this regard, green algae have been reported at higher abundances in several convergences between mining effluents and stream waters in natural environments (Das and Ramanujam, 2011). The mecanisms that favoured green algae tolerance to high metal polluted conditions was the decrease in the number of binding sites at the cell surface, internal detoxifying mechanisms (Gold et al., 2003) or additional enzymatic activity induced by metals (Bonet et al., 2014) can be the mechanisms favouring the green algae tolerance to heavy metal stress. Nevertheless, green algae did not differ between background, low and moderate metal (Zn) polluted sites (Bonet et al., 2013). These mechanisms are related to Zn toxicity which triggers the synthesis of the antioxidant response (dinoxanthin, antheroxanthin and diadinoxanthin,) activating the xanthophyll cycle of green algae as protective mechanisms (Corcoll et al., 2012). On the other hand, diatoms abundance increased, as lower the metal concentration was, as observed by Bonet et al. (2013).

In fact, diatom communities under higher metal concentrations (ME, SITE 1 and SITE 2) were significantly different from those exposed to lower metal concentrations (for instance SITE 4, 5 and NANT CELL). In this case, the species identified in biofilm in those sites containing higher levels of metals, are either pioneer and substrate-adherent species that are more tolerant to metals (Medley and Clements, 1998), and species frequently reported in metal contaminated environments (Morin et al., 2012). Diatom composition is driven by several environmental factors, such as chemical parameters or exposure to toxic agents (i.e., metals). Indeed, metal contamination favors tolerant species selection, whereas sensitive species tend to decrease in number or disappear (Morin et al., 2012). Apart from the diatom community, the macroinvertebrate communities were also affected by the metal content in water, showing less

species richness under higher metal concentrations. As previously reported by Clements, (2004), heavy metals in water have direct toxic effects to the macroinvertebrate community, reducing its diversity and abundance, while indirect effects include modification of species interaction, alteration of habitat conditions or trophic relationship. Amusan and Adu (2020) found that Zn might be responsible for changes in macroinvertebrate community structure in waterbodies. Kage (2012) reported that Zn had significant influence on the macroinvertebrate diversity by reducing it by 12%.

Certainly, the diatom community response varied along the metal concentration and pH environmental gradients. Regarding metal concentration in water, the diatom community change point was identified at 2 mg L^{-1} of Zn but some species, like *Cocconeis neothumensis* (CNTH), started to disappear at concentrations below 1 mg L^{-1}. Additionally, *Pinnularia borealis* (PBOR) and *Eunotia pectinalis* (EPEC), which are rare species mostly found in high Zn concentration environments (Rainbow, 2018; Hellawell, 1986), increased with the metal content. The negative responders were species mostly found in clean waters sensible to high polluted environments that commonly die or present deformities when exposed to increased metal concentrations (Morin et al., 2012; Falasco et al., 2009). Regarding the pH, the community change point was found at 6.3, although species, like CCSP and FUAC, presented their change point at lower pH values. PBOR is the only negative responder, and it is a species that occur at low pH and does not survive when it increases above 6 (Zheng, 2015). Positive responders are commonly present in neutral freshwater environments and clean waters (Stoermer, Smol and Kristiansen 1999). It was found that NSTL was an increased in pH but a decreaser in Zn concentrations, indicating that with the decrease of the metal concentrations and the increase of the pH, this species can grow.

Finally, the ecological quality indexes calculated showed inconsistencies between them. Our results demonstrated that, for the Frongoch catchment, the TDI were the most restrictive indicator, showing worst ecological status at all the sampling sites compared to the BMWP and ASTP. Additionally, the BMWP and the ASTP demonstrated variation between them, being the ASTP the less restricting. Indeed, Hering et al. (2006), suggested that the effects of toxic elements are most strongly reflected by benthic diatom assemblages than by macroinvertebrates communities. Additionally, the functional response of the biofilm community was significantly correlated to the TDI (Pearson correlation r = -0.79, p = 0.018), indicating less photosynthetic efficiency at higher TDI. Therefore, some evidence was provided about the potential use of the biofilm photosynthetic efficiency as a functional measure to

assess the ecological status of a stream. However, this issue should be further studied to demonstrate its feasibility.

The streams bioassessments are focused on structural elements, which provides an incomplete picture of the overall integrity (Ferreira et al., 2020). This supposes a problem since the structure and function can respond in a different way to environmental stress (Sandin and Solimini, 2009; Feckler and Bundschuh, 2020; Verdonschot and Lee, 2020), that can cause changes in functioning but not in the structure (McKie and Malmqvis, 2009; Riipinen et al., 2009). Besides, ecosystem functions are strictly linked to the ecosystem services on which human societies rely (Capon et al., 2013; Jackson et al., 2016). For those reasons, it is crucial to develop and standardize a multimetric index which includes the functional measurements that can be used to assess the complexity of environmental exposure.

In this regard, the biofilm responses in this study provided an overview of the ecosystem damage attributed to the metal contamination from the Frongoch abandoned mine. The results obtained confirm the potential use of biofilm as an indicator of metal pollution since the exposure to the metal concentration along the stream caused changes in the community structure (i.e., shift in the community composition and in the diatom species richness and diversity) and function (i.e., photosynthetic efficiency), which at the same time were dependent of the metal concentration in water at each sampling site. The response observed in the biofilm community could approach the effects into the trophic network since they are the first step of the food chain in fluvial ecosystems and thus the first to be affected by metal pollution, which can be rapidly transferred to the next trophic levels (Soldo and Behra, 2000; Morin et al., 2007; Dorigo et al., 2010; Corcoll et al., 2011; Bonet et al., 2013). However, the changes observed in biofilm between sampling sites, could be led by the continuous exposure over the years, which biofilm in turn, are able to integrate (Dorigo et al., 2004; Sabater et al., 2007). In this study, the photosynthetic efficiency was the variable that provided more information about the biofilm response, which highlight the need of include functional measures to assess the ecological status of streams. The determination of biofilm function can be done through measuring changes in system state using the photosynthetic efficiency and techniques such as biofilm metabolism or nutrient uptake to assess the ecological status of a stream. These techniques are faster to measure and include the response of the whole biofilm community.

Overall, the high metal concentrations found in Frongoch stream promoted the accumulation in biofilm communities affecting both functional and structural variables. Additionally, even though the WFD indices might provide relevant information to assess the ecological status, the

results obtained in this study indicated that the methodological approach proposed by the WFD, mainly based on chemical parameters and biological indices, provides an incomplete and potentially misleading picture of the overall ecological integrity, because the stream bioassessment proposed did not consider ecosystem functioning, despite the overall ecological integrity encompasses structural and functional integrity (Ferreira et al., 2020). In this regard, biofilm possess many attributes that make them useful ecological indicators in freshwater ecosystems. Their short generation time, sessile nature, rapid response to environmental characteristics and the availability of methodologies for both functional and structural metrics, make biofilm an ideal tool to be indicators of disturbances in freshwater ecosystems. This demonstrated that biofilm communities should be further testes as a bioindicator tool to assess abandoned mining effluents ecological impacts to natural streams.

To the management point of view, when designing a monitoring programme, the combination of both structural and functional biofilm attributes will allow the best assessment of impacts in freshwater ecosystems. Biofilm functional parameters provide an integrated, long-term measure of ecosystem function, with structural attributes such as biomass and diversity allowing historical comparisons from a great literature base. Monitoring programmes, with a well-founded scientific base and defined management outcomes will contribute to an increase on the understanding of freshwater ecosystems status.

CHAPTER 5.

Assessing the effects of metal mining effluents on freshwater ecosystems using biofilm as an ecological indicator: Comparison between nanofiltration and nanofiltration with electrocoagulation treatment technologies.

Photo: Pilot plant (Wales, UK), by Life DEMINE project

5. ASSESSING THE EFFECTS OF METAL MINING EFFLUENTS ON FRESHWATER ECOSYSTEMS USING BIOFILM AS AN ECOLOGICAL INDICATOR: COMPARISON BETWEEN NANOFILTRATION AND NANOFILTRATION WITH ELECTROCOAGULATION TREATMENT TECHNOLOGIES.

5.1. INTRODUCTION

Mining activities generate large amounts of highly concentrated wastewater due to the contact between water and various types of minerals. The origin of these effluents can be found in the distinct processes undertaken in mining, in addition to drainage from rainfall. Mining effluents can be caused by wash waters, flow process acids, water leaching, flotation and concentration and from the refining and gas scrubbers (European Commission, 2010). All these processes can generate highly polluted effluents, by carrying soluble substances (as heavy metals) or small particles through soil or rock to the rivers (Kumar, 2015).

In some cases, even long after the mining activities have ceased, the emitted metals throughout these effluents continue to persist in the environment (Jain et al., 2016). Historically, mine sites were often abandoned without any concerns regarding the potential risks to humans and the surrounding environment, nor with regard to visual impacts, land-scape integration or land-use (European Commission, 2012). Abandoned mines are certain to be of appreciable concern to nearby citizens, as they can affect regional water supplies, contaminate water resources and damage sensitive aquatic habitats (Jain et al., 2016). Specifically, heavy metals may be stored in aquatic ecosystems or seep into the water table, which leads to contamination of underground water courses (Johnson and Hallberg, 2005; Younger et al., 2003).

The specific hazards posed by heavy metals harboured in mining effluents to the aquatic environment are highly dependent on the long-term life of the metal, i.e., the metal remains dissolved in water or is adsorbed on suspended solids or sediment, which determines its bioavailability. Bioavailability controls the toxicity of the metal to aquatic communities, which leads to bioaccumulation behaviour and consequently the biomagnification of the metal throughout the trophic web (Younger et al., 2003). Heavy metals dissolved in water are easily absorbed by aquatic organisms, such as aquatic biofilms which are the primary producers of the aquatic ecosystems (Solomon, 2008). Metal pollution could lead to a variety of biofilm responses including structural and functional changes with different ecological implications. For example, kinetics of algal growth, photosynthetic activity, chlorophyll-a concentration, nutrient uptake capacity and community composition may be altered in response to chemical stressors

harboured in mine effluents (Corcoll et al., 2011). Specifically, metal exposure can produce metabolic and functional alterations on the biofilm and, after long-term exposures, when the accumulation of metals becomes higher, it causes structural changes (Wu, 2016) which indicates the relevance of using a multi-biomarker approach including functional and structural biomarkers (Bonnineau et al., 2010).

Within biofilm processes, photosynthesis is critical for algal groups and metal toxicity has been shown to promote its inhibition (Guasch et al., 2002; Serra, 2009; Corcoll et al., 2011). The evaluation of ecological impacts caused by metal mining effluents is not trivial (Wu, 2016). The use of biofilm communities as bioindicators can be considered as a good approach of the community ecotoxicology (Sabater et al., 2007).

Currently, some technologies exist to treat metal mining effluents in order to minimise the high environmental and ecological impacts that they are causing to water bodies. The conventional active methods for heavy metal removal from wastewaters include chemical precipitation, chemical oxidation, ion exchange, nanofiltration, reverse osmosis, electrocoagulation and electrodialysis (Tripathi and Rawat Ranjan, 2015). Despite the existence of these technologies, the treatment of metal effluents coming from abandoned mines continues to be a major environmental problem, due to the high treatment costs and the lack of establishment actors, responsible to deal with the treatment. In this context, LIFE DEMINE (LIFE16 ENV/ES/000218) is a demonstration project funded by the European Commission that puts in practice, tests and evaluates at pre-industrial scale an innovative treatment process that combines membrane technologies (mainly nanofiltration) and electrocoagulation. Nanofiltration is a relatively new membrane technology and has been in use since the early 1980 s. The technology uses the combination of small pore size (nanometre range, MWCO < 2000 Da) and charge to selectively remove divalent cations from solution while allowing monovalent ions to permeate (Mohammad et al., 2015). As a result, this technology has found industrial application in food and beverages, wastewater treatment and drinking water production (Oatley-Radcliffe et al., 2017). Electrocoagulation is essentially chemical precipitation of the metal species by formation of the metal hydroxide, in this case the hydroxyl ions are formed by splitting water at an electrode (Moussa et al., 2017). Any metal that is insoluble in hydroxyl form will then precipitate, thus removing heavy metals but allowing common salts to remain.

Mining effluents are very complex and are composed of several metals. As a result, there are very limited studies available that include representative effects of metal mine effluents on complex biofilm communities. In this study, the efficiency of nanofiltration technology and the combination of nanofiltration + electrocoagulation was evaluated by exposing aquatic biofilms

to a metal mining effluent, treated by these technologies or untreated, and structural and functional responses were measured throughout time. It is expected the untreated mine effluent will impact on both the biofilm structure and function, while the treated effluents would have reduced metal content with a consequent lower biological impact for each of the technologies. The maximum reduction should occur when the technologies are combined (Nanofiltration + Electrocoagulation) since this combined treatment was expected to achieve the maximum reduction of the metal content in water.

5.2. MATERIAL AND METHODS

5.2.1. MINING EFFLUENT

This study was conducted in laboratory microcosms using the mining effluent from Frongoch abandoned mine described in the materials and methods section. The Frongoch mining effluent has been treated at bench scale using the treatment technologies developed in LIFE DEMINE. This study has been performed using: an unpolluted stream water as control (C), (ii) the treated effluent using only the nanofiltration step (NF), (iii) the treated effluent using nanofiltration combined with electrocoagulation (NF + EC) and (iv) the untreated (U) effluent from Frongoch mine.

5.2.2. EXPERIMENTAL DESIGN

Twelve microcosms consisting of glass aquariums (described in the materials and methods sections) were used to assess the biofilm response under untreated and treated mining effluents (Fig. 1). Each microcosm contained 15 previously scraped and autoclaved stream cobbles that were used as substrata for natural biofilm colonization, and each microcosm was filled with 3-L of artificial water. Artificial water was prepared to mimic a pristine stream as described in Ylla et al. (2009). Water was recirculated in each aquarium by a submersible pump (EDEN 105, Eden Water Paradise, Italy). The water in the aquaria was completely renewed every 3–4 days to avoid nutrient depletion. The temperature and the photoperiod were set at 18 °C and 12 h light: 12 h dark using LEDs (LENB 135-lm, LENB/14.97/11.98). During the experiment, the irradiance reaching the substrata was 12 μmol photons $m^{-2}s^{-1}$.

To promote biofilm colonisation, 15 mL of natural biofilm suspension obtained by scraping cobbles collected from Viladrau pristine and forested stream (Natural Park of Montseny, Spain) were inoculated in each microcosm. This inoculum was added at the beginning of the experiment to favour biofilm settlement, as well as after each water renewal during the colonization period, which lasted for three weeks. After the colonization, the exposure period

started with the addition of water from the mining effluents. Four different treatments were tested to compare biofilm responses with means of a control (C) in which the conditions remained unvaried. The exposure was set to mimic the real dilution conditions in Afon Ysywyth river where a mining effluent of $4.3 \text{ m}^3 \text{ h}^{-1}$ reaches the Afon Ysywyth river of $100 \text{ m}^3 \text{ h}^{-1}$ (Edwards and Williams, 2016). To achieve these conditions, 0.2 L of each effluent was added to 2.8 L of artificial water in the respective microcosms and each experiment was performed in triplicate. During the exposure period, which lasted for 13 days, each effluent was added to the respective microcosms at each water renewal every 3–4 days.

Physicochemical parameters were measured using the multiparametric probe (YSI professional plus, YSI Incorporated, USA). Water samples were taken at each water renewal and were filtered through 0.22 µm pore diameter glass microfiber filter (Prat Dumas Filter Paper, Couze-St-Front, France) before the nutrient analysis (i.e. SRP, NH_4^+, NO_3^- and NO_2^-).

Biofilms were sampled before (t0) and after 1, 6 and 13 days of the effluent's addition, always during the day following the water renewal (Figure 5.1). At each sampling day, three random cobbles from each microcosm were scrapped and suspended in 10 mL of the corresponding microcosm water. The area of stones was measured as described in materials and methods. Biofilm photosynthetic activity and the phototrophic community composition were measured immediately after collection, whereas samples for AFDM and chlorophyll-a concentration on the biofilm were stored at −20 °C until analysis. Samples for the determination of metal bioaccumulation in biofilm were taken before the exposure (t0) and at the end of this period (t13).
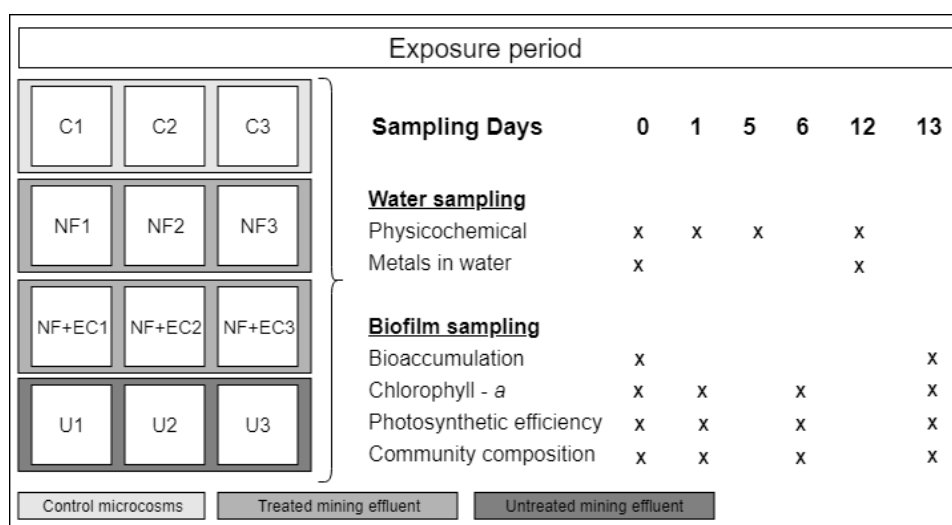
Figure 5.1: Experimental design and sampling strategy during the exposure period. C = control, U = untreated mining effluent, NF = nanofiltration and NF + EC = combined treatments.

5.2.3. DATA ANALYSIS

Physico-chemical data, photosynthetic efficiency, metal concentration in water, metal bioaccumulation and chlorophyll-a concentration in biofilm were evaluated using one-way repeated measures analysis of variance (ANOVA) in SPSS Statistics version 21, with treatment (C, NF, NF + EC and U) as factor and sampling date (time) as repeated measure. For physico-chemical data, a separate ANOVA was done for the colonisation and exposure period. Effects were analysed post hoc with a Tukey-b test when one-way ANOVA revealed significant differences among treatments. One-way ANOSIM tests (using Bray-Curtis similarity coefficients) were performed on relative abundances of the biofilm community composition at each sampling time with Bonferroni correction in Past3 version 3.23. Pearson correlation analysis was performed to explore the relationship between the community composition and the bioaccumulated metals in biofilm. A principal component analysis (PCA) using R Studio software (version 3.6.0) was performed to visualize the differences among treatments at the end of the exposure period (t13) based on the photosynthetic efficiency, metal bioaccumulation and the relative abundance of algal groups (cyanobacteria, green algae, and diatom) of the biofilm. Statistical significance was set at $p < 0.05$ for all the performed tests.

5.3. RESULTS

5.3.1. PHYSICO-CHEMICAL WATER PARAMETERS

During the colonisation period, the physico-chemical conditions did not show significant differences among microcosms. During the exposure period, dissolved oxygen, water temperature and pH remained stable with no significant deviations (Table 5.1). Nutrient concentrations showed similar behaviour in all microcosms and decreased between water renewals: SRP from 134 (± 12) to 62 (± 11) µg L^{-1} and NO$_3^-$ from 810 (± 20) to 450 (± 18) µg L^{-1}, the N/P ratio range during the whole experiment was between 14 and 18. The dissolved metal concentrations analysis showed that Zn was the most abundant metal during the exposure period in all the microcosms exposed to the effluents, with the highest concentration found in the microcosms exposed to the U compared to the treated ones and the C (one-way ANOVA F = 23.06p < 0.05; Tukey test, $p < 0.05$) (Table 5.1). By contrast, Pb and Cd concentrations in water were below the detection limit in all microcosms during the experiment (detection limit 0.01 mg L^{-1}).

Table 5.1. Physico-chemical conditions of the microcosms water during the colonisation (n=9) and exposure period (n=4) (mean ± SD). Zinc (Zn) concentration is expressed as the average between t0 and t12 (n=2). C= control, U=mining effluent, NF=nanofiltration and NF+EC=combined treatments. n.a = data not available, n.d =not detected.

	Colonisation period (n=9)	Exposure period (n=4)			
		C	NF	NF+EC	U
Temperature (°C)	21.85 (±0.44)	22.23 (±0.03)	21.79 (±0.03)	20.10 (±0.04)	21.53 (±0.03)
pH	7.93 (±0.10)	7.88 (±0.15)	8.01 (±0.06)	8.05 (±0.07)	7.76 (±0.06)
O_2 (mg L^{-1})	7.76 (±0.14)	7.26 (±0.15)	7.66 (±0.09)	6.97 (±0.12)	7.34 (±0.10)
Conductivity (µS cm^{-1})	147.01 (±2.21)	173.57 (±9.15)	151.68 (±3.26)	149.49 (±3.78)	174.96 (±2.72)
Zn (mg L^{-1})	n.a	n.d	0.36 (±0.03)	0.15 (±0.04)	4.25 ±1.15)

5.3.2. BIOFILM PARAMETERS

5.3.2.1. CHLOROPHYLL-A CONCENTRATION

Chlorophyll-a concentration in the biofilm decreased progressively during the exposure period in all treatments without significant differences among them in any of the sampling dates. Just before the starting of the exposure period (t0), the chlorophyll-a in all treatments was on average 3.5 (±1.9) µg cm^{-2} (n=36) while at the end of the exposure period (t13) it was 1.5 (±0.8) µg cm^{-2} (n=36).

5.3.2.2. PHOTOSYNTHETIC EFFICIENCY (YEFF)

The biofilm photosynthetic efficiency (Yeff) during the exposure period tended to increase over time in all treatments except for the case of U-exposed biofilm (Figure 5.2) which presented some significantly lower Yeff values than the rest of the treatments and C (ANOVA repeated measures, F = 48.88, $p < 0.05$; Tukey test, $p < 0.05$). In particular, the Yeff decreased drastically for the U effluent, since the first day of exposure (t1), when significant differences appeared between this treatment and the others (one-way ANOVA, F = 4.89, $p < 0.05$; Tukey test, $p < 0.05$). On the other hand, NF+EC treatment showed higher Yeff values than C and NF at the end of the exposure period (t13) (one-way ANOVA, F = 30.65, $p < 0.05$; Tukey test, $p < 0.05$).
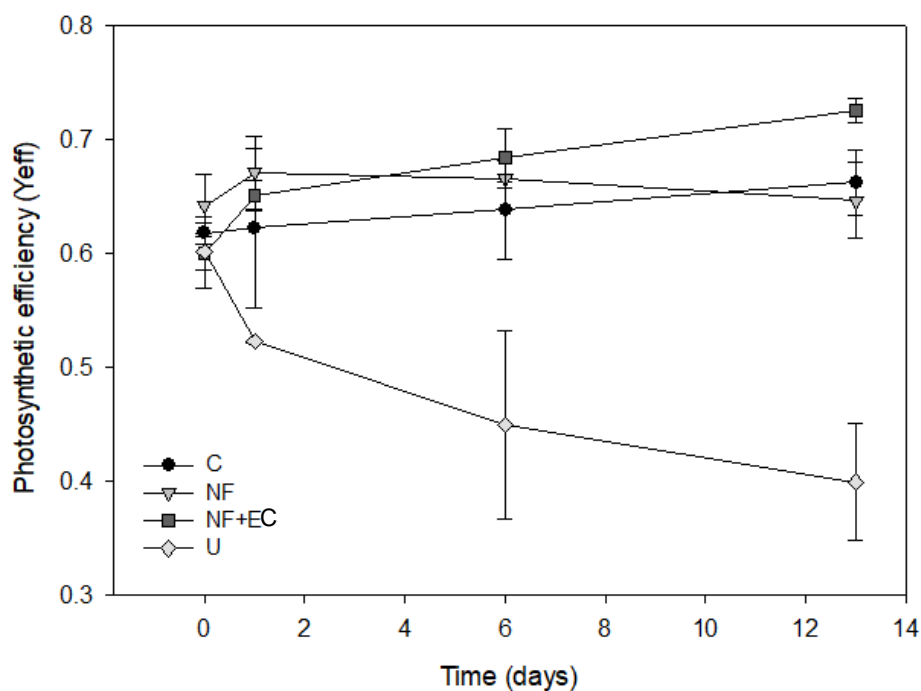
Figure 5.2: Photosynthetic efficiency (Yeff) of the biofilm on each treatment during the exposure period, mean ± SD (n=3). C= control, U= untreated mining effluent, NF= nanofiltration and NF+EC= combined treatments.

5.3.2.3. PHOTOSYNTHETIC COMMUNITY COMPOSITION

Just before the beginning of the exposure period (t0), all microcosms showed similar photosynthetic community composition (Figure 5.3), dominated by diatom (73±4%) followed by cyanobacteria (25±4%) and a negligible presence of green algae (1±1%) (ANOSIM, R = 0.02, p = 0.27). By contrast, a clear shift of the community composition was observed for the U effluent samples, just after 6 days of exposure (t6) (Figure 5.3), characterized by a significant increase of the relative abundance of green algae in the biofilm community compared to the other treatments (one-way ANOSIM, R = 0.04, p < 0.05). This trend continued until the end of the exposure period (t13) when green algae dominated (73±3%) the biofilm community in the U system, significantly differing from the other treatments (ANOSIM, R = 0.08, p < 0.05;) (Figure 5.3). The rest of treatments (NF and NF+EC) did not present changes in the biofilm photosynthetic community composition from t0 until t13, following the same trend as C (Figure 5.3).
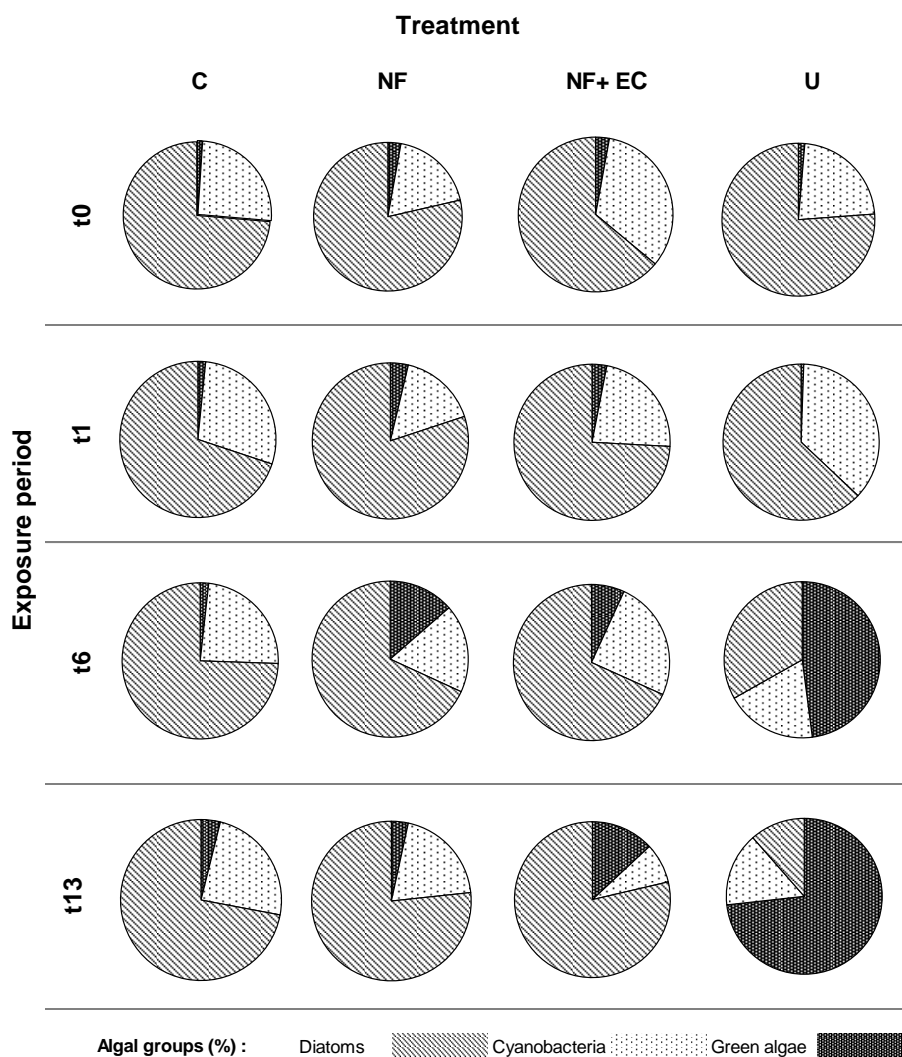
Figure 5.3: Relative abundance (%) of each algal group conforming the photosynthetic community composition of the biofilm on each treatment along the exposure period. C= control, U= untreated mining effluent, NF= nanofiltration and NF+EC= combined treatments. The results present the mean values of three replicates of each microcosm at each sampling date.

5.3.2.4. METAL BIOACCUMULATION

Just before the exposure (t0), the metal concentrations in the biofilm were similar among the microcosms. At the end of the exposure period (t13), significant differences were found in the Zn (one-way ANOVA, F = 23.5, p < 0.05), Pb (one-way ANOVA, F = 152.7, p < 0.05) and Cd (one-way ANOVA, F = 50.7, p < 0.05) metal content accumulated in the biofilm depending on the treatment. These differences were especially evident between the biofilm exposed to the U effluent and the C (Figure 5.4). Biofilm that was exposed to the U effluent contained 18-fold more Zn, 46-fold more Pb and 25-fold more Cd than C biofilm. On the other hand, the biofilm that was exposed to the effluent treated by NF+EC presented 3-fold more Zn bioaccumulation with respect to the C. In contrast, biofilm exposed to NF treated effluent did not present significant differences with the C for any of the metals measured (Figure 5.4Figure 5.4).
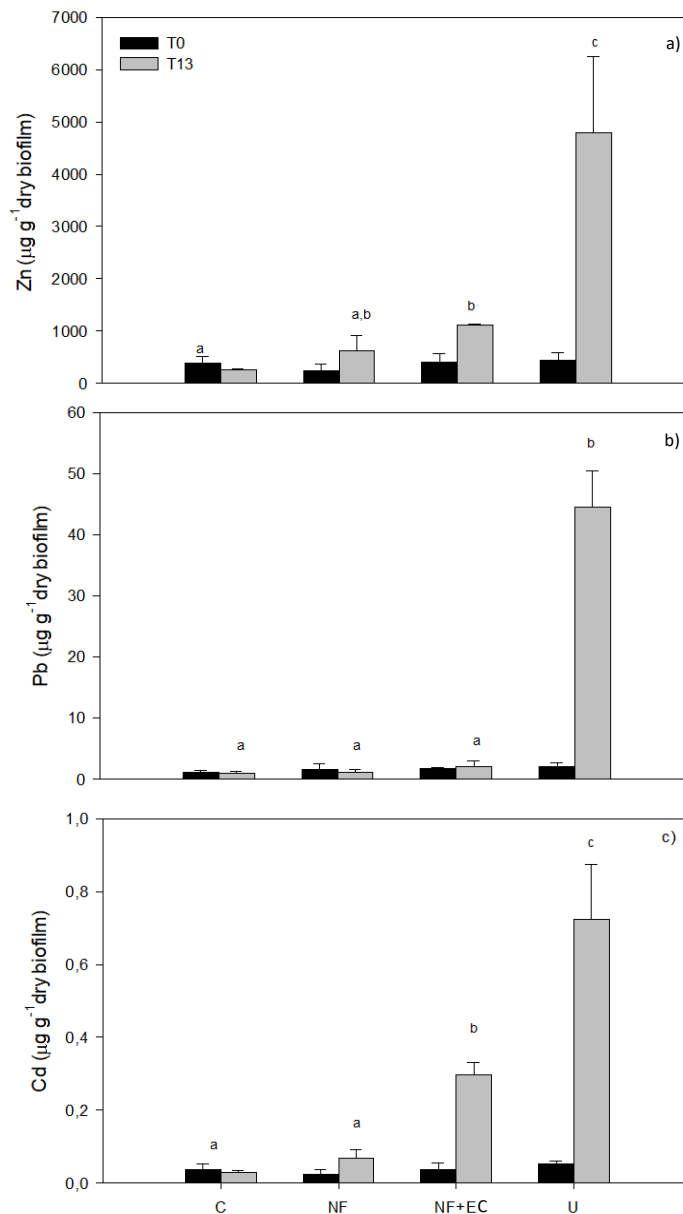
Figure 5.4. Metal bioaccumulation in biofilm just before the exposure period (t0) and after 13 days of exposure (t13) to the different treatments. C= control, U= untreated mining effluent, NF= nanofiltration and NF+EC= combined treatment. Mean ± SD (n = 3). The letters indicate significant differences (p < 0.05) between treatments after one-way ANOVA and Tukey's HSD test. a) indicates the Zn bioaccumulation. b) is for Pb bioaccumulation and c) Cd bioaccumulation in biofilm.

A significant positive correlation was found between green algal biomass, based on the main photosynthetic groups' densities, and Zn bioaccumulation (Pearson's correlation r = 0.83, p < 0.01) on the biofilm at the end of the exposure period (t13), which increased in a significant linear relationship (linear regression, R^2=0.69, p < 0.01). By contrast, a negative correlation between diatom biomass and Zn bioaccumulation was found (Pearson's correlation, r = -0.81, p < 0.01), which decreased in a significant linear relationship (linear regression, R^2 = 0.66, p < 0.01).
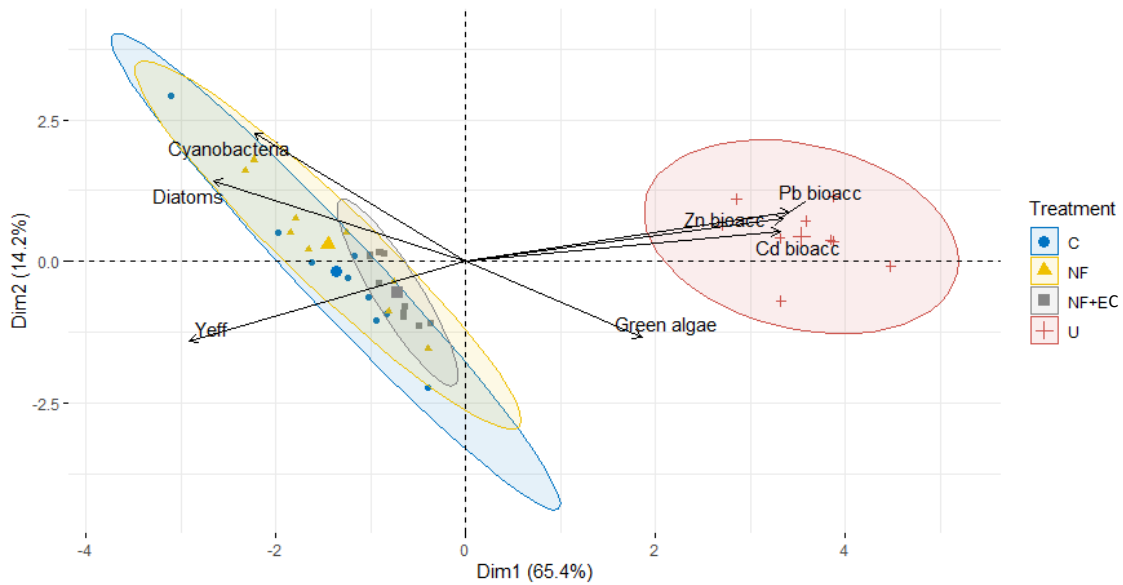
Figure 5.5: Biplot of the principal component analysis (PCA), with data points identified by treatment. Vectors plotted indicate the correlation scores between the community composition, metals bioaccumulation and photosynthetic efficiency at the end of the experiment (t13). The ellipses indicate 95% confidence around their centroids for treatment.

A principal component analysis (PCA) was used to visualize the difference among treatments at the end of the exposure period based on the community composition metal bioaccumulation and photosynthetic efficiency of the biofilm (Figure 5.5). The first axis of the PCA (explaining 65.4% of the variance) was linked to the pollution gradient, with higher values of metals bioaccumulated and the dominance of green algae in the U treatment. By contrast, C and treatments (NF and NF + E) appeared at the opposite side of this axis, indicating similar characteristics under a less impacted scenario. The data were plotted within the correlation circles and differentiated two main trends, the U treatment from the C, NF and NF+EC.

5.4. DISCUSSION

The primary aim of this work was to investigate the impacts of an abandoned metal mine effluent on freshwater ecosystems and the efficiency of different treatment technologies in reducing these impacts, using the aquatic biofilm as ecological indicator. The experimental setup allowed to simulate the chemical conditions generated by the entrance of a real metal mining effluent to a stream in order to assess the impact caused on natural aquatic biofilm, before and after the effluent treatment with two different technologies. The metal mining effluent used in this study was characterised by a high Zn concentration, thus the U effluent presented the highest Zn concentration in water (4.25 ± 1.15 mg Zn L^{-1}), which exceeded both European and US legislation limits, according to the Water Framework Directive (WFD) (Directive 2000/60/EC, 2000) and US Environmental Protection Agency (US EPA, 2014) respectively.

In this study, a variety of biofilm community alterations has been observed, including changes in the photosynthetic efficiency, community composition and metal bioaccumulation mainly caused by the exposure to U mine effluent waters. Photosynthetic efficiency, expressed as quantum yield is a sensitive indicator of metal toxicity to biofilm (Miller et al., 2017). In this study, as Tlili et al.(2011) and Bonet et al. (2014) demonstrated in similar studies, a drastical decrease in the photosynthetic efficiency was observed in biofilm under the untreated mining (U) effluent compared to the C just after 24h of exposure. The observed decrease of the photosynthetic efficiency indicated the damage produced by the metal exposure on the photosynthetic apparatus (Leal-Alvarado et al., 2016; Miller et al., 2017). In this regard, other studies evidenced that Zn concentrations of 450 μg Zn L^{-1} to 40 mg Zn L^{-1} in water, similar to those generated by the exposure to U mining effluent in our study, are enough to affect biofilm photosynthesis after short-term exposure (Bonet et al., 2013; Blanck et al., 2003). This decrease of the photosynthetic efficiency could be explained by the mode of action of Zn potentially targeting several photosynthetic processes of algae and cyanobacteria (Corcoll et al., 2012). For example, the in vivo substitution of magnesium, which is the central atom of chlorophyll-*a*, by heavy metals (such as Zn), could lead to a breakdown in photosynthesis (Corcoll et al., 2011).

In addition to the observed decrease in the photosynthetic efficiency, biofilm exposed to the U mining effluent also experimented a marked shift in the photosynthetic community composition after longer-term exposure (t13). Indeed, the relative abundance of green algae in this biofilm increased throughout the exposure period compared to the control, where diatom dominated during the whole experiment. Similar results were reported by Corcoll et al. (2011) and Ivorra et al. (2000) that found that green algae were favoured after several weeks of exposure to Zn in microcosms compared to diatom. In this sense, significant higher abundances of green algae have been reported at different confluences of mining effluents with stream waters in natural environments (Das and Ramanujam, 2011). Different mechanisms could enable green algae to tolerate chemical stress caused by heavy metal concentrations such as a decrease in the number of binding sites at the cell surface, internal detoxifying mechanisms (Gold et al., 2003) or additional enzymatic activity provided by metals (Pawlik-Skowronska 2003). These mechanisms were described by Corcoll et al. (2012) and are related to Zn toxicity that may enhance the synthesis of antioxidants causing the activation of the xanthophyll cycle of green algae as protective mechanisms to avoid Zn toxicity. By contrast, we observed a clear decrease in the relative abundance of diatom in the biofilm under the effect of the U mining effluent at the end of the exposure period. Higher abundances of deformed diatom have been reported in zinc polluted sites, which are indicative of toxic stress (Morin et al., 2014).

The functions of biofilm can be recovered after long term of exposure because the tolerant species ensure these functions by species replacement (Guasch et al., 2010, Corcoll et al., 2012, Tlili et al., 2010 and Barranguet et al., 2000). However, in the present study the biofilm functioning has not been recovered at the end of the exposure period. It is well known that high concentrations of Zn can inhibit the photosynthetic activity by blocking electron transfer at PSI and PSII levels, which stops oxygen production and CO_2 fixation (Ivorra et al., 1999).

Biofilm exposed to the U effluent indicated an ecological impact by showing inhibitory effects on photosynthetic efficiency just after 24 hours of exposure and a progressive shift of the photosynthetic community composition throughout the exposure period. This shift coincided with an increase of Zn, Pb and Cd bioaccumulation in this biofilm exposed to the U effluent compared to the C communities. Significant relationships between metal bioaccumulation in biofilm and dissolved metal concentration in water column have been found (Leguay et al., 2016), suggesting that the metal concentration in water explains a large amount of the variability in metal concentration inside biofilm. Biofilm has a large number of metal binding sites located in either mucopolysaccharide at the surface of cells or in the organic particles trapped by the biofilm. These substances can play an important role in the sorption of dissolved metals from water column on biofilm (Bere et al., 2012; Duong et al., 2008, 2010). The bioaccumulation of trace metals by algal cells is well known and generally increase with exposure time (Collard and Matagne, 1994). Green algae have the capacity to concentrate inorganic ions to amounts several thousand folds greater than in external dilute solutions by a variety of biological, chemical and physical mechanisms involving adsorption, precipitation and metabolism-dependent processes that operate simultaneously or in sequence (Bere et al., 2012). Metals become toxic for algae when intracellular metal is present at high concentrations and exerts a negative influence on the biochemical mechanisms occurring within the cells (Corcoll et al., 2012). The presence of metal ions can affect many aspects of biofilm communities including biomass, metabolic activity (e.g., enzyme activity, photosynthesis), and extracellular polymeric substances (EPS) productivity (Tang et al., 2017). In this regard, Zhu et al (2019) demonstrated that EPS productivity play the most important role in the community composition shift due to metal ion presence. EPS have many functional groups including carboxylates, hydroxyls, phosphates and sulphates (Sheng et al., 2010), which can change the size, distribution and surface properties of nanoparticles and thereby stabilize its dispersion or induce their aggregation (Quigg et al., 2013). As a result, EPS can be considered a protective barrier of microbial cells in periphytic biofilm from the exposure of nanoparticles (Joshi et al., 2012). However, the EPS production and composition changes of periphytic biofilm under nanoparticles exposure have been rarely reported (Liu et al., 2019).

Regarding the treatment technologies, biofilm exposed to the treated mining effluents showed similar responses than C biofilm, indicating the reduction of the ecological impact caused by the U, and therefore, the efficiency of the treatment technologies tested. In this regard, biofilm exposed to NF and NF+EC did not show any significant decrease in the photosynthetic efficiency compared to the control during the exposure period. However, the biofilm exposed to NF+EC treated effluent presented an increase of the photosynthetic efficiency above the control at the end of the experiment (t13). Ivorra et al. (2002) suggested that another adaptive response of individual algal species is the maintenance of a high photosynthetic efficiency under Zn stress. Indeed, the biofilm exposed to NF+EC treatment presented 3-fold more Zn bioaccumulation with respect to the C. It should be noted that the Zn content of the effluent obtained by both treatments were still exceed the EU standards (0.12 mg L^{-1}, EC 2000). The main reason for that is because NF and EC technologies were combined with the final aim to increase the water recovery rather than improving the NF permeate quality. In that sense, the EC step was treating the NF concentrate. After the E step, a sludge with a high metal concentration and a clean water effluent was obtained. The clean water effluent after the EC was mixed with the NF permeate, but the results obtained showed that the EC process was not very efficient and due to the high amount of metals present in the NF concentrate, the mixture of the two clean water effluents (NF+EC) resulted in a more polluted effluent than the NF.

The results obtained in this study contribute to a better understanding in the evaluation of the efficiency of treatment technologies that permit to reduce the ecological impact to the natural stream of a metal effluent, and additionally to the greater understanding of the response of fluvial biofilm to a metal mining effluent exposure. The technologies proposed to treat the metal mining effluents has proved to be a viable and valid option since the technology significantly reduced the amounts of metals present in the mine effluent. Due to this reduction, the biofilm functioning (photosynthetic efficiency) and structure (community composition) in biofilm exposed to the treated effluents did not show substantial differences respect to the C. At the same time, metal bioaccumulation in biofilm decreased drastically in biofilm exposed to these treated effluents compared to the U one, being equal to the C, in the case of NF. However, metal bioaccumulation on biofilm under the NF + E treatment was higher than the C, indicating that the mining effluent treated by these this technology could still cause certain environmental impact on the ecosystem, being evident only in the long-term.

5.5. CONCLUSIONS

Aquatic biofilm revealed that the tested treatment technologies offer an effective and viable solution to treat these metal effluents from abandoned mines. These technologies have the potential to significantly reduce the global environmental and ecological impact of mining operations and highlights the need to treat these highly polluting effluents. This study also evidences the ecological impact caused by the high concentrations of metals such as Zn, Cd and Pb in aquatic biofilm and the overall ecosystem as a result of abandoned metal mines. The work demonstrates the ability of biofilm to act as biological indicators of metal pollution due to their sensitivity and ability to accumulate metals from low concentrations in water, even below detection limits. In this regard, an effect in both functional and structural capacities as a shift of the phototrophic community composition and the decrease on the photosynthetic efficiency was observed. Therefore, the need to treat this metal effluent was highlighted, since the negative impact they generate on aquatic ecosystems was demonstrated. The development of this study has not only been useful to properly evaluate the negative ecological impacts caused by the metal mining effluents, but it has also been highly important to help in the improvement of the treatment system. Thanks to the results obtained, it has been seen that the combination of the NF and E technologies in the way initially planned (NF + E) was not as efficient as expected, indicating that combining the two technologies in a different way could be tested as an alternative to improve the efficiency of the technology in reducing the environmental and ecological impacts. However, it is also important to consider the dilution capacity of the natural stream where this effluents discharge since the ecological impact caused by mining effluents can be determined by both the efficiency of the treatment technology and the dilution capacity of the receiving stream. This dilution capacity will depend on the treated mining effluent load, the stream flow, and the heavy metals bioavailability, that could remain dissolved in water or adsorbed on suspended solids and sediments (Tchounwou et al., 2012). Besides, the potential capacity of these communities to recover from the impacts should be further addressed to determine whether the impacts posed by heavy metals on freshwater ecosystems would be permanent.

CHAPTER 6.

Responses and recovery of freshwater biofilms
receiving treated and untreated metal mining
effluents under different river dilution scenarios.

Photo: Artificial streams, by the author

6. EXPOSURE AND RECOVERY: THE EFFECT OF DIFFERENT DILUTION FACTORS OF TREATED AND UNTREATED METAL MINING EFFLUENT ON FRESHWATER BIOFILM FUNCTION AND STRUCTURE

6.1. INTRODUCTION

Metal effluents generated during mining activities are sources of water pollution that can arise while the mine is active but, without remedial action, this pollution source can persist long after the mining operation ceases (Younger et al., 2004). When mines are abandoned, mining effluents are discharged uncontrollably into the surrounding aquatic ecosystems. Due to that, around Europe, several river catchments are polluted by abandoned mines' effluents, which is considered an important source of pollution to freshwater ecosystems (Younger et al., 2004).

In mining effluents, when heavy metals are dissolved in water, they are easier to be absorbed or uptaken by aquatic organisms, leading to a bioaccumulative fate and biomagnification of the metal throughout the trophic network (Younger et al., 2003). Metal bioavailability in turn is determined by chemical speciation, which dictates that metals may be present in chemically different forms, i.e. as free ion or complexes with inorganic (e.g., Cl^-, $SO4_2^-$, CO_3^{2-}) and natural organic ligands; speciation is thus governed by water chemistry (Zhang et al., 2020). This is the case of aquatic biofilms, that are primary producers in freshwater ecosystems and represent the first level of the trophic food chain, from which metal bioaccumulation is transferred to higher trophic levels (Bere et al., 2012; Leguay et al., 2016; Hong et al., 2020).

Metal pollution could lead to a variety of biofilm responses including structural and functional changes with different ecological implications. Specifically, metal exposure can produce metabolic and functional alterations on the biofilm and, after long-term exposures, when the bioaccumulation of metals becomes higher, it can cause structural changes (Morin and Coste, 2006; Wu, 2016). For example, kinetics of algal growth, photosynthetic activity, chlorophyll-*a* concentration, nutrient uptake capacity and community composition may be altered in response to chemical stressors harboured in mining effluents (Corcoll et al., 2011; Vendrell-Puigmitja et al., 2020).

In order to reduce the impact of these mining effluents, different treatment processes such as chemical precipitation, chemical oxidation, ion exchange, nanofiltration, reverse osmosis, electrocoagulation and electrodialysis are used nowadays to treat metal mining effluents before discharging into the receiving stream (Tripathi and Rawat Ranjan, 2015). In this context, the LIFE

DEMINE project (LIFE16 ENV/ES/000218) has developed an innovative treatment process that combines electrocoagulation and microfiltration processes to effectively treat these effluents from abandoned mines with the final aim to obtain a non-polluting effluent to be discharge into the stream reducing its ecological impacts. This technology has been tested in Frongoch abandoned metal mine that exploited lead (Pb) and zinc (Zn) for almost 200 years and has been abandoned for nearly 200 years discharging uncontrollably since then to Afon Ysywyth catchment.

However, fluctuations in stream flow may determine the dilution capacity of the receiving stream, that can influence biogeochemical processes and surface water quality through complex interactions between hydrology and biogeochemical processes, including the production, release, and transport of pollutants such as heavy metals from mining effluents (Park et al., 2011). When a mining effluent is treated, the overall reduction in the ecological impact caused by the mining effluent will be determined not only by the efficiency of the selected treatment technology, but also by the dilution capacity of the receiving stream. This dilution capacity depends on the treated mining effluent load, the stream flow, and the heavy metals bioavailability, that could remain dissolved in water or adsorbed on suspended solids and sediments (Tchounwou et al., 2012).

The efficiency of the treatment technologies in reducing the ecological impacts to freshwater ecosystems were tested using biofilm communities as indicator. Biofilms are complex assemblages of algae, bacteria, fungi, protozoans, and meiofauna embedded in a matrix of extracellular polymeric substances (Sabater et al., 2007). Biofilms contribute to the overall river ecosystem functioning through key ecosystem functions such as nutrient uptake from the water column and the provisional or permanent retention of pollutants (Allan, 1995; Battin et al., 2016; Kaplan et al., 1987). Because biofilms are sensitive to several environmental factors (Romaní et al., 2013), they integrate environmental changes and present a rapid response to chemical pollution (Sabater et al., 2007), expressed as changes in biomass, community composition, and functionality (Taylor et al., 2004), making them good ecological indicators.

Although the toxic effects of heavy metals in freshwater communities have been widely described, very few studies have experimentally addressed the effects of a real and complex metal mining effluent on them. Additionally, the recovery capacity of stream biofilm communities after the exposure to a pollution source such as mining effluents has been less studied (but see Bonnineau et al., 2011; Lambert et al., 2012; Arini et al., 2012b; Bonet et al., 2013 and 2014; Pandey and Bergey, 2018). However, the interest in studying recovery

trajectories and community resilience in aquatic environments has increased in the recent years (Lambert et al., 2012). This growing interest comes from the increasing concern, especially through environmental policies such as the European Water Framework Directive (2000/60/EC), about the restoration of chemically contaminated aquatic ecosystems. In fact, during periods of exposure to pollutants, the community composition of aquatic organisms changes and loses ecological resilience which has long-term implications for ecosystem recovery (Clements et al., 2010). From the exposure to contaminants and other anthropogenic stressors, novel communities can result and form a new combination of species resulting from regime shifts that may provide very different ecosystem services (Wolff et al., 2019).

Given this background, the main purpose of the present study was to test the efficiency of the treatment technology proposed by the LIFE DEMINE project in reducing the ecological impact caused by mining effluents in freshwater ecosystems, using biofilm as bioindicator. Moreover, biofilm recovery capacity was assessed as well using untreated and treated mine effluent. To achieve these objectives, different dilutions capacities were used. We specifically focused on the following questions: (i) Which are the ecological effects caused by the treated and untreated mining effluent on the aquatic biofilm structure and functioning under different simulated stream dilution capacities? (ii) Are these communities able to recover their previous functions and structure when returning to steady conditions (during two weeks)? And iii) Do the treatment technologies decrease the overall ecological impact caused by the mining effluent? It was expected that the treated effluents would reduce the metal concentration in water and, as a consequence, lower ecological impacts would be observed. Additionally, the recovery of biofilm communities will depend on the impact caused by the exposure to the different metal concentrations during the exposure period. Although it is expected that those communities exposed to the treated effluent will be able to recover both function and structure after 16 days. By contrast, the untreated mining effluent will have chronic effects on biofilm communities and will be less effective in recovering since the biofilm structure and function will have been modified and therefore the corresponding ecosystems services.

6.2. MATERIALS AND METHODS

6.2.1. EXPERIMENT DESIGN

The experiment was conducted in eighteen independent recirculating Perspex channels (50 cm long x 12 cm wide). These artificial channels were designed to maintain the water column at 2 cm depth. Water input at the head of each channel unit was provided from a 5L carboy using a water pump connected with silicone tubes. The system was supplied with artificial water

simulating a pristine stream as described by Ylla et al. (2009). Water in the carboys was renewed every two days to prevent nutrient depletion during the whole experiment. Light-emitting diodes (SMD 5730 - 72) were used to provide natural light at an intensity of 110 µmol photons $m^{-2} s^{-1}$, following a 12h/12h light and dark cycle. The bottom of each channel was covered with 35 sandblasted tile glasses (1 x 1 cm, 3 x 3 cm, and 11 x 18 cm) as artificial substrate. Benthic biofilm colonization lasted for 21 days, and it was achieved by introducing aliquots of a natural biofilm suspension obtained from the pristine stream of Riera Major (Viladrau, Natural Park of Montseny, NE Spain) at each water renewal (every two days) during the colonization period.

The experiment included three different temporal periods: colonization (3 weeks), exposure (3 weeks) and recovery (2 weeks), and biofilm communities of each artificial stream were sampled at different times during each period (Figure 6.1). After the colonisation period, the exposure to the different treatments started. The experiment comprised four treatments that represented the treated (T) (0.8 mg L^{-1} of Zn, and not detected Pb and Cd) and untreated (U) (95, 8.6, and 0.7 mg L^{-1} of Zn, Pb and Cd respectively) metal mining effluent from Frongoch mine effluent, under two different flow conditions, obtaining a high dilution (HD) and low dilution (LD). These dilution factors mimicked the real dilution occurring when the metal mining effluent from Frongoch abandoned mine reached Frongoch stream under average or low flow conditions. The reference flow conditions were obtained of historical data from Frongoch stream provided by Natural Resources of Wales for the period 2004 to 2019. The historical average stream flow was 200 m^3 h^{-1} and the minimum 18 m^3 h^{-1}. Each treatment was performed in triplicate. Besides, three artifical streams were maintained with artficial water during all the experiment and used as a control (C). During the exposure and recovery periods, all the artificial streams were filled with artificial water for 14 days (recovery phase). Physico-chemical parameters (conductivity, dissolved oxygen, pH, and temperature) and nutrients concentration in water were measured in each channel before and after each water renewal. Benthic biofilm was sampled during the exposure (time 0, and after 1, 3, 7, 14 and 21 days) and the recovery period (after 1, 3, 7 and 16 days). At each sampling day, colonized glass tiles were randomly collected from each channel and analyzed for biofilm community composition, photosynthetic efficiency (Y_{eff}), soluble reactive phosphorous (SRP) and ammonium uptake capacity, chlorophyll-*a* concentration (chl-*a*), ash free dry mass (AFDM), metal accumulation in biofilm, microbial respiration, and different diatom metrics following methods described in Chapter 3 of this thesis.
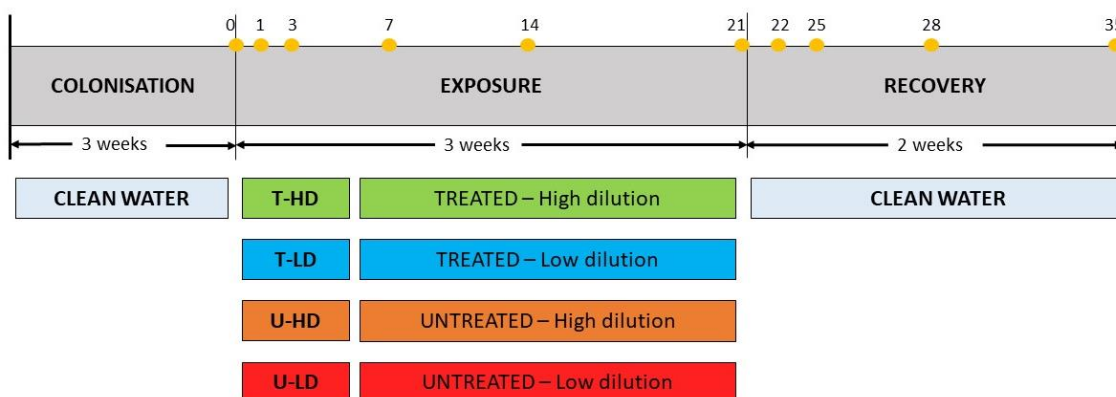
Figure 6.1: Experimental design and sampling times (yellow dots, in days) during the exposure and recovery periods.

6.2.2. DATA ANALYSIS

The effects of the treatment, dilution and their interaction on the biofilm response over time during the experiment were determined with data normalised to control using two-way repeated measures ANOVA (tw-rm-ANOVA). Differences among treatments were performed using post hoc with Tukey-b test. Differences in physico-chemical parameters between treatments during the colonisation, exposure and recovery periods were evaluated at each water renewal day using one-way ANOVA, as well as metal accumulation on biofilm and diatom metrics. Differences on physico-chemical parameters and diatom metrics over time between treatments were evaluated using one-way repeated measures ANOVA for the exposure and recovery period separately (rm-ANOVA), and using a post hoc with Tukey-b test. Normality was assessed with the Kolmogorov-Smirnov test and homogeneity of variances with the Bartlett test. All tests were performed using SPSS Statistics software (version 21). To determine differences among treatments on the biofilm community composition and the species conforming the diatom community within the biofilm, a one-way ANOSIM was carried out with Bonferroni correction using Past3 version 3.23 for the end of the exposure and the recovery periods. A principal component analysis (PCA) using R Studio software (version 3.6.0) was conducted to visualize the differences among treatments at the end of the exposure (t21d) and recovery (t14R) periods, based on both functional and structural variables evaluated. Pearson correlation analysis was performed to explore the relationship between biofilm variables.

The Threshold Indicator Taxa Analysis (TITAN, R package *TITAN2*) was used to classify the response of diatom taxa to significant environmental factors. TITAN is a combination of indicator species analysis and change point analysis (Dufrêne and Legendre, 1997). For each taxon, TITAN seeks an optimum observed change point that maximizes the indicator value (IndVal score) or its standardized IndVal score along a specific environmental gradient. Depending on the relative

abundance and occurrence frequency of the taxon on either side of the change point, it is assigned to a negative (vulnerable) or positive (tolerant) response group. The significant environmental factors were selected when a change point or threshold was detected, where there was a synchronous change in the abundance of a number of taxa lying within a narrow range of the predictor variable (Sultana et al., 2020).

6.3. RESULTS

6.3.1. WATER PHYSICO-CHEMICAL PARAMETERS

During the colonisation period, non-significant differences were found in the physico-chemical conditions among channels (Table 6.1). Water temperature and dissolved oxygen (DO) remained stable throughout the exposure period without differences between treatments (Table 6.1). By contrast, the pH was significatively lower than the control (C) at T-LD, U-HD and U-LD (Table 6.1, Tukey b $p < 0.05$) and the conductivity was significantly higher at T-LD and U-LD compared to the C (Table 6.1, Tukey b $p < 0.05$). Regarding the nutrient concentrations in water during the exposure period, soluble reactive phosphorus (SRP) did not differ between treatments (Table 6.1) while higher ammonium and nitrate concentrations were found at T-LD and U-LD compared to the C (Table 6.1, Tukey b $p < 0.05$). During the recovery period, only U-LD presented higher conductivity than the other treatments and the C (Table 6.1, Tukey b $p < 0.05$).

Regarding metal concentrations in water, during the exposure period any metal was detected in the C. At the end of the exposure period (t21d), Zn concentration differed among treatments and ranged between 0.19 ± 0.01 in T-HD to 21.3 ± 0.48 mg L^{-1} in U-LD (Table 6.1). Pb and Cd were detected only in U-LD (Table 6.1). At the recovery period, significant differences in Zn concentration were found between treatments T-LD, U-HD and U-LD compared to the C and among them (Table 6.1).

Table 6.1: Physico-chemical water variables measured in the streams during the colonization (n=12), exposure (n=9), and recovery periods (n=6) (Mean ± SD). bdl: below detection limit. DO, dissolved oxygen; T, temperature; Zn, zinc; Pb, lead; Cd, cadmium. n.a: not available. T-HD: treated high dilution, T-LD: treated low dilution, U-HD: untreated high dilution, U-LD: untreated low dilution. * rm-ANOVA; ** one-way ANOVA. The letters indicate significant differences (p < 0.05) between treatments after one-way and rm - ANOVA and Tukey b test.

	DO (mg L^{-1})	Conductivity (µS cm^{-1})	T (°C)	pH	N-NO$_3^-$ (mg L^{-1})	N-NH$_4^+$ (mg L^{-1})	SRP (mg L^{-1})	Zn (mg L^{-1})	Pb (mg L^{-1})	Cd (mg L^{-1})
Colonisation	9.53 (±0.04)	136 (±4.10)	15.8 (±0.17)	7.06 (±0.01)	0.36 (±0.05)	0.39 (±0.04)	0.12 (±0.00)	n.a	n.a	n.a
Exposure										
Control	9.64 (±0.58)	120 [a] (±6.32)	15.7 (±0.40)	6.96 [a] (±0.16)	0.38 [a] (±0.05)	0.30 [a] (±0.02)	0.11 (±0.01)	bdl	bdl	bdl
T-HD	9.52 (±0.52)	124 [b] (±7.43)	15.8 (±0.35)	6.96 [a] (±0.16)	0.39 [a] (±0.04)	0.32 [a,b] (±0.02)	0.11 (±0.01)	0.19 [a] (±0.01)	bdl	bdl
U-HD	9.41 (±0.46)	130 [c] (±4.64)	15.9 (±0.38)	6.72 [b] (±0.24)	0.39 [a] (±0.04)	0.35 [b,c] (±0.03)	0.11 (±0.02)	1.41 [b] (±0.06)	bdl	bdl
T-LD	9.49 (±0.48)	225 [d] (±12.0)	15.9 (±0.39)	6.69 [b] (±0.24)	0.56 [b] (±0.06)	0.39 [c,d] (±0.02)	0.12 (±0.02)	4.87 [c] (±0.25)	bdl	bdl
U-LD	9.47 (±0.40)	225 [d] (±10.6)	15.7 (±0.34)	6.29 [c] (±0.37)	0.60 [c] (±0.07)	0.43 [d] ±0.03)	0.10 (±0.01)	21.3 [d] (±0.48)	0.17 (±0.06)	0.04 (±0.01)
	n.s *	F = 393 p < 0.001 *	n.s *	F = 17.6 p < 0.001 *	F = 102 p < 0.001 *	F = 20.6 p < 0.001 *	n.s *	F = 42.5 p < 0.001 **	n.a	n.a
Recovery										
Control	9.86 (±0.45)	133 [a] (±7.09)	15.4 (±0.54)	7.00 (±0.30)	0.36 (±0.03)	0.30 [a] (±0.07)	0.11 (±0.01)	bdl	bdl	bdl
T-HD	9.92 (±0.23)	134 [a] (±8.75)	16.3 (±0.50)	7.15 (±0.51)	0.36 (±0.03)	0.36 [a,b] (±0.03)	0.13 (±0.01)	bdl	bdl	bdl
U-HD	9.95 (±0.20)	134 [a] (±7.81)	16.3 (±0.49)	7.11 (±0.11)	0.34 (±0.01)	0.33 [a,b] (±0.06)	0.12 (±0.02)	0.18 [a] (±0.02)	bdl	bdl
T-LD	9.80 (±0.24)	132 [a] (±1.85)	16.3 (±0.55)	7.12 (±0.12)	0.37 (±0.07)	0.34 [b,c] (±0.09)	0.13 (±0.01)	0.29 [b] (±0.04)	bdl	bdl
U-LD	9.78 (±0.12)	143 [b] (±6.14)	16.2 (±0.29)	7.04 (±0.09)	0.37 (±0.05)	0.38 [c] (±0.05)	0.12 (±0.01)	0.50 [c] (±0.04)	bdl	bdl
	n.s *	F = 502 p = 0.015 *	n.s *	n.s *	n.s *	F = 12.2 p = 0.001 *	n.s *	F = 13.3 p < 0.001 **	n.a	n.a

6.3.2. EFFECTS OF THE TREATMENT TECHNOLOGY AND MINE EFFLUENT DILUTIONS ON BIOFILM

6.3.2.1. PHOTOSYNTHETIC EFFICIENCY

The photosynthetic efficiency (Y_{eff}) of the biofilm significantly decreased after 24h of exposure in T-LD, U-HD and U-LD (Figure 6.2-a). Considering the Y_{eff}, the treatment process was only effective under the high-dilution scenario (T-HD), which remained equal to the control (C), but not in the T-LD that kept below the C, highlighting the dilution importance (tw-rm-ANOVA, F = 19.4, p < 0.001). By contrast, the untreated effluents maintained below the C (i.e., Y_{eff} < 0.45) independently of the dilution (Figure 6.2-a, tw-rm-ANOVA, F = 16.1, p < 0.001). During the recovery period, the photosynthetic efficiency recovered along time in all treatments without significant differences among them at the end of the recovery (Figure 6.2-b).
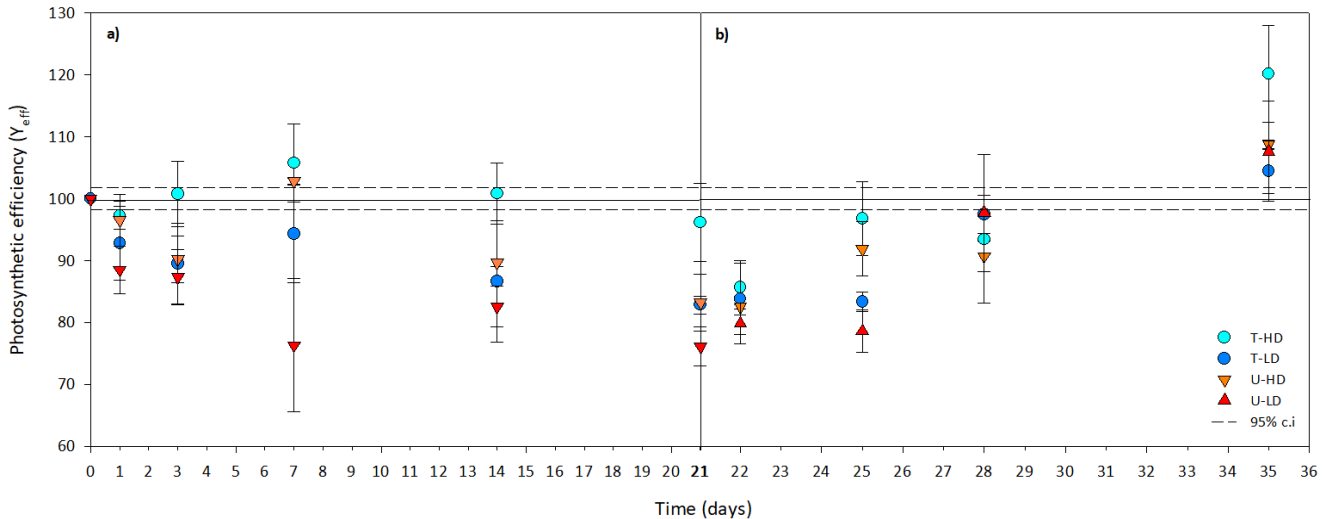
Figure 6.2: Photosynthetic efficiency (Yeff) of the biofilm communities under the different treatments during the exposure (a) and recovery (b) periods in % variation from control (black line). Values are mean ± SD (n = 3). c.i: 95% confidence interval (dash line). Circles correspond to the treated and the triangles to the untreated effluents. Light blue and orange correspond to high dilution and dark blue and red to the low dilution scenario. T-HD: treated high dilution, T-LD: treated low dilution, U-HD: untreated high dilution, U-LD: untreated low dilution.

6.3.2.2. NUTRIENT UPTAKE

During the exposure period, the P uptake rate coefficient (kSRP) significantly decreased and remained below the control for the cases: T-HD, T-LD and U-HD (Figure 6.3-a, Tukey-b test, p < 0.05) highlighting the effect of the interaction between treatment and dilution (tw-rm-ANOVA, F = 2.41, p < 0.001). By contrast, U-LD showed a significant increase in SRP compared to the control during all the exposure period (Figure 6.3-a). On the other hand, the NH_4^+ uptake rate coefficient (k NH_4^+) decreased drastically in all exposed biofilm compared to the C (Figure 6.3- c,

91

Tukey-b test, p < 0.05), despite T-HD remained above the other treatments (Tukey-b test p < 0.05) indicating significant influence of the treatment and dilution (tw-rm-ANOVA, F = 12.2, p < 0.05). Additionally, negative correlations were found between Zn accumulation and NH_4^+ uptake rate during the exposure period (Pearson's correlation r = -0.535, p = 0.040). During the recovery period, the nutrient uptake recovered in all treatments excepting for the T-HD and the U-LD (Figure 6.3-b,d). At the end of the recovery period, non-significant differences were found between the kSRP of the C and the T-HD, and $k$$NH_4^+$ of C and T-LD and U-HD (Figure 6.3-b,d) which evidenced a significant effect of the dilution and the treatment in the recovery (tw-rm-ANOVA (kSRP and $k$$NH_4^+$) F = 10.0, p < 0.05 and F = 27.7, p < 0.001, respectively)
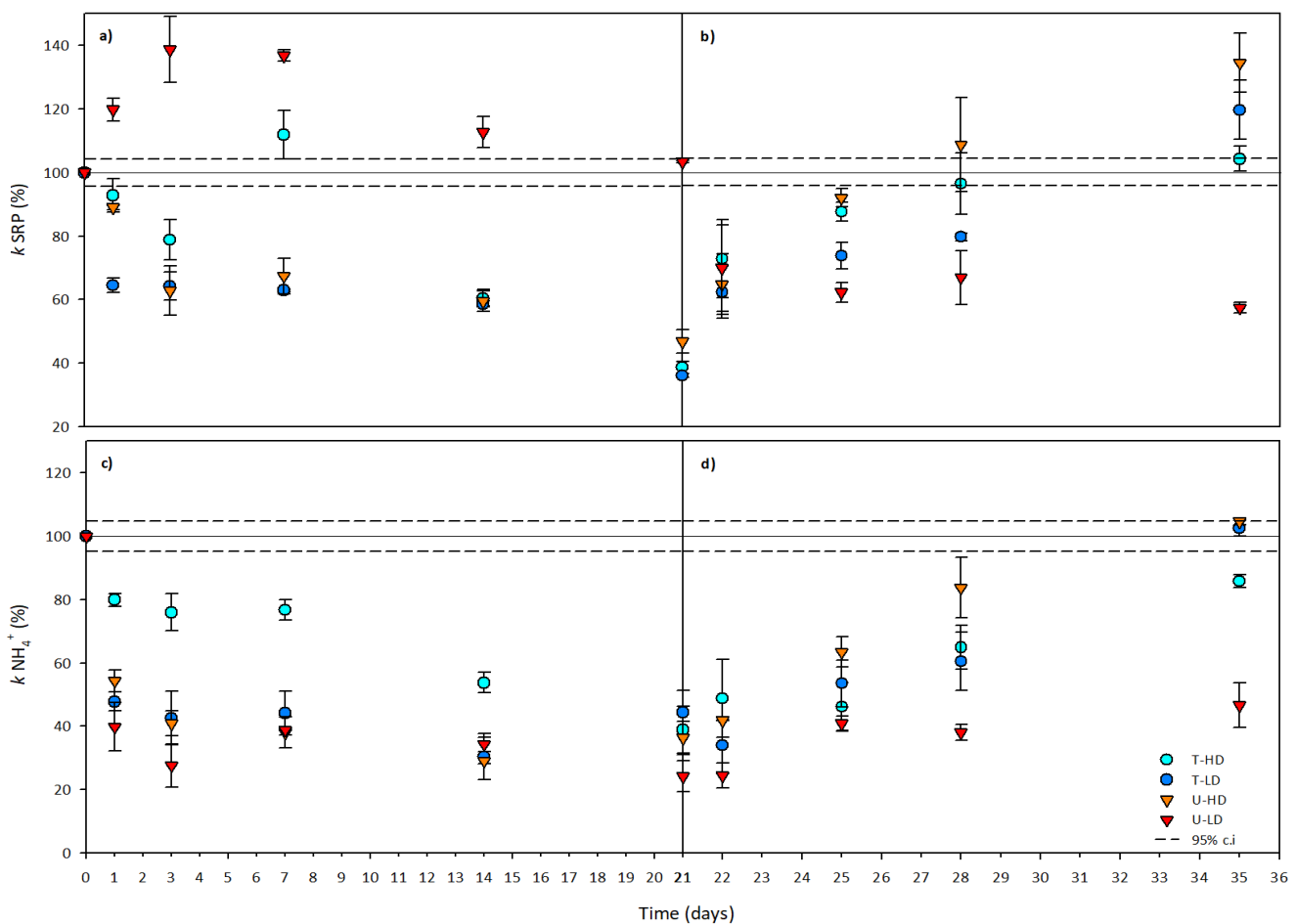
Figure 6.3: SRP and NH4+ uptake capacity of the biofilm communities under the different treatments during the exposure (a and c) and recovery (b and d) periods in % variation from control (black line). Values are mean ± SD (n = 3). c.i: 95% confidence interval (dash line). Circles correspond to the treated and the triangles to the untreated effluents. Light blue and orange correspond to high dilution and dark blue and red to the low dilution scenario. T-HD: treated high dilution, T-LD: treated low dilution, U-HD: untreated high dilution, U-LD: untreated low dilution.

6.3.2.3.   CHLOROPHYLL-*A*

The chlorophyll-*a* concentration (chl-*a*) in biofilm decreased significantly after 24h of exposure in all treatments compared to the control (C) (Figure 6.4-a). Even though treated effluents (T)

and U-HD recovered along time during the exposure period, they remained below the C at the end of this period. The dilution did not affect the treated effluents and non-significant differences were observed between T-HD and LD (Figure 6.4-a). By contrast, the interaction between treatment and dilution was significative in the response of the biofilm exposed to the untreated effluent (U) (tw-rm-ANOVA, F = 6.22, $p < 0.05$). In this regard, chl-a remained around 40% lower than the C until the end of the exposure period (Figure 6.4-a). During the recovery period, the U and the T-LD presented the lower chl-a highlighting the effect of the dilution and treatment (Figure 6.4-b, tw-rm-ANOVA, F = 14.4, $p < 0.05$ and F = 18.5, $p < 0.05$, respectively).
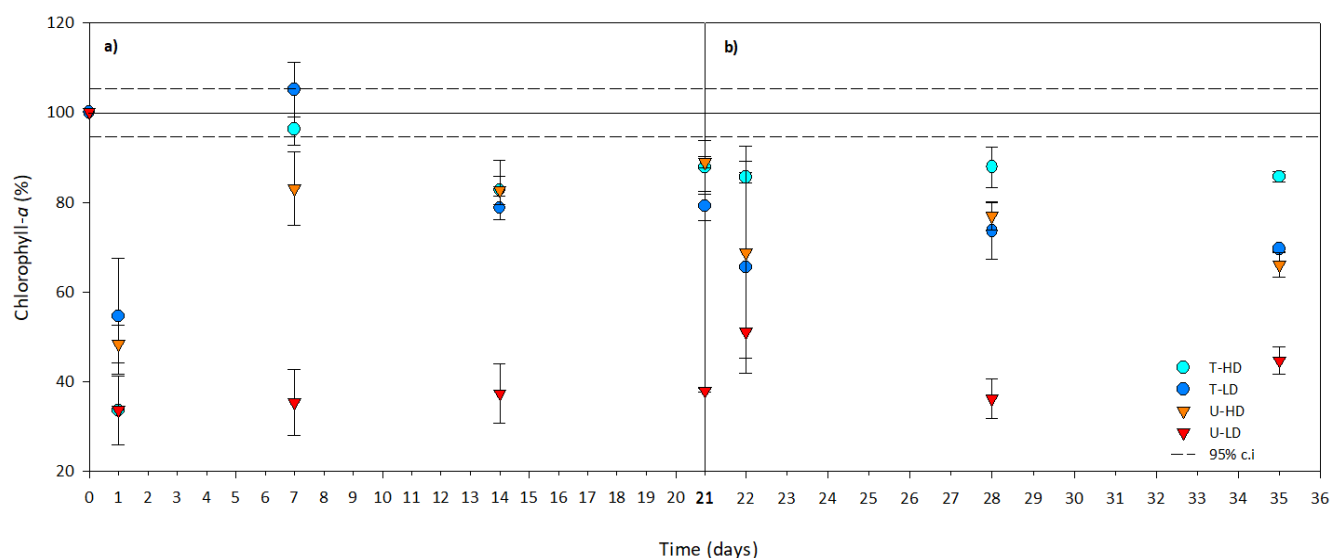
Figure 6.4: Biofilm chlorophyll-a concentration under the different treatments during the exposure (a) and recovery (b) periods in % variation from control (black line). Values are mean ± SD (n = 3). c.i: 95% confidence interval (dash line). Circles correspond to the treated and the triangles to the untreated effluents. Light blue and orange correspond to high dilution and dark blue and red to the low dilution scenario. T-HD: treated high dilution, T-LD: treated low dilution, U-HD: untreated high dilution, U-LD: untreated low dilution.

6.3.2.4.   BIOFILM COMMUNITY COMPOSITION

Regarding the biofilm community composition, diatoms dominated the biofilm community just before the starting of the exposure period, with an average relative abundance of 48.9 ± 3% in all channels (Figure 6.5). During the exposure period, the relative abundance of green algae increased in all treatments, being significantly higher than the C in T-LD, U-HD and U-LD at t21d (one-way ANOSIM R = 0.186, $p < 0.001$). At the end of the exposure period (t21d) a significant negative correlation was found between diatom abundance (based on the main photosynthetic group densities) and Zn concentration (Pearson's correlation r = -0.695, p = 0.004) in biofilm. During the recovery period, the communities kept dominated by green algae, even though an increase in the diatom relative abundance was observed in treatment U-HD compared to the C (one-way ANOSIM R = 0.365, $p < 0.001$).
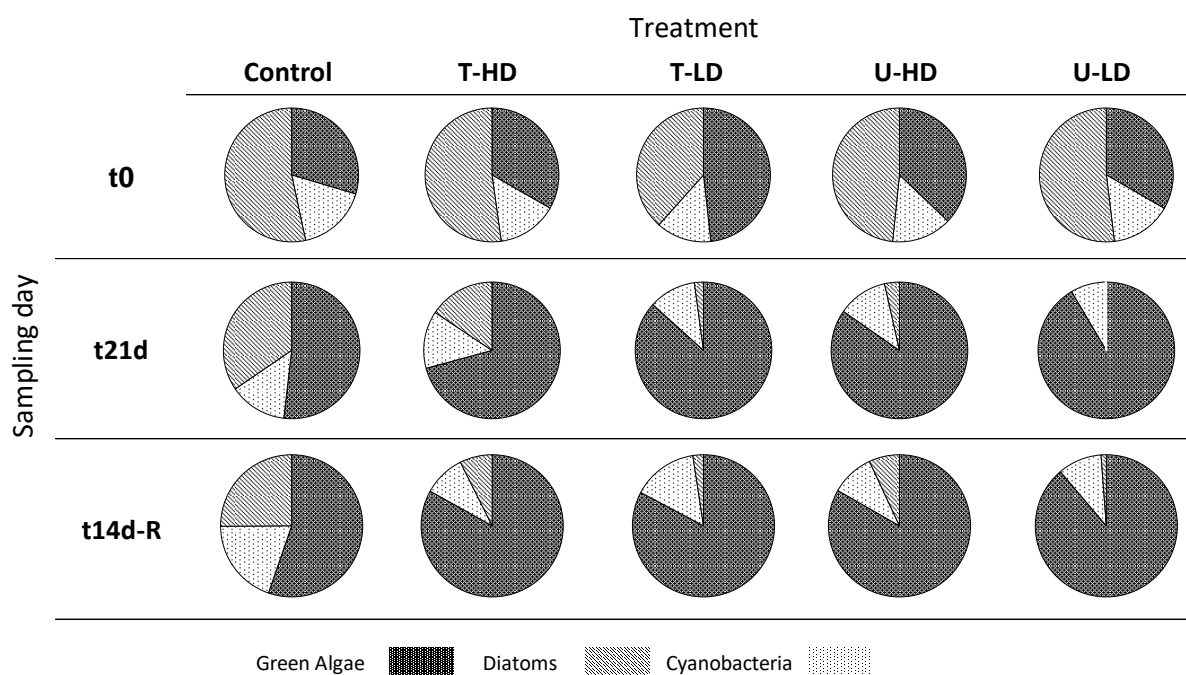
Figure 6.5: Relative abundance (%) of each algal group conforming the photosynthetic community composition of the biofilm on each treatment before the exposure period (t0) and after the exposure and recovery periods (t21d and t14R). The results present the mean values of three replicates of each treatment and sampling day. T-HD: treated high dilution, T-LD: treated low dilution, U-HD: untreated high dilution, U-LD: untreated low dilution. t0: before the exposure period, 21d: 21 days after the exposure, 14-R: 14 days after the recovery.

6.3.2.5.   METAL ACCUMULATION IN BIOFILM

Metal concentration in biofilm occurred throughout the exposure period. Significant differences were observed in the accumulation of Zn (one-way ANOVA, F = 93.2, p < 0.001), Pb (one-way ANOVA, F = 99.4, p < 0.001) and Cd (one-way ANOVA, F = 350, p < 0.001) in biofilm between treatments at the end of this period. These differences were especially evident in biofilm exposed to U-LD, that presented 80, 40 and 2-fold more Zn, Pb and Cd accumulation, respectively, than C biofilm (Figure 6.6). In contrast, biofilm exposed to T-HD did not show significant differences in metal accumulation respect to the C for any of the metals measured (Figure 6.6). At the end of the recovery period, still significant differences in the accumulation of Zn, (one-way ANOVA, F = 23.2, p < 0.001), Pb (one-way ANOVA, F = 4.97, p = 0.018) and Cd (one-way ANOVA, F = 30.2, p < 0.001) among treatments and the C were observed, being especially evident under U-LD that accumulated 23, 37 and 1.3-fold more Zn, Pb and Cd, respectively, than the C (Figure 6.6).

.
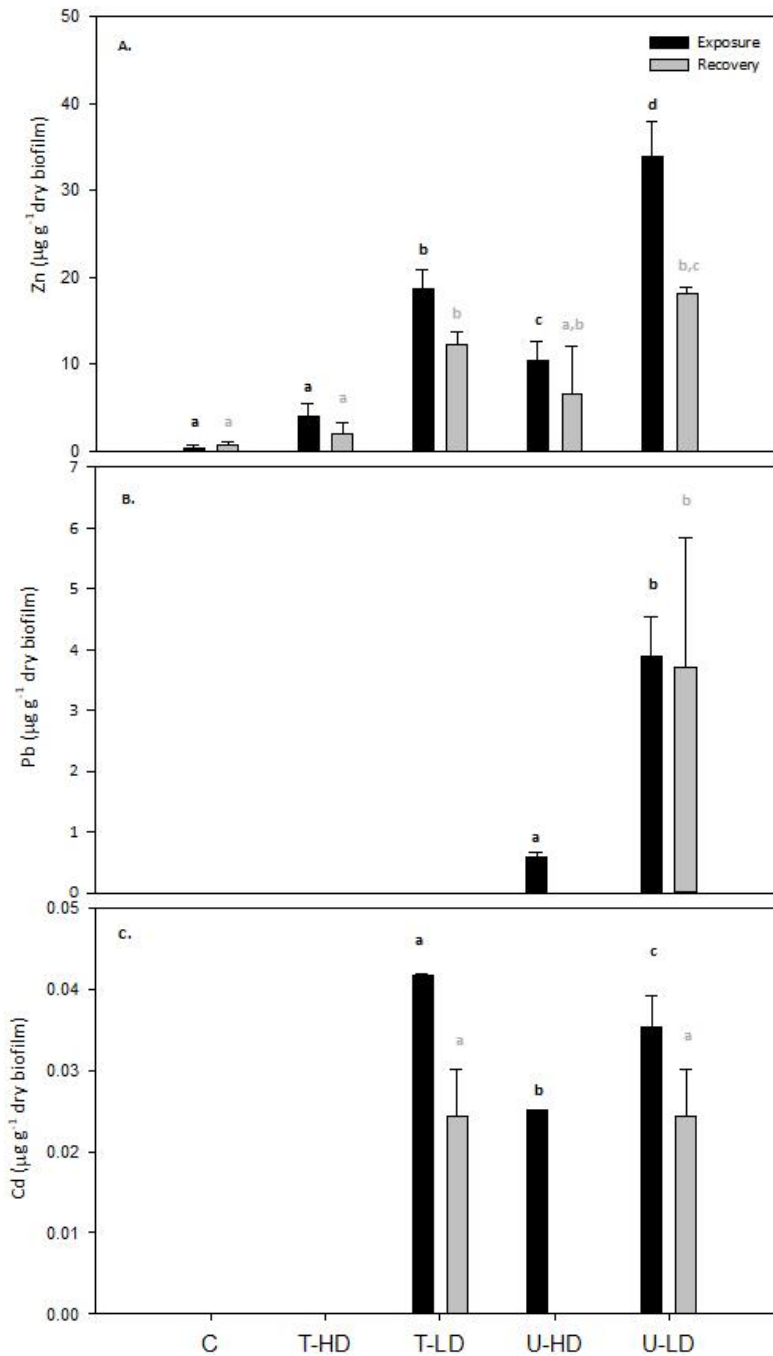
Figure 6.6: Metal accumulation in biofilms (A. Zn accumulation; B. Pb accumulation; C. Cd accumulation) under the different treatments at the end of the exposure (after 21 days) and recovery (after 14 days of recovery) period. T-HD: treated high dilution, T-LD: treated low dilution, U-HD: untreated high dilution, U-LD: untreated low dilution. Mean ± SD (n = 3). The letters indicate significant differences (p < 0.05) between treatments at each time (t21d and t14R) after one-way ANOVA and Tukey b test.

6.3.2.6.   DIATOM METRICS

After 7 days of exposure, a decrease in the diatom growth rate (GR) was observed in biofilm communities under T-HD, T-LD and U-LD compared to the control. These treatments remained below the C during all the exposure period (rm-ANOVA F = 6.86, p < 0.001) (Figure 6.7). The decrease was especially significant when exposed to treatment U-HD, however at the end of the

exposure period (t21d), nonsignificant differences were observed among the treated effluents (T) and U-HD, indicating the effect of the interaction between treatment and dilution (tw-rm-ANOVA, F = 372, p < 0.001). Eventually, diatom communities under all treatments presented a significant decrease in diatom cells size compared to the C (one-way ANOVA, F = 10.6, p < 0.001), being U-LD significantly smaller than the rest of treatments at t21d (Tukey b test, p < 0.05). In addition, a decrease on the diatom species richness after 3 days exposure (t3d) was observed and maintained during all the exposure period in all treatments (one-way ANOVA F = 1.72, p < 0.001) ranging the number of identified species from 34 in the C to 16 in the U-LD. From the different diatom samples collected, over 46 taxa were identified at the end of the exposure period (t21d) and significant differences were observed between the diatom communities exposed to the treatments compared to C (one-way ANOSIM, R = 1, p = 0.008, Figure 6.8). Furthermore, Zn accumulation presented negative correlation to the diatom GR (Pearson's correlation r = -0.785, p < 0.001), size (Pearson's correlation r = -0.794, p < 0.001) and species richness (Pearson's correlation r = -0.651, p = 0.009).

Nevertheless, during the recovery period an increase of the treatment was observed in the diatom growth rate (GR) compared to the exposure period. Biofilm exposed to T-HD increased above the C (10.3 ± 0.04 div day^{-1}), T-LD did not present significant differences to the C (10.1 ± 0.01 div day^{-1}), and those exposed to U-HD and U-LD maintained below the C (9.49 ± 0.03 and 9.88 ± 0.05 div day^{-1}) (Figure 6.7), being the treatment the significant variable in the recovery period (tw-rm-ANOVA, F = 89.2, p < 0.05). The diatom diversity did not recover under any treatment during the recovery period, and at t14R, it was observed similar diversity values than during the exposure period, ranging from 34 at C to 29, 21, 18 and 16 in biofilm exposed to T-HD, T-LD, U-HD and U-LD, respectively. Additionally, the species found under the different treatments presented significant smaller sizes than the C at t21d, in which the size ranged between 127µm in the C to 32.3µm in the U-LD (one-way ANOVA, F = 10.6, p < 0.001). At the end of the recovery period, the diatom size did not recover compared to the C and smaller forms were observed. However, at the end of this period, a significant change in the species dominance was observed in all treatments compared to the C. Specifically, it was observed an increase in *Navicula antonii* (Lange-Bertalot), which was the most abundant species under all treatments while *Nitzschia intermedia* (Hantzsch) disappeared (Figure 6.8).
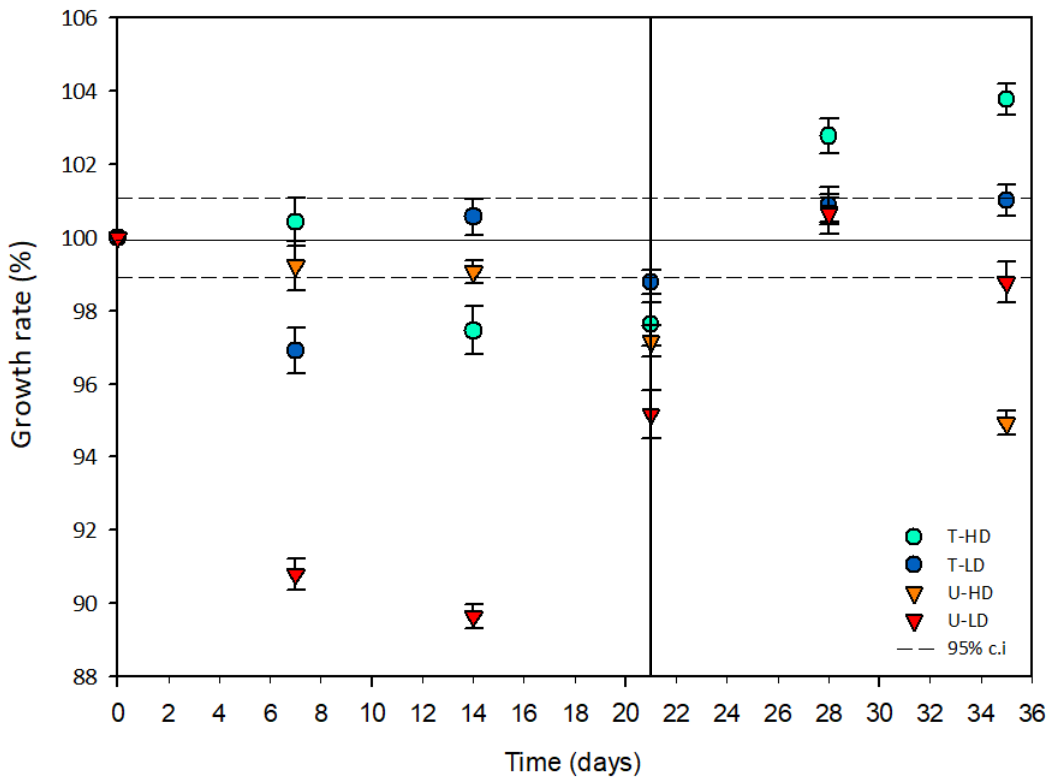
Figure 6.7: Diatom growth rate (div day^{-1}) (mean ± SD; n=3) at each treatment, during the exposure and recovery periods in % variation from control (black line). c.i: 95% confidence interval (dash line). Circles correspond to the treated and the triangles to the untreated effluents. Light blue and orange correspond to high dilution and dark blue and red to the low dilution scenario. T-HD: treated high dilution, T-LD: treated low dilution, U-HD: untreated high dilution, U-LD: untreated low dilution.
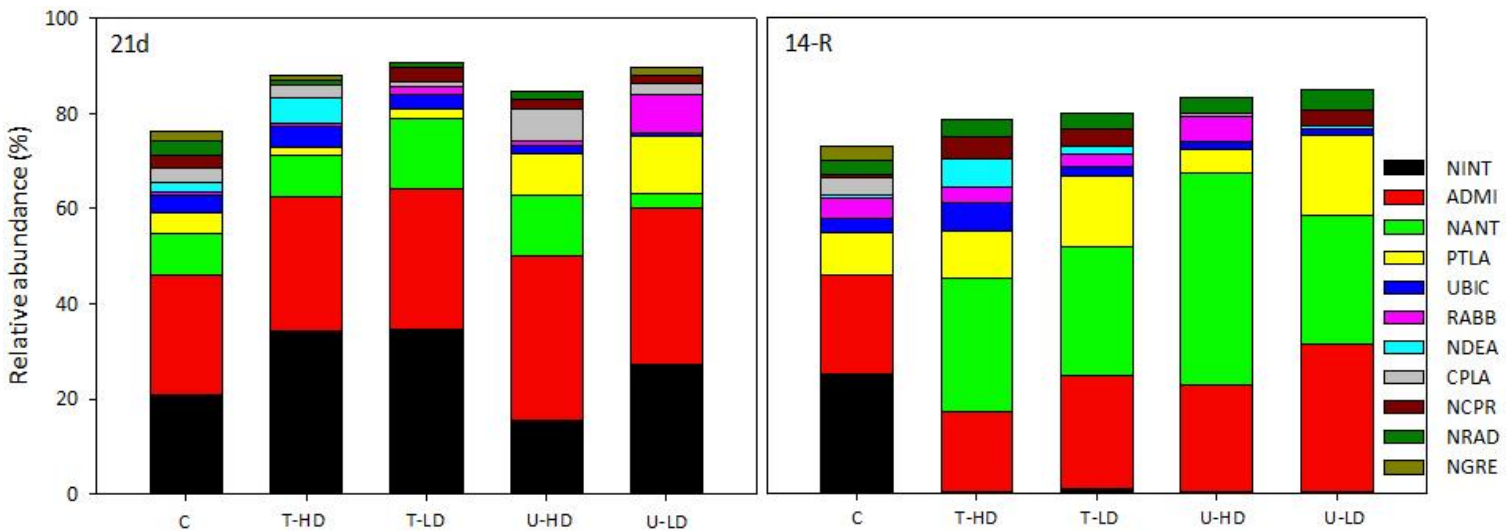
Figure 6.8: Relative abundance (mean value, n=3) of the ten major diatom species (>3%) within diatom communities collected in the artificial streams at the end of the exposure and recovery periods. Where *Nitzschia intermedia* (NINT), *Achnantidium minutissimum* (ADMI), *Navicula antonii* (NANT), *Plathonidium lanceolatum* (PTLA), *Ulnaria biceps* (UBIC), *Rhoicosphenia abbreviata* (RABB), *Navicula dealpiniana* (NDEA), *Cocconeis placentula* (CPLA), *Navicula capitoradiata* (NCPR), *Navicula radiosa* (NRAD), and *Navicula gregaria* (NGRE). 21d: 21 days after the exposure, 14-R: 14 days after the recovery.

6.3.3. THRESHOLD INDICATOR TAXA ANALYSIS (TITAN ANALYSIS)

TITAN analysis was applied to identify diatom indicator taxa and diatom community sensitivity thresholds to the pollution among the most abundant diatom taxa. The analysis was applied to the Zn and pH gradient since they showed the most significant response. The results demonstrated that the most negative responder taxa to Zn and pH gradient at t21d decreased at community-level change points of 0.79 mg Zn L^{-1} and pH 6.72, whereas at t14R, the decrease on the negative responders were found at 0.01 mg Zn L^{-1} and pH 7.06 (Figure 6.9). By contrast, the community-level change points for the positive responder taxa at t21d were calculated at 1.39 mg Zn L^{-1} and pH of 6.88, while at t14R the change points were found at 0.01 mg Zn L^{-1} and pH 7.09 (Figure 6.9). Most of the positive responder taxa were associated with higher pH, and negative responder taxa were related to high Zn concentrations. Using TITAN, we found that only a subset of the diatom taxa (range: 2%–20% of the 46 taxa depending on the environmental variable considered) responded reliably to the two environmental variables.
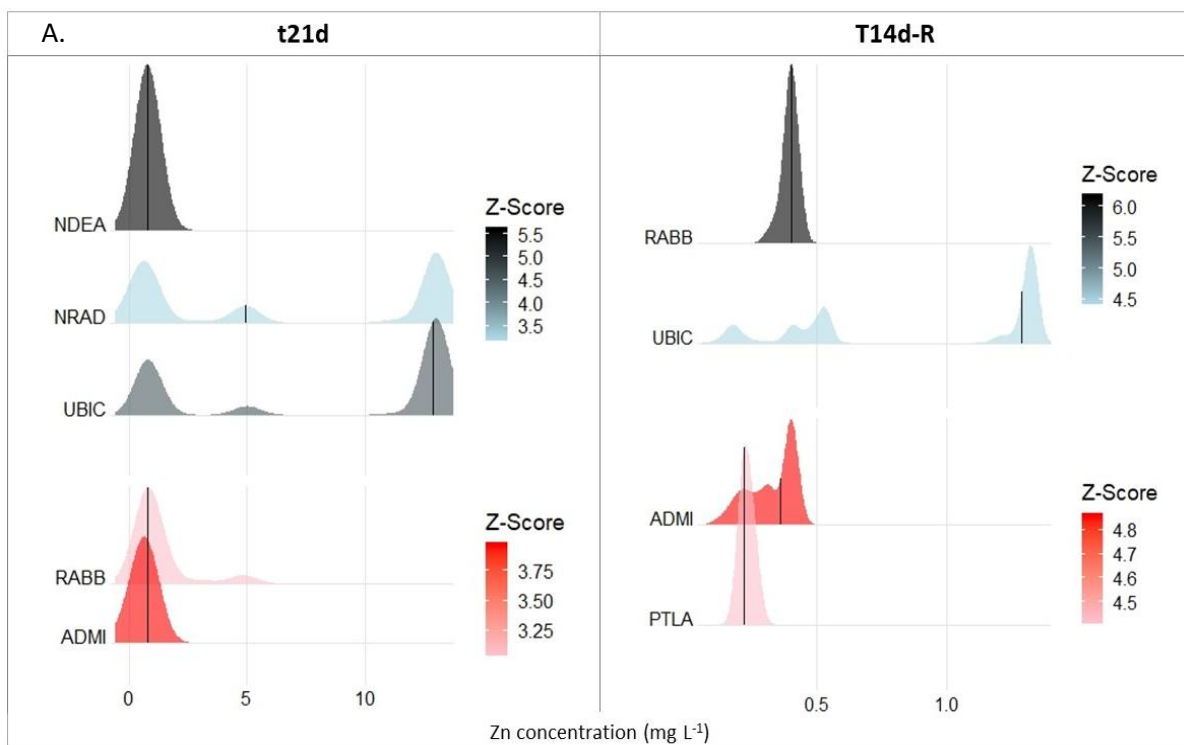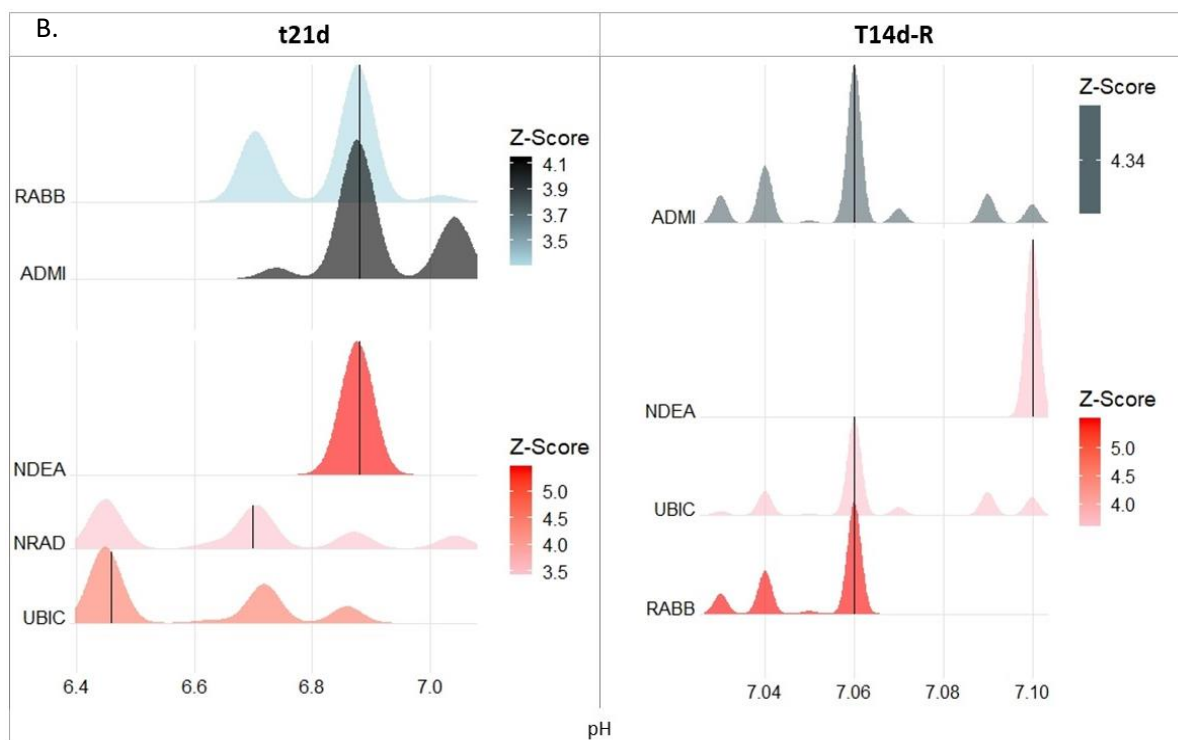
Figure 6.9: Plot of sum z-scores for responding diatom taxa along the A. Zn and B. pH gradient. Steep slopes indicate major change points in abundance. Red corresponds genera that increased with the increasing Zn and pH values (z+), and in blue the genera that negatively responded to the increase on pH and Zn (z-). 21d: 21 days after the exposure, 14-R: 14 days after the recovery.

6.3.4. OVERALL BIOFILM RESPONSES

A PCA biplot was performed at the end of the exposure and recovery periods to compare the overal structure and functional responses of the biofilm communities. The first axis of the PCA at t21d explained the 57.5% of the variance and was linked to the dilution factor (Figure 6.10-A). Treatments U-LD and T-LD were separated from the other treatments and the C, mostly driven by higher metal accumulation and green algae abundance in LD treatments. By contrast, the C showed the higher photosynthetic efficiency, nutrient uptake capacities, chl-*a* and diatom abundance. The second axis of the PCA explained the 21.2% of the variance and it was driven by cyanobacteria abundance and the IM, without any particular trend highlighted respect to the treatments.

On the other hand, the first axis of the PCA at t14R explained the 39.8% of the variance separating again LD treatments from the rest (Figure 6.10-B). These treatments are characterized by higher metal accumulation, green algae and cyanobacteria abundance. The second axis explained the 28.5% of the variance and separated treatments U-LD in the lower part of the PCA, from the rest. Regarding the second axis, treatment U-LD and T-LD were clearly

separated from the other treatments in the right part of the PCA at the end of the recovery period.
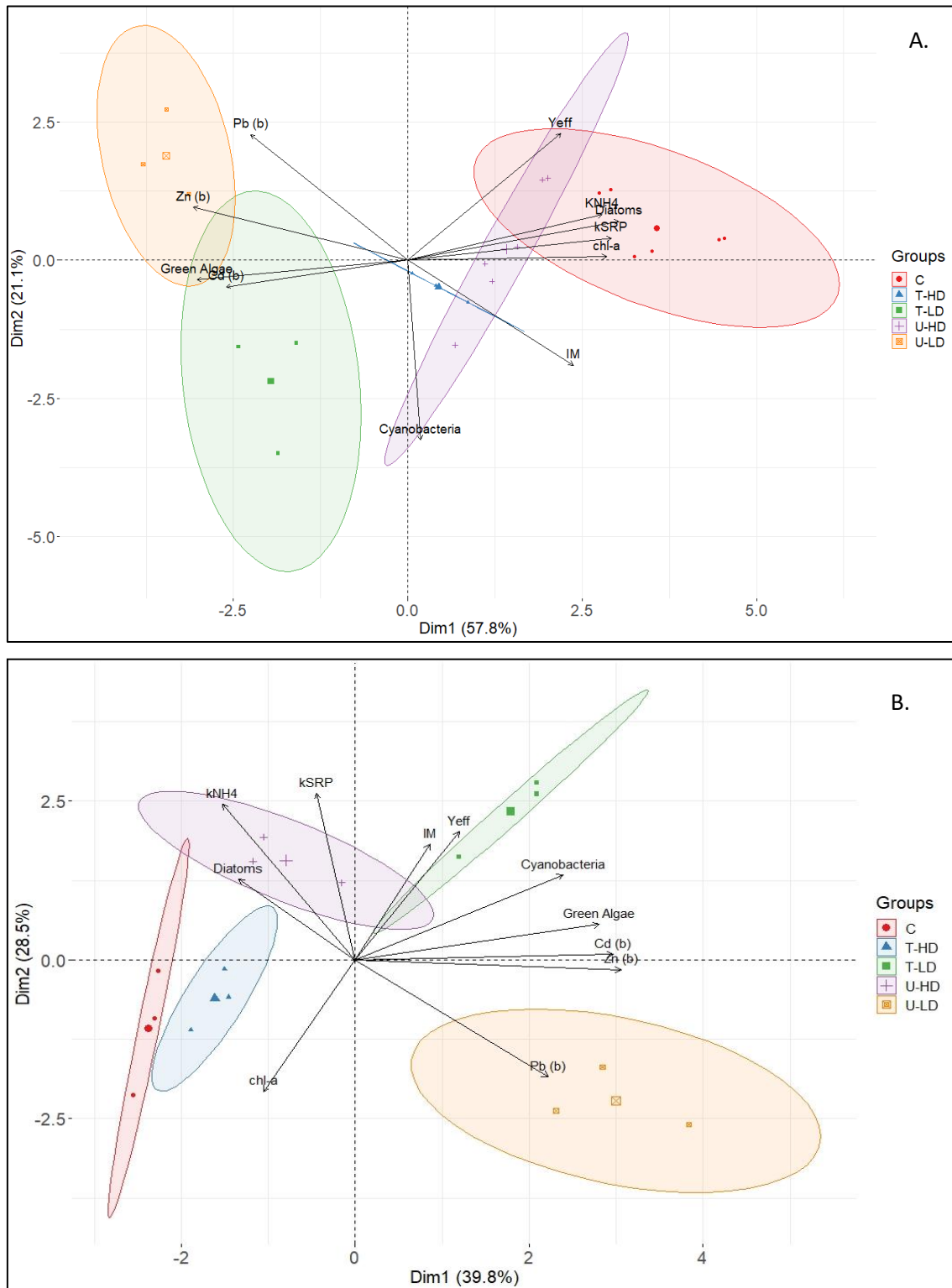
Figure 6.10: Biplot of the principal component analysis (PCA), with data points identified by treatment. Vectors plotted to indicate the correlation scores between the structural and functional variables evaluated at the end of the exposure (A) and recovery period (B). chl-a, chlorophyll-a; KNH4, ammonium uptake rate; KSRP, soluble reactive phosphate uptake rate; IM, Margalef index; Yeff, photosynthetic efficiency; Zn, Pb and Cd(b), metal accumulation. The ellipses indicate 95% confidence around their centroids for treatment. C: control in red circles, T-HD: treated high diluted in

blue triangles, T-LD: treated low diluted in green squares, U-HD: untreated high diluted in purple cross, U-LD: untreated low diluted in orange squares.

6.4. DISCUSSION

In this study, the efficiency of the technology developed in the LIFE DEMINE project (electrocoagulation + microfiltration) in reducing the ecological impact caused by the Frongoch mining effluent in the freshwater ecosystem was tested using the biofilm as bioindicator. Specifically, the effect of discharging the treated and untreated metal mining effluent when different dilutions occurred in the receiving stream were simulated using artificial streams. Additionally, the recovery capacity of these communities after being exposed to the treated and untreated metal mining effluent for 21 days was assessed. The experimental setup allowed us to simulate four different metal pollution scenarios that corresponded to the treated (T) and untreated (U) metal mining effluent under high (HD) and low dilution (LD) capacities of the receiving stream. Different biofilm alterations were observed, including changes in the photosynthetic efficiency, nutrient uptake rate, community composition, diatom metrics and metal accumulation mainly caused by the exposure to both treated and untreated mining effluent under the low diluted (LD) scenario.

6.4.1. BIOFILM FUNCTIONAL RESPONSES DURING THE EXPOSURE PERIOD

Regarding the functional changes, it was observed a drastic decrease in the photosynthetic efficiency (Y_{eff}) when biofilm was exposed to T-LD, and to all untreated treatments just after 24h of exposure that remained below the C until the end of the exposure. This effect has been previously described (Tlili et al., 2011 and Bonet et al., 2014), and might be explained by metals mode of action compromising different photosynthetic paths of biofilm communities (Admiraal et al., 1999; Prasad et al., 1999) where metal exposure inhibited the electron transport flow during the light period (Juneau et al., 2007). Similar results have been reported in the past when biofilm was exposed to 400 µg Zn L^{-1} under microcosms conditions (Corcoll et al., 2011). Additionally, the decay in the photosynthetic efficiency under Zn concentrations of 4.25 mg Zn L^{-1} was observed in the previous study performed with the same metal mining effluent but with a different set-up (see Chapter 5) (Vendrell-Puigmitja et al., 2020).

In addition to the decrease on the photosynthetic efficiency, the metal mining effluent caused a decrease in the SRP uptake capacity of biofilm exposed to T-LD, T-HD and U-HD, and in the NH_4^+ uptake capacity in biofilm exposed to all treatments. This indicated that the presence of heavy metals might have affected the biofilm capacity to assimilate P and NH_4^+ (Serra, 2009; Proia et al., 2017). The exposure to heavy metals is known to cause oxidative damage in the cells

that might have reduced the nutrient uptake capacity of exposed biofilm communities by oxidative stress (Sabater et al., 2007). The oxidative stress might have caused a change in the energy investment from nutrient uptake to antioxidant enzyme activities production as detoxification mechanisms (Morin et al., 2012; Bonet. 2013). This was also reported by Castro et al. (2015) and Tuulaikhuu et al. (2015) under arsenic (As) concentration of 130 µg L^{-1} and 37 µg L^{-1}, respectively.

However, an increase above the control on the SRP uptake rate during the exposure period in treatment U-LD was observed. During the nutrient uptake experiments, the biofilm communities that were exposed to the different metal mining effluents were spiked with four-fold more the background concentration of nutrients. In the highest metal concentration scenario, the increase in the SRP uptake might have been caused by abiotic removal of phosphorous promoted by the metal complexation with phosphate, such as $Zn_3(PO_4)_2$ and $Pb_5(PO_4)_3Cl$, leading to its precipitation (Zhu et al., 2016; Seshadri et al., 2017). In fact, in Lu et al. (2021) Zn precipitated with inorganic phosphate at Zn concentrations between 1 to 10 mg L^{-1}, which in this study the concentration was exceeded. This indicate that in the field, when the untreated mining effluent discharges to the stream in low flow conditions can cause phosphate removal from the water column through precipitation. This could be an impediment for freshwater organisms to growth and develop since SRP is an essential ion playing indispensable roles in ATP synthesis and mineralization, among other processes (Rumschik et al., 2009).

The decrease in the nutrient uptake capacity of biofilm communities might suggest that in the field, natural streams affected by metal mining effluents could have a decrease in the self-purification capacity, since biofilm directly participate in the nitrogen and phosphorus uptake and mineralization, which in front of a stressor, this function could be compromised (Bothwell 1988). This was observed by Castro et al. (2015) under realistic arsenic (As) concentrations. Furthermore, the nutrient uptake capacity of biofilm communities is influenced by the biofilm biomass (Guasch et al., 2003; Proia et al., 2017) which in this study decreased with the increase of the metal concentrations.

6.4.2. BIOFILM STRUCTURAL RESPONSES DURING THE EXPOSURE PERIOD

In addition to the different functional responses observed when exposed to different metal concentrations, structural changes were also detected. As previously exposed it was observed a decrease in biomass (i.e., chl-*a*) in those biofilms exposed to T-LD, U-HD and U-LD just after 24h of exposure and maintained below the C until the end of the exposure. This decrease was also observed after long-term exposures to 400 µg Zn L^{-1} in water by Corcoll et al. (2011) and up to

60 µg Cd g^{-1} dry weight and 1400 µg Zn g^{-1} dry weight accumulated in biofilm by Morin et al. (2007). This decrease could also be related to the substitution of magnesium, the central atom of chlorophyll, by heavy metals leading to an inhibition of chlorophyll production (Baumann et al., 2009; Corcoll et al., 2011).This observed decrease in the biomass, might imply effects on the freshwater ecosystems due to their role in the uptake or retention of inorganic and organic nutrients (Fishcer et al., 2002; Romaní et al., 2004), affecting the self-depuration processes, and transfer of energy to higher trophic levels (Corcoll et al., 2011). These effects were observed by Paulsson et al. (2002) at Zn concentrations between 6 and 25 µg L^{-1}. By contrast, Guasch et al. (2003), reported that Zn toxicity on biofilm was highly related to algal biomass thus the range of EC$_{10}$ values based on photosynthesis tests was very extensive (455 - 65,000 µg Zn L^{-1}). Regarding Cd, previous studies (Gold et al., 2003b; Morin et al., 2008) showed slight effects at 10 µg L^{-1}, and a prominent reduction of the biofilm biomass after chronic exposure to 100 µg L^{-1}. In relation to the Pb, Fechner et al. (2010) observed effects at Pb concentrations around 50 mg L^{-1}. In this study, the main effects in biofilm biomass and function (photosynthetic efficiency and nutrient uptake) were observed from Zn concentrations in water of 0.19 mg L^{-1}, and below the detection limit of Cd and Pb.

On the other hand, a shift in the biofilm community composition was observed at the end of the exposure period in all treatments, excepting for the T-HD. In this treatment, the relative abundance of green algae increased above the C, dominating the biofilm community. Additionally, as observed in the field (Chapter 4), the most polluted scenario (T-HD) did not differ significantly to the C even though green algae presented an increase. In fact, green algae are known to be favored after long-term exposure to Zn concentration in microcosms (Ivorra et al., 2000; Corcoll et al., 2011 and Vendell-Puigmitja et al., 2020). It is already known that green algae can be present in higher abundances in metal polluted natural environments (Das and Ramanujam, 2011). Different mechanisms could enable green algae to tolerate chemical stress caused by heavy metal concentrations such as a decrease in the number of binding sites at the cell surface, internal detoxifying mechanisms (Gold et al., 2003) or additional enzymatic activity provided by metals (Pawlik-Skowronska 2003). These mechanisms were described by Corcoll et al. (2012) and are related to Zn toxicity that may enhance the synthesis of antioxidants causing the activation of the xanthophyll cycle of green algae as protective mechanisms to avoid Zn toxicity. However, the observed increase in green algae could be an artifact of fluorescence interactions of some metals with the Benthotorch which artificially increase the green fluorescence, without any real increase of the abundance of chlorophytes (Paunov et al., 2018).

Despite diatom dominated (48.9 ± 3%) the biofilm community just before the exposure period started, this algal group drastically reduced its abundance during the exposure to T-LD, U-HD and U-LD, while remained similar to the control in T-HD. By contrast, the diatom size, biodiversity, and growth rate decreased in all treatments, including the T-HD. The diatom community response varied along the Zn concentration and pH gradient and the concentrations from which diatom abundance decreased was 0.79 mg Zn L^{-1} and pH 6.72. However, this response in the field (Chapter 4) was identified at 1 mg Zn L^{-1} and pH of 6.3. This might suggest that under field conditions, chronic exposures might promote adaptations to the pollution gradient. In this case, the diatom species identified above these thresholds were described as tolerant to metal concentration (Medley and Clements, 1998), and frequently reported in metal contaminated environments (Morin et al., 2012). Certainly, environmental factors such as the exposure to toxic agents (i.e., metals), determine the diatom composition by favoring tolerant species selection (Morin et al., 2012). On the other hand, diatom cell size and diversity decreased regardless of both treatment and dilution. In impacted sites, the decrease on the diatom cell size is related to the dominance of smaller growth forms (Sabater and Admiraal, 2005), since they are more effectively protected by the exopolysaccharidic matrix and thus its survival is favored under heavy metal pollution (Morin et al., 2012).

Furthermore, it was observed higher metal concentration inside biofilm when exposed to higher metal concentrations in water. However, even when Cd and Pb were not detected in water, they were found accumulated. Biofilms have a large number of metal binding sites located in either mucopolysaccharide at the surface of cells or in the organic particles trapped by the biofilm. These substances can play an important role in the sorption of dissolved metals from water column (Bere et al., 2012; Duong et al., 2008, 2010). The metals can slowly enter to the cells by active metal transport into the intracellular pool also called absorption or bio-uptake (Serra et al., 2009). The accumulation of metals by biofilm communities increase at larger exposure times (Collard and Matagne, 1994), and become toxic when intracellular metal is present at high concentrations and exerts a negative influence on the biochemical mechanisms of the cells (Corcoll et al., 2012). The presence of metal ions can affect many aspects of biofilm communities including biomass, metabolic activity (e.g., photosynthesis), and extracellular polymeric substances (EPS) production (Tang et al., 2017), which play the most important role in biofilm protection to metal toxiciyty (Zhu et al., 2019). In this study, biofilm presenting higher metal accumulation (T-LD, U-HD and U-LD), demonstrated the most significant changes in both functional (decrease in the photosynthetic efficiency and nutrient uptake rate) and structural responses (change in the algal biomass and a decrease in the diatom size, growth rate and

diversity) compared to the C. By contrast, T-HD did not presente differences in the metal accumulation compared to the C, but it was observed a decrease in the nutrient uptake rate, chlorophyll-*a* and diatom size, biodiversity and growth rate.

6.4.3. BIOFILM RESPONSES DURING THE RECOVERY PERIOD

During the recovery period, biofilm communities previously exposed to the mining effluent recovered the photosynthetic efficiency and algal biomass. Biofilm exposed to T-HD, T-LD and U-HD also recovered the nutrient uptake capacity during the transition to clean stream conditions. This recovery might be caused by the increase in the number of cell transporters excreting accumulated metals in cells as a consequence of a detoxification mechanism acquired after the exposure period (Castro et al., 2015). This extrusion was evidenced by the presence of Zn in water during the recovery phase (Table 6.1). However, during this phase, the presence of Zn in water could be caused by the metal desorption from the material of the artificial streams. By contrast, communities previously exposed to treatment U-LD did not recover the SRP and NH_4^+ uptake capacity, probably caused by the high metal accumulated still detected in these communities (Duong et al., 2009; Bere et al., 2011).

On the other hand, during the recovery period, green algae kept dominating communities previously exposed to treated and untreated effluents both under low and high diluted conditions, even though before the exposure period biofilm communities were dominated by diatom. Nevertheless, the diatom cell size and the growth rate of exposed biofilm still remained below the C at the end of the recovery period. Additionally, the diatom community composition of biofilm during the recovery period changed in comparison to the exposure period and the C. This shift in the diatom species dominance might be favored by the decrease of species dominant in the exposure period (mainly NINT) during the transition to clean conditions, that favored the growth of metal adapted ones such as *Rhoicosphenia abbreviata*. As Tlili et al. (2011b) reported, diatom composition changes are linked with the adaptation process to long-term Zn pollution. It is known that returning the adapted communities exposed to a pollutant to reference conditions may not be possible after crossing a critical threshold (Wolff et al., 2019). This suggest that the exposure to the metal mining effluent selected diatom species with a better capacity to regulate intracellular metal concentration by means of energy-dependent active transport systems (Castro et al., 2015) which might have favoured the growth and establishment of these species in the community that maintained the functional activity but not the structural recovery. Besides, adding new inoculum during the recovery period might have favoured the process where species physiologically affected by the metal exposure could be

replaced by more active species (Lambert et al., 2012). This indicated that structural changes could more prominent than the functional ones suggesting strong functional redundancy from the adapted community.

Differences observed in the community composition between treatment and the control might be explained by the duration of the recovery period. In this study, two weeks of recovery were simulated, and communities were not able to fully recover, indicating that a longer recovery period would be needed. For instance, Rimet et al. (2005) reported that diatom-dominated biofilm transferred from polluted to unpolluted site needed 40 to 60 days to recover according to the trophic diatom index (TDI). On the other hand, Arini et al. (2012a) reported incomplete biofilm recovery after 56 days of exposure to water free of metals. In addition, in our study, the fact that inoculum was not added during the recovery period could have affected the recovery of the biofilm community. Indeed, it was previously reported that the biofilm recovery was more pronounced when species immigration processes were possible (Ivorra et al., 1999; Morin et al., 2010). In this regard, Lambert et al. (2012) observed a full recovery after 4 weeks only when previously exposed communities were mixed with pristine communities, which favoured the diatom growth and green algae reduction. However, the retention of contaminants in the biofilm prevents complete removal of the stress even though it is no longer present in the bulk liquid phase (Ivorra et al., 1999), which might be the case of the most polluted scenario (U-LD).

According to the overall biofilm responses to the exposure period, functional and structural changes were more pronounced as higher the metal concentration in water was. In this regard, the treated metal mining effluent under high dilution (T-HD) presented the lowest metal concentration in water (0.19 mg Zn L^{-1}) achieving Zn removals of 97% compared to the U-LD, whereas under low dilution (T-LD) the metal concentration was higher (4.87 mg L^{-1}). In both cases, Pb and Cd were not detected in water. Specifically, T-HD exposed biofilm showed similar responses to the control (C) biofilm indicating a reduction in the overall ecological impact caused by the untreated mining effluent and therefore the efficiency of the treatment technology tested. However, treated mining effluent under low dilution conditions (T-LD) caused significant impacts in both functional and structural biofilm variables. In this case, the technology reduced the ecological impact, but it was demonstrated that is essential to consider the flow conditions of the receiving stream. In fact, the response of biofilm exposed to T-LD were similar to the untreated at both dilutions and it was observed that the metal concentration in the T-LD were higher than the metal concentration observed under the untreated mining effluent (U) at high dilution conditions (HD). Under low dilution, both treated and untreated caused an increase on the metal accumulation and a decrease on the biofilm' functionality (i.e., photosynthetic

efficiency and nutrient uptake rate) and structure (i.e., in the dominance, chlorophyll-*a* and diatom metrics).

6.5. CONCLUSIONS

This study indicated that metal mining effluents caused changes in the biofilm community composition and function. Early effects were mostly observed in functional variables of biofilm, such as photosynthetic efficiency and nutrient uptake. The long-term effects were observed in the biofilm community structure and diatom metrics. However, even though the technology achieved good metal removals and metals were not detected in the water, biofilm exposed to the treated effluents still presented higher metal accumulation compared to the C. This highlights the need to assess the efficiency of the treatment technologies under different flow conditions, since the ecological impact caused by the mining effluents on the receiving freshwater ecosystems depends on both, the effluent metal composition and concentration, and the dilution capacity of the receiving stream. In natural environments, lower flows and dilution capacities can occur, which might cause a decrease on the technology efficiency since higher metal reductions would have to be achieved to accomplish with the WFD limits of metal content in stream waters. In the treated effluent, the Zn concentrations in water remained above the EU limits, indicating that the dilution caused by the stream flow must be taken into account before discharging. Overall, the effects observed in this study were complex since the complexity of the effluent used, and so the expected responses in a real freshwater ecosystem would be even more variable.

CHAPTER 7.

Effects of an hypersaline effluent from an abandoned potash mine on freshwater biofilm and diatom communities.

.

Photo: Aquarium set-up, by the author

7. EFFECTS OF AN HYPERSALINE EFFLUENT FROM AN ABANDONED POTASH MINE ON FRESHWATER BIOFILM AND DIATOM COMMUNITIES.

7.1. INTRODUCTION

Freshwater salinisation has emerged as a topic of growing ecological concern (Cañedo-Argüelles et al., 2016; Kaushal et al., 2005). Salinity is considered as the total concentration of dissolved inorganic ions and it is an inherent component of all inland waters (Williams and Sherwood, 1994). Primary salinisation is considered when natural processes, as rainfall, rock weathering, seawater intrusion or aerosol deposits, lead to the ion content increase of inland surface waters (Cañedo-Argüelles et al., 2019). In contrast, the increase in ionic content of inland waters caused by human activities (i.e. construction activities, resource extraction or land cover changes increasing the transport of ions to surface), is considered as secondary salinisation (Kaushal et al., 2018; Steffen et al., 2011; Cañedo-Argüelles et al., 2019). Potash mining activities are considered an important driver of secondary salinisation (Cañedo-Argüelles et al., 2012), especially when these mines are abandoned, and uncontrolled polluted effluents are usually generated long after the end of the mining activity (Younger, 2000). In addition, the frequent lack of an effective regulatory framework to deal with abandoned mines in many regions contributes to perpetuate this legacy pollution. For example, despite the Mining Waste Directive (Directive, 2006/21/EC) of the European Parliament provides measures, procedures, and guidance to prevent or reduce any adverse effects on the environment, it does not clearly identify the administration that must deal with these effluents from abandoned mines, which frequently compromise the ecological status of the surrounding water bodies.

Freshwater salinisation has an impact on freshwater communities, including biofilm communities (Cañedo-Argüelles et al., 2017). These impacts on aquatic organisms affect the ecosystem structure and functioning (i.e. phosphorous removal from water column; Sauer et al., 2016) and can change the ecosystem services provided by freshwater ecosystems (Cañedo-Arguelles et al., 2020). In freshwater ecosystems, species richness decreases along a salinity gradient, and many freshwater species do not survive when a certain threshold of salinity is exceeded (Cañedo-Argüelles et al., 2019). Indeed, freshwater organisms have different sensitivities towards salinity stress and hence it is expected that the salinity increase alters the composition of the freshwater communities (Berger et al., 2019).

Biofilm are complex microbial communities, rich in species that can occur over a wide variety of environmental conditions and can display a rapid response to any change in the environment

(Besemer, 2015). Furthermore, microbial biofilm maintains the functioning of the ecosystem and contribute significantly to the mechanisms of absorption and processing of nutrient and pollutants, which lead to the self-depuration of running water ecosystems (Sabater et al., 2007). In addition, the Water Framework Directive (WFD) (Directive 2000/60/EC, 2000) identifies biofilm and specifically diatom as a biological compartment that should be targeted for assessing the ecological status of water bodies.

Biofilm responses to salinisation can lead to a reduction in algal cell density, growth and photosynthetic activity, as well as a shift in the taxon dominance when it is exposed to extremely high NaCl and $NaHCO_3$ concentrations in water (Entrekin et al., 2019). Regarding diatom, high salt concentrations have been reported to have effects on diatom communities reducing its density and altering its external morphology (Trobajo et al., 2011). In addition, chronic exposures can increase the percentage of nuclear abnormalities in the diatom assemblage (Cochero et al., 2017). However, little is known about the consequences of extreme salinities on its functioning and whether and to what extent changes in the species community structure can affect the biofilm functionality, and thus, the ecosystem functioning.

The main objective of this study was to assess the effects of a hypersaline effluent from an abandoned potash mine (Menteroda, Germany) on the structure and functioning of freshwater biofilm, especially on diatom communities, under laboratory conditions. It was initially hypothesized that high salt concentrations would have significant effects on aquatic biofilm community structure and function, likely a decrease in the algal and cyanobacteria biomass, and hence, on the photosynthesis capacity and nutrient uptake rates. Additionally, it was predicted a shift in the diatom community composition, since some taxa would increase in response to salinity, whereas others would decrease.

7.2. MATERIALS AND METHODS

7.2.1. EXPERIMENTAL DESIGN

This experiment was carried out using a mining effluent from the abandoned potash mine located in Menteroda described in the materials and methods section.

In a temperature-controlled chamber, six microcosms consisting of 6-L glass aquaria (as described in materials and methods) were used. Each microcosm contained 15 stream cobbles (previously scraped and autoclaved) used as substrates for natural biofilm colonization. The microcosms were filled with 3 L of artificial water, which was prepared to mimic a pristine stream as described in Ylla et al. (2009). A submersible pump (EDEN 105, Eden Water Paradise, Italy)

was installed in each microcosm to ensure the recirculation of water. During the whole experiment, the water of each microcosm was completely renewed every 2 days to avoid nutrient depletion. Temperature and photoperiod in the chamber were set at 20°C and 12 h light: 12 h dark using LEDs (LENB 135-lm, LENB/14.97/11.98), respectively.

In each microcosm, 15 mL of natural biofilm suspension obtained by scraping cobbles collected from the Riera Major at Viladrau (a pristine stream located in the Natural Park of Montseny, in NE Spain), was inoculated to promote the cobbles colonization. The biofilm suspension was added at the beginning of the experiment and at each water renewal during the colonization period to favor biofilm settlement.

After three weeks of colonization, the exposure period, which lasted for 16 days, started with the addition of water from the mining effluent. Two treatments were set: (i) the mining effluent from Menteroda abandoned mine (ME) and (ii) artificial water used as control (C). The exposure was set to mimic the realistic conditions of a river where a mining effluent of 4.30 m^3 h^{-1} reaches a river of 100 m^3 h^{-1}. To achieve these conditions, 0.20 L of the mining effluent was added to 2.80 L of artificial water in the respective microcosms creating a salinity concentration of 15.0 g L^-1, which was maintained at each water renewal. Each treatment was performed in triplicate.

7.2.2. PHYSICO-CHEMICAL CONDITIONS IN MICROCOSMS

Dissolved oxygen concentration and saturation, temperature (YSI professional plus, YSI Incorporated, USA), pH (G-PH7-2 portable pH meter XS PH7 + DHS), and conductivity (G-COND7-2 conductivity-meter portable XS COND 7+) were measured directly at each microcosm with sensor probes at each water renewal.

Triplicate water samples for each treatment (one sample *per* microcosms) were collected and filtered through a 0.22 μm pore diameter glass microfiber filter (Prat Dumas Filter Paper, Couze-St-Front, France). Water samples were frozen immediately and kept at -20°C until analysis. NO_2^-, NO_3^-, NH_4^+ and SRP were analyzed following APHA (1992a, b), Reardon et al. (1966) and Murphy and Riley, (1962) respectively.

7.2.3. BIOFILM SAMPLING

Biofilm was sampled before (T0) and after 1, 8 and 16 days of the addition of the mining effluents one day after water renewal. At each sampling day, three random cobbles were collected from each microcosm. Immediately after collection, photosynthetic activity and photosynthetic community composition were measured directly with an amplitude modulated flurimeter

(Mini-PAM fluorometer, Walz, Effeltrich, Germany) and BenthoTorch portable fluorimeter probe (bbe Moldaenke, Schwentinenta, DK) as defined in Vendrell-Puigmitja et al. (2020). Biofilm of the corresponding microcosm were then scraped using a toothbrush and suspended in water from the corresponding microcosm. Aliquots of 10 mL of biofilm suspension were then sub-sampled to analyze chlorophyll-a concentration, ash-free dry mass (AFDM) and diatom community (see below). The area of stones was measured by placing aluminum foil over the scratched surface and drawing the area of the stone and recalculating depending on the weight (Graham et al., 1988). Chlorophyll-a concentration and AFDM samples were stored at -20°C until analysis.

7.2.4. DATA ANALYSIS

Differences in physico-chemical variables, biofilm functional responses (photosynthetic efficiency and phosphorous uptake rate), and diatom metrics (diatom abundance, density, cell growth rate, size and species richness) between treatments were evaluated using one-way ANOVA for each sampling day. The effects of exposure throughout time were evaluated using one-way repeated measures analysis of variance (rm-ANOVA). Both analyses were carried out with SPSS Statistics software (version 21). One-way ANOSIM tests (using Bray-Curtis similarity coefficients) were carried out with Bonferroni correction on relative abundances of the biofilm community composition and diatom taxa in Past3 version 3.23. A principal component analysis (PCA) using R Studio software (version 3.6.0) was conducted to analyze the relationships between the biofilm parameters tested at the exposure period (T16). Statistical significance for all tests conducted was set at $p < 0.05$.

7.3. RESULTS

7.3.1. PHYSICO-CHEMICAL CONDITIONS OF THE MICROCOSMS

During the colonization period, the oxygen, temperature, conductivity, and pH remained stable with no significant deviations among microcosms (Table 7.1). Nutrient concentration decreased slightly between water renewals and nutrient depletion was prevented by the periodical water replacement every 2 days. Specifically, phosphate decreased from 120 (± 9) µg L^{-1} to 114 (± 8) µg L^{-1} on average at each water renewal, and the whole average nitrogen (DIN) decreased from 647 (± 47) µg L^{-1} to 509 (± 38) µg L^{-1} at each water renewal. Once the exposure period started, dissolved oxygen, water temperature and pH remained stable with no significant deviations, but the conductivity changed significantly in the ME treatment microcosms, increasing up to 13200 (± 268) µS cm^{-1} on average during the exposure period (Table 7.1).

Table 7.1. Physico-chemical conditions on each treatment (3 microcosms per treatment) during the colonisation (n= 9) and exposure (n= 4) period (mean ±SD). C= control, ME=mining effluent.

Period	Treatment	Physico-chemical parameters					
		Oxygen (mg L^{-1})	Oxygen (%)	Conductivity (µS cm^{-1})	Temperature (°C)	pH	SRP (µg L^{-1})
Colonization	C	7.80 (±0.10)	88.0 (±0.57)	2000 (±3.17)	21.1 (±0.20)	7.00 (±0.15)	120 (± 9.17)
	ME	7.60 (±0.08)	87.5 (±1.03)	196 (±7.80)	21.1 (±0.25)	7.00 (± 0.39)	119 (± 8.56)
Exposure	C	7.30 (±0.20)	81.0 (±2.01)	215 (±9.20)	20.4 (±0.62)	6.20 (±0.34)	122 (± 7.45)
	ME	7.50 (±0.09)	83.0 (±3.50)	13200 (±268)	19.8 (±0.55)	6.70 (±0.33)	110 (± 9.38)

7.3.2. BIOFILM COMMUNITY COMPOSITION AND FUNCTIONING

7.3.2.1. CHLOROPHYLL-A CONCENTRATION AND AFDM

Chlorophyll-*a* concentration in the biofilm increased progressively during the exposure period in C and ME, being slightly higher in ME than C at the end of the exposure (Table 7.2). Just before the exposure period started (T0), the chlorophyll-*a* was 1.76 (±0.72) µg cm^{-2}, whereas at the end of the exposure period (T16) it was 4.44 (±0.42) µg cm^{-2} for C and 5.13 (± 0.09) µg cm^{-2} for ME. AFDM reached its maximum at T8 in both cases, being 0.58 (±0.71) mg cm^{-2} in C and 1.15 (± 1.78) mg cm^{-2} in ME, without significant differences between them (one-way ANOVA F = 0.7, p = 0.570). At the end of the experiment (T16), both treatments showed a significant decrease in the AFDM from T8, but without significant differences between them (rm- ANOVA F = 2.5, p = 0.100).

7.3.2.2. PHOTOSYNTHETIC COMMUNITY COMPOSITION

The photosynthetic community composition of the biofilm over time was mainly formed by diatom on both treatments. ME exposure leaded to a significant change in community structure, and diatom were significantly affected over time (Table 2). Specifically, diatom abundance resulting significantly higher in ME-exposed biofilm particularly from T8 (Table 7.2) until the end of the exposure (T16) when its abundance doubled that of C biofilm (Figure 7.1, Table 7.2).
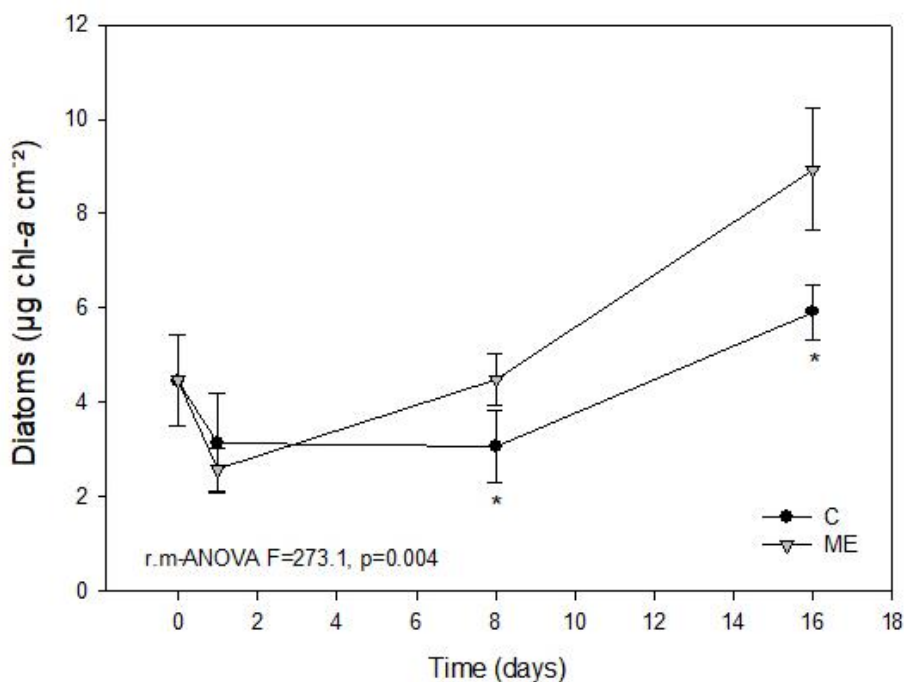
Figure 7.1: Diatom abundance (µg chl-a cm^{-2}) (mean ± SD), n=3. ✳: significant difference (p < 0.05).

7.3.2.3.   DIATOM METRICS

During the experiment, an increase in the diatom growth rate (GR) was observed for both C and ME-exposed biofilm. Nevertheless, at the end of the experiment the GR was significantly higher in ME-exposed biofilm than in the C (Figure 7.2-a, Table 7.2). In addition, after 8 days of exposure, and until the end of the experiment, an increase of diatom cell density was observed in ME-exposed biofilm ($1.65 \cdot 10^7 \pm 5.14 \cdot 10^4$ cell div mL^{-1}) being higher than in the C at the end of the experiment (Figure 7.2-b, Table 7.2). By contrast, a significant decrease in the average cell size was observed in ME-exposed biofilm (9.42 ± 0.71 µm) compared to the C (30.1 ± 3.14 µm) (Figure 7.2-c, Table 7.2).

Over 44 diatom taxa were identified from the different biofilm samples collected in all sampling times. Species richness (S) and diversity index (H') were significantly different between the C and the ME at the end of the experiment (Table 7.2). Under the influence of the mining effluent (ME), a loss of species richness (S_{ME} = 9, S_C = 42) and diversity (H'$_{ME}$ = 1.15, H'$_C$ = 2.79) of diatom communities within biofilm were observed at T16. Taxonomic composition and relative abundance of diatom species were markedly different between C and ME-exposed biofilm (Figure 7.3, Table 7.2). ME-exposed diatom communities were characterized by significantly smaller species (Table 2) such as *Fragilaria crotonensis* Kitton (FCRO), *Navicula reichardtiana* Lange-Bertalot (NRCH), *Nitzschia intermedia* Hantzsch ex Cleve and Grunow (NINT),

Rossithidium pusillum (Grunow) *Round and Bukhtiyarova* (RPUS) and *Rhoicosphenia abbreviata* (C.Agardh) Lange-Bertalot (in less than the 2%) (Figure 7.3). For the C biofilm, the predominant taxa were *Fragilaria crotonensis* (FCRO), *Navicula reichardtiana* (NRCH), *Nitzschia tropica Hustedt* (NTRO), *Ulnaria biceps* (Kützing) Compère (UBIC) and *Cocconeis euglypta* Ehrenberg (CEUG) (Figure 7.3).
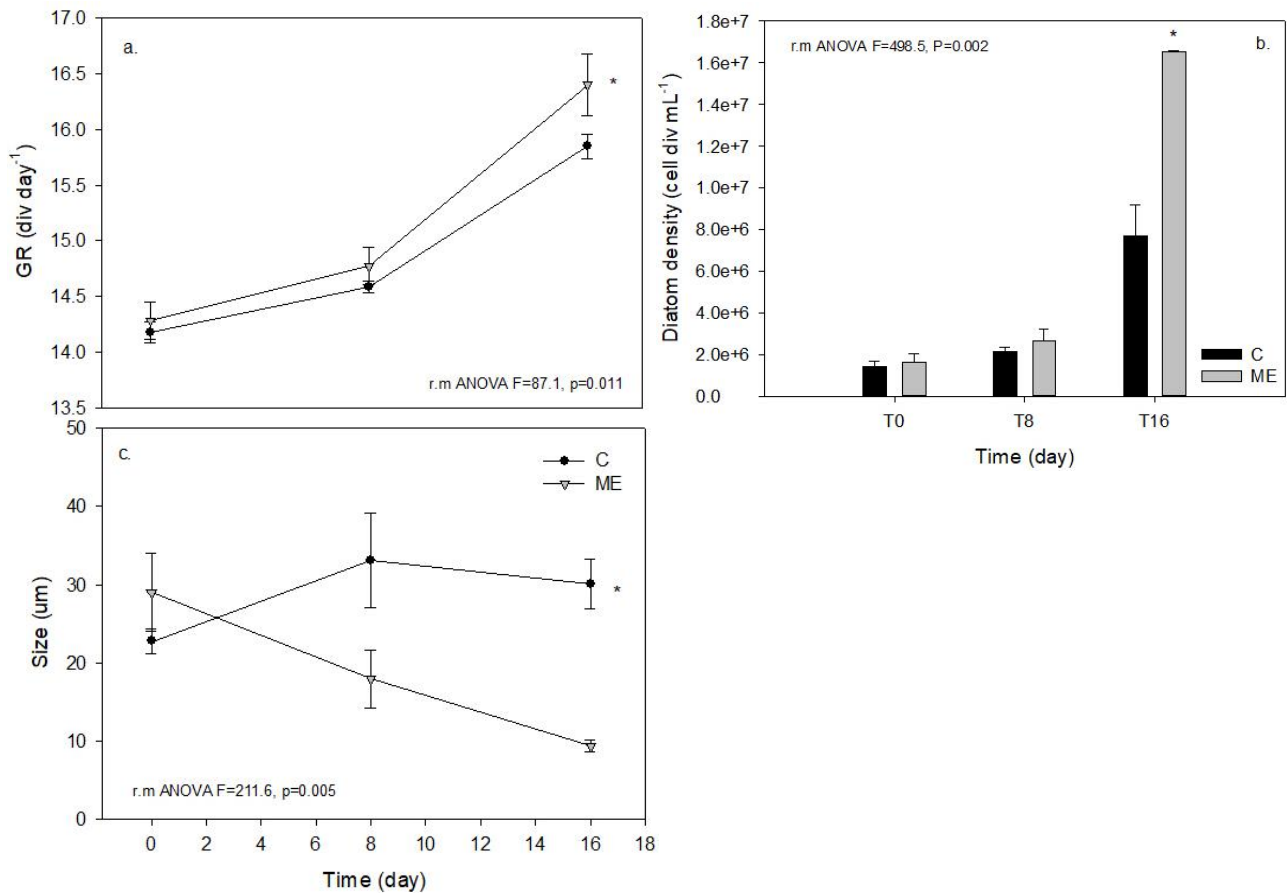
Figure 7.2. **a**. Diatom growth rate (div day^{-1}) (mean ± SD), n=3, **b**. diatom density (cell division mL^{-1}) (mean ± SD), n=3 and **c**. average diatom cell size (μm^2) (mean ± SD), n=3. C=control and ME= Mining effluent during the exposure period. ✳: significant difference (p < 0.05).
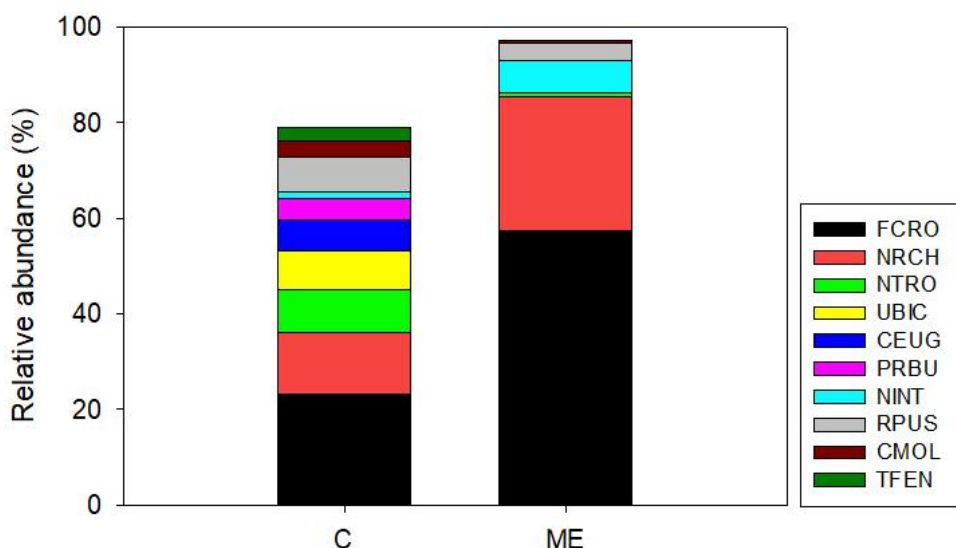
Figure 7.3: Relative abundance (mean value, n=3) of the 10 major diatom species (>3%) within diatom communities collected in the microcosms (C and ME) at t16. Where *Fragilaria crotonensis* (FCRO), *Navicula reichardtiana* (NRCH), *Nitzschia tropica* (NTRO), *Ulnaria biceps* (UBIC), *Cocconeis euglypta* (CEUG), *Planothidium robustius* (Hustedt) Lange-Bertalot (PRBU), *Nitzschia intermedia* (NINT), *Rossithidium pusillum* (RPUS), *Caloneis molaris* (Grunow) Krammer (CMOL) and *Tabellaria fenestra* (Lyngbye) Kützing (TFEN).

7.3.2.4.   PHOTOSYNTHETIC EFFICIENCY

The biofilm photosynthetic efficiency (Yeff) during the exposure period was stable over time in the C, but decreased significantly after one day of exposure (T1) in the ME treatment (Table 7.2, Figure 7.4-a). After 8 days of exposure (T8) the Yeff of ME biofilm were still significantly lower than in C microcosms (Table 7.2, Figure 7.4). Finally, the Yeff values of ME biofilm were recovered at the end of the exposure period (T16) being not significantly different from the C biofilm (Figure 7.4-a). Overall, the repeated measures analysis of variance confirmed that ME exposure significantly affected the photosynthetic efficiency of treated biofilm with respect to C (Table 7.2).

7.3.2.5.   PHOSPHOROUS UPTAKE RATE

The biofilm P-uptake rate was affected by ME, decreasing significantly after one day of exposure (0.17 ± 0.02 μgP $h^{-1}cm^{-2}$) compared to the C (0.31 ± 0.06 μgP $h^{-1}cm^{-2}$) (Figure 7.4-b, Table 7.2), but recovered from T8 until the end of the exposure. Overall,significant differences were observed over time between treatments (Figure 7.4-b, Table 7.2).
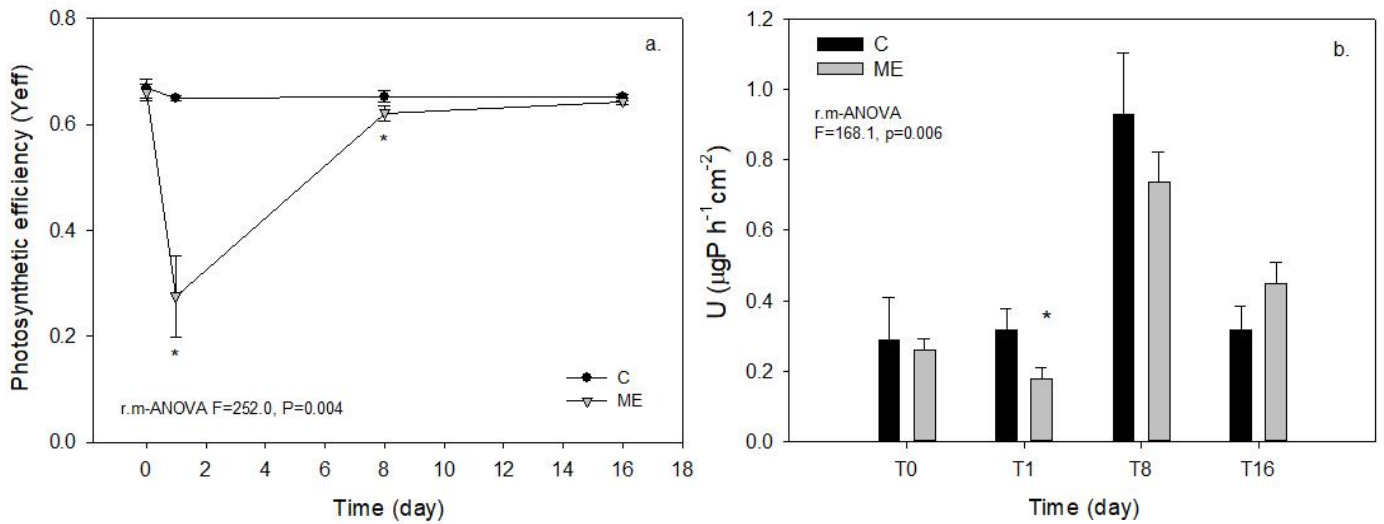
Figure 7.4. **a**. Photosynthetic efficiency (Yeff) (Yield) (mean ± SD), n=3, and **b.** P-uptake rate ($\mu gP\ h^{-1}\ cm^{-2}$) of the biofilm during the exposure period, (mean ± SD), n=3. C= control, ME= mining effluent. ✳ significant difference ($p < 0.05$).

7.3.2.6.   OVERALL BIOFILM RESPONSES

The principal component analysis (PCA) revealed a clear effect of ME exposure on the overall biofilm response at the end of the experiment (T16) (Figure 7.5). The first axis separates the ME treatment with biofilm showing the highest diatom growth rate (GR), diatom abundance and more chlorophyll-a, with respect to the control (C). PCA ordination highlighted that higher diatom density and GR (found in ME exposed biofilm) corresponded to lower cell size and biodiversity (*H'*) of diatom species of the respective community. Photosynthetic efficiency was lower under ME whereas the phosphorous uptake rate was higher.
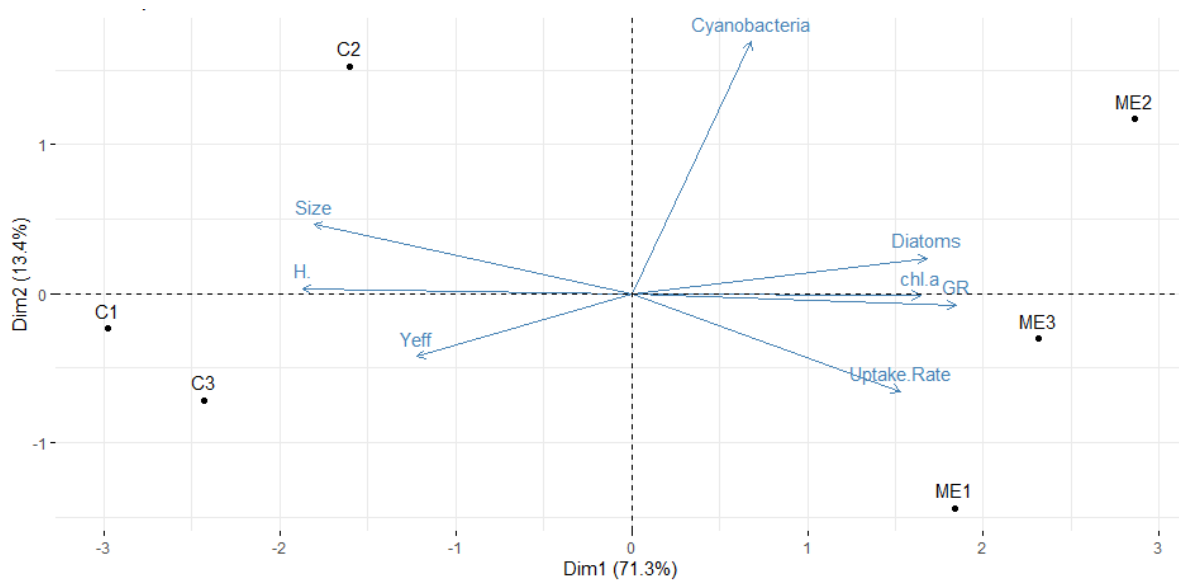
Figure 7.5. Principal component analysis (PCA). Plotted vectors indicate the correlation scores between the community composition, photosynthetic efficiency (Yeff), phosphorous uptake rate, chlorophyll-a (chl-a) and diatom metrics (growth rate, size, Shannon index H') at the end of the experiment (T16).

Table 7.2: F and p values of one-way ANOVA, one-way repeated measures ANOVA, and one-way ANOSIM test performed during the exposure period. Non-significant differences were found at T0 (just before the exposure) in any of the parameters evaluated. The most responsive endpoints are reported.

| | one-way ANOVA | | | | | | Repeated-measures (ANOVA) | |
| | T1 | | T8 | | T16 | | | |
	F	p	F	p	F	p	F	p
Conductivity (µS cm^{-1})	1760.8	<0.001	966.4	<0.001	805.4	<0.001	31.1	0.031
Diatom:								
Abundance (µg chl-a cm^{-2})	n.s		6.3	0.045	7.2	0.002	273.1	0.004
GR (div day^{-1})	-		n.s		3.4	0.037	87.1	0.011
Density (cell div ml^{-1}l)	-		n.s		103.3	<0.001	498.5	0.002
Cell size (µm)	-		22.0	<0.001	66.6	<0.001	211.6	0.005
H'	-		38.4	0.003	403.2	<0.001	98.6	0.010
Biofilm:								
Chl-a (µg cm^{-2})	n.s		n.s		7.9	0.048	311.3	0.003
Yeff	69.8	<0.001	8.7	0.050	n.s		252.0	0.004
Phosphorus uptake (µg P h^{-1} cm^{-2})	4.5	0.015	n.s		n.s		168.1	0.006
one-way ANOSIM								
	R	p	R	p	R	p		
Photosynthetic community composition (µg cm^{-2})	n.s		n.s		0.3	0.011	-	
Diatom taxa	-		n.s		0.6	0.040	-	

7.4. DISCUSSION

Our study revealed alterations on the biofilm structure and functioning caused by the hypersaline mining effluent from an abandoned potash-mine. Freshwater salinisation, induced by the abandoned potash-mine, impacted firstly on the biofilm functioning, causing a strong decrease of photosynthetic efficiency and a slight reduction of P-uptake capacity after only one day of exposure that was recovered throughout time. Thereafter, alterations also occurred at the biofilm structure level, with a significant increase of the diatom growth rate associated with a decrease of its cell size, species richness and diversity.

In agreement with what was previously described by Cañedo-Argüelles et al. (2017), the hypersaline mining effluent did not influence the dominance among algal groups within biofilm during the whole experiment in our study. Previous studies suggested that the threshold for detecting steady effects of freshwater salinisation on freshwater biofilm communities (i.e. drastic reductions in abundance and/or the number of surviving taxa) may occur around 3 g L^{-1} of salinity (Cañedo-Argüelles et al., 2017). However, the tolerable threshold that biofilm communities can resist has not been determined yet. Our study revealed that freshwater salinisation, induced by an effluent from potash mining with a salinity concentration of 15 g L^{-1}

created in each microcosm, caused a drastic shift on the biofilm structure and functioning, although the latter was able to recover over time.

Biofilm community structure may be affected by freshwater salinisation (Loureiro et al., 2013; Venancio et al., 2019). Our results showed that, salinisation caused a shift in the diatom community of the exposed biofilm, favoring salt-tolerant diatom species that occupied the niches left by the sensitive ones. Previous works report high abundances of extremely salt-tolerant diatom species (i.e., Rhoicosphenia abbreviata) in biofilm exposed to hypersaline mining effluents under conductivities between 10–16 mS cm $^{-1}$ (Rovira et al., 2012). Indeed, salinisation can cause drastic changes in freshwater diatom communities, affecting the diatom stability and leading to a transition to a new stable state (Herbert et al., 2015). Some of these changes may be related to salinity effects on diatom valve morphology, which may be taxon specific (Trobajo Pujadas, 2003). In this regard, we observed a direct effect of salinity on cell size probably as a consequence of the energy allocated to osmoregulation processes under high ion concentrations (Entrekin et al., 2019). The elongation of the diatom is driven by the osmotic pressure which breaks down siliceous components of the cell wall. The diatom, at high salt concentrations, may not be able of producing the necessary intracellular osmolarity to produce the same pressure as at low salt concentrations (Entrekin et al., 2019). Consequently, if cell elongation is less efficient under hypersaline conditions, cell size can decrease faster than under non-polluted conditions (Mitra et al., 2014). Indeed, in our study we observed that the smaller and salt-tolerant taxa occupied the space left by larger diatom species. Moreover, cell size is a key trait determining a species' ability to recover after disturbance due to the fact that smaller cells have typically higher growth rates that confer greater resilience (Lange et al., 2016). In addition, in those communities exposed to the hypersaline mining effluent, a decrease in the diatom species richness was observed. In the ME microcosms, higher densities but smaller cell sizes of the species Fragilaria crotonensis, Navicula reichardtiana and Nitzschia intermedia were observed, whereas higher densities of Fragilaria crotonensis, Navicula reichardtiana, Nitzschia tropica, Ulnaria biceps and Cocconeis euglypta were found in the control biofilm. Rovira et al. (2012) report that diatom react to Cl$^-$ changes as low as 100 mg L^{-1}. (Ziemann et al., 2001) report a shift in the diatom composition of river Wipper after salinisation and established that it should not exceed a maximum chloride concentration of 400 mg L^{-1} to preserve diatom diversity. In the salinized section of the River Werra (27 000 mg Cl L^{-1}), a decrease in species richness is also observed (Bäthe and Coring, 2011). Our study demonstrated that, despite diatom dominance within the biofilm assemblages increased in response to freshwater salinisation, the diversity and species richness of these communities tended to decrease during the exposure.

The biofilm functioning was also affected by the hypersaline effluent, in conjunction with the structural changes observed, particularly in the diatom community. After one day of exposure significant inhibition of autotrophic activity was observed, followed by a rapid recovery. It is well known that short-term exposure to high salt concentration immediately reduces the biofilm photosynthetic efficiency (Cook and Francoeur, 2013). The decrease in photosynthetic efficiency was caused by the photoinhibitory stress induced by the high salt concentration *per se*.

It has been described that a drastic increase in the cellular sodium (Na) content can inhibit the CO_2 assimilation processes causing that the cells may down-regulate their light harvesting capacity to acclimatate their low carbon metabolic capacity (Lu and Zhang, 2000). The subsequent recovery can be explained by two key factors: i) the rapid ions extrusion from the cells, which is probably associated with the sodium proton antiporter (Lu and Zhang, 2000) and ii) the salt-tolerant species' functional redundancy that continued to sustain its activity under stress (Rovira et al., 2012). On the other hand, at the end of the experiment, the phosphorous uptake capacity of ME biofilm was also affected, being significantly lower than the C just after one day of the exposure and recovered along time at the end of the experiment. Despite the poorly described effects on nutrient uptake capacities under salt exposures (Entrekin et al., 2019), it is known that chemical stressors can affect the ability of biofilm to assimilate SRP since they can be less effective in removing it from the water column (Proia et al., 2017). In this study, the increase in diatom abundance along with the reduction in size could have caused an increase, above the control of the SRP uptake capacity since the species with high surface:volume ratios (i.e the small ones) are characterized by higher nutrient uptake rates per unit biomass (Den Haan et al., 2016). Therefore, smaller cells have higher nutrient uptake rates relative to the larger ones (Lange et al., 2016).

We investigated biofilm structure and functioning related to processes that can be relevant at the ecosystem scale, such as photosynthetic efficiency (for the energy supply) or P-uptake (for the self-depuration capacity). The effects of the hypersaline mining effluent did compromise the functioning of the biofilm only in the short-term, though a significant decrease was appreciated in the diatom richness, highlighting the potential long-term effects of salinisation on biofilm biodiversity. In this context, it would be relevant to investigate the effects on the biodiversity of the other microbial components conforming the biofilm. To quantify the overall effects of freshwater salinisation on ecosystem services related to biofilm-driven processes, temporal data and more variables (i.e., organic matter breakdown or community metabolism) should also be considered. Furthermore, given that biofilm is the basal level of the stream food webs, further

research is needed to assess the direct and indirect effects of freshwater salinisation on higher trophic levels.

7.5. CONCLUSIONS

The present study indicates that freshwater salinisation from potash mining effluents has the potential to significantly alter the photosynthetic communities of receiving streams. The high salt concentration created by the hypersaline effluent addition in our microcosm, resulted in a significant decline in diatom biodiversity, leading to a community dominated by tolerant species, and an immediate decrease in the photosynthetic efficiency and nutrient uptake capacity that were recovered throughout the experiment. Hence, freshwater salinisation threatens not only aquatic biodiversity, but also ecosystem functioning and services (Estévez et al., 2019). Thus, this is an issue that requires further investigation since the expected increase in water scarcity and desertification in many regions of the world, which would be induced by climate change, is expected to increase the amount of salinized rivers around the world, exacerbating the biological degradation and ultimately supposing a risk to human health (Rotter et al., 2013; Kaushal 2016). Therefore, the salinity tolerance thresholds on biofilm communities should be further investigated as well as the effect of different time exposures (chronic vs pulses) to protect ecosystem integrity. Additionally, the recovery capacity of these communities previously exposed need to be addressed to investigate the potential permanent damage caused to the ecosystem.

CHAPTER 8.

Exposure and recovery: the effect of a salinisation gradient on the structure and function of freshwater biofilm communities.
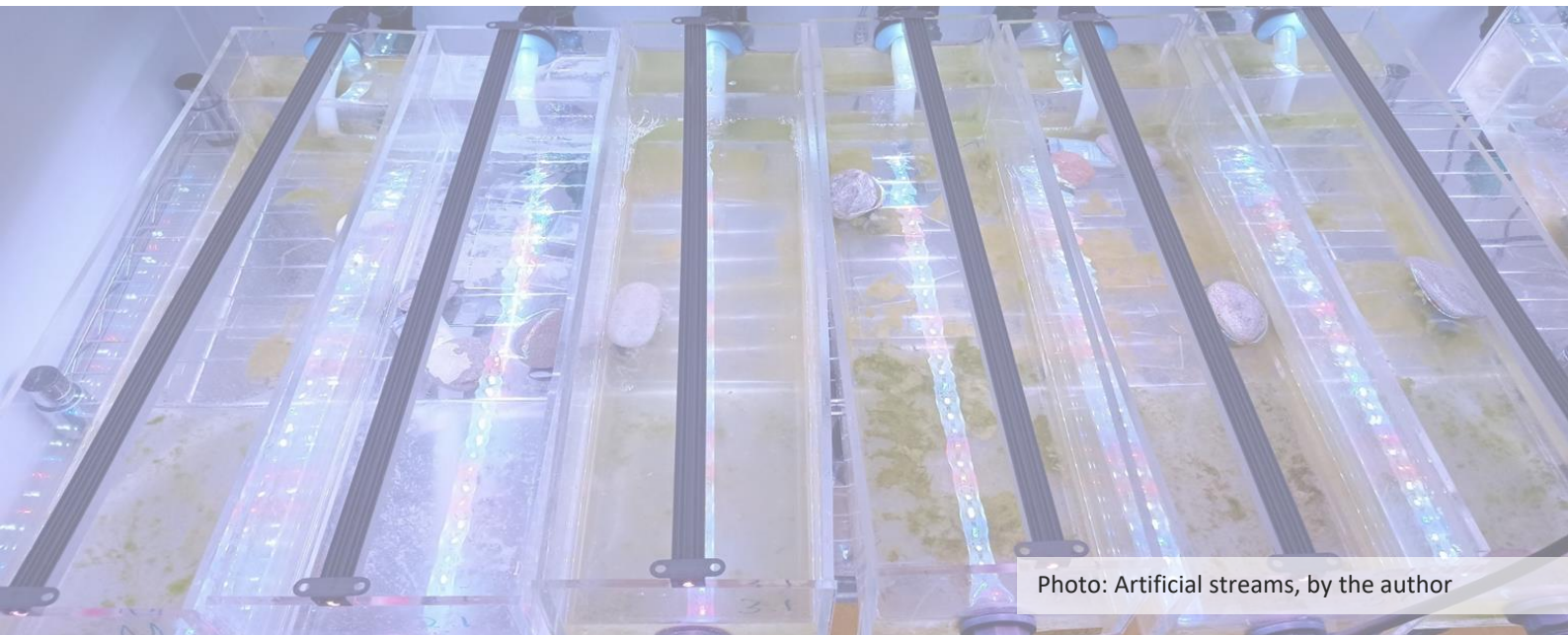
Photo: Artificial streams, by the author

8. EXPOSURE AND RECOVERY: THE EFFECT OF A SALINISATION GRADIENT ON THE STRUCTURE AND FUNCTION OF FRESHWATER BIOFILM COMMUNITIES.

8.1. INTRODUCTION

Salinisation of freshwater ecosystems is a global environmental problem that threatens freshwater biodiversity, functions, and services (Kaushal et al., 2018). Anthropogenic activities such as mining, agriculture, and the application of de-icing salts are increasing the salt concentration of freshwaters (Cañedo-Argüelles et al., 2013; Kaushal et al., 2018), and this pollution is expected to increase in the future due to climate and land-use changes (Olson, 2019; Le et al., 2018). Despite these evidences, salinisation effects on freshwater ecosystems remain poorly studied compared to other human stressors, such as heavy metals or antibiotics (Cañedo-Argüelles et al., 2020). The few studies performed until the date suggested that current water regulations and standards are insufficient to prevent freshwater salinisation (Schuler et al., 2018).

To date, few studies have examined salinity tolerance thresholds on biofilm communities (Bonada et al., 2004; Cañedo-Argüelles et al., 2017). Threshold salinity concentrations and exposure times at which sub-lethal effects occur need to be identified to protect ecosystem integrity (Cañedo-Arguelles et al., 2016). Freshwater biofilms play an important role in river ecosystem functioning by driving metabolism and biogeochemical cycles through nutrient uptake and transfer to higher trophic levels (Battin et al., 2016; Allan and Castillo, 2007). They are essential as a basal resource for in-stream food webs and key elements in the self-purification processes occurring in rivers and streams (Wu et al., 2018; Hall and Meyer, 1998; Power and Dietrich, 2002). Biofilm functionality and structure can respond to extensive environmental changes (Ponsati et al., 2016; Pereda et al., 2019; Pu et al., 2019), including salinisation (Vendrell-Puigmitja et al., 2020).

Few studies assessing the salinity effects on biofilm exists nowadays. Within these studies, the impacts on freshwater organisms of different saline concentrations and ion compositions were assessed (i.e., SO_4^{2-}, Cl^-, K^+, Mg^{2+}, Ca^{2+}, Na^+, HCO_3^-) (Bonada et al., 2004; Cañedo-Arguelles et al., 2017; Canhoto et al., 2017). However, the toxic effects of salinity depend on the salt concentration, the ionic composition, and the type of exposure (chronic or pulse) (Sala et al., 2016; Hintz and Relyea, 2017; Olson and Hawkins, 2017; Velasco et al., 2019; Martínez et al., 2019). These previous studies have indicated that salinities between 4 and 10 g L^{-1} can affect the algal biomass (Silva et al., 2000; Dunlop et al., 2008; Ros et al., 2009; Kefford et al., 2011; Rotter

et al., 2013). Additionally, under short-term exposures to salinities of 15 g L^{-1}, significant effects were observed in the photosynthetic efficiency and nutrient uptake capacity of the biofilm and a significant decline in its diatom biodiversity (Vendrell-Puigmitja et al., 2020). At the same time, freshwater salinisation may also affect other key ecosystem functions such as leaf litter decomposition or microbial respiration under salinities of 6 g L^{-1} (Martinez et al., 2020). Besides, catabolism-related functions influencing respiration and activity of extracellular enzymes was also at 0.25 g NaCl L^{-1} (Martínez et al., 2020). Yet, higher salinities had been reported in the field, as in River Werra (Germany) where peaks of 30 g L^{-1} of Cl^{-} were registered near salt mines (Coring and Bäthe, 2011), or in Tajo-Segura River (Spain) where the salinity of the stream reached almost 100 g L^{-1} due to anthropogenic activities (Velasco et al., 2006).

Besides, it is not only important to assess the effects during the exposure, but also during the recovery. This is important to overcome the environmental variations and underscore biofilm recovery potential in response to, exclusively, chemical improvement. Only a few studies have addressed the biofilm community's recovery capacity after the stressor disappearance. Gutiérrez-Cánovas et al. (2009) reported that a decrease in the salinity in a previous impacted stream changed the primary producers' community which lead to a higher primary production, supporting greater secondary production. Under microcosms conditions, Cochero et al. (2017) exposed biofilm communities during 72h to water enriched with 24.6 g L^{-1} NaCl and observed a recovery of the bacterial density and in oxygen consumption 72h after the exposure stopped.

Freshwater salinisation and its effects on freshwater ecosystems may be caused by hypersaline effluents derived from abandoned potash mines, as they pour into the river very high concentrations of salts. Potash mining activities are considered an important driver of secondary salinisation (Cañedo-Argüelles et al., 2012) since they generate tailings of wastes dominated by NaCl, KCl and MgCl$_2$ that are one of the world's largest chronic waste concerns (Tallin et al., 1990). These wastes are stored in impoundments near the mines, from where they can reach surface waters by infiltrations through embankments or the base of the tailings pile, causing severe effects of freshwater communities (Hudson-Edwards et al., 2011). Mining effluents from abandoned mines are among the most relevant sources of freshwater salinisation, acting as a stressor of biological activity (Weiss et al., 2016).

For that reason, this study aimed to explore the effects of freshwater salinisation under different realistic concentrations on the biofilm structure and functioning caused by an abandoned potash mining effluent and its ability to recover once the effluent has been removed. To do that, we used the Menteroda (Germany) abandoned potash mine effluent composition (Chapter 3). We

analysed the response patterns of freshwater biofilm communities to an increasing salinity gradient using the real mining effluent from Menteroda potash abandoned mine as a reference for the ionic composition. After 21 days of exposure to different salinities defined according to the salinity ranges reported in previous studies and those found in the environment (3, 6, 15, 30 and 100 g L^{-1}), we also assessed the biofilm recovery capacity and the effects of adding a pulse of salt during 24h at the end of the recovery period. The pulse addition was performed to investigate whether or not the historical exposure of communities to the different salinities could provide acquired tolerance towards high salinity pulses. We specifically focus on the following questions: (i) What is the salinisation effect on the freshwater biofilm structure and functioning along the salinity gradient? (ii) Are these microbial communities able to recover their functions and structure after salinity stress removal? If yes, (iii) After the exposure period, is there an overall increase in tolerance to salinisation? To this end, we performed a microcosms experiment using artificial streams to study the potential impact of different salinity concentrations on freshwater biofilms and their ability to recover from this impact.

8.2. MATERIALS AND METHODS

8.2.1. EXPERIMENTAL DESIGN

This experiment was performed using a set of microcosms formed by eighteen methacrylate artificial streams (50 cm long x 12 cm wide) placed in a temperature and light-controlled chamber. The bottom of each artificial stream was covered by sandblasted glasses as artificial substrata of three different sizes: 1, 3, and 200 cm^2. The artificial streams were filled with 3L of simulated river water, recirculated using a submersible pump (EDEN 105, Eden Water Paradise, Italy). Artificial water was prepared following Ylla et al. (2009) to mimic a pristine stream's chemical composition. It was obtained by dissolving pure salts in distilled water to achieve a chemical composition of 0.75 mg N L^{-1}, 0.10 mg P L^{-1}, 15.83 mg Na$^+$ L^{-1}, 8.17 mg Ca^{2+} L^{-1}, 0.52 mg K$^+$ L^{-1}, 0.19 mg Mg^{2+} L^{-1}, 8.89 mg SO$_4^{2-}$ L^{-1}, 10.71 mg SiO$_3^2$ L^{-1} , 14.94 mg Cl^{2-} L^{-1} and 14.52 mg HCO$_3^-$ L^{-1}. During the experiment, all the water from each channel was renewed every two days to avoid nutrient depletion. The temperature was set at 15°C and the photoperiod at 12:12h day/light (PAR set at 110) using LEDs (SMD 5730 - 72). The irradiance reaching the glass substrata ranged between 96.9 and 126 mmol photons m^{-2} s^{-1}.

The experiment comprised four different temporal periods: colonisation (4 weeks), exposure (3 weeks), recovery (2 weeks) and pulse (24h). During the colonisation period, 50 mL of biofilm suspension obtained by scraping several cobbles from a pristine stream (Riera Major, Viladrau, Spain) was added at each artificial stream at each water renewal to promote colonisation.

Once the biofilm was attached uniformly to the artificial substrate, the exposure period started. The experiment comprised five treatments that represented an increasing salinity gradient: (i) 3 g L^{-1}, (ii) 6 g L^{-1}, (iii) 15 g L^{-1}, (iv) 30 g L^{-1}, (v) 100 g L^{-1}. The ion composition of real effluent from Menteroda (Germany) was used as reference to reproduce the same concentrations assessed in this study. The ionic composition and concentration of this effluent were reproduced under laboratory conditions to obtain an effluent of 216 g L^{-1} of salinity (191 g L^{-1} NaCl, 12 g L^{-1} KCl, 12.5 g L^{-1} Cl$_2$Mg·6H$_2$O) that mimicked the concentration of the mining effluent, used as mother solution. Each treatment was performed in triplicate, and artificial water was used as a control (C). Following the exposure phase, all the artificial streams were filled with artificial water (unpolluted) for 16 days (recovery phase). At the end of the exposure period, we added a pulse of 24h of 100 g L^{-1} of salinity in all artificial streams (Figure 8.1).
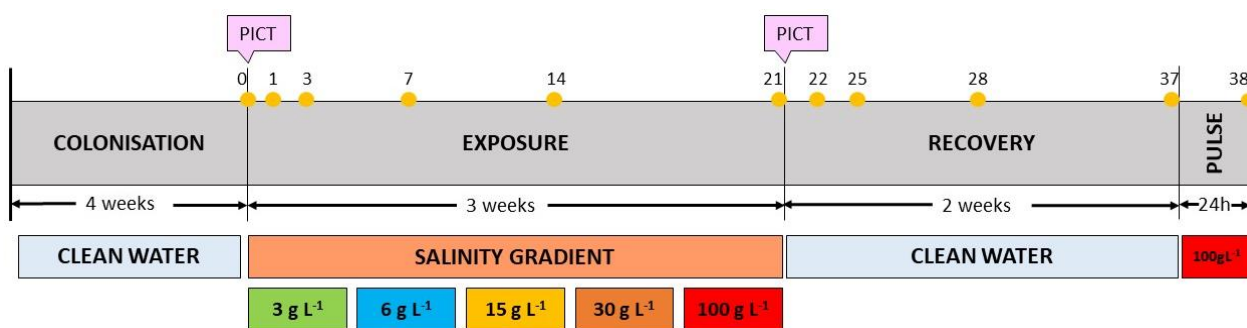
Figure 8.1: Experimental design and sampling times (yellow circles) during the exposure, recovery, and pulse addition periods. Pollution -induced community tolerance (PICT) was performed just before the exposure period started (t0) and at the end of the exposure period (t21d).

8.2.2. PHYSICO-CHEMICAL CONDITIONS

The water physico-chemical conditions on each artificial stream were monitored every time that the water was renewed during the whole experiment (every two days). Dissolved oxygen concentration and saturation, temperature, pH, and conductivity were measured using a portable sensor probe (YSI professional plus, YSI Incorporated, USA). Simultaneously, replicate water samples from each treatment were obtained and filtered through a 0.22 µm pore glass microfiber filter (Prat Dumas Filter Paper, Couze-St-Front, France) to analyse inorganic nutrients (DIN, SRP) and Cl$^-$ concentration since it was the most abundant ion in the mining effluent tested in this study.

8.2.3. BIOFILM SAMPLING

Biofilm was sampled just before the exposure period (t0) started, during the exposure period at 1, 3, 7, 14, and 21 days, during the recovery period at 1, 3, 7, and 16 days and after the 24h pulse at the end of the experiment (Figure 8.1). At each sampling day, three 3 cm^2 glass substrata were

collected from each artificial stream. The photosynthetic activity and photosynthetic community composition of the biofilm were measured directly with an amplitude modulated fluorimeter (Mini-PAM fluorometer, Walz, Effeltrich, Germany) and BenthoTorch portable fluorimeter probe (bbe Moldaenke, Schwentinenta, DK), respectively. Then, biofilm was scraped using a toothbrush and suspended in 15 mL of water from the corresponding stream. The suspension was distributed to analyse chlorophyll-a (chl-a), ash-free dry mass (AFDM) and microbial respiration (mgCO_2 produced) at 1, 7,14, 21 days of the exposure period, 22, 28 and 37 days of the recovery period, and after the pulse, and then stored at -20°C until analysis. A additional subsample of this biofilm suspension was obtained in all sampling times for determining diatom metrics and, preserved with Ethanol 90% and kept at 4°C until analysis. Diatom diversity was calculated using the Shannon-Weaver index (H') (Shannon and Weaver, 1963). From diatom species relative abundances and their biovolumes, a mean cell length (cm^2) of the community was calculated as described in Barral-Fraga et al. (2016).

The nutrient uptake capacity of the biofilm was also measured at each sampling day. For this purpose, the 200 cm^2 glass substrate was collected from each artificial stream and placed in a 6-L glass aquarium filled with the same water. The basal nutrient concentration on each aquarium was increased four-fold and the biofilm incubated for 240 minutes. Water samples (10 mL) from each aquarium were obtained at 1, 5, 15, 30, 60, 90, 120, 180, and 240 minutes after the nutrient addition, and filtered through a 0.22 μm glass microfiber filter (Prat Dumas Filter Paper, Couze-St-Front, France) to determine (SRP, NH_4^+ and NO_3^-) concentrations over time and obtain nutrient uptake rates. We calculated the nutrient decay rate (k) from the nutrient decay along time as it fitted a negative exponential model (Chapter 3).

The potential Pollution-Induced Community Tolerance (PICT) (Blanck et al, 1988) was assessed before (t0) and at the end of the exposure period (21d) (Figure 8.1). Eight small glass substrata (1 cm^2) were taken from each artificial stream and exposed to eight increasing salt concentrations, which included all the concentrations tested in the channels and two additional higher concentrations (0, 4.5, 9.0, 18.0, 36.3, 72.5, 145, and 290 g L^{-1}) for 24 hours. The increasing salt concentrations were created from a stock solution of 290 g L^{-1} (265 g L^{-1} NaCl, 17.1 g L^{-1} KCl and 17.1 g L^{-1} Cl$_2$Mg·6H$_2$O) which included two concentrations above the most concentrated treatment that allowed to assess potential tolerances of the most concentrated treatment (Blanck, 2002). After 24 hours of incubation, photosynthetic efficiency was measured and used as an end-point to obtain the communities' responses to the different treatments compared to those under the C. From the results obtained, the EC$_{50}$ values were calculated.

Finally, after two weeks of recovery in all channels, a pulse of 24h of salinity 100 g L^{-1} was performed (Figure 8.1) in all artificial channels (including the control ones) by making the correspondig solution using the mother solution of 208 g L^{-1}, as performed during the exposure period. After 24h, samples to analyse all biofilm functional and structural variables were collected.

8.2.4. DATA ANALYSIS

Differences between treatments in water physicochemical parameters, biofilm structural and functional parameters and diatom metrics were evaluated using one-way ANOVA for each sampling day. Differences in these parameters over time among treatments during the exposure and the recovery period were assessed using one-way repeated measures ANOVA (rm-ANOVA). Based on EC$_{50}$ estimates obtained after the PICT, one-way ANOVA was used to test the differences in the community tolerance in biofilm among treatments. When a significant difference was observed in the ANOVA, post hoc comparisons were performed with a Tukey's test. Both tests were performed using SPSS Statistics software (version 21). Pearson correlation analysis was performed to explore the relationship between biofilm variables. To determine differences among treatments on the biofilm community composition and the species conforming the diatom community within the biofilm, a one-way ANOSIM was carried out with Bonferroni correction using Past3 version 3.23.

Structural equation modelling (SEM) was used to assess the salinity effects on the biofilm structure and functioning at the end of the exposure, using the "lavaan" package of R Studio software (version 3.6.0). SEM is based on the variance-covariance matrices between predictor and response variables, and it uses correlations between these variables and their statistical significance to evaluate direct and indirect causal pathways (Franier et al., 2014). The model contained 54 sampling units which included all sampling events (i.e. six treatments x three replicates x three sampling times), and ten explanatory/response variables (microbial respiration, photosynthetic efficiency (Yield), chlorophyll-a, green algae and diatom abundance, kSRP, kNH$_4^+$, diatom size, species richness and GR). Additionally, salinity was set as the predictor variable. SEM is based on an assessment of overall model fit (i.e., root mean square error of approximation (RMSEA), comparative fit index (CFI)), which indicates if a model structure fits the data structure rather than on the statistical significance of individual relationships within the model. It is considered that CFI values of 0.9 or greater indicate good fit, and values less than 0.90 indicate poor fit (Schumacker and Lomax, 2010), and values below 0.05 of RMSEA indicate good model fit.

8.3. RESULTS

8.3.1. WATER PHYSICO-CHEMICAL PARAMETERS DURING THE COLONISATION, EXPOSURE, AND RECOVERY PERIOD

Water physicochemical parameters during the colonisation period remained stable without significant differences among treatments (Table 8.1). During the exposure period, water temperature, pH, and oxygen saturation did not differ among treatments (Table 8.1) and ranged between 14.7 ($\pm$ 3.33) and 16.1 ($\pm$ 0.34) °C, pH of 6.31 ($\pm$ 0.96) and 7.00 ($\pm$ 0.28) and 8.81 ($\pm$ 1.11) and 9.71 ($\pm$ 0.44) mg O_2 L^{-1} throughout the exposure (Table 8.1). Water conductivity increased according to the salinity gradient (Pearson correlation, r = 0.95, p < 0.001), and it ranged from 4273 ($\pm$ 1045) μS cm^{-1} in the 3 g L^{-1} treatment to 109875 ($\pm$ 8048) μS cm^{-1} in the 100 g L^{-1} treatment (Table 8.1). At the recovery period, treatments presented a gradual decrease in the conductivity over time, achieving the same conductivity as the control (C) after one week of recovery (t7R).

Regarding inorganic nutrient concentration in stream water, soluble reactive phosphate (SRP) and dissolved inorganic nitrogen (DIN) concentrations during the colonisation period decreased significantly between water renewals from 120 ($\pm$ 1.13) μg L^{-1} to 103 ($\pm$ 5.07) μg L^{-1} (one-way ANOVA, F = 115, p < 0.001) and from 739 ($\pm$ 73.9) μg L^{-1} to 618 ($\pm$ 61.5) μg L^{-1} (one-way ANOVA, F = 206, p < 0.001), respectively. However, during the exposure period, nutrient concentrations did not decrease between water renewals at the 100 g L^{-1} salinity treatment, being 75.8 ($\pm$ 8.6) μg L^{-1}, SRP and 805.9 ($\pm$ 37.3) μg L^{-1} of whole average nitrogen (DIN before renewals. All treatments showed similar SRP concentrations during the recovery period, without significant differences with the C (Table 8.1).

Table 8.1: Water physico-chemical parameters on each treatment (3 artificial streams per treatment) during the colonization (n = 12), exposure (n = 9), and recovery (n = 6) period (mean ± S*D*). Results of rm-ANOVA and Tukey b test (p < 0.05) are provided. DO, dissolved oxygen; T, temperature; EC, Electrical conductivity. ns, no significative. *conductivity values at the end of the recovery period. The letters indicate significant differences (p < 0.05) between treatments after rm - ANOVA and Tukey b test.

Period	Treatment	Physico-chemical parameters					
		DO (mg L^{-1})	T (°C)	pH	EC (µS cm^{-1})	SRP (µg L^{-1})	DIN (µg L^{-1})
Colonisation		9.52 (± 0.04)	15.7 (± 0.25)	6.84 (± 0.05)	120 (± 1.13)	123 (± 8.61)	739 (± 73.9)
Exposure	**Control**	9.30 (± 1.16)	15.6 (± 0.35)	6.45 (± 0.79)	157 [a] (± 2.28)	129 [a] (± 5.47)	711 [a] (± 69.7)
	3g L^{-1}	9.43 (± 1.22)	15.6 (± 0.40)	6.30 (± 0.93)	4273 [b] (± 1045)	118 [a,b] (± 13.3)	626 [a] (± 82.2)
	6g L^{-1}	9.21 (± 1.20)	15.9 (± 0.31)	6.30 (± 0.95)	9307 [c] (± 1024)	110 [b] (± 15.6)	605 [a] (± 74.1)
	15g L^{-1}	9.26 (± 1.20)	15.9 (± 0.34)	6.32 (± 0.96)	20343 [d] (± 1848)	102 [b] (± 7.84)	739 [a] (± 75.7)
	30g L^{-1}	9.01 (± 1.16)	16.1 (± 0.34)	6.31 (± 0.96)	38052 [e] (± 4187)	115 [b] (± 4.07)	808 [a] (± 56.6)
	100g L^{-1}	8.81 (± 1.11)	15.9 (± 0.46)	6.29 (± 0.94)	109875 [f] (± 8048)	187 [c] (± 14.0)	1262 [b] (± 99.6)
rm-ANOVA		n.s	n.s	n.s	F = 9959 p < 0.001	F = 127 p < 0.001	F = 49.3 p < 0.001
Recovery	**Control**	9.90 (± 0.21)	15.8 (± 3.56)	6.67 (± 1.50)	136 [a] (± 2.45) *	125 [a] (± 9.09)	656 [a] (± 96.1)
	3g L^{-1}	9.10 (± 1.25)	14.7 (± 3.33)	6.60 (± 1.51)	139 [a] (± 3.55) *	129 [a] (± 7.02)	646 [a] (± 80.8)
	6g L^{-1}	9.06 (± 1.51)	14.9 (± 3.35)	6.69 (± 1.51)	134 [a] (± 2.76) *	138 [b] (± 2.52)	618 [a] (± 90.7)
	15g L^{-1}	9.29 (± 1.27)	15.7 (± 0.33)	7.00 (± 0.28)	137 [a] (± 3.81) *	128 [a] (± 10.8)	605 [a] (± 92.4)
	30g L^{-1}	9.35 (± 1.31)	15.8 (± 0.37)	6.95 (± 0.24)	137 [a] (± 3.31) *	113 [a] (± 13.2)	597 [a] (± 87.2)
	100g L^{-1}	9.71 (± 0.44)	15.7 (± 0.24)	6.58 (± 1.50)	149 [b] (± 6.75) *	130 [a] (± 8.73)	771 [b] (± 113)
rm-ANOVA		n.s	n.s	n.s	F = 630 p < 0.001	F = 120 p = 0.010	F = 25.8 p < 0.001

8.3.2. BIOFILM RESPONSE DURING THE EXPOSURE PERIOD

The biofilm's photosynthetic efficiency decreased in all treatments just after 24h of exposure to the salinity gradient compared to the control (one-way ANOVA F = 28.6, p < 0.001). However, this decrease was statistically significant only in those treatments with higher salinity concentrations (30 and 100 g L^{-1}) compared to the C. Treatment 30 g L^{-1} presented on average 25% less efficiency than the control, while treatment 100 g L^{-1} was 80% below the C during the exposure period (Figure 8.2).
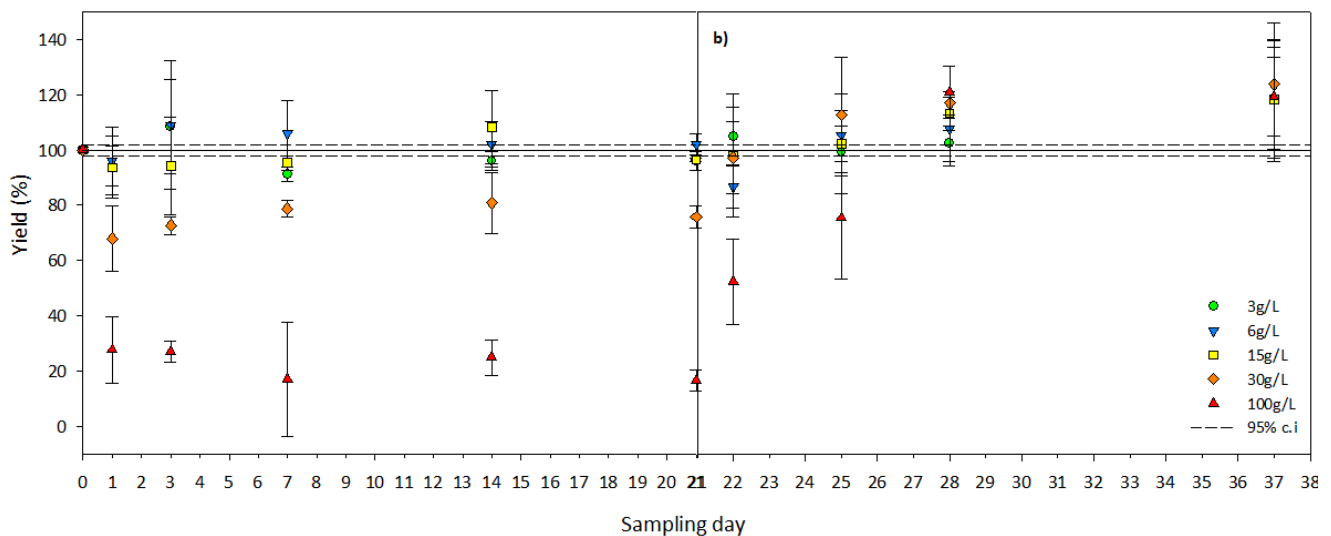
Figure 8.2: Photosynthetic efficiency of the biofilm communities along the salinity gradient during the exposure (a) and recovery (b) periods in % variation from control (black line). Values are mean ± SE (n = 3). c.i: 95% confidence interval (dash line). The colours represent the increasing salinity concentrations, from less concentrated (green circle) to more concentrated (red triangle).

Nutrients (SRP and NH_4^+) uptake capacity of the biofilm were signficantly affected by the salinity increase (one-way rm-ANOVA F = 50.3, p < 0.001 and F = 123, p < 0.001, respecitvely). Results showed a decrease in both SRP and NH_4^+ uptake rate of biofilm (measured as *k*) exposed to all treatments after 24h of exposure. Treatments 30 and 100 g L^{-1} remained significantly below the C during all the exposure period (t21d. Treatments 3 and 6 g L^{-1} recovered after t3d and did not present significant differences respect to the C during the rest of the exposure period (Figure 8.3).
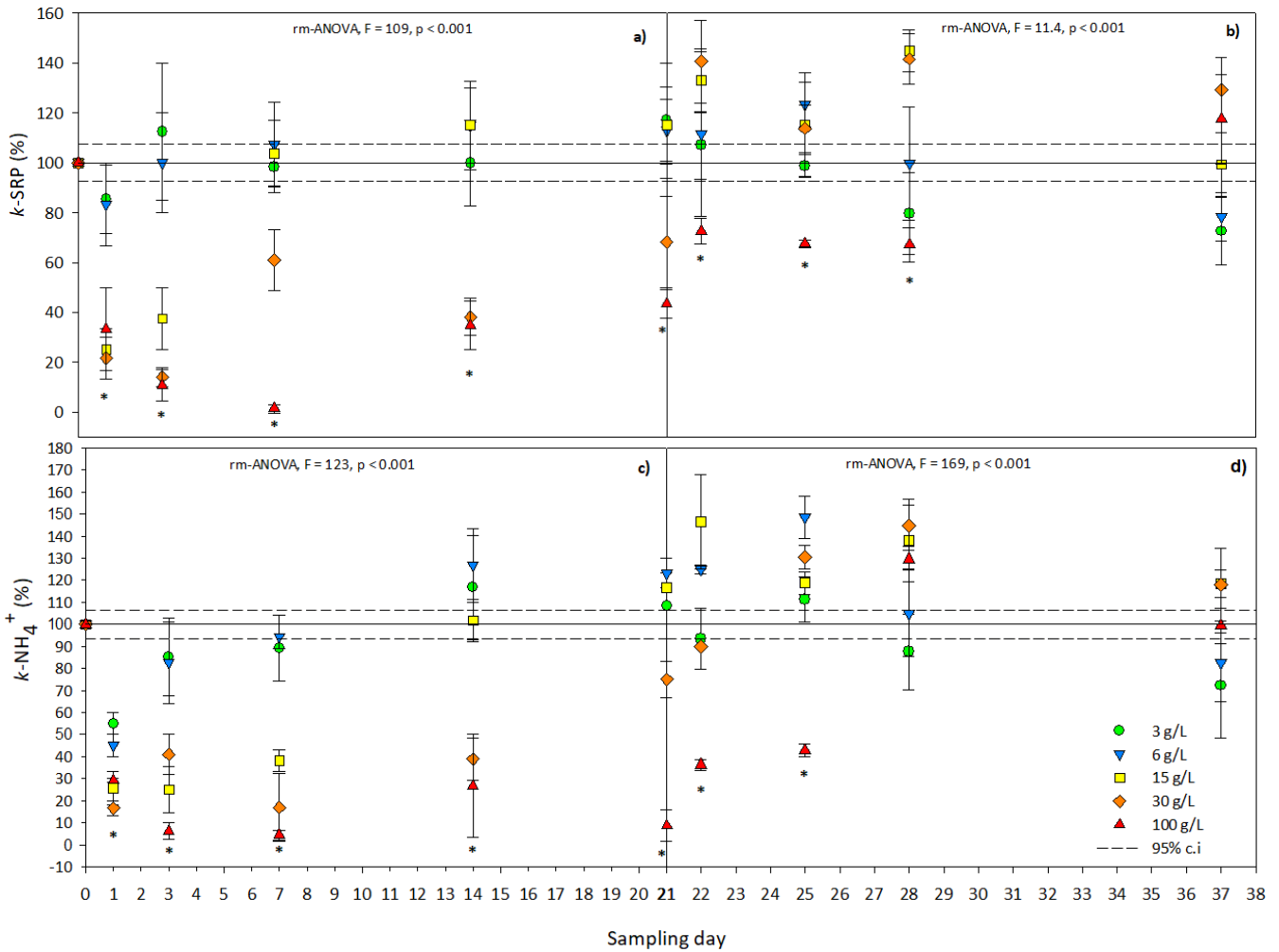
Figure 8.3: SRP and NH4+ uptake capacity of the biofilm communities under the different treatments during the exposure (a and c) and recovery (b and d) periods in % variation from control (black line). Values are mean ± SD (n = 3). c.i: 95% confidence interval (dash line). The colours represent the increasing salinity concentrations, from less concentrated (green circle) to more concentrated (red triangle). For each sampling time, an ANOVA has been performed to detect significant differences between treatments indicated by *.

The microbial respiration of the biofilm communities showed different dynamics between treatments during the exposure period (rm-ANOVA F = 85.1, p < 0.01), but at the end of it, no significant differences were found respect to the C (Figure 8.4).

133
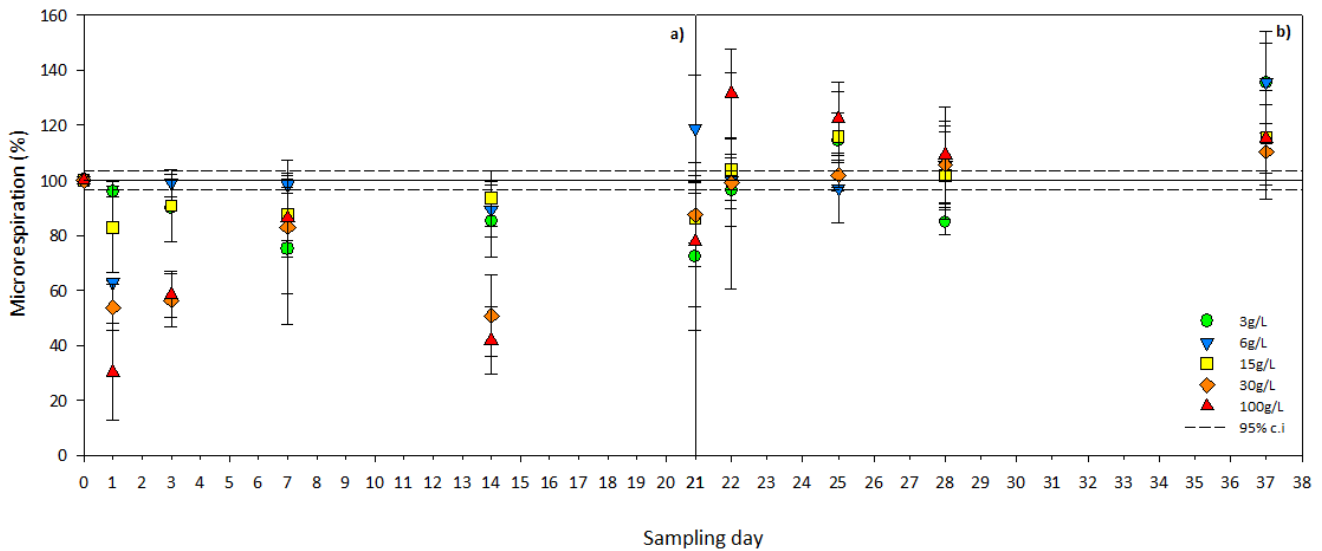
Figure 8.4: Microbial respiration of the biofilm under the different treatments during during the exposure (a) and recovery (b) periods in % variation from control (black line). Mean ± SE (n = 3). c.i: 95% confidence interval (dash line). The colours represent the increasing salinity concentrations, from less concentrated (green circle) to more concentrated (red triangle).

Biofilm exposed to treatments 30 and 100 g L^{-1} presented a significant decrease in the chl-a concentration after a week of exposure (one-way ANOVA F = 3.7, p = 0.006) but the 30 g L^{-1} recovered over time. In contrast, treatment 100 g L^{-1} remained significantly below the C during all the exposure period (rm-ANOVA, F = 13.9, p < 0.001) (Figure 8.5). Green algae were the dominant algal group conforming the biofilm community in all treatments at t0. During the exposure period, the abundance of this algal group decreased significantly in those biofilm exposed to the highest salinity concentrations (30 and 100 g L^{-1}) compared to the C. By contrast, green algae abundance increased over time during the exposure period compared to the control in those treatments with less salinity (3, 6, and 15 g L^{-1}) concentrations (Figure 8.5). On the other hand, diatom remained the second dominant group within the community in all treatments during the exposure period by reducing its relative abundance under treatments 30 and 100 g L^{-1}.

134
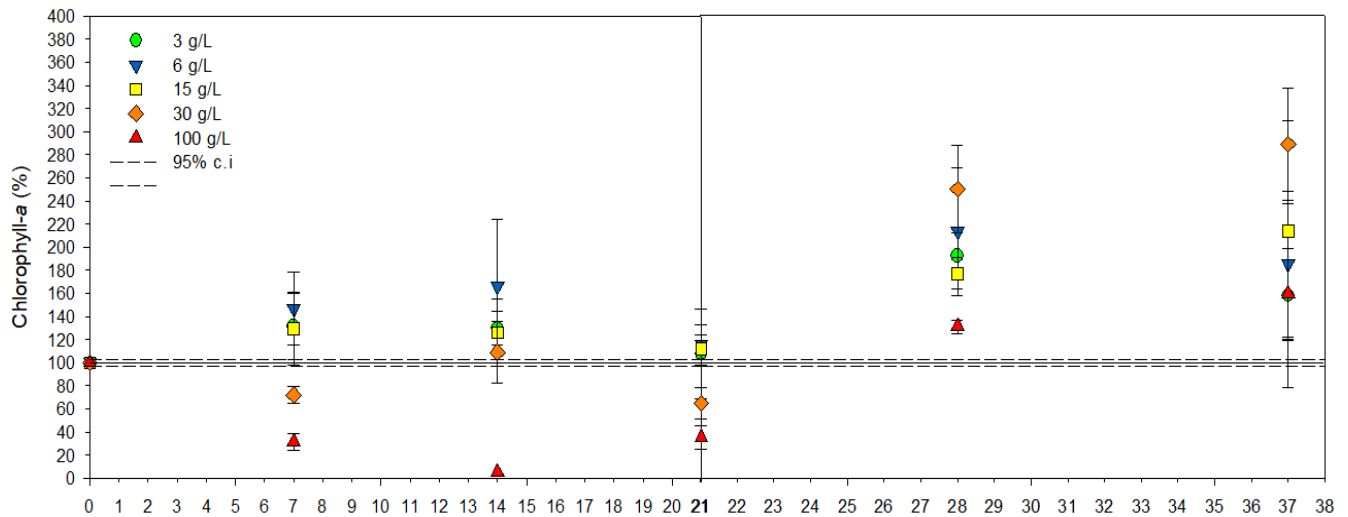
Figure 8.5: Comparison of biofilm chlorophyll-a under the different treatments during the exposure and recovery period in % variation from control (black line). Mean ± SE (n = 3). c.i: 95% confidence interval (dash line). The colours represent the increasing salinity concentrations, from less concentrated (green circle) to more concentrated (red triangle).

Within the diatom species pool, 42 diatom taxa were identified from the different biofilm samples collected at t0, t21d and t16d R. At t0, diatom species richness (S) and Shannon diversity index (H') were 23 (± 4) and 1.89 (± 0.21), respectively (Table 8.2). At the end of the exposure period (t21d), a significant decrease in S and H' was observed along the salinity gradient (Table 8.2). However, different trends between treatments were observed in the diatom cell density and growth rate (GR). These variables were higher than the C in treatments 6, 15, and 30 g L^{-1} at t21d, while at treatment 100 g L^{-1} remained below the C (Table 8.2). *Nitzschia intermedia* (Hantzsch) and *Achnanthidium minutissimum* (Kützing) were the dominant species in all treatments during the exposure period. In the control treatment, *Planothidium lanceolatum* (Brébisson ex Kützing), *Platessa hustedtii* (Krasske), and *Reimeria sinuata* (W.Gregory) were also present in abundances >3% (Table 8.3, Figure 8.6). In treatments 3, 6, and 15 g L^{-1} *Gomphonema micropus* (Kützing) was found in greater abundance than 6%. Besides, different diatom taxa were identified under the influence of the different treatments (3, 6, 15, 30 and 100 g L^{-1}) with abundances over the 5%; *Platessa hustedtii* (Krasske), *Navicula dealpina* (Lange-Bertalot), *Planothidium lanceolatum* (Brébisson ex Kützing), Nitzschia linearis (c. Agardh) and *Gomphonema micropus* (Kützing), respectively (Table 8.3,Figure 8.6). Those species found at t21d under 30 g L^{-1} presented smaller sizes. Concentrations of 30 g L^{-1} seem to be a threshold from which the size remains constant not being significantly different to those exposed to 100 g L^{-1} (Table 8.2).

Table 8.2: Diatom metrics of all treatments at the beginning of the experiment (t0) and after the exposure (t21d) and recovery (t16d-R) periods. *C, control.* The letters indicate significant differences (p < 0.05) between treatments after one-way ANOVA and Tukey b test.

Treatment		Species richness (S)	Shannon diversity index (H')	Size (μm)	Density (cell mL⁻¹)	Growth rate (div day⁻¹)
t0		23 (± 4)	1.89 (± 0.21)	12.1 (± 1.23)	31289 (± 7531)	10.2 (± 0.41)
t21d	C	21 [a] (± 2)	2.03 [a] (± 0.33)	12.0 [a] (± 1.32)	34613 [a] (± 5253)	10.5 [a] (± 0.76)
	3 g L⁻¹	19 [a,b] (± 1)	1.84 [b] (± 0.07)	11.7 [b] (± 0.93)	24640 [b] (± 4472)	10.1 [b] (± 0.87)
	6 g L⁻¹	17 [b] (± 3)	2.09 [a] (± 0.70)	10.3 [c] (± 0.12)	88977 [c] (± 7501)	11.4 [c] (± 1.08)
	15 g L⁻¹	12 [c] (± 3)	1.70 [c] (± 0.09)	9.29 [d] (± 0.10)	118272 [d] (± 26295)	11.7 [d] (± 0.69)
	30 g L⁻¹	10 [c,d] (± 0)	1.55 [c] (± 0.33)	8.22 [e] (± 0.16)	73724 [e] (± 9817)	11.2 [e] (± 0.49)
	100 g L⁻¹	9 [d] (± 2)	0.87 [d] (± 0.02)	7.83 [f] (± 0.41)	13102 [f] (± 4839)	9.50 [f] (± 0.29)
one-way ANOVA	F	11.5	1.23	375	3063	8.8
	p	< 0.001	<0.001	< 0.001	< 0.001	< 0.001
t16d-R	C	28 [a] (± 4)	1.61 [a] (± 0.51)	12.9 [a] (± 1.24)	19360 [a] (± 8720)	9.98 [a] (± 1.24)
	3 g L⁻¹	16 [b] (± 1)	0.55 [b] (± 0.03)	10.9 [b] (± 1.17)	52330 [b] (± 5946)	10.9 [b] (± 1.39)
	6 g L⁻¹	15 [b] (± 0)	0.58 [b] (± 0.06)	10.8 [b] (± 0.95)	32657 [c] (± 5946)	10.4 [c] (± 1.09)
	15 g L⁻¹	17 [b] (± 2)	0.71 [c] (± 0.09)	9.94 [b] (± 0.77)	56711 [d] (± 6678)	10.9 [d] (± 0.67)
	30 g L⁻¹	10 [c] (± 3)	0.19 [d] (± 0.12)	9.77 [b,c] (± 0.30)	77635 [e] (± 2957)	11.3 [e] (± 0.87)
	100 g L⁻¹	15 [b] (± 2)	0.41 [e] (± 0.09)	9.68 [c] (± 0.22)	23662 [f] (± 2074)	10.1 [a] (± 0.70)
one-way ANOVA	F	9.1	0.75	44.9	2327	2.5
	p	<0.001	<0.001	< 0.001	< 0.001	< 0.001
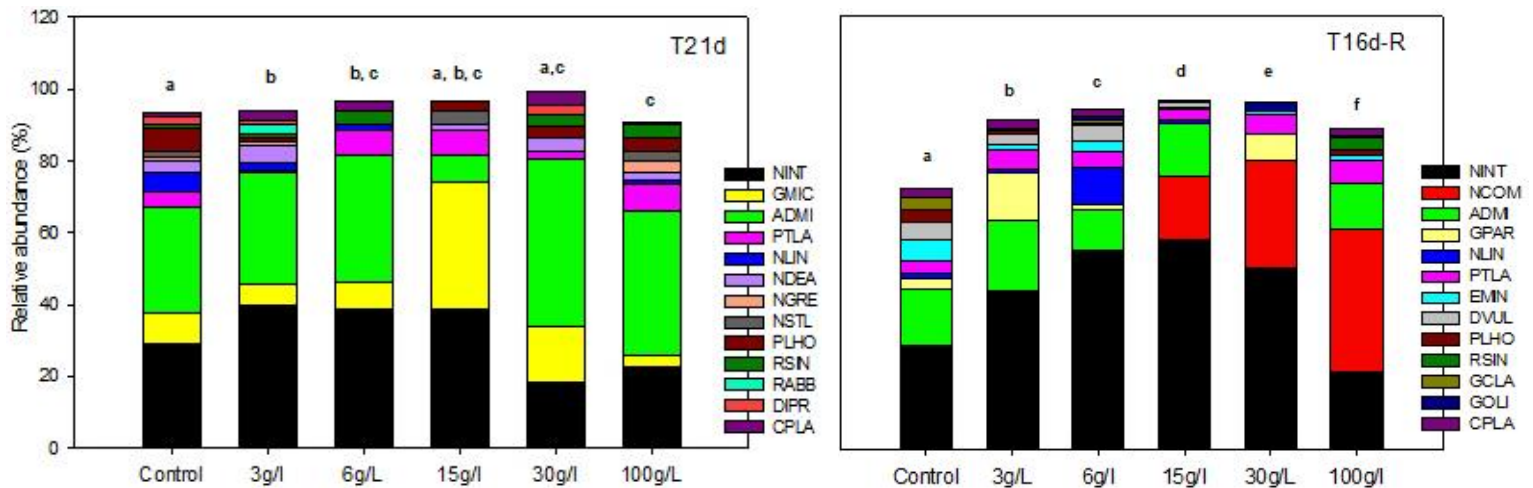
Figure 8.6: Relative abundance of the 13 major diatom species (>3%) within biofilm communities collected in the artificial streams at t21d and t16d-R. Where *Nitzschia intermedia* Hantzsch (NINT), *Gomphonema micropus* Kützing (GMC), *Achnanthidium minutissimum* (ADMI), *Planothidium lanceolatum* (Brébisson ex Kützing) Lange-Bertalot (PTLA), *Nitzschia linearis* c. Agardh (NLIN), *Navicula dealpina* Lange-Bertalot (NDEA), *Navicula gregaria* Donkin (NGRE), *Navicula striolata* Grunow (NSTL), *Platessa hustedtii* Krasske (PLHO), *Reimeria sinuata* Gregory (RSIN), *Rhoicosphenia abbreviata* c. Agardh (RABB), *Diatama problematica* Lange-Bertalot (DIPR), *Cocconeis placentula* Ehrenberg (CPLA), *Nitzschia communis* Rabenhorst (NCOM), *Gomphonema parvulum* Kützing (GPAR), *Encyonema minitum* (EMIN), *Diatama vulgaris* Bory (DVUL), *Gomphonema clavatum* Ehrenberg (GCLA) and *Gomphonema olivaceum* Hornemann (GOLI). p < 0.05.

SEM was performed for the exposure period to evaluate the effects of salinity on biofilm variables and their relationship. The SEM performed had a CFI index of 0.90 and RMSEA below 0.05, which denoted a good fit of the model structure. According to the results obtained, the most substantial adverse effects of salinity in structural variables were in total algal biomass as chl-*a* concentration (-0.35), green algae (-0.45) and diatom (-0.29) abundance. Regarding the diatom community metrics, it was observed that salinity negatively affected the species richness and size (-0.49 and -0.97). Besides, diatom species richness and diatom size presented a positive relationship (0.51). On the other hand, the affected biofilm functional variables by salinity were microbial respiration (-0.60), photosynthetic efficiency (-0.63), and the overall uptake rate of SRP (-0.45) and NH_4^+ (-0.36) (Figure 8.7).

Concerning the relationship between functional and structural variables, it was found that the algal biomass, as chl-*a* concentration, was positively related to diatom (0.13) and green algae (0.13) abundance and photosynthetic efficiency (0.39). In addition, photosynthetic efficiency were strongly correlated to diatom abundance (0.34). Likewise, green algae and diatom related positively to the uptake of NH_4^+ (0.47 and 0.20). On the other hand, green algae presented a negative relationship with the uptake of SRP (-0.17), whereas the relationship between diatom and SRP uptake were positive (0.33). Microbial respiration was related positively to the NH_4^+ uptake (0.22) and negatively to the SRP uptake (-0.35) (Figure 8.7).

These results suggests that diatom and green algae communities had a key role in the functional response to salinisation. Salinisation affected the diatom and green algae community by drastically reducing its abundance, and this reduction seem to cause an inhibition on the photosynthetic efficiency and a decrease on the NH_4^+ uptake capacity. By contrast, the SRP uptake capacity was favoured by diatom but interfered by green algae. In this study, it was observed an increase of the abundance of green algae in detriment of diatom, which might lead to a reduction on the SRP uptake.
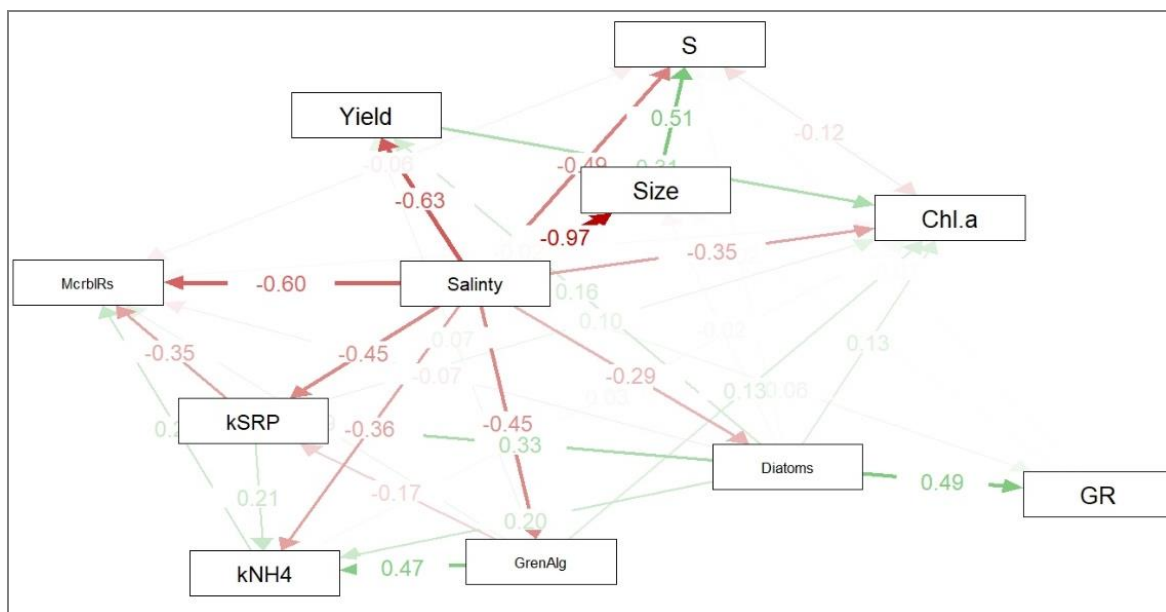
Figure 8.7: Structural equation model for the exposure period, where it is presented the effects of the salinity on the functional and structural variables evaluated and the relationships between them. Salinity: Salinity (g L^{-1}), Chl.a: chlorophyll-a (µg cm^{-2}), Diatom: Diatom abundance (µg chl-a cm^{-2}), GreenAlg: Green algae abundance (µg chl-a cm^{-2}), McrblRsp: microbial respiration (mg CO_2 produced/mg AFDM cm^{-2}), Yield: photosynthetic efficiency, kNH4 and kSRP: are the NH_4^+ and SRP uptake rate coefficient (min^{-1}), GR: diatom growth rate (div day^{-1}), Size: diatom size (µm), and S: diatom species richness. The red lines describe the adverse effects, and the green lines indicate the positive effects. Model fit indexes were set at CFI ≥ 0.90 and RMSEA ≤ 0.05.

8.3.3. POLLUTION-INDUCED COMMUNITY TOLERANCE (PICT)

At the beginning of the experiment (t0) and at end of the exposure period (t21d), the biofilm Pollution-Induced Community Tolerance (PICT) was measured using the photosynthetic efficiency as an end-point. The photosynthetic efficiency was measured on six random microcosms at t0 and on each treatment after the exposure of the biofilm to an increasing salinity concentration (0 to 290 g L^{-1}) during 24 hours. At t0, non significant differences were found between sampled streams. At t21d the C presented the same PICT (estimated based on EC$_{50}$) that at t0, showing the lowest tolerance to the salinity compared to the other treatments (EC$_{50}$ = 34.7 and 34.2 g L-1 respectively). Moreover, significant differences were found between treatments and the C (Figure 8.8). Additionally, a positive correlation was observed between the salinity concentration (from 0 to 30 g L^{-1}) and the EC$_{50}$ values measured (Pearson correlation r = 0.95, p = 0.005). According to the results obtained, the EC$_{50}$ for the100 g L^{-1} treatment was no possible to calculate precicely because if felt out of the range tested, thus the estimated EC$_{50}$ for this treatment was excluded from the statistical analysis (Figure 8.8).
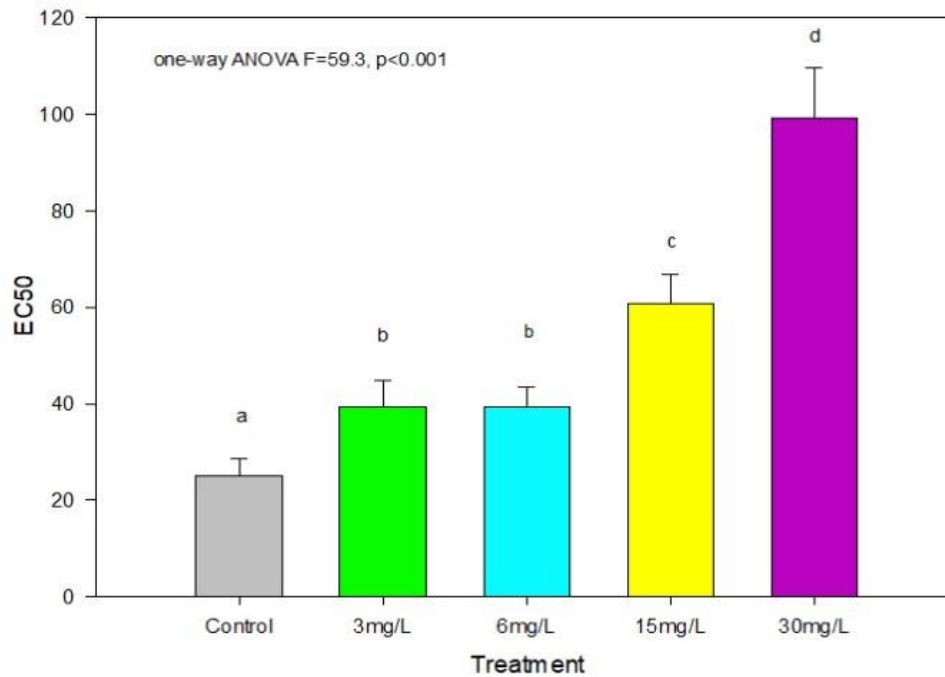
Figure 8.8: Effective concentrations (EC_{50}) as a measure of community tolerance to salinity after 21 days of exposure. Three replicate microcosms were conducted per treatment, mean ± SE (n = 3). EC_{50} was calculated from concentration-response relationships based on photosynthetic efficiency. Letters represent significant different groups after the post hoc Tukey b test when one-way analysis of variance (ANOVA) resulted significant (p < 0.05).

8.3.4. BIOFILM RESPONSE DURING THE RECOVERY PERIOD

At the end of the recovery period, non-significant differences were found among the control and treatments in the photosynthetic efficiency and the SRP and NH_4^+ uptake capacities of the biofilm. By contrast, the chl-*a* concentration of those biofilm exposed to the salinity gradient increased during the recovery period, being 6, 15 and 30 g L^{-1} significantly higher than the C at the end of the experiment (Figure 8.5).

Regarding the biofilm community composition, the green algae and diatom abundance increased in all treatments compared to the C during the recovery period. Regarding the diatom metrics, even though the diatom community had greater abundances and increased cell density and growth rates (GR) in all treatments during recovery (Table 8.2), the diatom diversity and species richness remained below the C at the end of the recovery period under all treatments. Simultaneously, the diatom species' dominance within the biofilm community changed compared to the C, especially in treatments previously exposed to 15, 30 and 100 g L^{-1} salinity (Table 8.2). Although at t16d-R, *Nitzschia intermedia* (Hantzsch) was the dominant species under all treatments, except for the most concentrated one, significant differences were found among all the communities (Table 8.2, Figure 8.6)

At the end of the exposure period, treatment 3 g L^{-1} showed similar behaviour than the C, even tough treatments 6 and 15 g L^{-1} had higher green algae and diatom abundances and growth rate, and treatments 3 and 6 g L^{-1} showed greater nutrient uptake capacities and photosynthetic efficiency, non significant differences respect to the C were found. By contrast, treatments 30 and 100 g L^{-1} had lower functional capacities, less green algae and diatom abundances, smaller diatom cells and little species richness compared to the C. Even though C showed larger diatom species and species richness at the end of the recovery period respect to the treatments, and those biofilm exposed to the different treatments, demonstrated higher functional responses than the C.

8.3.5. BIOFILM RESPONSE AFTER A 24H PULSE SALT ADDITION

After the recovery period, a pulse addition of 100 g L^{-1} of salinity was performed. After 24h of pulse, the biofilm functional and structural parameters were evaluated and non-significant differences in the nutrient uptake capacity were observed. By contrast, higher abundance of, green algae, diatom and chl-*a* (Table 8.3) were observed in biofilm communities from treatment 30 g L^{-1} compared to the C. Additionally, higher microbial respiration were observed under treatments 30 and 100 g L^{-1} and higher photosynthetic efficiency in treatment 100 g L^{-1} after the pulse addition (Table 8.3).

Table 8.3: Biofilm responses after the pulse addition. One-way ANOVA was performed to analyse statistical differences between treatments. C, control. n.s, no significant. The letters indicate significant differences ($p < 0.05$) between treatments after one-way ANOVA and Tukey b test.

	Microbial respiration (mg CO$_2$ cm^{-2})	Chl-*a* (µg cm^{-2})	Photosynthetic efficiency (Yield)	k – SRP (min^{-1})	Green algae	Diatom (µg chl-a cm^{-2})	Cyanobacteria
C	0.47 [a] (±0.11)	0.07 [a] (±0.07)	0.11 [a] (±0.04)	0.42 (±0.07)	0.34 [a,b] (±0.41)	0.08 [a,b] (±0.09)	0.07 (±0.09)
3 g L^{-1}	0.59 [a] (±0.15)	0.06 [a] (±0.02)	0.08 [a] (±0.05)	0.37 (±0.20)	0.36 [a,b] (±0.37)	0.09 [a,b] (±0.09)	0.09 (±0.08)
6 g L^{-1}	0.64 [a] (±0.21)	0.12 [a] (±0.03)	0.08 [a] (±0.02)	0.42 (±0.19)	0.48 [a,b] (±0.24)	0.07 [a,b] (±0.02)	0.11 (±0.06)
15 g L^{-1}	0.56 [a] (±0.10)	0.14 [a] (±0.00)	0.13 [a,b] (±0.03)	0.49 (±0.22)	0.93 [a,b] (±0.16)	0.19 [a,b] (±0.08)	0.24 (±0.07)
30 g L^{-1}	0.82 [b] (±0.05)	0.43 [b] (±0.12)	0.15 [a,b] (±0.04)	0.53 (±0.21)	1.76 [a] (±0.54)	0.53 [a] (±0.41)	0.60 (±0.32)
100 g L^{-1}	1.02 [c] (±0.09)	0.12 [a] (±0.02)	0.19 [b] (±0.02)	0.49 (±0.16)	0.33 [b] (±0.22)	0.04 [b] (±0.03)	0.02(±0.01)
one-way ANOVA	F = 4.49 p = 0.002	F = 11.8 p < 0.001	F = 4.36 p = 0.002	n.s	F = 8.00 p = 0.002	F = 3.30 p = 0.042	n.s

8.4. DISCUSSION

In this study, realistic salinity gradient concentrations (based on the real mining effluent from Menteroda abandoned mine and bibliography regarding freshwater salinization) were tested using artificial streams to assess and provide new evidence of its effects on biofilm communities, the salinity tolerance thresholds, and the ability of these communities to recover after the stress. As well as to reproduce different dilution scenarios of a real mine effluent discharging in a

freshwater stream to explore the potential salinity threshold from which irreversible impact can occur.

8.4.1. BIOFILM RESPONSES DURING THE EXPOSURE PERIOD

The salinity gradient had significant effects on different water physico-chemical variables, specifically on the nutrient concentration and conductivity. The increase reported in nutrient concentration under treatments 30 and 100 g L^{-1} between water removals, might be caused by the reduction of biofilm community growth and activity led by the high ion content during the exposure period. There is little information on the effects of salinity on biofilm functioning, but it is known that chemical stressors can affect the ability of biofilm to assimilate SRP since they can be less effective in removing it from the water column (Proia et al., 2017). These effects might be caused by the toxic effects of ions which caused the blocking of the synthesis of fatty acids, jeopardising the permeability-barrier functions and destabilise the cell membranes (McMurry et al., 1998; Villalaín et al., 2001; Phan and Marquis 2006). In this study, the biofilm community affected by the high ion content were not effective in removing the nutrient which lead to an accumulation of these nutrients in the water column as well as a reduction in the nutrient uptake capacity.

In addition to reducing the nutrient uptake capacities, just after one day of exposure, significant inhibition of the photosynthetic activity and microbial respiration were observed under the highest salinities (i.e., 30 and 100 g L^{-1}). High ion concentration is known to play a key role in regulating primary photochemical reactions (Berry and Dowton, 1982). When salinity increases, photosynthesis by epilithic algae also changes due to ionic and osmotic effects, which affect both photosynthetic reactions and general cell physiology, respectively (Martinez et al., 2020). Therefore, increased salinity results in changes in photosynthetic efficiency and in turn, primary production in stream habitats (Berger et al., 2019). However, these changes were observed only under salinities of 30 and 100 g L^{-1}.

Despite the extreme conditions, green algae are commonly the dominant primary producers in salinized ecosystems (Costelloe and Subramanyam, 2005). As observed in this study, the biofilm community composition exposed to the salinities of 3, 6 and 15 g L^{-1} showed an increase in the green algae abundance after 24h of exposure. Green algae possess great plasticity and adaptability to most abiotic stresses requiring drastic changes in the morphology and osmolyte concentrations in the short term and accumulation of advantageous mutations in the long run (Shetty et al., 2019a). Biofilm exposed to 30 g L^{-1} presented a different trend with decrease in the green algae abundance compared to other treatments. Those exposed to 100 g L^{-1} presented

a drastical reducction in the green algae abundance and in the overall total biomass. The mechanisms causing this reduction in biofilm biomass exposed to high salinities is not described, but it was described that under a given stressor, the decrease in chlorophyll levels in plants is considered as a common symptom of oxidative stress (Smirnoff, 1996), and it is attributed to the chlorophyll synthesis inhibition and with the activation of its degradation by the enzyme chlorophyllase (Taïbi et al., 2016). The reduction of chlorophyll indicates a photoprotection mechanism by reducing light absorbance by decreasing chlorophyll contents due to either slow synthesis or fast breakdown (Taïbi et al., 2016).

Additionally, regarding the the diatom community, its species richness, biodiversity, and cell size decreased in all treatments. By contrast, cell density increased under the 6, 15 and 30 g L^{-1} and the growth rate decrease in those exposed to 100 g L^{-1} treatment. Salinisation caused a shift in the exposed diatom community by favouring small forms of salt-tolerant diatom species. In fact, cell size is an important trait determining a species' ability to recover after disturbance due to the fact that smaller cells have typically higher growth rates, and therefore increased cell densities that confer greater resilience (Lange et al., 2016). Specifically, under treatment with higher salinities, it was abundant *Navicula gregaria* (Donkin), a species commonly found in marine and brackish waters (Hällfors, 2004). *Cocconeis placentula* (Ehrenberg) is another species that can grow in marine environments (Hällfors, 2004), and it was abundant under the influence of treatments 3, 6, and 30 g L^{-1}. Besides, treatments 15 and 30 g L^{-1} favoured the growth of *Gomphonema micropus* (Kützing), which is commonly found in marine waters (Hällfors, 2004) too. However, there is limited information regarding the evolutionary adaptation of freshwater taxa to hypersaline conditions. But non-genetic adaptive shifts can also occur through plastic changes involving acclimation within generations and acclimated responses across generations, including epigenetic changes (Kefford et al., 2021).

Furthermore, the direct effect of salinity on cell size might be caused by the energy invested in the osmoregulation process (Entrekin et al.,2019). Diatom could not produce enough intracellular osmolarity under high ionic concentrations to make the same pressure as smaller ionic content (Entrekin et al.,2019). Consequently, cell elongation is more inefficient, and cell size decreases faster (Mitra et al., 2014). In this study, the smaller diatom forms within the diatom community exposed to the different salinities occupied the more prominent species' remaining space.

At the end of the exposure period, the strongest effects were observed in those communities exposed to salinities between 15 and 100 g L^{-1}. At these concentrations, an apparent increase in

community tolerance to salinity was observed as higher the exposure to the ionic concentration was. To date, there is no study assessing the tolerance of biofilm communities to a gradient of realistic salinity concentrations. In this regard, the EC_{50} values of the biofilms exposed by the highest salinity concentration (30 g L^{-1}) were 2.6 times higer than the control biofilm. This observation wcould be explained because communities with high sensitivity experienced the highest selection pressure upon highest salinities and the sensitive species that are not able to withstand a given concentration of salinity would need physiological adaptations or be suppressed by more tolerant species. This sensitivity distributions enable a visualization of the community changes brought about by the exposure to a toxicant (Tlili et al., 2016). In fact, the resitance of an ecosystem to antropogenic pollution relies on tolerant species and their abilities to maintain ecosystem functions (Tlili et al., 2016). in this study a shift on the community composition was observed in biofilms exposed to the different salinities and tolerant species were favoured, which probably caused the increase on the community tolerance. This was also reported by Tlili et al. (2011b) in biofilms exposed to Zn pollution and by Pesce et al. (2016) when biofilms were exposed to herbicides. However, the adaptation to a new stressor situation might increase community sensitivity to other stressors because of the cost associated with tolerance acquisition (Clements & Rohr, 2009). For instance, Courtney & Clements (2000) reported that communities tolerant to metals were more sensitive to low pH, compared to communities not previously exposed to metals. Likewise, Kashian et al. (2007) showed that metal-tolerant benthic stream communities became sensitive to UV-B. Besides, the biofilm community-tolerance to hypersaline effluents shoulf be further studied.

8.4.2. RESPONSES IN THE RECOVERY PERIOD

Following the exposure period, two weeks of recovery were assessed. The replacement of the colonisation conditions in all the artificial channels gave back the physicochemical parameters uniformity after t7d of recovery. Functional variables responded quickly once the exposure period ended and demonstrated the highest recovery capacity in that biofilm exposed to the highest salinities, especially regarding the photosynthetic efficiency. On the other hand, the chl-*a* concentration was the structural variable with the quicker response, and the biofilm community structure recovered during the recovery period, remaining green algae the dominant group.

However, the diatom cell size, species richness, and biodiversity increased along the recovery period but did not recover to the C values. In this regard, cell size is considered an essential trait determining the species' ability to recover after a disturbance since smaller cells typically have

higher growth rates that give better resilience (Lange et al., 2016). However, the species found to be dominant at both the end of the exposure and recovery period differ between them and to the community observed at the beginning of the experiment (t0), suggesting that during the exposure period, the salinity concentrations may have opened niches for populations that were either more capable of tolerating higher salinities (Navada et al., 2019). Mainly, species that can survive in marine environments were found under the influence of salinity treatments, such as *Gomphonema parvulum* (Kützing), *Nitzschia linearis* (c. Agardh), and *Gomphonema olivaceum* (Hornemann). Nevertheless, one of the most abundant specie exclusively found in treatments 15, 30, and 100 g L^{-1} was *Nitzschia communis* (Rabenhorst), a euryhaline specie described to grow good over a conductivity range of 10 to 70 mS cm^{-2}. The tolerance of this species to a wide range of conductivities would allow them to proliferate in most natural saline waters (Dempster and Sommerfeld. 1988).

On the other hand, a pulse of 100 g L^{-1} were performed at the end of the recovery period to determine whether the historical exposure of communities to the different salinities could provide acquired tolerance towards high salinity pulses. These pulses can occur at any time due to leakages end up in the rivers and streams. In this study, even though all the biofilm communities presented a recovery of the functionality during the recovery phase, after the pulse addition, only those biofilm communities exposed to 30 and 100 g L^{-1} during the exposure period presented a better performance in all variables. The timing of the exposure could have had legacy effects to the species conforming the biofilm community that determined the resistance and resilience of these communities. In fact, the composition and diversity and of the diatom community were not altered significantly, despite that it is well known that diatom can react to rather small changes in salinity (Zimmermann-Timm, 2007; Trobajo et al., 2011; Rovira et al., 2012). This could be linked to the fact that the community was already adapted from the exposure period developing tolerances to higher salinity concentrations. Due to these adaptations that promoted functional redundancy, those communities exposed to the most polluted treatment demonstrated significantly higher SRP capacities (Shetty et al., 2019a).

8.5. CONCLUSIONS

This study indicated that hypersaline effluents caused changes in the biofilm community composition and function by increasing the salinity concentration in stream water. In this case, biofilm functions were compromised by reducing photosynthetic efficiency and nutrient uptake capacity. Additionally, communities exposed to the different treatments produced persistent effects on biofilm structure, this being evident by the incomplete recovery when saline

treatments were removed. Specifically, severe changes in the diatom species richness, growth rate and size were observed under all treatments. This shift in the community composition caused an increase of the community tolerance as higher the salinity concentrations were. Nevertheless, the community tolerance to hypersaline mining effluents should be further studied since there is no other evidences of it. However, the removal of the hypersaline effluent favoured the recovery of all the functional variables assessed but did not promote the biofilm structure recovery, which might be chronically affected. Additionally, after the recovery period, the pulse addition had an effect in those communities exposed to all treatments except for the most concentrated one.

Our results indicated that salinity concentrations of 15 g L^{-1} were the threshold from which more severe changes were observed in both structure and functionality of the biofilm communities. Nevertheless, freshwater salinisation is an environmental problem that requires further investigation since expected to increase in many regions of the world as a consequence of the global change (Le et al., 2019; Olson 2019).

CHAPTER 9.

GENERAL DISCUSSION

Photo: Microcosms and Frongoch stream (Wales, UK), by the author

9. GENERAL DISCUSSION

Mining effluents are complex mixture of substances composed by several elements that can become toxic to freshwater organisms. Due to its complexity, there are very limited studies available that include the effects of mining effluents on freshwater communities (Wu, 2016), including biofilm communities. These effluents can be produced from several processes such as run-off (surface flow from precipitation), acid mine drainage or leaching (flow into or out of the ground) that can generate highly polluted effluents, by carrying soluble substances (as heavy metals or ions) or small particles through soil or rock to the rivers and groundwater (Kumar, 2015). However, these effluents can persist long after the mining operation ceases, and the mine is abandoned. Therefore, the environmental problem caused by mining effluents is especially critical for effluents from abandoned mines. The study of biofilm communities exposed to these effluents could be a useful tool to test its effects at ecosystem level since they are complex communities integrating functional and structural responses. Additionally, they are the first step of the food chain integrating the effects of different environmental conditions and stressors over time. Finally, using their responses as metrics they can provide toxicological responses as indicators related with pollution.

Currently, some remediation techniques exist to treat mining effluents from abandoned mines in order to minimise the high environmental and ecological impacts that they are causing to water bodies worldwide (Tripathi and Rawat Ranjan, 2015; Abdel-Raouf and Abdul-Raheim, 2017). In this thesis, we investigated the ecological impacts of a metal (Chapter 4, 5 and 6) and a hypersaline (Chapter 7 and 8) mining effluents from abandoned mines on freshwater ecosystems and the efficiency of different remediation techniques in reducing these impacts, using the aquatic biofilms as bioindicator. Specifically, these methods consist of i) the use of innovative technologies based on electrocoagulation and membrane processes to treat metal mining effluents, and ii) testing different dilutions of the hypersaline effluent to define the salinity thresholds in which non-reversible ecological impacts occurred.

It was initially hypothesized that mining effluents from abandoned mines would have severe impacts on freshwater biofilm functionality and structure. However, these communities would recover its functional and structural characteristics when the pollution source from the mining effluents disappears by extruding the toxicants from their cells. Additionally, as hypothesized, different treatment technologies would potentially reduce the ecological impact of metal mining effluents. On the other hand, the dilution of both metal and hypersaline mining effluents could reduce the impact to freshwater ecosystems.

9.1. ECOLOGICAL IMPACT CAUSED BY METAL MINING EFFLUENTS ON FRESHWATER ECOSYSTEMS.

The specific hazards posed by heavy metals harboured in mining effluents in the aquatic environment may produce toxic effects on aquatic organisms since they are highly dependent on the long-term life of the metal, and if the metal remains dissolved in water or is adsorbed on suspended solids or sediment, which determines its bioavailability. The bioavailability controls the toxicity of the metal to biofilm, which leads to bioaccumulation behaviour and consequently the biomagnification of the metal throughout the trophic web (Ivorra et al., 2002; Corcoll et al., 2012; Bonet et al., 2014). In agreement with that and the initial hypothesis, biofilm communities presented short-term responses in the functionality and alterations in the structure after mid-term exposures to abandoned metal mining effluents. Since Frongoch mine was a former exploitation of zinc (Zn), this metal was found to be the most abundant metal in the mining effluent used as reference in this thesis. Besides, lead (Pb) and cadmium (Cd) were also detected in low concentrations. Specifically, the Zn concentration tested in this thesis ranged from 133 mg Zn L^{-1} in Frongoch stream, to 0.19 mg Zn L^{-1} in the artificial stream set-up (Table 9.1).

Table 9.1: Summary of the functional and structural biofilm responses during the exposure period to the different Zn concentrations tested in this thesis. ↑, high; ↓, low; ≠, different and =, not different from the control. U, untreated; T, treated; LD, low-dilution; HD, high-dilution; NF, nanofiltration; EC, electrocoagulation. Grey fills; not tested. [1] Chapter 4; [2] Chapter 5; [3] Chapter 6.

	TREATED				UNTREATED			
	T-HD[3]	NF+EC[2]	NF[2]	T-LD[3]	U-HD[3]	U[2]	U-LD[3]	Frongoch Stream[1]
Zn in water (mg L^{-1})	0.19	0.25	0.36	4.87	1.41	4.26	21.3	133
BIOFILM RESPONSES								
Metal accumulation	↓	↓	↑	↑	↑	↑	↑	↑
FUNCTIONAL								
Photosynthetic efficiency	↑	↑	↑	↓	↓	↓	↓	↓
SRP uptake	↓			↓	↓		↑	
NH$_4^+$ uptake	↓			↓	↓		↓	
STRUCTURAL								
Algal biomass	↓	↓	↓	↓	↓	↓	↓	↓
Community composition	≠	=	=	≠	≠	≠	≠	≠

In the field, the Frongoch stream presented higher Zn concentrations compared to the worst scenario reproduced in the laboratory experimental set-up (low dilution (LD) in the artificial stream set-up). Even though the flow conditions in the field during the sampling were similar to the conditions simulated in the U-LD scenario using artificial streams (18 $m^3 h^{-1}$), the differences

might be caused because the flow of the mining effluent on the field was higher (7.4 m^3h^{-1}) compared to the simulation performed in the laboratory (4 m^3h^{-1}).

9.1.1. FUNCTIONAL EFFECTS

Biofilm communities exposed to the untreated effluent presented more Zn, Pb and Cd accumulated than the control (C) biofilm. However, even though in the field higher metal concentrations in water were observed, the metal bioaccumulated in biofilm were lower than in the artificial streams set-up where less metal in water were detected. This effect might be caused since laboratory tests focus on bioaccumulation associated with a single exposure route, which do not represent field situations. Besides, laboratory exposures may overwhelm metabolic capabilities for biotransformation and overestimate bioaccumulation compared to the field (Weisbrod et al., 2009). Dosing test substances in "clean" laboratory water (lacking organic complexing agents) may also exaggerate bioavailability compared to the field (Kiparissis et al. 2003). On the other hand, field determination of chemical bioaccumulation integrates all corresponding exposure routes and dissipation processes (i.e., growth, metabolism, elimination, bioavailability). Such bioaccumulation metrics may be affected by ecosystem variables, such as chemical concentrations that can change with natural temporal and spatial variability in exposure sources, sediment–water column chemical relationships, temperature, and other environmental factors (Weisbrod et al., 2009).

The observed bioaccumulation was accompanied by short-term functional changes, such as changes in the photosynthetic efficiency of the biofilm. The decrease on the photosynthetic efficiency might be caused by the mode of action of Zn (as the most accumulated metal) affecting several photosynthetic processes of algae and cyanobacteria (Corcoll et al., 2012), although Pb and Cd could have played a key role since they were detected in biofilm even when they were not detected in water (Chapter 5 and 6). In fact, Cd toxicity to the photosynthetic apparatus has been observed at water concentration < 100 μg L^{-1} (Hill et al., 2000) whereas the Pb toxicity threshold is set at 2.5 μg L^{-1} (Corcoll et al., 2012) which in Chapter 6, this threshold was exceeded (170 μg L^{-1}). On the other hand, the toxicity threshold proposed for Zn is 120 μg L^{-1} (US EPA, 2006), however several authors reported Zn concentrations in different polluted streams from 25 to 3000 μg L^{-1} (Ivorra et al., 2002; Le Faucheur et al., 2005; Morin et al., 2008; Bonnineau et al., 2011; Corcoll et al., 2012). In this thesis, these effects on the photosynthetic efficiency of biofilms were mainly at Zn concentrations in water above 1.41 mg L^{-1} (Chapter 6).

Besides, metal mining effluents are very complex and are composed of a complex mixture of compounds leading to a variability in the biofilm responses (Younger et al., 2003).

On the other hand, the nutrient uptake capacity of biofilm exposed to metal effluents was negatively affected under a wide range of metal concentration in water (0.19 to 21.3 mg Zn L^{-1}) (Chapter 5 and 6). This decrease in the nutrient uptake capacity could be caused by oxidative damage in the cells (Sabater et al., 2016). The oxidative stress might have caused a change in the energy investment from nutrient uptake to antioxidant enzyme activities production as detoxification mechanisms (Morin et al., 2012; Bonet. 2013). A similar decrease was observed by Castro et al. (2015) and Tuulaikhuu et al. (2015) under arsenic (As) concentration of 130 µg L^{-1} and 37 µg L^{-1}, respectively. This decrease in the nutrient uptake capacity under polluted scenarios might suggest that in the field, natural streams affected by metal mining effluents could have a decrease in its self-purification capacity and, consequently, increase the eutrophication. This might be caused because biofilms directly participate in the nutrient uptake and mineralization, which make this communities relevant actors in the self-depuration processes occurring in rivers (Pusch et al., 1998).

9.1.2. STRUCTURAL EFFECTS

Apart from the functional effects, the metal mining effluent caused changes in the biofilm structure too. Specifically, the algal biomass estimated from chlorophyll-*a* concentration in biofilm decreased during the exposure to the most polluted treatments in the artificial streams (Chapter 6) as well as in the most polluted sampling sites in the field (Chapter 4). However, a different pattern in this decrease was observed among different experiments. Under controlled conditions, the algal biomass decreased at Zn concentrations around 5 mg L^{-1} (Chapter 6), whereas in the field, this decrease occurred at Zn water concentrations around 35 mg Zn L^{-1} (Chapter 4) compared to the reference sampling site (Nant Cell). The different responses observed between the field sampling and experiments could be attributed to an adaptation process of the biofilm community caused by the chronic exposure to heavy metals from the abandoned mining effluent in the field, where sensitive species to metals were replaced by tolerant ones with higher resistance to metal pollution than communities used in the microcosm experiment (Corcoll et al., 2012; Bonet et al., 2013; Bonet et al., 2014). Nevertheless, this different responses between field and laboratory-based experiments could also be an influence of other cofounding environmental factors given in natural streams affecting biofilm community composition (including nutrients, dissolved organic carbon, pH, temperature, hydrodynamic parameters, and pollutants) (Besemer. 2015). Regardless, the decrease in the algal biomass

might have effects on the overall ecosystem functioning due to their role in the uptake or retention of inorganic and organic nutrients (Fishcer et al., 2002; Romaní et al., 2004), affecting the self-depuration processes, and transfer of energy to higher trophic levels (Corcoll et al., 2011).

Regarding the community composition, in Chapter 5 and 6, the relative abundance of green algae in biofilm exposed to mid-term metal pollution increased as well as it was observed in the field. This pattern has been reported by previous studies performed under laboratory conditions (Corcoll et al., 2011; Ivorra et al., 2000) and in natural environments at different confluences of mining effluents with stream waters (Das and Ramanujam, 2011). The mechanisms favouring the growth of green algae under high Zn concentration in water could be related to the response to Zn toxicity that may enhance the synthesis of antioxidants causing the activation of the xanthophyll cycle of green algae as protective mechanisms to avoid Zn toxicity (Corcoll et al., 2012). Despite this evidence, in Chapter 4 (in the field), the relative abundance of green algae in Frongoch stream decreased after the entrance of the mining effluent into the stream, where the highest metal concentration was found. This decrease in the green algae community might have bene caused by other environmental perturbation such as flow conditions that are highly variable (Ghosh and Gaur, 1994) or the substrate typology (which in this sampling points were artificial). The substrate typology also affected the biofilm algal growth since those communities growing in rocks, gravel and boulders are more resistant to the adverse environmental factors (Burns and Ryder, 2001; Pandey, 2020).

By contrast, diatoms, which were the algal group dominating the biofilm community before the exposure period in Chapter 4 and 6, were strongly affected by metal concentrations. During the exposure period, lower growth rates, smaller cell sizes and a decrease in diatom biodiversity were observed in both chapters. The diatom community varied between studies, and the Zn concentrations and pH from which diatom abundance drastically decreased was observed at 0.79 mg Zn L^{-1} and pH 6.72 in the artificial streams (Chapter 6), whereas this response in the field (Chapter 4) was identified at 1 mg Zn L^{-1} and pH of 6.3. This indicated that in the field, adaptations to the pollution gradient might occur due to chronic exposures to heavy metal. In fact, the diatom species identified under the metal stress in the field (i.e., *Achnanthidium minutissimum, Pinnularia borealis* or *Rhoicosphenia abbreviata*) were more tolerant to metals (Medley and Clements, 1998) and species frequently reported in metal contaminated environments (Morin et al., 2012). These species favoured by the metal contaminated environments are usually smaller, since they are more effectively protected by the exopolysaccharidic matrix and thus favored their survival under heavy metal pollution (Morin et al., 2012). In this thesis, the size in

those biofilms exposed to metal concentration (Chapter 4 and 6) gradually decreased between 43% (T-HD) to 70% (U-LD) compared to the C. With the selection of adapted species with smaller cells, the larger species disappeared and hence a decrease in the biodiversity was observed (Chapter 4 and 6).

9.1.3. RECOVERY CAPACITY

In Chapter 6, the recovery capacity of biofilm communities after being exposed to the treated and untreated metal mining effluent was assessed. During this period, biofilm communities showed a rapid response, firstly recovering the photosynthetic efficiency and increasing algal biomass (chlorophyll-*a* concentration). This recovery might be caused by the increase in the number of cell transporters excreting accumulated metals in cells as a consequence of a rapid detoxification mechanism promoting rapid metal extrusion (Lambert et al., 2012; Castro et al., 2015). By contrast, the nutrient uptake capacity was not recovered in that biofilm exposed to the highest metal concentration (U-LD) probably due to the high amount of metal still detected accumulated in these communities (Duong et al., 2009; Bereet al., 2011; Corcoll et al., 2011) that kept causing the oxidative stress and therefore the shift on the energy investment to produce antioxidant enzyme activities as detoxification mechanisms.

On the other hand, the community composition kept dominated by green algae at the end of the recovery period and the diatom cell size, growth rate and biodiversity remained below the control biofilm (C). In addition, the diatom composition of the biofilm during the recovery period changed compared to the end of the exposure period and the C biofilm. The change in the species dominance might be favored by the loss of dominant species during the exposure period, which might have left spaces for the adapted ones to growth. In fact, returning the adapted communities exposed to a pollutant to reference conditions may not be possible after crossing a critical threshold and changing to an alternative state (Wolff et al., 2019). This suggests that the exposure to the metal mining effluent selected diatom species with a better capacity to regulate intracellular metal concentration by means of energy-dependent active transport systems (Castro et al., 2015) which might have favoured the growth and establishment of these species in the community that maintained the functional but not the structural recovery, through functional redundancy that sustained its activity under stress (Liu et al., 2017).

The fact that the community composition of those biofilms exposed to the different metal concentrations did not structurally recover might be caused by the duration of the recovery period. In this study, where two weeks of recovery were performed, the biofilm structure on the biofilms previously exposed to the metal effluent was not fully recovered. This suggests that

longer periods of recovery should be assessed to determine whether this lack of recovery could be a matter of time as previously reported by Rimet et al. (2005) and Arini et al. (2012a). Besides, the fact that no new biofilm inoculum was added during the recovery period probably limited the potential recovery of the pre-exposure values of the algal biomass and the community composition. In this regard, it was previously reported that the recovery was more pronounced when species immigration processes were possible (Ivorra et al., 1999; Morin et al., 2010; Lambert et al., 2012). Besides, at the end of the recovery period, metal accumulation was still higher in communities under T-LD, U-HD and U-LD than the C biofilm, which suggests that the experimental set-up did not allow the complete metal dissipation since artificial streams were used in a recirculating mode and water was renewed every two days, thus limiting dissipation kinetics.

9.2. EFFICIENCY OF DIFFERENT TREATMENT TECHNOLOGIES IN REDUCING ECOLOGICAL IMPACTS FROM ABANDONED METAL MINING EFFLUENTS

Within the Life DEMINE project, the efficiency of different treatment technologies to treat abandoned metal mining effluents and reduce its ecologically impact was tested. Specifically, the technologies tested were: nanofiltration (NF) and the combination of NF followed by electrocoagulation (NF+EC) at laboratory scale, and the combination of EC with microfiltration (EC+MF) at pilot plant scale. The efficiency of these technologies in reducing the ecological impacts of metal mining effluents from abandoned mines on freshwater ecosystems was tested in the framework of this thesis using biofilm communities as a bioindicator under microcosm conditions.

The treatment technologies tested, NF, NF+EC and EC+MF, presented Zn removals in water of 91%, 96% and 97%, respectively (Chapter 6). However, even though metals were not detected in the water, biofilm exposed to the treated effluents still presented higher metal accumulation compared to the C; biofilms exposed to the mining effluent treated by NF+EC presented 3 and 10-fold more Zn and Cd than the C, while those exposed to EC+MF at low dilution (T-LD) presented 7 and 0.04-fold more Zn and Cd than the C. It has been reported that metal toxicity in biofilm is more related to extracellular metal accumulation than to metal concentration in the water column, which commonly may not be detected at low concentrations (Corcoll et al., 2012; Bonet et al., 2014). Throughout this thesis, even when metals were not detected in water, they were detected accumulated in biofilm affecting its performance. Additionally, it was observed that the metal concentration in water, hence their toxicity, depends on both the treatment

technology efficiency in removing metals and the dilution capacity of the receiving stream (Chapter 6).

The NF and NF+EC efficiency were assessed by exposing biofilm communities to these treated effluents mimicking the real dilution conditions of the field under microcosm conditions (aquarium). Biofilm responses to the different metal concentrations demonstrated that the combination of NF+EC was the technology with higher metal removal rates and biofilm exposed to this technology presented similar functional and structural responses than the control biofilm (C). By contrast, NF presented lower metal removals but no differences in the metal accumulation were found compared to the C. The lower metal removals could promote an increase in the metal accumulation under longer exposure periods (Chapter 6).

In that sense, it is important to assess the efficiency of the treatment technologies under different flow conditions to assure that they will be successful in reducing the impacts caused by the polluted effluents. The ecological impact caused by the mining effluents on the receiving freshwater ecosystems depends on both, the effluent metal composition and concentration, and the dilution capacity of the receiving stream (Morgan et al., 2021). In natural environments, the river flow might have more acute changes and hence lower flows and dilution capacities. This scenario may decrease the technology efficiency as higher metal reductions would have to be achieved to accomplish with the WFD limits of metal content in stream waters. With the NF, NF+EC and EC+MF technologies, Zn removals of 91 and 96% and 97% were obtained in the mining effluent, respectively. However, the Zn content in the treated effluent (Chapter 5 and 6) still exceeded the limits established by the EU (0.12 mg L^{-1}, European Commission. 2000), indicating that the stream flow has to be considered to calculate the metal concentrations in the stream before discharging the treated effluent. On the other hand, treated effluent could be diluted with upstream water before reaching the stream to achieve permitted limits thus increase the dilution when discharging to the stream.

The efficiency of combining EC + MF in reducing the ecological impact were tested using artificial streams (Chapter 5). To assess the efficiency as accurately as possible, four treatments were set representing the treated and untreated metal mining effluent from Frongoch abandoned mine discharged into the receiving stream under two different dilution capacities depending on its average and minimum stream flow rate. In this regard, we observed that under low dilution conditions both, treated and untreated effluents, showed an increase on the metal accumulation and a decrease on the biofilm functionality (i.e., photosynthetic efficiency and nutrient uptake rate) and structure (i.e., in the dominance, chlorophyll-*a* and diatom metrics).

154

On the other hand, the treated effluent under high dilution were similar to the control. This indicated that the treatment technology was efficient enough to reduce the ecological impacts to the receiving stream under high dilution conditions.

9.3. ECOLOGICAL IMPACT CAUSED BY HYPERSALINE MINING EFFLUENTS ON FRESHWATER ECOSYSTEMS.

As observed with the metal mining effluents, freshwater salinisation induced by mining effluents from abandoned potash mines had effects on the biofilm functionality and structure (Table 9.2). These effluents impacted firstly on the biofilm functionality, causing a strong decrease on the photosynthetic efficiency, the microbial respiration, and a reduction in the nutrient uptake capacity. At the same time, freshwater salinisation altered the biofilm structure, causing a significant shift of the biofilm community composition at mid-term exposure.

Table 9.2: Summary of the functional and structural biofilm responses during the exposure period to the different salinity concentrations tested in this thesis. ↑, high; ↓, low; ≠, different and =, not different from the control. Grey fills; not tested.

Salinity	Chapter 7	Chapter 8				
	15 g L^{-1}	3 g L^{-1}	6 g L^{-1}	15 g L^{-1}	30 g L^{-1}	100 g L^{-1}
Conductivity (μS cm^{-1})	13200	4273	9307	20343	38052	109875
BIOFILM RESPONSES						
FUNCTIONAL						
Photosynthetic efficiency	↑	↑	↑	↑	↓	↓
SRP uptake	↑	↑	↑	↑	↓	↓
NH_4^+ uptake		↑	↑	↓	↓	↓
STRUCTURAL						
Algal biomass	↑	↑	↑	↑	↓	↓
Community composition	≠	≠	≠	≠	≠	≠

9.3.1. FUNCTIONAL EFFECTS

The high ionic content of these hypersaline effluents caused a significant inhibition of the photosynthetic efficiency after short-term exposures to salinities up to 15 g L^{-1} (Chapter 7 and 8). In fact, high ion concentration is known to play a key role in regulating primary photochemical reactions due to ionic and osmotic effects (Berry and Dowton, 1982; Martinez et al., 2020) causing the inhibition of photosynthetic CO_2 assimilation capacity. This suggests that the cells may down-regulate their light-harvesting capacity to acclimate their low carbon metabolic capacity (Lu and Zhang, 2000). Likewise, the work done in this thesis has shown significant short-term effects in the nutrient uptake capacity of those biofilm exposed to salinity concentrations

below 15 g L^{-1}, that were able to recover after 3 days of exposure (Chapter 7 and 8). By contrast, the nutrient uptake of the biofilm exposed to concentrations up to 30 g L^{-1} remained significantly below the control during all the exposure period (Chapter 8). These effects could be caused by the toxic effects of ions that blocked the synthesis of fatty acids, jeopardising the permeability-barrier functions and destabilise the cell membranes preventing the nutrient uptake (McMurry et al., 1998; Villalaín et al., 2001; Phan and Marquis 2006). Besides, after short-term exposure to the different salinity concentrations (from 3 to 100 g L^{-1}), the microbial respiration presented a decrease, but in those biofilm exposed to concentrations below 15 g L^{-1} recovered just after three days of exposure. Osmotic stresses may play a role in restricting respiration since the ion-stress mechanisms involve a change in the osmotic potential, accumulation of hazardous components (such as hydrogen sulfide) as a byproduct of different composts reduction and a disturbance to nutrient cycles (Yang et al., 2018).

The functional recovery of biofilm communities exposed to 3, 6 and 15 g L^{-1} (Chapter 7 and 8) were probably due to the rapid ion extrusion from the cells, associated with the sodium proton antiporter (Lu and Zhang, 2000) and the salt-tolerant species' functional redundancy that continued to sustain its activity under stress (Rovira et al., 2012). This recovery was not observed at higher concentrations, probably because these salinities could exceed the salinity threshold at which sub-lethal effects occur (Cañedo-Arguelles, 2020). Moreover, biofilm exposed to 30 and 100 g L^{-1} (Chapter 8) presented a drastic decrease in its algal biomass as chl-*a*, suggesting that the ion content caused an oxidative stress (Smirnoff, 1996) inhibiting the chlorophyll synthesis and activating its degradation, which is a photoprotection mechanism that reduce light absorvance by decrasing chlorophyll contents (Taïbi et al., 2016).

9.3.2. STRUCTURAL EFFECTS

In addition, it is interesting to note that, despite the biofilm inoculum added in both microcosm studies using the hypersaline effluent (Chapter 7 and 8) were taken from the same reference stream (Riera Major, Viladrau, NE Spain), the community composition of the initial biofilm colonizing aquaria in Chapter 7 differed from the community observed in the artificial channels in Chapter 8. This might be caused because the experiment was carried out in different times and seasons, thus the biofilm composition could be different. During the colonisation period, in both experimental set-ups the community were dominated by diatoms. However, during the exposure period, in biofilms exposed to the salinity of 15 g L^{-1} in the aquaria approach (Chapter 7) the community were dominated by diatoms, whereas in the artificial streams, biofilms exposed to the same concentration showed an increase in the green algae relative abundance

just after 24h of exposure (Chapter 8). The different responses observed in biofilm communities could be caused by differences in the effluent composition used in the different experimental approaches, even though the initial salinity of both hypersaline effluents were similar. In this regard, the original hypersaline mining effluent from Menteroda used in Chapter 7 could have added other compounds (not identified in this thesis) affecting the biofilm response, whereas the ion concentration of the hypersaline effluent made up in the laboratory in Chapter 8 simulated the Menteroda effluent was strictly known. Along with the composition, the different experimental approaches might have played an important role in the biofilm community composition, since the mining effluent from Menteroda mining site was used in aquarium conditions characterised by steady flow conditions, whereas a synthetic hypersaline effluent based on the ion composition of Menteroda mining site was used in indoor artificial streams with a continuous flow regime. Indeed, under laminar flow conditions diatom communities might have more difficulties to growth, which allow other species with higher flow tolerances (i.e., green algae) dominate the community (Besemer et al., 2007). It is therefore important to consider the conditions simulated in microcosms to assess the ecological impacts of different stressors, including hypersaline effluents.

Moreover, it is known that the effects of salinisation on the freshwater biota can depend on factors such as the magnitude and frequency of exposure, and ionic composition, as well as on the base-line salt concentration in the stream water (Pilkaitytë et al., 2004; Nielsen et al., 2003; Gutiérrez-Cánovas et al., 2012; Cañedo-Argüelles et al., 2014). Direct effects of salinity on diatom taxa dominance, species richness, growth rate and cell size were observed under all salinities (from 3 to 100 g L^{-1}) tested in this thesis (Chapter 7 and 8). Some of these changes may be related to salinity effects on diatoms valve morphology (Trobajo Pujadas, 2003), such as the effect of salinity on cell size caused by the energy invested to maintain the osmoregulation processes (Entrekin et al., 2019). Moreover, salinisation affected the diatom community stability and led to a transition to a new stable state (Herbert et al., 2015) favoring salt-tolerant diatom species occupy the niches left by the sensitive ones such as *Navicula gregaria* (Donkin) and *Cocconeis placentula* (Ehrenberg).

To date, few studies have reported the effects of freshwater salinisation in biofilm community functionality and structure (Loureiro et al., 2013; Venancio et al., 2019). However, in this thesis, it was found that effects of salinity in biofilm structure might have affected its functionality (Chapter 8). Specifically, we observed that diatom and green algae communities had a key role in the functional response to salinisation. Salinisation affected the diatom and green algae

community by drastically reducing its abundance, and this reduction caused a photosynthetic inhibition and a decrease on the NH_4^+ uptake capacity (Chapter 8). By contrast, the SRP uptake capacity increased with the presence of diatom but it was reduced when green algae dominated the community. According to that, the decrease on the SRP uptake rate observed under salinity concentrations from 15 to 100 g L^{-1} might have been favoured by the dominance of green algae in the biofilm which activity is known to be limited by salinity (von Alvensleben et al., 2016).

9.3.3. RECOVERY CAPACITY

On the other hand, as observed in the biofilm exposed to the metal mining effluent, functional variables responded quickly once the exposure period ended and demonstrated the highest recovery capacity in that biofilm previously exposed to the highest salinities, especially regarding the photosynthetic efficiency (Chapter 8). In this regard, it is reported that the existence of a high degree of functional redundancy in microbial communities could promote the functional recovery of communities previously exposed to a polluted effluent (Hill et al., 2008). In fact, when a community is exposed to pollution, they may response in three ways to sustain or recover their functions: resistance, resilience, and redundancy (Allison and Martiny, 2008). For a community with multiple species, functional redundancy is the main response way to maintain its functions under disturbance, because some individual species may be damaged and makes it most unlikely to return to the original composition. When recovering, functional redundancy of a community indicates that the altered community by previous exposure can perform at the same rate as the original community, since the old community may contain functionally redundant taxa (Liu et al., 2017). This was observed during the recovery period (Chapter 6), where the communities previously exposed to the different salinities recovered its functionality, even though the community composition was different between salinities.

The biofilm composition did not change during the recovery period and green algae remained the dominant group until the end of this period (14 days). Additionally, even though diatom did not dominate, they increased their cell size, species richness, and biodiversity during the recovery period in biofilms previously exposed to salinities from 3 to 100 g L^{-1}. The reduction in diatom size and an increase in its density was observed in biofilm exposed to all the salinity concentrations tested, especially to salinities > 15 g L^{-1}. Besides, differences between the dominant diatom species at the end of the exposure and recovery periods were observed. During the exposure period, the salinity concentrations may have opened niches for populations that were either more capable of tolerating higher salinities (i.e., as *Gomphonema parvulum* (Kützing), *Nitzschia linearis* (c. Agardh), *Gomphonema olivaceum* (Hornemann) and *Nitzschia*

communis (Rabenhorst). These species were well established when the recovery period started (thus increasing its dominance) which did not allow the most sensible ones to recover since the niches were already occupied by the tolerant ones. On the other hand, microcosms conditions could have affected this recovery since no new biofilm inoculum were added during the recovery period as it would occur in natural streams (Ivorra et al., 1999; Morin et al., 2010; Lambert et al., 2012), adding new species that could favour the community recovery. However, further investigations concerning the recovery duration should be addressed since longer periods might favour the community structure recovery.

Yet, after the exposure period, biofilm communities exposed to the different salinities during the exposure period, responded differently to a 24h pulse of a high salinity (100 g L^{-1}), indicating differences between them on salinity tolerance (Chapter 8). These differences in the responses to a salt pulse were detected after 2 weeks of recovery in which all communities were left under the same unpolluted conditions. After the pulse, only those biofilm communities previously exposed to 30 and 100 g L^{-1} during the exposure period were less affected in all variables, which might be explained by the previous adaptation of the community to the most polluted treatments. The biofilm reorganised into different alternative state (i.e., shift from one stability domain to another) in which resistant species were favoured.

Salinity has not been considered a major problem in most European countries, even though the salinisation of European rivers might compromise the achievement of the Water Framework Directive (WFD) aims in several river basins. Additionally, neither water quality indicators nor EQS values have been defined for freshwater salinisation (Cañedo-Arguelles et al., 2013). As a consequence, there is a lack of solid methodological standards, guidelines and best practices for prediction and evaluation of negative impacts of freshwater salinisation in inland water bodies (Böhme, 2011).

Throughout this thesis, it was explored the salinity thresholds from which irreversible impact can be observed on the biofilm structure and functioning, and thus the optimal concentration to be achieved when discharging hypersaline mining effluents to the receiving water bodies. By using artificial streams, which provided a feasible approach of a stream conditions, the impact of realistic salinity concentrations on the biofilm performance was assessed. In this regard, although structural effects were observed in biofilm exposed to all salinities tested, significant effects on functionality were observed in that biofilm exposed to salinity concentration above 15 g L^{-1}. In this study, this threshold has been identified between 6 and 15 g L^{-1}, that coincides with other published field studies that identified salinity concentrations of 4 to 10 g L^{-1} as the

threshold at which most freshwater species are eliminated (Cañedo-Argüelles, 2020) but it can vary widely among taxa (Kefford et al., 2012).

According to the results obtained in this thesis and previous studies, one feasible solution to reduce the impact of hypersaline mining effluents on freshwater ecosystems could be to control that the salinity concentrations in the receiving river do not exceed a salinity between 6 and 15 g L^{-1}. However, the toxic effects of salinity depend on the ion composition, but also on the type of exposure (chronic or pulse), as well as the dilution of the saline effluent on the receiving stream (William et al., 2016; Gutierrez-Canovas et al., 2018). It should also be considered that salinity in freshwaters can present can temporal variability due to changes in river flows (affecting the dilution capacity), precipitation (affecting run-off) and salinity point sources. These issues should be further addressed because they can determine the response of freshwater organisms to salinization and the resistance and resilience mechanisms to adapt to it (Cañedo-Argüelles, 2020).

9.4. BIOFILM AS A BIOINDICATOR TOOL

Common responses of biofilm communities exposed to both hypersaline and metal mining effluents were observed throughout this thesis. In all cases, functional variables of biofilm were the ones responding faster to the stress. Specifically, the exposure to the different pollutants caused a decrease in the photosynthetic efficiency and the nutrient uptake rate after short-term exposure. In addition, the structure of biofilm communities changed during the mid-term exposure under both pollutant source by decreasing the diatom species richness, cell size, growth rate and taxa dominance. Likewise, after the pollution removal during the recovery period, the functional variables were the first ones to respond. By contrast, in both cases, the biofilm community structure could not fully recover during the two weeks of recovery period, and despite the diatom abundance increased, green algae remained the dominant group. Overall, biofilm communities responded to both types of pollution, and showed similar effects, especially on its functionality. Within the functional variables, photosynthetic efficiency was the one that responded faster, indicating the potential use of this variable as an indicator. On the other hand, even though Pb and Cd were not detected in water, it was detected bioaccumulated in the biofilm (Chapter 5 and 6). The presence of this metals accumulated in biofilms can play an important role in its response since they can become toxic to freshwater organisms (Hill et al., 2000; Corcoll et al., 2012). Although metal pollution might not be detected in water, its impacts in biofilm communities due to bioaccumulation along time could be observed. This demonstrates the ability of biofilm communities to accumulate metals, indicating that biofilms

can serve as a reliable parameter for biomonitoring the heavy metal effects over time in freshwater ecosystems.

The stream bioassessments are commonly focused on structural elements, which provides an incomplete picture of the overall integrity because function is not considered (Ferreira et al., 2020). This supposes a problem since the structure and function can respond in a different way to environmental stress (Sandin and Solimini, 2009; Feckler and Bundschuh, 2020; Verdonschot and Lee, 2020). Besides, ecosystem functions are strictly linked to the ecosystem services of which human societies depend (Capon et al., 2013; Jackson et al., 2016), and thus, evaluating ecosystem functionality is essential to understanding the impacts on ecosystem services (Jackson et al., 2016). Based the results of obtained in the field sampling (Chapter 4) where different indexes proposed by the WFD were calculated, the diatom indexes (thus, biofilm endpoints) were more restrictive and sensitive to *in situ* metal pollution than macroinvertebrate indices (Chapter 4). Additionally, diatom index correlated with the photosynthetic efficiency which highlight the use of this functional measure as an indicator of freshwater pollution. Functional measures should be included to assess the ecological status of streams since it would complete the ecosystem impact assessment and, as it was observed in this thesis, functional variables rapidly responded to the impacts and its variations (i.e., the impact removal).

These functional parameters are faster to measure than the structural ones and include the response of the whole biofilm community. The measurement of functional biofilm attributes provides knowledge of ecosystem processes which are fundamental to river health that are not available through quantifying structural attributes (Burns and Ryder, 2001). For instance, functional attributes such as respiration, nutrient uptake or photosynthetic efficiency of biofilm are suitable measures of system integrity since they provide an integrated response to an extensive range of disturbances. Additionally, in this thesis we observed that even though some metals can be very low in water or below the detection limit, they can be accumulated in biofilm (Bonet et al., 2013 and 2014).

Frequently, ecotoxicological test have been used as a tool to assess the effects of environmental pollutants to aquatic ecosystems. These tests are commonly performed in the laboratory, on small populations of certain species and, although they provide useful information on effects of these toxicants, they are not full trustworthy to predict effects in natural systems (Serra, 2009) since they do not allow the understanding of the effects of toxicants at community level (Sabater et al., 2007) and lacks ecological realism (Bonet et al., 2014). In this regard, the results obtained in this thesis using biofilm as a bioindicator demonstrated a more realistic assessment than using

the established tests based on single species. The combination of structural and functional biofilm attributes in monitoring programmes might allow a better impact assessment in freshwater ecosystems.

CHAPTER 10.

GENERAL CONCLUSIONS
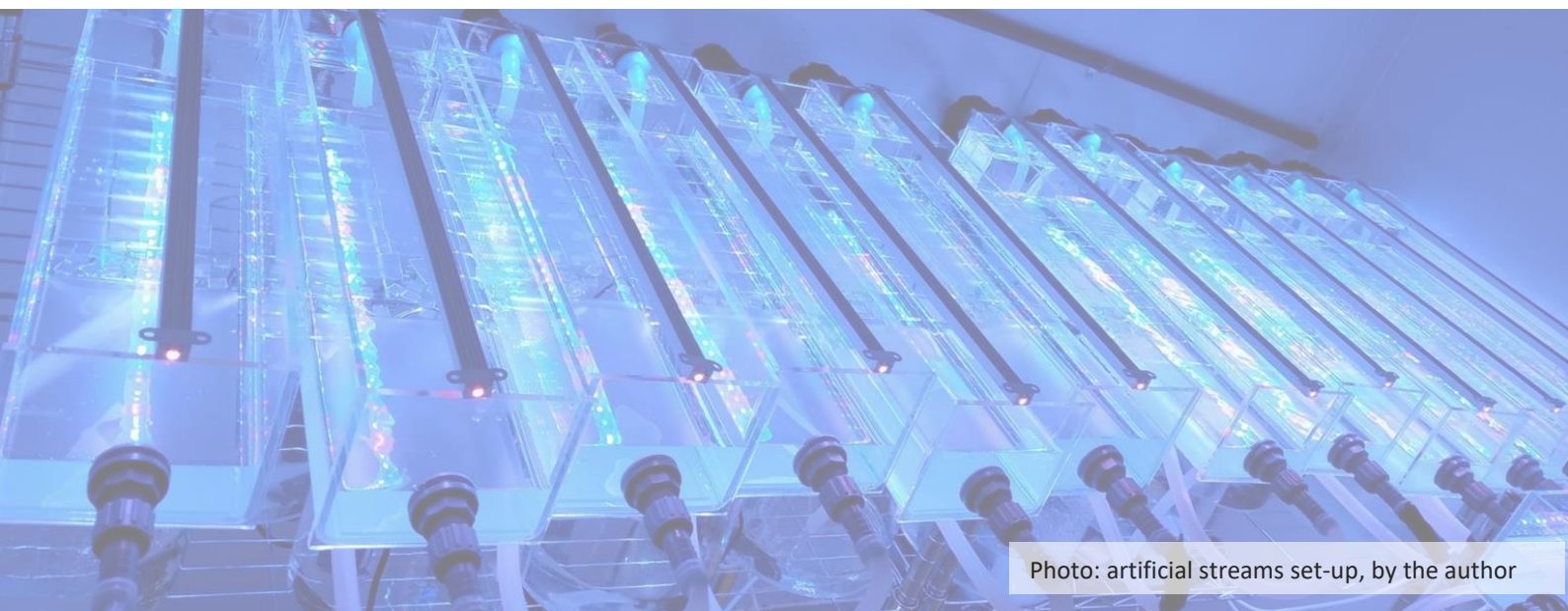
Photo: artificial streams set-up, by the author

10. CONCLUSIONS

In this thesis, biofilm communities were used to evaluate the ecological impact caused by abandoned mining effluents on freshwater ecosystems and the efficiency of different remediation methods to reduce these impacts. Specifically, it was tested the potential of different treatment technologies to reduce the ecological impacts caused by metal mining effluents as well as the potential salinity threshold from which the damage to the ecosystem could be irreversible. The main conclusions of this thesis can be summarized as follows.

- Frongoch stream was affected by the metal mining effluent from the abandoned mine, which was characterised by an increase in zinc and lead concentrations in water after the discharge of the mining effluent, a reduction in the pH and a high metal bioaccumulation in biofilm after chronic exposure (Chapter 4).

- The negative impacts of metal mining effluents on biofilm inhabiting in the receiving stream were mainly in its photosynthetic efficiency and its structure presenting significant differences in the diatom community composition compared to the reference sampling site (Chapter 4).

- Under chronic exposures of heavy metals (Chapter 4), biofilm communities develop adaptations to the pollution and become more tolerant.

- Abandoned mining effluents had severe effects in both functional and structural variables of biofilm communities. Short-term exposures to metal mining effluents caused rapid responses in biofilm functionality, while the structural shifts were appreciated after mid-term (Chapter 5, 6, 7 and 8).

- Abandoned mining effluents promote changes in the diatom growth rate, size, biodiversity, and taxa dominance favouring pioneer and tolerant species to growth (Chapter 6, 7 and 8). These traits make diatom community a good indicator of the water quality.

- Biofilm communities exposed to both metal and hypersaline mining effluents gradually recovered its functionality when the polluted effluent was removed, but the structure remained affected (Chapter 6 and 8)

- Treating the metal mining effluents with appropriate technologies offers an effective solution to treat these metal effluents from abandoned mines, having the potential to significantly reduce the ecological impact of mining (Chapter 5 and 6). However, this technology is not enough efficient on its own highlighting that the dilution capacity of the receiving stream is a crucial factor to assure this reduction.

- The dilution of mining effluent in the receiving stream has a key role in the technologies efficiency since it is the factor determining the metal concentration in the stream and therefore the ecological impact. Low dilution would cause higher metal concentrations in water and thus, ecological implications (Chapter 6).
- Biofilm communities are a good tool to assess the treatment technologies efficiency in reducing the ecological impacts caused by metal mining effluents in freshwaters (Chapter 5 and 6).
- Salinities below 15 g L^{-1} had short-term functional impacts that recovered along time due to the presence of salt tolerant species sustaining the functionality of biofilm communities. In contrast, higher salinities had functional effects (Chapter 7 and 8).
- Salinity exposure caused changes in the biofilm structure that affected its functionality (Chapter 7 and 8).
- Biofilm communities under the higher salinities developed resilience towards salinity that favoured its recovery after the exposure and less impacts during the pulse (Chaper 7 and 8).
- The threshold of salinity of hypersaline effluents from which irreversible impacts are caused could be between 6 and 15 g L^{-1} (Chapter 7and 8).
- Despite the fact that the WFD establishes guidelines to assess the ecological status of streams based on chemical parameters and biological indices, these methodologies are potentially misleading the overall ecological integrity since it is not considered the ecosystem function.
- The diatom-based indexes the ecological status of the Frongoch stream that were obtained correlated with the photosynthetic efficiency indicating that the functional measurements could be a good and easier to measure indicator. Additionally, the functional traits respond faster to the perturbations and the recovery.
- Metal bioaccumulation should be included in the prediction of ecosystem impacts since event though no metals were detected in water, they were found bioaccumulated.
- According to the evidence obtained throughout this work, biofilm can be considered a good tool assess the ecological impacts of abandoned mining effluents on freshwater ecosystems and the efficiency of different treatment technologies in reducing this impact, since it integrates structure and functionality effects which can be a good approach of the ecosystem impacts.

REFERENCES

Admiraal, W., Blanck, H., Buckert-De Jong, M., Guasch, H., Ivorra, N., Lehmann, V., ... & Sabater, S. (1999). Short-term toxicity of zinc to microbenthic algae and bacteria in a metal polluted stream. Water Research, 33(9), 1989-1996.

Abdel-Raouf, M. S., & Abdul-Raheim, A. R. M. (2017). Removal of Heavy Metals from Industrial Waste Water by Biomass-Based Materials: A Review. J Pollut Eff Cont 5: 180. doi: 10.4172/2375-4397.1000180 Page 2 of 13 Volume 5• Issue 1• 1000180 J Pollut Eff Cont, an open access journal ISSN: 2375-4397 The Top Six Toxic Threats: Estimated Population at risk at Identified Sites*(million people) Estimated Global Impact**(million people) 1. Lead 10 18-22 2. Mercury, 8, 15-19.

Ajah, K. C., Ademiluyi, J., & Nnaji, C. C. (2015). Spatiality, seasonality and ecological risks of heavy metals in the vicinity of a degenerate municipal central dumpsite in Enugu, Nigeria. Journal of Environmental Health Science and Engineering, 13(1), 1-15.

Akcil, A., & Koldas, S. (2006). Acid Mine Drainage (AMD): causes, treatment and case studies. Journal of cleaner production, 14(12-13), 1139-1145.

Alba-Tercedor, J. (1996). Macroinvertebrados acuáticos y calidad de las aguas de los ríos. In IV Simposio del agua en Andalucía (SIAGA). Almería (Vol. 2, pp. 203-213).

Allan, J. D., & Castillo, M. M. (2007). Stream ecology: structure and function of running waters. Springer Science & Business Media.

Allison, S. D., & Martiny, J. B. (2008). Resistance, resilience, and redundancy in microbial communities. Proceedings of the National Academy of Sciences, 105(Supplement 1), 11512-11519.

Amezaga, J. M., Rötting, T. S., Younger, P. L., Nairn, R. W., Noles, A. J., Oyarzún, R., & Quintanilla, J. (2011). A rich vein? Mining and the pursuit of sustainability.

APHA (American Public Health Association), 1992a. Method 4500 - NO2-. Nitrogen (Nitrite)*. Standard Methods for the Examination of Water and Wastewater, 18th ed. Washington, D.C.

APHA (American Public Health Association), 1992b. Method 4500-NO3-. Nitrogen (Nitrate)*. Standard Methods for the Examination of Water and Wastewater, 18th ed. Washington, D.C.

Arini, A., Feurtet-Mazel, A., Maury-Brachet, R., Pokrovsky, O. S., Coste, M., & Delmas, F. (2012). Recovery potential of periphytic biofilms translocated in artificial streams after industrial contamination (Cd and Zn). Ecotoxicology, 21(5), 1403-1414.

Armitage, P. D., Moss, D., Wright, J. F., & Furse, M. T. (1983). The performance of a new biological water quality score system based on macroinvertebrates over a wide range of unpolluted running-water sites. Water research, 17(3), 333-347.

Azapagic, A. (2004). Developing a framework for sustainable development indicators for the mining and minerals industry. Journal of cleaner production, 12(6), 639-662. 1016/S0959-6526(03)00075-1.

Baker ME, King RS (2010) A new method for detecting and interpreting biodiversity and ecological community thresholds. Method Ecol Evol 1:25–37

Balt, K., & Goosen, R. L. (2020). MSAHP: An approach to mining method selection. Journal of the Southern African Institute of Mining and Metallurgy, 120(8), 451-460.

Barrado, E., Prieto, F., Vega, M., & Fernández-Polanco, F. (1998). Optimization of the operational variables of a medium-scale reactor for metal-containing wastewater purification by ferrite formation. Water Research, 32(10), 3055-3061.

Barral-Fraga, L., Morin, S., Rovira, M. D., Urrea, G., Magellan, K., & Guasch, H. (2016). Short-term arsenic exposure reduces diatom cell size in biofilm communities. Environmental Science and Pollution Research, 23(5), 4257-4270.

Barranguet, C., Charantoni, E., Plans, M., & Admiraal, W. (2000). Short-term response of monospecific and natural algal biofilms to copper exposure. European journal of phycology, 35(4), 397-406.

Basile, A., Cassano, A., & Rastogi, N. K. (Eds.). (2015). Advances in membrane technologies for water treatment: materials, processes and applications. Elsevier.

Bäthe, J., & Coring, E. (2011). Biological effects of anthropogenic salt-load on the aquatic fauna: a synthesis of 17 years of biological survey on the rivers Werra and Weser. Limnologica, 41(2), 125-133.

Battin, T. J., Besemer, K., Bengtsson, M. M., Romani, A. M., & Packmann, A. I. (2016). The ecology and biogeochemistry of stream biofilms. Nature Reviews Microbiology, 14(4), 251.

Baulch, H. M., Turner, M. A., Findlay, D. L., Vinebrooke, R. D., & Donahue, W. F. (2009). Benthic algal biomass—measurement and errors. Canadian Journal of Fisheries and Aquatic Sciences, 66(11), 1989-2001.

Baumann, H. A., Morrison, L., & Stengel, D. B. (2009). Metal accumulation and toxicity measured by PAM—chlorophyll fluorescence in seven species of marine macroalgae. Ecotoxicology and Environmental Safety, 72(4), 1063-1075.

Bearcock, J., Palumbo-Roe, B., Banks, V., & Klinck, B. (2010). The hydrochemistry of Frongoch Mine, mid Wales.

Bellwood, D. R., Hughes, T. P., Folke, C., & Nyström, M. (2004). Confronting the coral reef crisis. Nature, 429(6994), 827-833.

Bere, T., Chia, M. A., & Tundisi, J. G. (2012). Effects of Cr III and Pb on the bioaccumulation and toxicity of Cd in tropical periphyton communities: Implications of pulsed metal exposures. Environmental pollution, 163, 184-191. 12.028.

Berger, E., Frör, O., & Schäfer, R. B. (2019). Salinity impacts on river ecosystem processes: a critical mini-review. Philosophical Transactions of the Royal Society B, 374(1764), 20180010.

Berry, J. A., & Downton, W. J. S. (1982). Environmental regulation of photosynthesis. Photosynthesis, 2, 263-343.

Besemer, K. (2015). Biodiversity, community structure and function of biofilms in stream ecosystems. Research in microbiology, 166(10), 774-781.

Besemer, K., Singer, G., Limberger, R., Chlup, A. K., Hochedlinger, G., Hödl, I., ... & Battin, T. J. (2007). Biophysical controls on community succession in stream biofilms. Applied and environmental microbiology, 73(15), 4966-4974.

Bian, Z., Miao, X., Lei, S., Chen, S. E., Wang, W., & Struthers, S. (2012). The challenges of reusing mining and mineral-processing wastes. Science, 337(6095), 702-703.

Birk, S., Bonne, W., Borja, A., Brucet, S., Courrat, A., Poikane, S., ... & Hering, D. (2012). Three hundred ways to assess Europe's surface waters: an almost complete overview of biological methods to implement the Water Framework Directive. Ecological indicators, 18, 31-41.

Blanck, H., Admiraal, W., Cleven, R. F. M. J., Guasch, H., Van den Hoop, M. A. G. T., Ivorra, N., ... & Tubbing, G. M. J. (2003). Variability in zinc tolerance, measured as incorporation of radio-labeled carbon dioxide and thymidine, in periphyton communities sampled from 15 European river stretches. Archives of Environmental Contamination and Toxicology, 44(1), 0017-0029.

Blanck, Hans, S-Å. Wängberg, and Sverker Molander. "Pollution-induced community tolerance—a new ecotoxicological tool." Functional testing of aquatic biota for estimating hazards of chemicals. ASTM International, 1988.

Böhme, D. (2011). Evaluation of brine discharge to rivers and streams: methodology of rapid impact assessment. Limnologica, 41(2), 80-89.

Bonada, N., Zamora-Munoz, C., Rieradevall, M., & Prat, N. (2004). Ecological profiles of caddisfly larvae in Mediterranean streams: implications for bioassessment methods. Environmental pollution, 132(3), 509-521.

Bonet Sánchez, B. (2013). Antioxidant enzyme activities in fluvial biofilms as biomakers of metal pollution.

Bonet, B., Corcoll, N., & Guasch, H. (2012). Antioxidant enzyme activities as biomarkers of Zn pollution in fluvial biofilms. Ecotoxicology and environmental safety, 80, 172-178.

Bonet, B., Corcoll, N., Acuňa, V., Sigg, L., Behra, R., & Guasch, H. (2013). Seasonal changes in antioxidant enzyme activities of freshwater biofilms in a metal polluted Mediterranean stream. Science of the total environment, 444, 60-72.

Bonet, B., Corcoll, N., Tlili, A., Morin, S., & Guasch, H. (2014). Antioxidant enzyme activities in biofilms as biomarker of Zn pollution in a natural system: an active bio-monitoring study. Ecotoxicology and environmental safety, 103, 82-90.

Bonnineau, C., Bonet, B., Corcoll, N., & Guasch, H. (2011). Catalase in fluvial biofilms: a comparison between different extraction methods and example of application in a metal-polluted river. Ecotoxicology, 20(1), 293-303.

Bonnineau, C., Guasch, H., Proia, L., Ricart, M., Geiszinger, A., Romaní, A. M., & Sabater, S. (2010). Fluvial biofilms: a pertinent tool to assess β-blockers toxicity. Aquatic Toxicology, 96(3), 225-233.

Bonnineau, C., Moeller, A., Barata, C., Bonet, B., Proia, L., Sans-Piché, F., ... & Segner, H. (2012). Advances in the multibiomarker approach for risk assessment in aquatic ecosystems. In Emerging and priority pollutants in rivers (pp. 147-179). Springer, Berlin, Heidelberg.

Bradac, P., Wagner, B., Kistler, D., Traber, J., Behra, R., & Sigg, L. (2010). Cadmium speciation and accumulation in periphyton in a small stream with dynamic concentration variations. Environmental Pollution, 158(3), 641-648.

Bunn, S. E., Abal, E. G., Smith, M. J., Choy, S. C., Fellows, C. S., Harch, B. D., ... & Sheldon, F. (2010). Integration of science and monitoring of river ecosystem health to guide investments in catchment protection and rehabilitation. Freshwater Biology, 55, 223-240.

Burns, A., & Ryder, D. S. (2001). Potential for biofilms as biological indicators in Australian riverine systems. Ecological Management & Restoration, 2(1), 53-64.

Campbell, C. D., Chapman, S. J., Cameron, C. M., Davidson, M. S., & Potts, J. M. (2003). A rapid microtiter plate method to measure carbon dioxide evolved from carbon substrate amendments so as to determine the physiological profiles of soil microbial communities by using whole soil. Applied and environmental microbiology, 69(6), 3593-3599.

Canhoto, C., Simões, S., Gonçalves, A. L., Guilhermino, L., & Bärlocher, F. (2017). Stream salinization and fungal-mediated leaf decomposition: a microcosm study. Science of the Total Environment, 599, 1638-1645.

Cañedo-Argüelles, M. (2020). A review of recent advances and future challenges in freshwater salinization. Limnetica, 39(1), 185-211.

Cañedo-Argüelles, M., Brucet, S., Carrasco, S., Flor-Arnau, N., Ordeix, M., Ponsá, S., & Coring, E. (2017). Effects of potash mining on river ecosystems: an experimental study. Environmental Pollution, 224, 759-770.

Cañedo-Argüelles, M., Bundschuh, M., Gutiérrez-Cánovas, C., Kefford, B. J., Prat, N., Trobajo, R., & Schäfer, R. B. (2014). Effects of repeated salt pulses on ecosystem structure and functions in a stream mesocosm. Science of the Total Environment, 476, 634-642.

Cañedo-Argüelles, M., Grantham, T. E., Perrée, I., Rieradevall, M., Céspedes-Sánchez, R., & Prat, N. (2012). Response of stream invertebrates to short-term salinization: a mesocosm approach. Environmental Pollution, 166, 144-151.

Cañedo-Argüelles, M., Hawkins, C. P., Kefford, B. J., Schäfer, R. B., Dyack, B. J., Brucet, S., ... & Coring, E. (2016). Saving freshwater from salts. Science, 351(6276), 914-916.

Cañedo-Argüelles, M., Kefford, B. J., Piscart, C., Prat, N., Schäfer, R. B., & Schulz, C. J. (2013). Salinisation of rivers: an urgent ecological issue. Environmental pollution, 173, 157-167.

Cañedo-Argüelles, M., Kefford, B., & Schäfer, R. (2019). Salt in freshwaters: causes, effects and prospects-introduction to the theme issue.

Cañedo-Argüelles, M., Sala, M., Peixoto, G., Prat, N., Faria, M., Soares, A. M., ... & Kefford, B. (2016). Can salinity trigger cascade effects on streams? A mesocosm approach. Science of the Total Environment, 540, 3-10.

Capon, S. J., Chambers, L. E., Mac Nally, R., Naiman, R. J., Davies, P., Marshall, N., ... & Williams, S. E. (2013). Riparian ecosystems in the 21st century: hotspots for climate change adaptation?. Ecosystems, 16(3), 359-381.

Cardinale, B. J., Hillebrand, H., & Charles, D. F. (2006). Geographic patterns of diversity in streams are predicted by a multivariate model of disturbance and productivity. Journal of Ecology, 94(3), 609-618.

Cassard, D., Bertrand, G., Billa, M., Serrano, J. J., Tourlière, B., Angel, J. M., & Gaál, G. (2015). ProMine Mineral Databases: New tools to assess primary and secondary mineral resources in Europe. In 3D, 4D and Predictive Modelling of Major Mineral Belts in Europe (pp. 9-58). Springer, Cham.

Castro, M. C. R., Urrea, G., & Guasch, H. (2015). Influence of the interaction between phosphate and arsenate on periphyton's growth and its nutrient uptake capacity. Science of the total environment, 503, 122-132.

Ceto, N., & Mahmud, S. (2000). Abandoned mine site characterization and cleanup handbook. Agency, EP (Ed.). USEPA, Seattle, WA, 129.

Charbonnier, P. (2001). Management of mining, quarrying and ore-processing waste in the European Union. BRGM service EPI, France.

Choi, T. S., Kang, E. J., Kim, J. H., & Kim, K. Y. (2010). Effect of salinity on growth and nutrient uptake of Ulva pertusa (Chlorophyta) from an eelgrass bed. Algae, 25(1), 17-26.

Christensen, A. M., Nakajima, F., & Baun, A. (2006). Toxicity of water and sediment in a small urban river (Store Vejleå, Denmark). Environmental Pollution, 144(2), 621-625.

Clements, W. H. (2004). Small scale experiments support causal relationships between metal contamination and macroinvertebrate community responses. Ecological Applications, 14, 954– 967.

Clements, W. H., & Kotalik, C. (2016). Effects of major ions on natural benthic communities: an experimental assessment of the US Environmental Protection Agency aquatic life benchmark for conductivity. Freshwater Science, 35(1), 126-138.

Clements, W. H., & Rohr, J. R. (2009). Community responses to contaminants: using basic ecological principles to predict ecotoxicological effects. Environmental Toxicology and Chemistry: An International Journal, 28(9), 1789-1800.

Clements, W. H., Vieira, N. K., & Church, S. E. (2010). Quantifying restoration success and recovery in a metal-polluted stream: A 17-year assessment of physicochemical and biological responses. Journal of Applied Ecology, 47(4), 899-910.

Clements, W.H. and Newman, M.C. 2002. Community ecotoxicology. John Wiley and Sons (Eds.). Chichester, U. K. 336 pp

Clothier, B. E., & Green, S. (2005). Leaching processes.

Cochero, J., Licursi, M., & Gómez, N. (2017). Effects of pulse and press additions of salt on biofilms of nutrient-rich streams. Science of the Total Environment, 579, 1496-1503.

Coclet, C., Garnier, C., D'Onofrio, S., Durrieu, G., Pasero, E., Le Poupon, C., ... & Briand, J. F. (2021). Trace Metal Contamination Impacts Predicted Functions More Than Structure of Marine Prokaryotic Biofilm Communities in an Anthropized Coastal Area. Frontiers in microbiology, 12, 292.

Coelho, P. C. S., Teixeira, J. P. F., & Gonçalves, O. N. B. S. M. (2011). Mining activities: health impacts.

Collard, J. M., & Matagne, R. F. (1994). Cd2+ resistance in wild-type and mutant strains of Chlamydomonas reinhardtii. Environmental and experimental botany, 34(2), 235-244.

Cook, L. J., & Francoeur, S. N. (2013). Effects of simulated short-term road salt exposure on lotic periphyton function. Journal of Freshwater Ecology, 28(2), 211-223.

Corcoll, N., Bonet, B., Leira, M., & Guasch, H. (2011). Chl-a fluorescence parameters as biomarkers of metal toxicity in fluvial biofilms: an experimental study. Hydrobiologia, 673(1), 119-136.

Corcoll, N., Bonet, B., Morin, S., Tlili, A., Leira, M., & Guasch, H. (2012). The effect of metals on photosynthesis processes and diatom metrics of biofilm from a metal-contaminated river: a translocation experiment. Ecological indicators, 18, 620-631.

Coring, E., & Bäthe, J. (2011). Effects of reduced salt concentrations on plant communities in the River Werra (Germany). Limnologica, 41(2), 134-142.

Coste, M., Boutry, S., Tison-Rosebery, J., & Delmas, F. (2009). Improvements of the Biological Diatom Index (BDI): Description and efficiency of the new version (BDI-2006). Ecological indicators, 9(4), 621-650.

Costelloe, J. F., Powling, J., Reid, J. R., Shiel, R. J., & Hudson, P. (2005). Algal diversity and assemblages in arid zone rivers of the Lake Eyre Basin, Australia. River Research and Applications, 21(2-3), 337-349.

Courtney, L. A., & Clements, W. H. (2000). Sensitivity to acidic pH in benthic invertebrate assemblages with different histories of exposure to metals. Journal of the North American Benthological Society, 19(1), 112-127.

D.V. Chapman. (1996). World health organization, united nations educational and scientific organization & united nations environment programme Water Quality Assessments: a Guide to the Use of Biota, Sediments and Water in Environmental Monitoring, Edited by Deborah Chapman, Second ed., E & FN Spon, London, UK

D'angelo, D. J., Webster, J. R., & Benfield, E. F. (1991). Mechanisms of stream phosphorus retention: an experimental study. Journal of the North American Benthological Society, 10(3), 225-237.

Das, M., & Ramanujam, P. (2011). Metal content in water and in green filamentous algae Microspora quadrata hazen from coal mine impacted streams of Jaintia Hills District, Meghalaya, India. International Journal of Botany, 7(2), 170-176.

de Paiva Magalhães, D., da Costa Marques, M. R., Baptista, D. F., & Buss, D. F. (2015). Metal bioavailability and toxicity in freshwaters. Environmental Chemistry Letters, 13(1), 69-87.

DeFaveri, J., & Merilä, J. (2014). Local adaptation to salinity in the three-spined stickleback?. Journal of Evolutionary Biology, 27(2), 290-302.

DEFRA. (2014). Water Framework Directive implementation in England and Wales: new and updated standards to protect the water environment.

Dempster TA, Sommerfeld MR (1998) Effects of environmental conditions on growth and lipid accumulation in Nitzschia com-munis (Bacillariophyceae). J. Phycol. 34: 712-721.

Den Haan, J., Huisman, J., Brocke, H. J., Goehlich, H., Latijnhouwers, K. R., Van Heeringen, S., ... & Visser, P. M. (2016). Nitrogen and phosphorus uptake rates of different species from a coral reef community after a nutrient pulse. Scientific reports, 6(1), 1-13. Rep. 6 (1), 1–13

DGRC. Dresden Groundwater Research Center. 2018. DE A.2 Database of mining effluents composition and treatment from different European mines. Life DEMINE.

Dorigo U, Berard A, Rimet F, Bouchez A, Montuelle B (2010) In situ assessment of periphyton recovery in a river contaminated by pesticides. Aquat Toxicol 98:396–406

Dufrêne, M., & Legendre, P. (1997). Species assemblages and indicator species: the need for a flexible asymmetrical approach. Ecological monographs, 67(3), 345-366.

Dunlop, J. E., Horrigan, N., McGregor, G., Kefford, B. J., Choy, S., & Prasad, R. (2008). Effect of spatial variation on salinity tolerance of macroinvertebrates in Eastern Australia and implications for ecosystem protection trigger values. Environmental Pollution, 151(3), 621-630.

Duong, T. T., Morin, S., Herlory, O., Feurtet-Mazel, A., Coste, M., & Boudou, A. (2008). Seasonal effects of cadmium accumulation in periphytic diatom communities of freshwater biofilms. Aquatic toxicology, 90(1), 19-28.

Earl, S. R., Valett, H. M., & Webster, J. R. (2006). Nitrogen saturation in stream ecosystems. Ecology, 87(12), 3140-3151.

Echenique-Subiabre, I., Dalle, C., Duval, C., Heath, M. W., Couté, A., Wood, S. A., ... & Quiblier, C. (2016). Application of a spectrofluorimetric tool (bbe BenthoTorch) for monitoring potentially toxic benthic cyanobacteria in rivers. Water research, 101, 341-350.

Edwards, P & Williams, T. (2016). Abandoned Mine Case Study: Cwmystwyth Lead Mine. Natural Resources of Wales.

Edwards, P., Williams, T., & Stanley, P. (2016) Surface water management and encapsulation of mine waste to reduce water pollution from Frongoch Mine, Mid Wales.

Elosegi, A., Nicolás, A., & Richardson, J. S. (2018). Priming of leaf litter decomposition by algae seems of minor importance in natural streams during autumn. Plos one, 13(9), e0200180.

Emsley, J. (2011). Nature's building blocks: an AZ guide to the elements. Oxford University Press.

Entrekin, S. A., Clay, N. A., Mogilevski, A., Howard-Parker, B., & Evans-White, M. A. (2019). Multiple riparian–stream connections are predicted to change in response to salinization. Philosophical Transactions of the Royal Society B, 374(1764), 20180042.

Environment Agency Wales (2008). Report on the impact of metal mine pollution from the Cwmystwyth, Frongoch-Wemyss and Dylife mines on macroinvertebrates, diatoms and fish.

Ermite Consortium. (2004). Mining impacts on the fresh water environment: technical and managerial guidelines for catchment scale management. Mine water and the environment, 23(Supplement 1), S2-S80.

Espinoza, D., Goycoolea, M., Moreno, E., & Newman, A. (2013). MineLib: a library of open pit mining problems. Annals of Operations Research, 206(1), 93-114.

Euromines. (n.d.). Mining in Europe. Retrieved 25 February 2021, from http://www.euromines.org/mining-europe

European Comission (2012), Supporting document on closure methodologies for closed and abandoned mining waste facilities. Annex 3. https://ec.europa.eu/environment/waste/mining/pdf/Annex3_closure_rehabilitation%20.pdf

European Comission. (2012). Establishment of guidelines for the inspection of mining waste facilities, inventory and rehabilitation of abandoned facilities and review of the BREF document. Annex 3. (070307/2010/576108/ETU/C2).

European Commission (2016). Raw Materials Information System (RMIS). Potash. https://rmis.jrc.ec.europa.eu/uploads/rmprofiles/

European Commission, 2000. Directive 2000/60/EC ofthe European Parliament and of the Council—Establishing a Framework for Community Action in the Field of Water Policy. European Commission, Belgium

European Commission. (2017). Assessment of Member States' performance regarding the implementation of the Extractive Waste Directive; appraisal of implementation gaps and their root causes; identification of proposals to improve the implementation of the Directive. Luxembourg: Publications Office of the European Union.

Eurostat, S. E. (2018). Waste statistics. https://ec.europa.eu/eurostat/statistics-explained/index.php/Waste_statistics#Total_waste_generation

Eurostat, S. E. (2021). Material flow accounts and resource productivity.

Falasco, E., Bona, F., Badino, G., Hoffmann, L., & Ector, L. (2009). Diatom teratological forms and environmental alterations: a review. Hydrobiologia, 623(1), 1-35.

Fashola, M. O., Ngole-Jeme, V. M., & Babalola, O. O. (2016). Heavy metal pollution from gold mines: environmental effects and bacterial strategies for resistance. International journal of environmental research and public health, 13(11), 1047.

Fechner, L. C., Gourlay-Francé, C., Uher, E., & Tusseau-Vuillemin, M. H. (2010). Adapting an enzymatic toxicity test to allow comparative evaluation of natural freshwater biofilms' tolerance to metals. Ecotoxicology, 19(7), 1302-1311.

Feckler, A., & Bundschuh, M. (2020). Decoupled structure and function of leaf-associated microorganisms under anthropogenic pressure: Potential hurdles for environmental monitoring. Freshwater Science, 39(4), 652-664.

Ferreira, V., Elosegi, A., D Tiegs, S., Schiller, D. V., & Young, R. (2020). Organic Matter Decomposition and Ecosystem Metabolism as Tools to Assess the Functional Integrity of Streams and Rivers—A Systematic Review. Water, 12(12), 3523.

Fischer, H., Sachse, A., Steinberg, C. E., & Pusch, M. (2002). Differential retention and utilization of dissolved organic carbon by bacteria in river sediments. Limnology and Oceanography, 47(6), 1702-1711.

Förstner, U., & Prosi, F. (1979). Heavy Metal Pollution in Freshwater Ecosystems. Biological Aspects of Freshwater Pollution, 129–161. doi:10.1016/b978-0-08-023442-7.50011-6

Garrett, D. E. (2012). Potash: deposits, processing, properties and uses. Springer Science & Business Media.

Ghosh, M., & Gaur, J. P. (1994). Algal periphyton of an unshaded stream in relation to in situ nutrient enrichment and current velocity. Aquatic Botany, 47(2), 185-189.

Gold, C., Feurtet-Mazel, A., Coste, M., & Boudou, A. (2003). Impacts of metals (Cd, Zn) on the development of periphytic diatom communities within outdoor artificial streams along a pollution gradient. Arch. Environ. Toxicol, 44, 189-197.

Gómez-Ordóñez, E., Alonso, E., & Rupérez, P. (2010). A simple ion chromatography method for inorganic anion analysis in edible seaweeds. Talanta, 82(4), 1313-1317.

Graham, A. A., McCaughan, D. J., & McKee, F. S. (1988). Measurement of surface area of stones. Hydrobiologia, 157(1), 85-87.

Gray, N. F. (1998). Acid mine drainage composition and the implications for its impact on lotic systems. Water Research, 32(7), 2122-2134.

Griffith, M. B. (2014). Natural variation and current reference for specific conductivity and major ions in wadeable streams of the conterminous USA. Freshwater Science, 33(1), 1-17.

Guasch H et al (2012) How to link field observations with causality? Field and experimental approaches linking chemical pollution with ecological alterations. In: Guasch H, Ginebreda A, Geiszinger A (eds) Emerging and priority pollutants in rivers, vol 19. The Handbook of environmental chemistry. Springer Berlin Heidelberg, pp 181–218. doi:10.1007/978-3-642-25722-3_7

Guasch, H., & Sabater, S. (1998). Estimation of the annual primary production of stream epilithic biofilms based on photosynthesis-irradiance relations. Archiv für Hydrobiologie, 141(4), 469-481.

Guasch, H., Admiraal, W., & Sabater, S. (2003). Contrasting effects of organic and inorganic toxicants on freshwater periphyton. Aquatic toxicology, 64(2), 165-175.

Guasch, H., Artigas, J., Bonet, B., Bonnineau, C., Canals, O., Corcoll, N., ... & Serra, A. (2016). The use of biofilms to assess the effects of chemicals on freshwater ecosystems. Aquatic Biofilms: Ecology Water Quality and Wastewater Treatment; Caister Academic Press: Rofo, UK, 125-144.

Guasch, H., Atli, G., Bonet, B., Corcoll, N., Leira, M., & Serra, A. (2010). Discharge and the response of biofilms to metal exposure in Mediterranean rivers. In Global Change and River Ecosystems—Implications for Structure, Function and Ecosystem Services (pp. 143-157). Springer, Dordrecht. 143–157. https://doi.org/10.1007/s10750-010-0116-z.

Guasch, H., Bonet, B., Bonnineau, C., Corcoll, N., López-Doval, J. C., Munoz, I., ... & Clements, W. (2012). How to link field observations with causality? Field and experimental approaches linking chemical pollution with ecological alterations. In Emerging and priority pollutants in rivers (pp. 181-218). Springer, Berlin, Heidelberg.

Guasch, H., Ginebreda, A., & Geiszinger, A. (Eds.). (2012). Emerging and priority pollutants in rivers: bringing science into river management plans (Vol. 19). Springer Science & Business Media.

Guasch, H., Paulsson, M., & Sabater, S. (2002). EFFECT OF COPPER ON ALGAL COMMUNITIES FROM OLIGOTROPHIC CALCAREOUS STREAMS1. Journal of Phycology, 38(2), 241-248.

Guillard, R. R., & Lorenzen, C. J. (1972). Yellow-green algae with chlorophyllide C 1, 2. Journal of Phycology, 8(1), 10-14.

Gupta, S., & Bux, F. (2019). Application of microalgae in wastewater treatment. Springer, Switzerland.

Gutiérrez-Cánovas, C., Hernández, J., Millán, A., & Velasco, J. (2012). Impact of chronic and pulse dilution disturbances on metabolism and trophic structure in a saline Mediterranean stream. Hydrobiologia, 686(1), 225-239.

Gutiérrez-Cánovas, C., Velasco, J., & Millán, A. (2009). Effects of dilution stress on the functioning of a saline Mediterranean stream. Hydrobiologia, 619(1), 119-132.

Hall Jr, R. O., & Meyer, J. L. (1998). The trophic significance of bacteria in a detritus-based stream food web. Ecology, 79(6), 1995-2012.

Hall, R. J. O., Bernhardt, E. S., & Likens, G. E. (2002). Relating nutrient uptake with transient storage in forested mountain streams. Limnology and oceanography, 47(1), 255-265.

Hallfors, G. (2004). Checklist of Baltic Sea phytoplankton species (including some heterotrophic protistan groups).

Hawkes, H. A. (1998). Origin and development of the biological monitoring working party score system. Water research, 32(3), 964-968.

Heikkinen, P., Noras, P., Salminen, R., Mroueh, U. M., Vahanne, P., Wahlström, M. M., ... & Komppa, V. (2008). Environmental Techniques for the Extractive Industries. Mine Closure Handbook; Outokumpu: Helsinki, Finland.

Hellawell J.M. (1986) Biological Indicators of Freshwater Pollution and Environmental Management. Elsevier Ap- plied Science, London

Herbert, E. R., Boon, P., Burgin, A. J., Neubauer, S. C., Franklin, R. B., Ardón, M., ... & Gell, P. (2015). A global perspective on wetland salinization: ecological consequences of a growing threat to freshwater wetlands. Ecosphere, 6(10), 1-43.

Hering, D., Borja, A., Carstensen, J., Carvalho, L., Elliott, M., Feld, C. K., ... & van de Bund, W. (2010). The European Water Framework Directive at the age of 10: a critical review of the achievements with recommendations for the future. Science of the total Environment, 408(19), 4007-4019.

Hering, D., Johnson, R. K., Kramm, S., Schmutz, S., Szoszkiewicz, K., & Verdonschot, P. F. (2006). Assessment of European streams with diatoms, macrophytes, macroinvertebrates and fish: a comparative metric-based analysis of organism response to stress. Freshwater biology, 51(9), 1757-1785.

Hill, P. W., Farrar, J. F., & Jones, D. L. (2008). Decoupling of microbial glucose uptake and mineralization in soil. Soil Biology and Biochemistry, 40(3), 616-624.

Hill, W. R., Bednarek, A. T., & Larsen, I. L. (2000). Cadmium sorption and toxicity in autotrophic biofilms. Canadian Journal of Fisheries and Aquatic Sciences, 57(3), 530-537.

Hintz, W. D., & Relyea, R. A. (2017). A salty landscape of fear: responses of fish and zooplankton to freshwater salinization and predatory stress. Oecologia, 185(1), 147-156.

Holding, K. L., Gill, R. A., & Carter, J. (2003). The relationship between epilithic periphyton (biofilm) bound metals and metals bound to sediments in freshwater systems. Environmental Geochemistry and Health, 25(1), 87-93.

Holling, C. S. (1973). Resilience and stability of ecological systems. Annual review of ecology and systematics, 4(1), 1-23.

Hong, Y. J., Liao, W., Yan, Z. F., Bai, Y. C., Feng, C. L., Xu, Z. X., & Xu, D. Y. (2020). Progress in the research of the toxicity effect mechanisms of heavy metals on freshwater organisms and their water quality criteria in China. Journal of Chemistry, 2020.

Howarth, R. B. (2007). Towards an operational sustainability criterion. Ecological economics, 63(4), 656-663.

Hudson-Edwards, K. A., Macklin, M. G., Brewer, P. A., & Dennis, I. A. (2008). Assessment of metal mining-contaminated river sediments in England and Wales.

Issaka, S., & Ashraf, M. A. (2021). Phytorestoration of mine spoiled:"Evaluation of natural phytoremediation process occurring at ex-tin mining catchment". In Phytorestoration of Abandoned Mining and Oil Drilling Sites (pp. 219-248). Elsevier.

Ivorra, N., Barranguet, C., Jonker, M., Kraak, M. H., & Admiraal, W. (2002). Metal-induced tolerance in the freshwater microbenthic diatom Gomphonema parvulum. Environmental Pollution, 116(1), 147-157.

Ivorra, N., Bremer, S., Guasch, H., Kraak, M. H., & Admiraal, W. (2000). Differences in the sensitivity of benthic microalgae to Zn and Cd regarding biofilm development and exposure history. Environmental Toxicology and Chemistry: An International Journal, 19(5), 1332-1339.

Ivorra, N., Hettelaar, J., Tubbing, G. M. J., Kraak, M. H. S., Sabater, S., & Admiraal, W. (1999). Translocation of microbenthic algal assemblages used for in situ analysis of metal pollution in rivers. Archives of Environmental Contamination and Toxicology, 37(1), 19-28.

Ixer, R.A. and Budd, P. (1998) The mineralogy of Bronze Age copper ores from the British Isles: implications for the composition of early metalwork. Oxford Journal of Archaeology 17, 15-4

Jackson, M. C., Weyl, O. L. F., Altermatt, F., Durance, I., Friberg, N., Dumbrell, A. J., ... & Woodward, G. (2016). Recommendations for the next generation of global freshwater biological monitoring tools. Advances in ecological research, 55, 615-636.

Jackson, M. C., Weyl, O. L. F., Altermatt, F., Durance, I., Friberg, N., Dumbrell, A. J., ... & Woodward, G. (2016). Recommendations for the next generation of global freshwater biological monitoring tools. Advances in ecological research, 55, 615-636.

Jain, M. K., & Das, A. (2017). Impact of mine waste leachates on aquatic environment: a review. Current Pollution Reports, 3(1), 31-37.

Jain, R. K., Cui, Z. C., & Domen, J. K. (2016). Environmental impacts of mining. Environmental Impact of Mining and Mineral Processing, 53-157.

Jarvis, A. P., Alakangas, L., Azzie, B., Lindahl, L., Loredo, J., Madai, F., ... & Wolkersdorfer, C. (2012, May). Developments and challenges in the management of mining wastes and waters in Europe. In 9th International Conference on Acid Rock Drainage, Ottawa, Canada (p. 203).

Jeffrey, S. T., & Humphrey, G. F. (1975). New spectrophotometric equations for determining chlorophylls a, b, c1 and c2 in higher plants, algae and natural phytoplankton. Biochemie und physiologie der pflanzen, 167(2), 191-194.

Johnson, B. R., Haas, A., & Fritz, K. M. (2010). Use of spatially explicit physicochemical data to measure downstream impacts of headwater stream disturbance. Water Resources Research, 46(9).

Johnson, D. B., & Hallberg, K. B. (2005). Acid mine drainage remediation options: a review. Science of the total environment, 338(1-2), 3-14.

Johnston, D. (2004, September). A metal mines strategy for Wales. In Proceedings of the International Mine Water Association Symposium, Newcastle upon Tyne, UK (pp. 20-25).

Johnston, D., Potter, H., Jones, C., Rolley, S., Watson, I., & Pritchard, J. (2008). Abandoned mines and the water environment. Environment Agency Science project SC030136-41.

Juneau, P., Qiu, B., & Deblois, C. P. (2007). Use of chlorophyll fluorescence as a tool for determination of herbicide toxic effect. Toxicological and Environ Chemistry, 89(4), 609-625.

Juneau, P., Qiu, B., & Deblois, C. P. (2007). Use of chlorophyll fluorescence as a tool for determination of herbicide toxic effect. Toxicological and Environ Chemistry, 89(4), 609-625.

Kaasalainen, H., Lundberg, P., Aiglsperger, T., & Alakangas, L. (2019). Impact of declining oxygen conditions on metal (loid) release from partially oxidized waste rock. Environmental Science and Pollution Research, 26(20), 20712-20730.

Kage, F. G. (2012). Impact of heavy metal pollution on the composition and abundance of benthic macroinvertebrates along Nariobi river, Kenya. Kenyatta University Institutional Repository, 45, 142–151.

Kanda, J. (1995). Determination of ammonium in seawater based on the indophenol reaction with o-phenylphenol (OPP). Water Research, 29(12), 2746-2750.

Kaplan, D., Christiaen, D., & Malis-Arad, S. (1987). Binding of heavy metals by algal carbohydrates. Algal Biotechnology.

Kashian, D. R., Zuellig, R. E., Mitchell, K. A., & Clements, W. H. (2007). The cost of tolerance: Sensitivity of stream benthic communities to UV-B and metals. Ecological Applications, 17(2), 365-375.

Kaushal, S. S. (2016). Increased salinization decreases safe drinking water.

Kaushal, S. S., Groffman, P. M., Likens, G. E., Belt, K. T., Stack, W. P., Kelly, V. R., ... & Fisher, G. T. (2005). Increased salinization of fresh water in the northeastern United States. Proceedings of the National Academy of Sciences, 102(38), 13517-13520.

Kaushal, S. S., Likens, G. E., Pace, M. L., Utz, R. M., Haq, S., Gorman, J., & Grese, M. (2018). Freshwater salinization syndrome on a continental scale. Proceedings of the National Academy of Sciences, 115(4), E574-E583.

Keerthi, V., V., & Balasubramanian, N. (2013). Removal of heavy metals by hybrid electrocoagulation and microfiltration processes. Environmental Technology, 34(20), 2897–2902. doi:10.1080/09593330.2013.796005

Kefford, B. J., & Nugegoda, D. (2005). No evidence for a critical salinity threshold for growth and reproduction in the freshwater snail Physa acuta. Environmental Pollution, 134(3), 377-383.

Kefford, B. J., Hickey, G. L., Gasith, A., Ben-David, E., Dunlop, J. E., Palmer, C. G., ... & Piscart, C. (2012). Global scale variation in the salinity sensitivity of riverine macroinvertebrates: Eastern Australia, France, Israel and South Africa. PloS one, 7(5), e35224.

Kefford, B. J., Marchant, R., Schäfer, R. B., Metzeling, L., Dunlop, J. E., Choy, S. C., & Goonan, P. (2011). The definition of species richness used by species sensitivity distributions approximates observed effects of salinity on stream macroinvertebrates. Environmental Pollution, 159(1), 302-310.

Kelly, M. G., & Whitton, B. A. (1995). The trophic diatom index: a new index for monitoring eutrophication in rivers. Journal of Applied Phycology, 7(4), 433-444.ç

Khatri, N., & Tyagi, S. (2015). Influences of natural and anthropogenic factors on surface and groundwater quality in rural and urban areas. Frontiers in Life Science, 8(1), 23-39.

Kiffney, P. M., Clements, W. H., & Cady, T. A. (1997). Influence of ultraviolet radiation on the colonization dynamics of a Rocky Mountain stream benthic community. Journal of the North American Benthological Society, 16(3), 520-530.

Kiparissis, Y., Akhtar, P., Hodson, P. V., & Brown, R. S. (2003). Partition-controlled delivery of toxicants: a novel in vivo approach for embryo toxicity testing. Environmental science & technology, 37(10), 2262-2266.

Kivinen, S. (2017). Sustainable post-mining land use: are closed metal mines abandoned or re-used space?. Sustainability, 9(10), 1705.

Kondoh, M. (2001). Unifying the relationships of species richness to productivity and disturbance. Proceedings of the Royal Society of London. Series B: Biological Sciences, 268(1464), 269-271.

Kozak, G. M., Brennan, R. S., Berdan, E. L., Fuller, R. C., & Whitehead, A. (2014). Functional and population genomic divergence within and between two species of killifish adapted to different osmotic niches. Evolution, 68(1), 63-80.

Kunz JL, Conley JM, Buchwalter DB, Norberg-King TJ, Kemble NE, Wang N, Ingersoll CG (2013) Use of reconstituted waters to evaluate effects of elevated major ions associated with mountaintop coal mining on freshwater invertebrates. Environ Toxicol Chem 32:1–10

Kupilas, B., Friberg, N., McKie, B. G., Jochmann, M. A., Lorenz, A. W., & Hering, D. (2016). River restoration and the trophic structure of benthic invertebrate communities across 16 European restoration projects. Hydrobiologia, 769(1), 105-120.

Lambert, A. S., Morin, S., Artigas, J., Volat, B., Coquery, M., Neyra, M., & Pesce, S. (2012). Structural and functional recovery of microbial biofilms after a decrease in copper exposure: influence of the presence of pristine communities. Aquatic toxicology, 109, 118-126.

Lange, K., Townsend, C. R., & Matthaei, C. D. (2016). A trait-based framework for stream algal communities. Ecology and Evolution, 6(1), 23-36.

Lange-Bertalot, H. and Metzeltin, D. (1996) Indicators of oligotrophy - 800 taxa representative of three ecologically distinct lake types, Carbonate buffered - Oligodystrophic - Weakly buffered soft water. Lange-Bertalot, H. (ed.), Iconographia Diatomologica. Annotated Diatom Micrographs. Vol. 2. Ecology, Diversity, Taxonomy. Koeltz Scientific Books. Königstein, Germany, 2:390 pp.

Larson, C., & Passy, S. I. (2005).Spectral fingerprinting of algal communities: A novel approach to biofilm analysis and biomonitoring 1. Journal of Phycology, 41(2), 439-446.

Lawrence, J. R., Swerhone, G. D., Wassenaar, L. I., & Neu, T. R. (2005). Effects of selected pharmaceuticals on riverine biofilm communities. Canadian Journal of Microbiology, 51(8), 655-669.

Le Faucheur, S., Behra, R., & Sigg, L. (2005). Thiol and metal contents in periphyton exposed to elevated copper and zinc concentrations: a field and microcosm study. Environmental science & technology, 39(20), 8099-8107.

Le, T. D. H., Kattwinkel, M., Schützenmeister, K., Olson, J. R., Hawkins, C. P., & Schäfer, R. B. (2019). Predicting current and future background ion concentrations in German surface water under climate change. Philosophical Transactions of the Royal Society B, 374(1764), 20180004.

Le, T. D. H., Schreiner, V. C., Kattwinkel, M., & Schäfer, R. B. (2021). Invertebrate turnover along gradients of anthropogenic salinisation in rivers of two German regions. Science of The Total Environment, 753, 141986.

Leal-Alvarado, D. A., Espadas-Gil, F., Sáenz-Carbonell, L., Talavera-May, C., & Santamaría, J. M. (2016). Lead accumulation reduces photosynthesis in the lead hyper-accumulator Salvinia minima Baker by affecting the cell membrane and inducing stomatal closure. Aquatic Toxicology, 171, 37-47.

Leguay, S., Lavoie, I., Levy, J. L., & Fortin, C. (2016). Using biofilms for monitoring metal contamination in lotic ecosystems: The protective effects of hardness and pH on metal bioaccumulation. Environmental toxicology and chemistry, 35(6), 1489-1501.

Lehmann V, Tubbing GMJ, Admiraal W (1999) Induced metal tolerance in microbenthic communities from three lowland rivers with different metal loads. Arch Environ Contam Toxicol 36:384–391

Leira, M., & Sabater, S. (2005). Diatom assemblages distribution in Catalan rivers, NE Spain, in relation to chemical and physiographical factors. Water Research, 39(1), 73-82.

Lepori, F., Palm, D., Brännäs, E., & Malmqvist, B. (2005). Does restoration of structural heterogeneity in streams enhance fish and macroinvertebrate diversity?. Ecological applications, 15(6), 2060-2071.

Link, M., Peter, C., Voß, K., & Schäfer, R. B. (2017). Comparison of dilution factors for German wastewater treatment plant effluents in receiving streams to the fixed dilution factor from chemical risk assessment. Science of The Total Environment, 598, 805-813.

Lisle, J. T. (2020). Nutrient Removal and Uptake by Native Planktonic and Biofilm Bacterial Communities in an Anaerobic Aquifer. Frontiers in Microbiology, 11, 1765.

Liu, J., Tang, J., Wan, J., Wu, C., Graham, B., Kerr, P. G., & Wu, Y. (2017). Functional sustainability of periphytic biofilms in organic matter and Cu 2+ removal during prolonged exposure to TiO 2 nanoparticles. Journal of Hazardous Materials. doi:10.1016/j.jhazmat.2017.08.068

Liu, J., Tang, J., Wan, J., Wu, C., Graham, B., Kerr, P. G., & Wu, Y. (2019). Functional sustainability of periphytic biofilms in organic matter and Cu2+ removal during prolonged exposure to TiO2 nanoparticles. Journal of hazardous materials, 370, 4-12.

Loureiro, C., Pereira, J. L., Pedrosa, M. A., Gonçalves, F., & Castro, B. B. (2013). Competitive outcome of Daphnia-Simocephalus experimental microcosms: salinity versus priority effects. PloS one, 8(8), e70572.

Lozano RB, Pratt JR (1994) Interaction of toxicants and communities – the role of nutrients. Environ Toxicol Chem 13(3):361–368

Lu, C., & Zhang, J. (2000). Role of light in the response of PSII photochemistry to salt stress in the cyanobacterium Spirulina platensis. Journal of Experimental Botany, 51(346), 911-917.

Lu, X., Huang, Z., Liang, Z., Li, Z., Yang, J., Wang, Y., & Wang, F. (2021). Co-precipitation of Cu and Zn in precipitation of struvite. Science of The Total Environment, 764, 144269.

Margalef, R. (1983). Limnologia. Ediciones Omega. SA, Barcelona.

Martínez, A., Barros, J., Gonçalves, A. L., & Canhoto, C. (2020). Salinisation effects on leaf litter decomposition in fresh waters: Does the ionic composition of salt matter?. Freshwater Biology, 65(8), 1475-1483.

Martínez, A., Gonçalves, A. L., & Canhoto, C. (2020). Salinization effects on stream biofilm functioning. Hydrobiologia, 847(6), 1453-1459.

Mayes, W. M., Jarvis, A. P., & Younger, P. L. (2005, September). Assessing the importance of diffuse mine water pollution: a case study from County Durham, UK. In Proceedings of the 9th International Mine Water Association Congress, 5th–7th September (pp. 497-506).

McKie, B. G., & Malmqvist, B. (2009). Assessing ecosystem functioning in streams affected by forest management: increased leaf decomposition occurs without changes to the composition of benthic assemblages. Freshwater Biology, 54(10), 2086-2100.

Mcmurry, L. M., Oethinger, M., & Levy, S. B. (1998). Overexpression of marA, soxS, or acrAB produces resistance to triclosan in laboratory and clinical strains of Escherichia coli. FEMS microbiology letters, 166(2), 305-309.

Meals, D. W., Richards, R. P., & Dressing, S. A. (2013). Pollutant load estimation for water quality monitoring projects. Tech Notes, 8, 1-21.

Medley, C. N., & Clements, W. H. (1998). Responses of diatom communities to heavy metals in streams: the influence of longitudinal variation. Ecological applications, 8(3), 631-644.

Medley, C. N., & Clements, W. H. (1998). Responses of diatom communities to heavy metals in streams: the influence of longitudinal variation. Ecological applications, 8(3), 631-644.

Meylan, S., Behra, R., & Sigg, L. (2003). Accumulation of copper and zinc in periphyton in response to dynamic variations of metal speciation in freshwater. Environmental science & technology, 37(22), 5204-5212.

Meylan, S., Behra, R., & Sigg, L. (2003). Accumulation of copper and zinc in periphyton in response to dynamic variations of metal speciation in freshwater. Environmental science & technology, 37(22), 5204-5212.

Meylan, S., Odzak, N., Behra, R., & Sigg, L. (2004). Speciation of copper and zinc in natural freshwater: comparison of voltammetric measurements, diffusive gradients in thin films (DGT) and chemical equilibrium models. Analytica Chimica Acta, 510(1), 91-100.

Miller, R. J., Muller, E. B., Cole, B., Martin, T., Nisbet, R., Bielmyer-Fraser, G. K., ... & Lenihan, H. S. (2017). Photosynthetic efficiency predicts toxic effects of metal nanomaterials in phytoplankton. Aquatic Toxicology, 183, 85-93. efficiency predicts toxic effects of metal nanomaterials in phytoplankton. Aquat. Toxicol. 183, 85–93. https://doi.org/10.1016/j.aquatox.2016.12.009.

MINAE. (2007). Regulation for the Evaluation and Classification of the Quality of Surface Water Bodies Executive Decree No. 33903-MINAE (2007) Costa Rica

Mining Waste Directive, 2006. Directive 2006/21/EC of the European Parliament and of the Council of 15 March 2006 on the Management of Waste from Extractive Industries and Amending Directive 2004/35/EC.

Mitra, A., Flynn, K. J., Burkholder, J. M., Berge, T., Calbet, A., Raven, J. A., ... & Zubkov, M. V. (2014). The role of mixotrophic protists in the biological carbon pump. Biogeosciences, 11(4), 995-1005.

Mohammad, A. W., Teow, Y. H., Ang, W. L., Chung, Y. T., Oatley-Radcliffe, D. L., & Hilal, N. (2015). Nanofiltration membranes review: Recent advances and future prospects. Desalination, 356, 226-254.

Morgan, A., Vicenç, A., Wolfgang, G., Ignasi, R. R., Manuel, P., & Lluís, C. (2021). Climate change impact on EU rivers´ dilution capacity and ecological status. Water Research, 117166.

Morin, S., & Coste, M. (2006). Metal-induced shifts in the morphology of diatoms from the Riou Mort and Riou Viou streams (South West France). Use of algae for monitoring rivers VI. Hungarian Algological Society, Göd, Hungary, Balatonfüred, 91-106.

Morin, S., Corcoll, N., Bonet, B., Tlili, A., & Guasch, H. (2014). Diatom responses to zinc contamination along a Mediterranean river. Plant Ecology and Evolution, 147(3), 325-332.

Morin, S., Cordonier, A., Lavoie, I., Arini, A., Blanco, S., Duong, T. T., ... & Sabater, S. (2012). Consistency in diatom response to metal-contaminated environments. In Emerging and priority pollutants in rivers (pp. 117-146). Springer, Berlin, Heidelberg.

Morin, S., Duong, T. T., Dabrin, A., Coynel, A., Herlory, O., Baudrimont, M., ... & Coste, M. (2008). Long-term survey of heavy-metal pollution, biofilm contamination and diatom community structure in the Riou Mort watershed, South-West France. Environmental Pollution, 151(3), 532-542.

Morin, S., Proia, L., Ricart, M., Bonnineau, C., Geiszinger, A., Ricciardi, F., et al., (2010). Effects of a bactericide on the structure and survival of benthic diatom communities. Life Environ. 60, 107–114.

Morin, S., Vivas-Nogues, M., Duong, T. T., Boudou, A., Coste, M., & Delmas, F. (2007). Dynamics of benthic diatom colonization in a cadmium/zinc-polluted river (Riou-Mort, France). Fundamental and applied limnology, 168(2), 179.

Mossa, J., & James, L. A. (2013). 13.6 Impacts of Mining on Geomorphic Systems.

Motsi, T., Rowson, N. A., & Simmons, M. J. H. (2009). Adsorption of heavy metals from acid mine drainage by natural zeolite. International Journal of Mineral Processing, 92(1-2), 42-48.

Mount, D. R., Erickson, R. J., Highland, T. L., Hockett, J. R., Hoff, D. J., Jenson, C. T., ... & Wisniewski, S. (2016). The acute toxicity of major ion salts to Ceriodaphnia dubia: I. Influence of background water chemistry. Environmental toxicology and chemistry, 35(12), 3039-3057.

Moussa, D. T., El-Naas, M. H., Nasser, M., & Al-Marri, M. J. (2017). A comprehensive review of electrocoagulation for water treatment: Potentials and challenges. Journal of environmental management, 186, 24-41.

Mulholland, P. J., Steinman, A. D., Palumbo, A. V., Elwood, J. W., & Kirschtel, D. B. (1991). Role of nutrient cycling and herbivory in regulating periphyton communities in laboratory streams. Ecology, 72(3), 966-982.

Mullinger N (2004) Review of Environmental and Ecological Impacts of Drainage from Abandoned Metal Minesin Wales. Environment Agency Wales report EATW/04/02.

Muralidharan, M., Selvakumar, C., Sundar, S., & Raja, M. (2010). Macroinvertebrates as potential indicators of environmental quality. Ind. J. Biotechnol, 1, 23-28.

Murphy, J. A. M. E. S., & Riley, J. P. (1962). A modified single solution method for the determination of phosphate in natural waters. Analytica chimica acta, 27, 31-36.

Murray-Bligh J. (1999). Procedures for Collecting and Analysing Macroinvertebrate Samples-BT001. The Environment Agency: Bristol; 176.

National Water Council. (1981). River quality: the 1980 survey and future outlook (pp. 1-41). London: National Water Council.

Navada, S., Vadstein, O., Tveten, A. K., Verstege, G. C., Terjesen, B. F., Mota, V. C., ... & Kamstra, A. (2019). Influence of rate of salinity increase on nitrifying biofilms. Journal of Cleaner Production, 238, 117835.

Navarro, E., Robinson, C. T., & Behra, R. (2008). Increased tolerance to ultraviolet radiation (UVR) and cotolerance to cadmium in UVR-acclimatized freshwater periphyton. Limnology and Oceanography, 53(3), 1149-1158.

Nielsen, D. L., Brock, M. A., Rees, G. N., & Baldwin, D. S. (2003). Effects of increasing salinity on freshwater ecosystems in Australia. Australian Journal of Botany, 51(6), 655-665.

Nuy, J. K., Lange, A., Beermann, A. J., Jensen, M., Elbrecht, V., Röhl, O., ... & Boenigk, J. (2018). Responses of stream microbes to multiple anthropogenic stressors in a mesocosm study. Science of The Total Environment, 633, 1287-1301.

O'Callaghan, P., & Kelly-Quinn, M. (2013). Performance of selected macroinvertebrate-based biotic indices for rivers draining the Merendon Mountains region of Honduras. UNED Research Journal, 5(1), 45-54.

Oatley-Radcliffe, D. L., Walters, M., Ainscough, T. J., Williams, P. M., Mohammad, A. W., & Hilal, N. (2017). Nanofiltration membranes and processes: A review of research trends over the past decade. Journal of Water Process Engineering, 19, 164-171.

Ober, J. A. (2016). Mineral commodity summaries 2016. US Geological Survey.

Oksanen, J., Blanchet, F. G., Kindt, R., Legendre, P., Minchin, P. R., O'hara, R. B., ... & Oksanen, M. J. (2013). Package 'vegan'. Community ecology package, version, 2(9), 1-295.

Olson, J. R. (2019). Predicting combined effects of land use and climate change on river and stream salinity. Philosophical Transactions of the Royal Society B, 374(1764), 20180005.

Olson, J. R., & Hawkins, C. P. (2017). Effects of total dissolved solids on growth and mortality predict distributions of stream macroinvertebrates. Freshwater Biology, 62(4), 779-791.

Palumbo-Roe, B., Bearcock, J., & Banks, V. J. (2012). Hydrogeochemical observations to improve site characterisation and remediation of Frongoch Mine, Wales.

Pandey, L. K. (2020). In situ assessment of metal toxicity in riverine periphytic algae as a tool for biomonitoring of fluvial ecosystems. Environmental Technology & Innovation, 18, 100675.

Pandey, L. K., & Bergey, E. A. (2016). Exploring the status of motility, lipid bodies, deformities and size reduction in periphytic diatom community from chronically metal (Cu, Zn) polluted waterbodies as a biomonitoring tool. Science of the Total Environment, 550, 372-381.

Pandey, L. K., & Bergey, E. A. (2018). Metal toxicity and recovery response of riverine periphytic algae. Science of the total environment, 642, 1020-1031.

Pandey, L. K., Han, T., & Gaur, J. P. (2015). Response of a phytoplanktonic assemblage to copper and zinc enrichment in microcosm. Ecotoxicology, 24(3), 573-582.

Park, J. H., Inam, E., Abdullah, M. H., Agustiyani, D., Duan, L., Hoang, T. T., ... & Wirojanagud, W. (2011). Implications of rainfall variability for seasonality and climate-induced risks concerning surface water quality in East Asia. Journal of Hydrology, 400(3-4), 323-332.

Parmar, T. K., Rawtani, D., & Agrawal, Y. K. (2016). Bioindicators: the natural indicator of environmental pollution. Frontiers in life science, 9(2), 110-118.

Pattrick, R.A.D. and Polya, D.A. (1993) Mineralization in the British Isles. Chapman and Hall, London

Paul, W. L., Cook, R. A., Suter, P. J., Clarke, K. R., Shackleton, M. E., McInerney, P. J., & Hawking, J. H. (2018). Long-Term Monitoring of Macroinvertebrate Communities Over 2,300 km of the Murray River Reveals Ecological Signs of Salinity Mitigation Against a Backdrop of Climate Variability. Water Resources Research, 54(9), 7004-7028.

Paulsson M, Nystrom B, Blanck H (2000) Long-term toxicity of zinc to bacteria and algae in periphyton communities from the river Gota Alv, based on a microcosm study. Aquat Toxicol 47: 243–257

Paulsson, M., Månsson, V., & Blanck, H. (2002). Effects of zinc on the phosphorus availability to periphyton communities from the river Göta Älv. Aquatic Toxicology, 56(2), 103-113.

Paunov, M., Koleva, L., Vassilev, A., Vangronsveld, J., & Goltsev, V. (2018). Effects of different metals on photosynthesis: Cadmium and zinc affect chlorophyll fluorescence in durum wheat. International journal of molecular sciences, 19(3), 787.

Pawlik-Skowrońska, B. (2003). When adapted to high zinc concentrations the periphytic green alga Stigeoclonium tenue produces high amounts of novel phytochelatin-related peptides. Aquatic toxicology, 62(2), 155-163.

Pereda O., Acuña V., von Schiller D., Sabater S. & Elosegi A. (2019). Immediate and legacy effects of urban pollution on river ecosystem functioning: A mesocosm experiment. Ecotoxicology and Environmental Safety, 169: 960-970. doi: 10.1016/j.ecoenv.2018.11.103

Pereda, O., Solagaistua, L., Atristain, M., de Guzmán, I., Larrañaga, A., von Schiller, D., & Elosegi, A. (2020). Impact of wastewater effluent pollution on stream functioning: A whole-ecosystem manipulation experiment. Environmental Pollution, 258, 113719.

Pesce, S., Margoum, C., & Foulquier, A. (2016). Pollution-induced community tolerance for in situ assessment of recovery in river microbial communities following the ban of the herbicide diuron. Agriculture, Ecosystems & Environment, 221, 79-86.

Peterson, C. G., & Stevenson, R. J. (1990). Post-spate development of epilithic algal communities in different current environments. Canadian journal of botany, 68(10), 2092-2102.

Phan, T. N., & Marquis, R. E. (2006). Triclosan inhibition of membrane enzymes and glycolysis of Streptococcus mutans in suspensions and biofilms. Canadian journal of microbiology, 52(10), 977-983.

Pilkaitytë, R., Schoor, A., & Schubert, H. (2004). Response of phytoplankton communities to salinity changes–a mesocosm approach. Hydrobiologia, 513(1), 27-38.

Pinto, E., Sigaud-kutner, T. C., Leitao, M. A., Okamoto, O. K., Morse, D., & Colepicolo, P. (2003). Heavy metal–induced oxidative stress in algae 1. Journal of phycology, 39(6), 1008-1018.

Ponsatí, L., Corcoll, N., Petrović, M., Picó, Y., Ginebreda, A., Tornés, E., ... & Sabater, S. (2016). Multiple-stressor effects on river biofilms under different hydrological conditions. Freshwater Biology, 61(12), 2102-2115.

Potter, H.A.B. and Jarvis, A.P., 2006. Managing mining pollution to deliver the

Power, M. E., & Dietrich, W. E. (2002). Food webs in river networks. Ecological Research, 17(4), 451-471.

Proia, L., Romaní, A. M., & Sabater, S. (2012). Nutrients and light effects on stream biofilms: a combined assessment with CLSM, structural and functional parameters. Hydrobiologia, 695(1), 281-291.

Proia, L., Romaní, A., & Sabater, S. (2017). Biofilm phosphorus uptake capacity as a tool for the assessment of pollutant effects in river ecosystems. Ecotoxicology, 26(2), 271-282.

Prygiel, J., & Coste, M. (1993). The assessment of water quality in the Artois-Picardie water basin (France) by the use of diatom indices. Hydrobiologia, 269(1), 343-349.

Quigg, A., Chin, W. C., Chen, C. S., Zhang, S., Jiang, Y., Miao, A. J., ... & Santschi, P. H. (2013). Direct and indirect toxic effects of engineered nanoparticles on algae: role of natural organic matter. ACS Sustainable Chemistry & Engineering, 1(7), 686-702.

Rainbow, P. S. (2018). Trace metals in the environment and living organisms: the British Isles as a case study. Cambridge University Press.

Rapport, D. J., Regier, H. A., & Hutchinson, T. C. (1985). Ecosystem behavior under stress. The American Naturalist, 125(5), 617-640.

Reardon, J., Foreman, J. A., & Searcy, R. L. (1966). New reactants for the colorimetric determination of ammonia. Clinica Chimica Acta, 14, 403-405.

Reichl, C., Schatz, M., & Zsak, G. (2016). World Mining Data-Minerals Production. Vienna: International Organizing Committee for the World Mining Congresses.

Riipinen, M. P., Davy-Bowker, J. O. H. N., & Dobson, M. (2009). Comparison of structural and functional stream assessment methods to detect changes in riparian vegetation and water pH. Freshwater Biology, 54(10), 2127-2138.

Rimet, F., Cauchie, H. M., Hoffmann, L., & Ector, L. (2005). Response of diatom indices to simulated water quality improvements in a river. Journal of Applied Phycology, 17(2), 119-128.

Romaní, A. M., Giorgi, A., Acuna, V., & Sabater, S. (2004). The influence of substratum type and nutrient supply on biofilm organic matter utilization in streams. Limnology and Oceanography, 49(5), 1713-1721.

Ros, M. D., Marín-Murcia, J. P., & Aboal, M. (2009). Biodiversity of diatom assemblages in a Mediterranean semiarid stream: implications for conservation. Marine and Freshwater Research, 60(1), 14-24.

Rotter, S., Heilmeier, H., Altenburger, R., & Schmitt-Jansen, M. (2013). Multiple stressors in periphyton–comparison of observed and predicted tolerance responses to high ionic loads and herbicide exposure. Journal of applied ecology, 50(6), 1459-1468.

Roussel, H., Ten-Hage, L., Joachim, S., Le Cohu, R., Gauthier, L., & Bonzom, J. M. (2007). A long-term copper exposure on freshwater ecosystem using lotic mesocosms: primary producer community responses. Aquatic Toxicology, 81(2), 168-182.

Rovira, L., Trobajo, R., Leira, M., & Ibáñez, C. (2012). The effects of hydrological dynamics on benthic diatom community structure in a highly stratified estuary: the case of the Ebro Estuary (Catalonia, Spain). Estuarine, Coastal and Shelf Science, 101, 1-14.

Rumschik, S. M., Nydegger, I., Zhao, J., & Kay, A. R. (2009). The interplay between inorganic phosphate and amino acids determines zinc solubility in brain slices. Journal of neurochemistry, 108(5), 1300-1308.

Sabater S, Guasch H, Ricart M, Romaní A, Vidal G, Klünder C, Schmitt- Jansen M (2007) Monitoring the effect of chemicals on biological communities. The biofilm as an interface. Anal Bioanal Chem 387: 1425–1434

Sabater, S., & Admiraal, W. (2005). Periphyton as biological indicators in managed aquatic ecosystems. Periphyton: ecology, exploitation and management, 159-177.

Sabater, S., Barceló, D., De Castro-Català, N., Ginebreda, A., Kuzmanovic, M., Petrovic, M., ... & Muñoz, I. (2016). Shared effects of organic microcontaminants and environmental stressors on biofilms and invertebrates in impaired rivers. Environmental pollution, 210, 303-314.

Sabater, S., Guasch, H., Romaní, A., & Muñoz, I. (2002). The effect of biological factors on the efficiency of river biofilms in improving water quality. Hydrobiologia, 469(1), 149-156.

Sala, M., Faria, M., Sarasúa, I., Barata, C., Bonada, N., Brucet, S., ... & Cañedo-Arguelles, M. (2016). Chloride and sulphate toxicity to Hydropsyche exocellata (Trichoptera, Hydropsychidae): exploring intraspecific variation and sub-lethal endpoints. Science of the Total Environment, 566, 1032-1041.

Sandin, L., & Solimini, A. G. (2009). Freshwater ecosystem structure–function relationships: from theory to application. Freshwater Biology, 54(10), 2017-2024.

Sauer, F. G., Bundschuh, M., Zubrod, J. P., Schäfer, R. B., Thompson, K., & Kefford, B. J. (2016). Effects of salinity on leaf breakdown: dryland salinity versus salinity from a coalmine. Aquatic Toxicology, 177, 425-432.

Schuler, M. S., Cañedo-Argüelles, M., Hintz, W. D., Dyack, B., Birk, S., & Relyea, R. A. (2019). Regulations are needed to protect freshwater ecosystems from salinization. Philosophical Transactions of the Royal Society B, 374(1764), 20180019.

Serra Gasa, A. (2009). Fate and effects of copper in fluvial ecosystems: the role of periphyton. Universitat de Girona.

Serra, A., Corcoll, N., & Guasch, H. (2009). Copper accumulation and toxicity in fluvial periphyton: the influence of exposure history. Chemosphere, 74(5), 633-641.

Seshadri, B., Bolan, N. S., Choppala, G., Kunhikrishnan, A., Sanderson, P., Wang, H., ... & Kim, G. (2017). Potential value of phosphate compounds in enhancing immobilization and reducing bioavailability of mixed heavy metal contaminants in shooting range soil. Chemosphere, 184, 197-206.

Shannon, C.E., Weaver, W.W. (1963). The Mathematical Theory of Communication. University of Illinois Press, Urbana.

Sheng, G. P., Yu, H. Q., & Li, X. Y. (2010). Extracellular polymeric substances (EPS) of microbial aggregates in biological wastewater treatment systems: a review. Biotechnology advances, 28(6), 882-894.

Silva, E. I. L., Shimizu, A., & Matsunami, H. (2000). Salt pollution in a Japanese stream and its effects on water chemistry and epilithic algal chlorophyll-a. Hydrobiologia, 437(1), 139-148.

Smirnoff, N. (1996). Botanical briefing: the function and metabolism of ascorbic acid in plants. Annals of botany, 78(6), 661-669.

Society for Mining, Metallurgy, and Exploration, Inc. (SME). (2008). Management Technologies for Metal Mining Influenced Water – Basics of Metal Mining Influenced Water. V.T. McLemore (Ed.).

Soldo, D., & Behra, R. (2000). Long-term effects of copper on the structure of freshwater periphyton communities and their tolerance to copper, zinc, nickel and silver. Aquatic toxicology, 47(3-4), 181-189.

Solomon, F. (2008). Impacts of metals on aquatic ecosystems and human health.

Starke, L. (2002). Breaking new ground: mining, minerals, and sustainable development: the report of the MMSD project (Vol. 1). Earthscan.

Steele, D. J., Franklin, D. J., & Underwood, G. J. (2014). Protection of cells from salinity stress by extracellular polymeric substances in diatom biofilms. Biofouling, 30(8), 987-998.

Steffen, W., Grinevald, J., Crutzen, P., & McNeill, J. (2011). The Anthropocene: conceptual and historical perspectives. Philosophical Transactions of the Royal Society A: Mathematical, Physical and Engineering Sciences, 369(1938), 842-867.

Steinaman, A. D., & McIntire, C. D. (1986). EFFECTS OF CURRENT VELOCITY AND LIGHT ENERGY ON THE STRUCTURE FO PERIPHYTON ASSEMBLAGE IN LABORATORY STREAMS 1. Journal of Phycology, 22(3), 352-361.

Stoenner, E. F., Smol, J. P., & Kristiansen, J. (1999). Reviews-The Diatoms: Applications for the Environmental and Earth Sciences. Nordic Journal of Botany, 19(3), 384.

Südharz. S and Sommer. T (2014). Studie Abflussverhältnisse der Halde Menteroda als Grundlage für die Minderung des Niederschlagswasser-Anteils am Haldensickerwasser.

Sultana, J., Tibby, J., Recknagel, F., Maxwell, S., & Goonan, P. (2020). Comparison of two commonly used methods for identifying water quality thresholds in freshwater ecosystems using field and synthetic data. Science of The Total Environment, 724, 137999.

Taïbi, K., Taïbi, F., Abderrahim, L. A., Ennajah, A., Belkhodja, M., & Mulet, J. M. (2016). Effect of salt stress on growth, chlorophyll content, lipid peroxidation and antioxidant defence systems in Phaseolus vulgaris L. South African Journal of Botany, 105, 306-312.

Tallin, J. E., Pufahl, D. E., & Barbour, S. L. (1990). Waste management schemes of potash mines in Saskatchewan. Canadian Journal of Civil Engineering, 17(4), 528-542.

Tang, J., Zhu, N., Zhu, Y., Liu, J., Wu, C., Kerr, P., ... & Lam, P. K. (2017). Responses of periphyton to Fe2O3 nanoparticles: a physiological and ecological basis for defending nanotoxicity. Environmental science & technology, 51(18), 10797-10805.

Tchounwou, P. B., Yedjou, C. G., Patlolla, A. K., & Sutton, D. J. (2012). Heavy metal toxicity and the environment. Molecular, clinical and environmental toxicology, 133-164.

Ter Braak, C. T., & Smilauer, P. (1998). CANOCO reference manual and user's guide to Canoco for Windows: software for canonical community ordination (version 4).

Ternjej, Ivancica and Mihaljevic, Zlatko. (2017). "Ecology" Physical Sciences Reviews, vol. 2, no. 10, 2017. https://doi.org/10.1515/psr-2016-0116

Tessier, A., & Turner, D. R. (Eds.). (1995). Metal speciation and bioavailability in aquatic systems (pp. p-679). Chichester: Wiley.

Tipping, E., Jarvis, A. P., Kelly, M. G., Lofts, S., Merrix, F. L., & Ormerod, S. J. (2009). Ecological indicators for abandoned mines, Phase 1: Review of the literature.

Tlili, A., Berard, A., Blanck, H., Bouchez, A., Cássio, F., Eriksson, K. M., ... & Behra, R. (2016). Pollution-induced community tolerance (PICT): towards an ecologically relevant risk assessment of chemicals in aquatic systems. Freshwater Biology, 61(12), 2141-2151.

Tlili, A., Bérard, A., Roulier, J. L., Volat, B., & Montuelle, B. (2010). PO43– dependence of the tolerance of autotrophic and heterotrophic biofilm communities to copper and diuron. Aquatic Toxicology, 98(2), 165-177.

Tlili, A., Corcoll, N., Bonet, B., Morin, S., Montuelle, B., Bérard, A., & Guasch, H. (2011b). In situ spatio-temporal changes in pollution-induced community tolerance to zinc in autotrophic and heterotrophic biofilm communities. Ecotoxicology, 20(8), 1823-1839.

Tlili, A., Montuelle, B., Triquet, C. A., Rainbow, P. S., & Roméo, M. (2011). Microbial pollution-induced community tolerance.

Torrisi, M., Scuri, S., Dell'Uomo, A., & Cocchioni, M. (2010). Comparative monitoring by means of diatoms, macroinvertebrates and chemical parameters of an Apennine watercourse of central Italy: The river Tenna. Ecological Indicators, 10(4), 910-913.

Townsend, S. A., & Douglas, M. M. (2014). Benthic algal resilience to frequent wet-season storm flows in low-order streams in the Australian tropical savanna. Freshwater Science, 33(4), 1030-1042.

Tripathi, A., & Ranjan, M. R. (2015). Heavy metal removal from wastewater using low cost adsorbents. J Bioremed Biodegr 6 (6): 1–5.

Trobajo Pujadas, R. (2003). Ecological analysis of periphytic diatoms in Mediterranean coastal wetlands (Empordà wetlands, NE Spain). Universitat de Girona.

Trobajo, R., Rovira, L., Mann, D. G., & Cox, E. J. (2011). Effects of salinity on growth and on valve morphology of five estuarine diatoms. Phycological Research, 59(2), 83-90.

Truchy, A., Angeler, D. G., Sponseller, R. A., Johnson, R. K., & McKie, B. G. (2015). Linking biodiversity, ecosystem functioning and services, and ecological resilience: towards an integrative framework for improved management. Advances in ecological research, 53, 55-96.

Tuulaikhuu, B. A., Romaní, A. M., & Guasch, H. (2015). Arsenic toxicity effects on microbial communities and nutrient cycling in indoor experimental channels mimicking a fluvial system. Aquatic Toxicology, 166, 72-82.

USEPA (United States Environmental Protection Agency), 2014. Reference Guide to Treatment Technologies for Mining-Influenced Water. EPA 542-R-14-001.

Vannote, R. L., Minshall, G. W., Cummins, K. W., Sedell, J. R., & Cushing, C. E. (1980). The river continuum concept. Canadian journal of fisheries and aquatic sciences, 37(1), 130-137.

Velasco, J., Gutiérrez-Cánovas, C., Botella-Cruz, M., Sánchez-Fernández, D., Arribas, P., Carbonell, J. A., ... & Pallarés, S. (2019). Effects of salinity changes on aquatic organisms in a multiple stressor context. Philosophical Transactions of the Royal Society B, 374(1764), 20180011.

Velasco, J., Millán, A., Hernández, J., Gutiérrez, C., Abellán, P., Sánchez, D., & Ruiz, M. (2006). Response of biotic communities to salinity changes in a Mediterranean hypersaline stream. Saline systems, 2(1), 1-15.

Venâncio, C., Castro, B. B., Ribeiro, R., Antunes, S. C., Abrantes, N., Soares, A. M. V. M., & Lopes, I. (2019). Sensitivity of freshwater species under single and multigenerational exposure to seawater intrusion. Philosophical Transactions of the Royal Society B, 374(1764), 20180252.

Vendrell-Puigmitja, L., Abril, M., Proia, L., Angona, C. E., Ricart, M., Oatley-Radcliffe, D. L., ... & Llenas, L. (2020). Assessing the effects of metal mining effluents on freshwater ecosystems using biofilm as an ecological indicator: Comparison between nanofiltration and nanofiltration with electrocoagulation treatment technologies. Ecological Indicators, 113, 106213.

Verdonschot, P. F., & van der Lee, G. H. (2020). Perspectives on the functional assessment of multi-stressed stream ecosystems. Freshwater Science, 39(4), 605-620.

Villalaín, J., Mateo, C. R., Aranda, F. J., Shapiro, S., & Micol, V. (2001). Membranotropic effects of the antibacterial agent triclosan. Archives of biochemistry and biophysics, 390(1), 128-136.

Villeneuve A, Bouchez A, Montuelle B (2010) Influence of slight differences in environmental conditions (light, hydrodynamics) on the structure and function of the periphyton. Aquat Sci 72(1):33–44

Vinten, A. J. A., Artz, R. R. E., Thomas, N., Potts, J. M., Avery, L., Langan, S. J., ... & Singh, B. K. (2011). Comparison of microbial community assays for the assessment of stream biofilm ecology. Journal of microbiological methods, 85(3), 190-198.

von Alvensleben, N., Magnusson, M., & Heimann, K. (2016). Salinity tolerance of four freshwater microalgal species and the effects of salinity and nutrient limitation on biochemical profiles. Journal of applied phycology, 28(2), 861-876.

Weber, C. I. (Ed.). (1980). Biological field and laboratory methods for measuring the quality of surface waters and effluents (Vol. 73, No. 1). National Environmental Research Center, Office of Research and Development, US Environmental Protection Agency.

Weisbrod, A. V., Woodburn, K. B., Koelmans, A. A., Parkerton, T. F., McElroy, A. E., & Borgå, K. (2009). Evaluation of bioaccumulation using in vivo laboratory and field studies. Integrated Environmental Assessment and Management: An International Journal, 5(4), 598-623.

Weiss, F. T., Leuzinger, M., Zurbrügg, C., & Eggen, H. I. (2016). Chemical pollution in low-and middle-income countries. Eawag.

Williams, W. D., & Sherwood, J. E. (1994). Definition and measurement of salinity in salt lakes. International Journal of Salt Lake Research, 3(1), 53-63.

Wirth, P., & Harfst, J. (2012). Challenges of Post-Mining Regions in Central Europe. München: IÖR.

Wolff, B. A., Duggan, S. B., & Clements, W. H. (2019). Resilience and regime shifts: Do novel communities impede ecological recovery in a historically metal-contaminated stream?. Journal of Applied Ecology, 56(12), 2698-2709.

Wu, Y. (2016). Periphyton: functions and application in environmental remediation. Elsevier.

Yang, J., Zhan, C., Li, Y., Zhou, D., Yu, Y., & Yu, J. (2018). Effect of salinity on soil respiration in relation to dissolved organic carbon and microbial characteristics of a wetland in the Liaohe River estuary, Northeast China. Science of the total environment, 642, 946-953.

Ylla, I., Borrego, C., Romaní, A. M., & Sabater, S. (2009). Availability of glucose and light modulates the structure and function of a microbial biofilm. FEMS microbiology ecology, 69(1), 27-42.

Ylla, I., Sanpera-Calbet, I., Muñoz, I., Romaní, A. M., & Sabater, S. (2011). Organic matter characteristics in a Mediterranean stream through amino acid composition: changes driven by intermittency. Aquatic sciences, 73(4), 523-535.

Younger, P. L., & Wolkersdorfer, C. (2004). Mining impacts on the freshwater environment: technical and managerial guidelines for catchment scale management. Mine water and the environment, 23, s2.

Zhang, P., He, L., Fan, X., Huo, P., Liu, Y., Zhang, T., ... & Yu, Z. (2015). Ecosystem service value assessment and contribution factor analysis of land use change in Miyun County, China. Sustainability, 7(6), 7333-7356.

Zhang, X., Li, B., Deng, J., Qin, B., Wells, M., & Tefsen, B. (2020). Advances in freshwater risk assessment: improved accuracy of dissolved organic matter-metal speciation prediction and rapid biological validation. Ecotoxicology and environmental safety, 202, 110848.

Zhu, G., Wang, Q., Yin, J., Li, Z., Zhang, P., Ren, B., ... & Wan, P. (2016). Toward a better understanding of coagulation for dissolved organic nitrogen using polymeric zinc-iron-phosphate coagulant. Water research, 100, 201-210.

Zhu, N., Wang, S., Tang, C., Duan, P., Yao, L., Tang, J., ... & Wu, Y. (2019). Protection mechanisms of periphytic biofilm to photocatalytic nanoparticle exposure. Environmental science & technology, 53(3), 1585-1594.

Ziemann, H., Kies, L., & Schulz, C. J. (2001). Desalinization of running waters: III. Changes in the structure of diatom assemblages caused by a decreasing salt load and changing ion spectra in the river Wipper (Thuringia, Germany). Limnologica, 31(4), 257-280.

Zimmermann-Timm, H. (2007). Salinisation of inland waters. Water Uses and Human Impacts on the Water Budget. Verlag Wissenschaftliche Auswertungen/GEO, Hamburg, 133-136.